Biomagnetic fluid flows over a stretching sheet

A Thesis Submitted to

University of Dhaka, Dhaka

In Partial Fulfilment of the Requirements for the Degree of

DOCTOR OF PHILOSOPHY

in

Applied Mathematics

By

Md. Ghulam Murtaza Talukder

Registration No. 73

Session: 2015-16

Under the supervision of

Dr. Mohammad Ferdows
Professor
Department of Applied mathematics
University of Dhaka
Dhaka, Bangladesh

Dr. Efstratios E. Tzirtzilakis
Associate Professor
Department of Mechanical Engineering
Technological Educational Institute of
western Greece, Greece.

December 2018

Acknowledgements

A lot of people contributed to the success of this PhD thesis. In the first instance, I am deeply indebted to Professor Mohammad Ferdows, Department of Applied Mathematics, University of Dhaka, Bangladesh and Associate Professor Efstratios E. Tzirtzilakis, Department of Mechanical Engineering, Technological Educational Institute of Western Greece, Greece for the inspiring, patient supervision and support throughout my study in the development of my skills and the writing of this thesis. I have experienced an excellent academic study under their supervision and their invaluable recommendations and support encouraged me to plan my future academic studies and independent thinker which will be very much helpful during my teaching profession. Without their help and support, this work would never have been possible.

I would like to give my special thanks to Professor J. C. Misra, Indian Institute of Engineering Science and Technology, India and Dr. Swati Mukhopaddy, University of Burdwan, India, for their valuable scientific advice, useful discussion and guidance regarding the numerical aspects of my study.

Furthermore, I would like to thanks Professor Md. Shafiqul Islam, Chairman, Department of Applied Mathematics, University of Dhaka for his cordial support during my study period.

I am sincerely and deeply indebted to Professor Mahmud Alam, Mathematics Discipline, Khulna University, for his assistance, valuable comments and all kind of supports.

It is my pleasure to acknowledge to all the faculty member, Department of Applied Mathematics, University of Dhaka, for their kind support, assistances, unending inspiration and valuable suggestions.

I would like to thanks all of my family members specially my wife Mhafuza Matin and my son Munem Shaharier for their never-ending love, patient and encouragement.

The support of my colleagues, Comilla University, is appreciated. I would also like to thank Comilla University for allowing me a study leave for the whole period of my study.

Lastly, I would also like to acknowledge the Ministry of Science and Technology, Bangladesh for the financial support during my academic study.

CERTIFICATE

We hereby recommended that the thesis presented under our supervision by **Mr. Md. Ghulam Murtaza Talukder** entitled **"Biomagnetic fluid flows over a stretching sheet"** be accepted in partial fulfilment of the requirements for the Degree of Doctor of Philosophy in Applied Mathematics. Further, this thesis work as a whole or a part thereof has not been submitted elsewhere for the award of any other degree, diploma or any other qualification.

Professor Mohammad Ferdows
Supervisor
Department of Applied mathematics
University of Dhaka
Dhaka-1000, Bangladesh

Associate Professor Efstratios E. Tzirtzilakis
Co-Supervisor
Department of Mechanical Engineering
Technological Educational Institute of western Greece, Greece

Abstract

Biomagnetic fluid (Blood) is a fluid that exists in a living creature and its flow is influenced by the presence of a magnetic field. Blood is considered to be a typical biomagnetic fluid due to the interaction of intercellular proteins, membrane and the hemoglobin. Studies on biomagnetic fluid flow and heat transfer under the influence of external magnetic fields have been received much attention of researchers owing to their important applications in bioengineering and clinical sciences. Design and development of magnetic devices for cell separation, reduction of blood flow during surgery, targeted transport of drugs through the use of magnetic particles as drug carriers, magnetic resonance imaging (MRI) of specific parts of the human body, electromagnetic hyperthermia in cancer treatment are among these applications.

In this thesis, we emphasized to the theoretical and numerical investigations of both two-three dimensional, steady-unsteady, Newtonian, viscous, incompressible and laminar biomagnetic fluid flow and heat transfer over stretching-shrinking sheets under various boundary geometry with the action of an applied magnetic field.

Throughout this thesis, we first perform the biomagnetic fluid flow (BFD) over an elastic flat stretching sheet in the presence of a magnetic dipole. For the mathematical formulation of this problem both magnetization and electrical conductivity of blood are taken into account and consequently both principles of Magnetohydrodynamics (MHD) and FerroHydroDynamics (FHD) are adopted. The biomagnetic fluid flow and heat transfer in three-dimensional unsteady stretching/shrinking sheet in the presence of ferromagnetic phenomena has also been investigated. The main contribution is the study of three dimensional time dependent BFD flow which has not been considered yet to our best knowledge. Then, we investigate the time-dependent two-dimensional biomagnetic fluid flow (BFD) over a stretching sheet under the action of electrical conductivity and magnetization. A detailed stability and convergence analysis is performed to determine the restrictions for the values of the problem parameters like magnetic parameter which are of crucial importance for the formation of the flow fields. This could be predicted numerically by the application of the simple efficient finite difference method (EFDM).

Later on, we have analyzed the steady biomagnetic fluid flow which is stretched with a velocity proportional to $(dis\tan ce)^n$ i. e. nonlinear stretching sheet considering variable thickness. In this model, we assume that the fluid is electrically conducting due to an applied magnetic field and mathematical formulation also incorporates the space and time dependent

internal heat generation. Internal heat generation accelerates the mechanical strength of fluid flows throughout the boundary layer. We have also investigated the effects of variable fluid properties on the flow and heat transfer of three dimensional biomagnetic fluid over a stretching surface in the presence of a magnetic dipole. In this problem, the dynamic viscosity and thermal conductivity of biomagnetic fluid is considered to be temperature dependent whereas the magnetization of the fluid varies as a linear function of temperature and magnetic field strength. Also the surface temperature distribution across the sheet is non-linear.

To solve the above mathematical problem, the governing boundary layer equations with associated boundary conditions, are transformed into a system of nonlinear coupled ordinary differential equations by using suitable similarity transformations. Numerical solutions for the governing momentum and energy equations are obtained by efficient numerical techniques based on the common finite difference method with central differencing, on a tridiagonal matrix manipulation and on an iterative procedure.

Our next intention is to characterize the existence of duality of mathematical problem solutions and their physical realizable. The dual solutions are obtained by setting different initial guesses for the missing values of the skin friction coefficient and the local Nusselt number, where all profiles satisfy the far field boundary conditions asymptotically. For the first time, we have examined the dual solutions in biomagnetic fluid flow and heat transfer over a nonlinear stretching or shrinking sheet in the presence of a magnetic dipole with/without prescribed heat flux. This problem has been treated mathematically by using Lie group transformation and the resulting equations are solved numerically by using bvp4c function available in MATLAB and reported the existence of dual solution (stable solution and unstable solution) in the flow analysis. A stability analysis has also been carried out and presented here. Results from the stability analysis depict that the first solution (upper branch) is stable and physically realizable, while the second solution (lower branch) is unstable.

In all these analysis, influence of various physical parameters involved like as hydrodynamic, magnetohydrodynamic and ferromagnetic interaction parameters, unsteadiness parameter, suction/injection parameters, stretching ratio and heat generation parameter, viscosity parameter, thermal conductivity parameter, and velocity/temperature index parameter on the fluid flow are investigated and the results have been presented graphically. Missing slope like as the skin friction coefficient, , heat transfer rate and relative wall pressure is revealed and special case with change in hydrodynamic and ferromagnetic parameters have also been illustrated. The results of the present study have been compared with those of an earlier study reported in available literatures in order to ascertain the validity

of the computational results. Once we achieved good accuracy we go further for detailed results. The numerical results of the study reveal that the characteristics of blood flow are significantly affected by the presence of a magnetic dipole which gives rise to a magnetic field, sufficiently strong to saturate the biofluid.

Publications based on this thesis

1. **Murtaza**, **M. G.,** Tzirtzilakis, E. E. & Ferdows, M. (2018). Numerical solution of three dimensional unsteady biomagnetic flow and heat transfer through stretching/shrinking sheet using temperature dependent magnetization, *Archives of mechanics*, 70 (2), 161-185.
2. **Murtaza**, **M. G.,** Tzirtzilakis, E. E. & Ferdows, M. (2018). Similarity Solutions of Nonlinear Stretched Biomagnetic Flow and Heat Transfer with Signum Function and Temperature Power Law Geometries, *International Journal of Mathematical and Computational Sciences*, 12 (2), 9-14.
3. **Murtaza**, **M. G.,** Tzirtzilakis, E. E. & Ferdows, M. (2018). A Note on MHD Flow and Heat Transfer over a Curved Stretching Sheet by Considering Variable Thermal Conductivity. *International Journal of Mathematical and Computational Sciences,* 12(2), 23-27.
4. **Murtaza**, **M. G.,** Tzirtzilakis, E. E. & Ferdows, M. (2017). Effect of electrical conductivity and magnetization on the biomagnetic fluid flow over a stretching sheet, *Zeitschrift f¨ur angewandte Mathematik und Physik (ZAMP),* 68:93. DOI 10.1007/s00033-017-0839-z.
5. Robiul Awal, Ferdows, M., **Murtaza, M. G**., & Tzirtzilakis, E. E. (2018). Effect of mixed convective parameter on flow and heat transfer over a linear stretching sheet in a biomagnetic fluid with magnetization. *LAP Lambert academic publishing, Beau Bassin, Mauritius.*
6. **Murtaza**, **M. G.,** Tzirtzilakis, E. E. & Ferdows, M. (2018). Dual solutions in boundary layer flow and heat transfer of biomagnetic fluid over a stretching/shrinking sheet in the presence of a magnetic dipole and prescribed heat flux, *Zeitschrift f¨ur Angewandte Mathematik und Physik (ZAMP), Accepted.*
7. **Murtaza**, **M. G.,** Tzirtzilakis, E. E. & Ferdows, M. (2018). Biomagnetic fluid flow past a stretching/shrinking sheet with slip conditions using Lie group transformation. *8th BSME International Conference on Thermal Engineering, American Institute of Physics (AIP) conference proceeding.*
8. **Murtaza**, **M. G.,** Tzirtzilakis, E. E. & Ferdows, M. (2018). Three dimensional Biomagnetic flow and heat transfer over a stretching surface with variable fluid properties. *Second International Conference on Modern Mathematical Methods and High*

Performance Computing in Science and Technology (M3HPCST 2018), Advance in mechanics and mathematics,41, 403-414.

9. **Murtaza**, **M. G.,** Tzirtzilakis, E. E. & Ferdows, M. (2018). Effect of variable viscosity and variable thermal conductivity of biomagnetic fluid flow and heat transfer over a stretching sheet in the presence of magnetic dipole. *1st International Conference on Industrial and Mechanical Engineering and Operations Management (IMEOM), American Institute of Physics (AIP) conference proceeding.*

Contents

List of Figures

List of Tables

Nomenclature

(x, y, z)	Cartesian coordinates (m)
(u, v, w)	Velocity components in the x, y, z direction. (ms^{-1})
(U, V)	Dimensionless velocity components.
(ξ, ζ, η)	Non-dimensional coordinates
P	Fluid pressure (kg / ms^2)
$\overrightarrow{M}$	Magnetization (A/m)
H	Magnetic field intensity (A/m)
B	Magnetic induction (A/m)
B_s	Saturation magnetic induction (A/m)
M_s	Saturation magnetization (A/m)
T	Fluid temperature inside the boundary layer (K)
T_c , T_∞	Fluid temperature far away from sheet (K)
T_w	Temperature of the sheet (K)
P_1, P_3, P_5	Dimensionless pressure
(f', g')	Dimensionless velocity components in the x *and* y directions
$(\theta_1, \theta_3, \theta_5)$	Dimensionless Temperature
ρ	Density of fluid (kg / m^3)
μ	Dynamic viscosity (kg / ms)
ν	Kinematic viscosity (m^2 / s)
μ_0	Magnetic permeability $(Kg.m / A^2 s^2)$
A	Unsteadiness parameter
C_p	Specific heat constant pressure $(J / Kg.K)$

k	Thermal conductivity (J/msK)
a, c	Linear stretching constant
λ_1	Stretching parameter
P_r	Prandtl number
λ_a	Viscous dissipation parameter
ε	Dimensionless Curie temperature
β	Ferromagnetic interaction parameter
δ	Dimensionless distance
φ	Dissipation function
t	Time(t)
ψ	Stream function (m^2s^{-1})
τ	Dimensionless time
u_w	Stretching velocity
τ_w	Wall shear stress
Nu_x	Local Nusselt number
q_w	Wall heat flux
C_{fx}	Skin friction coefficient
Re_x	Local Reynolds number
$f''(0)$	Skin friction
$\theta'(0)$	Wall heat transfer gradient
s	Suction parameter
(m)	Velocity or temperature exponent parameter
M_n	Magnetohydrodynamic interaction parameter
q'''	Non-uniform heat source/sink
A^*	Coefficient of space dependent heat source/ sink
B^*	Coefficient of temperature dependent heat source/ sink

List of Abbreviations

BFD	Biomagnetic Fluid Dynamics
MHD	Magnetohydrodynamics
FHD	Ferrohydrodynamics
FDM	Finite Difference Method
PDE	Partial Differential Equation
ODE	Ordinary Differential Equation

Chapter 1

Introduction

In this chapter, the main terminologies used in the thesis are defined. The synthesis of biomagnetic fluid namely, blood and its properties are briefly discussed. A detailed review of the applications of biofluid is given in this chapter. The aims, objectives and important of the study are also discussed here.

1.1 Boundary Layers Concept

On August 12, 1904 at the third international mathematical congress in Heidelberg, Germany, Ludwig Prandtl presented a paper entitle "Uber Fliiussigkeitsbewegungen bei sehr kleiner Reibung" (English) "On fluid flow with very little friction". He explained that the viscosity of a fluid plays a vital role in a thin layer adjacent to the surface, which he called "Uebergangsschicht" or "Grenzschicht". The English terminology is boundary layer or shear layer. He also simplified the equations of fluid flow by dividing the flow field into two areas: one inside the boundary layer, dominated by viscosity and creating the majority of drag experienced by the boundary body; and one outside the boundary layer, where viscosity can be neglected without significant effects on the solution.

The first summary of boundary layer theory is to be found in two articles by Tollmien (1931) in the Handbuch der Experimental physic. Some years later, Prandtl's comprehensive contribution appeared in Aerodynamic Theory, edited by W. F. Durand, Prandtl (1935). In the six decades since then, the extent of this research area has become extraordinary large. Cf. Schlichting (1960) and also Evans (1968), Alfred Walz (1969), Tani (1977), Young (1989), Oleinik, Samokhin (1999). In spite of these developments concerning the numerical solutions of the full Navier-Stokes equations it can also be noticed that in recent years the extensions of boundary layer theory received increasing attention. Several text books have been published recently. Such as the interactive boundary layer theory by Sobey (2000), Schlichting and Gersten (Ed.) (2017), Kluwick (2014), Ruban (2017).

In physics and fluid mechanics, boundary layer is an important concept and refers to the layer of fluid in the immediate vicinity of a bounding surface where the effects of viscosity are significant. The boundary layer provides an important link between ideal fluid

and real fluid flow. For fluids having relatively small viscosity, the effect of internal friction in a fluid is appreciable only in a narrow region surrounding the fluid boundaries. Since the fluid at the boundaries has zero velocity, there is a steep velocity gradient from the boundary into the flow. This velocity gradient in a real fluid sets up shear forces near the boundary that reduce the flow speed to that of the boundary. That fluid layer which has had its velocity affected by the boundary shear is called the boundary layer. The overall flow field is found by coupling the boundary layer and the inviscid outer region. The coupling process (both physically and mathematically) will also receive ample attention.

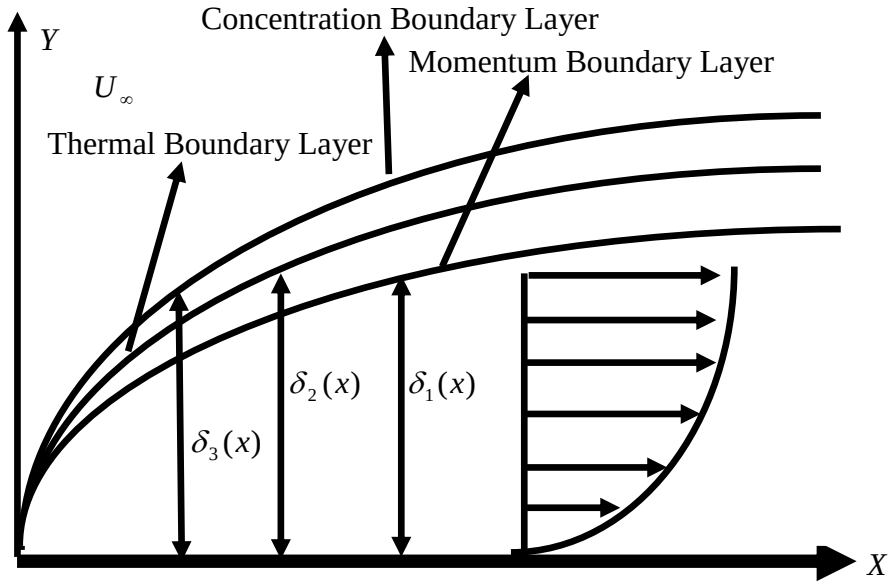

Fig. 1.1 Boundary layer formulation.

Depending on the nature of the fluid flow in consideration, we can study either one or a combination of the boundary layers discussed below.

(a) Velocity boundary layer (δ_1)**:** Fluid particles in contact with a stationary surface assume zero tangential velocity. Similarly, fluid particles in contact with a moving surface will move at the velocity of the surface.

In fluid dynamics this phenomenon is called the no slip condition. When a fluid flows, there occurs a net momentum transport from regions of high velocity to regions of low velocity thus creating a viscous shear stress in the direction of the flow. The significance of the velocity boundary layer is to determine the surface (or skin) friction of the fluid.

(b) Thermal boundary layer (δ_2)**:** The thermal boundary layer develops due to the presence of temperature gradients between the surface and the free stream region. The thermal boundary layer is important in determining the rate of convection heat transfer.

(c) Concentration boundary layer (δ_3)**:** A concentration boundary layer develops in a fluid region where concentration gradients exist between the surface and the free stream. The significance of this boundary layer is in determining the rate of convection mass transfer.

1.2 Heat Transfer

Heat transfer involves the study of energy transfer taking place between material bodies as a result of temperature difference. The different modes of heat transfer include conduction, convection and radiation.

(a) Conduction heat transfer: This is the energy transfer from the more energetic to the less energetic particles of a substance as a result of interactions between the particles.

(b) Radiation heat transfer: This is the energy emitted by matter due to changes in electron configuration of the constituent atoms or molecules. It is transported by electromagnetic waves (or alternatively photons).

(c) Convection heat transfer: If the heat transport process is affected by the flow of a fluid such that two different portions of a fluid mix then the mode of heat transfer is termed as convection. This mode of heat transfer can further be classified as free, forced or mixed convection. In free or natural convection, fluid motion is as a result of density gradients created by temperature or concentration gradients existing in the fluid mass. Forced convection fluid motion takes place due to external forces such as those from a pump or fan acting on the fluid. A special case called mixed convection arises when both free and forced convection fluid motions exist simultaneously.

1.3 Basic Definitions

1.3.1 Magnetic field: A magnetic field is the magnetic effect of electric current and magnetic materials. The magnetic field at any given point is specified by both a direction and a magnitude: such as it is represented by a vector field. The term is used for two distinct but closely related fields denoted by the symbols B and H, where H is measured in units of Amperes per meter (symbol: A/m). B is measured in Teslas (Symbol: T) and Newton per meter per ampere (symbol: N/A/m). B is almost commonly define in terms of Lorentz force it exerts on moving electric charges.

1.3.2 Magnetic Field Intensity (**H):** Magnetic field intensity at a point is the number of magnetic lines of force crossing per unit area around that point, the area being held

perpendicular to the direction of lines of force. In SI system, the unit of magnetic intensity is Ampere per metre (symbol: A/m).

1.3.3 Magnetic Induction (B): When a magnetic material is placed in a uniform magnetising field of magnetic field strength intensity (**H**), it acquires magnetism and develops its own magnetic field due to induction. As a result of this induction, the original magnetic field is modified both inside as well as outside the magnetic material. This modified or resultant field is called magnetic induction and is measured as the number of lines of induction passing normally through unit area of the material and is denoted by **B.** It is expressed in Tesla in SI units. Thus total number of magnetic lines crossing per unit area normally through a magnetic substance is called magnetic induction.

1.3.4 Intensity of Magnetization (**M**): It is a measure of the extent to which a substance gets magnetized. Intensity of magnetization **M** of a magnetic substance is defined as its magnetic moment per unit volume, the specimen being so small that its magnetization can be supposed to be uniform. In SI system, the unit of intensity of magnetization is Weber/metre^2.

1.3.5 Magnetic Susceptibility (χ): It measures the ease with which a specimen takes magnetism. Magnetic susceptibility of a magnetic substance is defined as the ratio of the intensity of magnetization **M** induced in the substance to the strength of magnetizing field **H** in which the substance is placed. Mathematically, $\chi = M / H$

Susceptibility is zero for air, is positive in case of paramagnetism, ferromagnetism and negative in case of diamagnetism. As it is the ratio of same quantities, so it has no units.

1.3.6 Magnetic Permeability (μ_0): It measures the degree to which the specimen can be penetrated. The magnetic permeability of a material is defined as the ratio of magnetic induction **B** to the strength of magnetization **H**. Mathematically, $\mu_0 = B / H$.

Units: In SI system, the unit μ_0 is henry/metre. For free space, permeability is $4\pi \times 10^{-7}$ henry/metre.

1.4 Curie Temperature

In physics and materials science, the Curie temperature (T_c) is the temperature at which certain materials loses their permanent magnetic properties, to be replaced by induced magnetism. The Curie temperature is named after Pierre Curie, who showed that magnetism was lost at a critical temperature The force of magnetism is determined by the magnetic moment, a dipole moment within an atom which originates from the angular momentum

and spin of electrons. Materials have different structures of intrinsic magnetic moments that depend on temperature; the Curie temperature is the critical point at which a material's intrinsic magnetic moments change direction.

Permanent magnetism is caused by the alignment of magnetic moments and induced magnetism is created when disordered magnetic moments are forced to align in an applied magnetic field (Fan (1987)). For example, the ordered magnetic moments (ferromagnetic, Figure 1) change and become disordered (paramagnetic, Figure 2) at the Curie temperature. Higher temperatures make magnets weaker, as spontaneous magnetism only occurs below the Curie temperature. Magnetic susceptibility above the Curie temperature can be calculated from the Curie–Weiss law, which is derived from Curie's law (Jullian and Guinier (1989)).

In analogy to ferromagnetic and paramagnetic materials, the Curie temperature can also be used to describe the phase transition between ferroelectricity and Para electricity. In this context, the order parameter is the electric polarization that goes from a finite value to zero when the temperature is increased above Curie temperature.

Below T_c		**Above** T_c
Ferromagnetic	↔	Paramagnetic
Ferrimagnetic	↔	Paramagnetic
Antiferromagnetic	↔	Paramagnetic

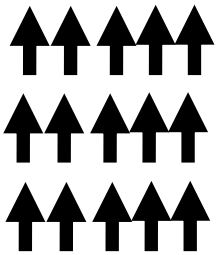

Figure 1.2

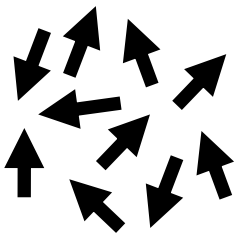

Figure 1.3(a)

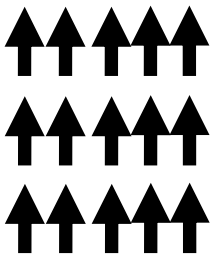

Figure 1.3(b)

Figure 1.2. Below the Curie temperature, neighbouring magnetic spins align parallel to each other in ferromagnet in the absence of an applied magnetic field.

Figure 1.3. Above the Curie temperature, the magnetic spins are (a) disordered in the absence of an applied magnetic field and (b) ordered in the presence of an applied magnetic field.

Ferromagnetic, paramagnetic, ferrimagnetic and antiferromagnetic materials have different intrinsic magnetic moment structures (Harald and Hans (2009), (Robert (1968)). At

a material's specific Curie temperature, these properties change. The transition from antiferromagnetic to paramagnetic (or vice versa) occurs at the Néel temperature, which is analogous to Curie temperature.

1.5 Stretching Sheet/Surface

The analysis of the magnetohydrodynamic (MHD) flow field of an electrically conducting fluid in a boundary-layer due to the stretching sheet/surface is an important part in fluid dynamics and heat transfer in the recent years due to the extensive engineering applications as well as bioengineering applications, such as the cooling of metallic plates in a cooling bath, the aerodynamic extrusion of plastic sheets, polymer sheet extruded continuously from a dye and heat-treated materials that travel between feed and wind-up rolls or on a conveyer belt possesses the characteristics of a moving continuous surfaces.

Blood flows in the whole body through capillaries, arties and veins. Capillaries carry the blood through skin and muscles and arteries carry the blood away from the heart where veins carry the blood towards the heart. Also we know skins, muscles, arteries and veins are stretched continuously and we say skin and muscles as a stretching/shrinking surface whereas artery and vein as a stretching/shrinking cylinder. That's why blood flow is applicable in stretching/shrinking surfaces.

The assumption of steady flow in many physical situations offers a serious limitation because in some situations such as sudden stretching of the sheet or due to sudden change in temperature of the sheet, the flow becomes unsteady. Thus, it becomes necessary to consider time variation of velocity, temperature and physical quantities of ow. In such situations, the flow behavior as well as the heat transfer rate vary with time, depending upon the associated engineering and industrial processes. Unsteady fluid flow hinges upon time dependent flow properties: velocity, pressure, temperature etc. This type of fluid flow can be observed in human body due to much impulsive body movement, vibration, unintentional abrupt body acceleration while riding any vehicle or in various kinds of physical competition.

Non-linearity arises in different biomagnetic fluid flow under various circumstances. Such as if the blood flow in human body encounters stenosis arteries, and then the flow can be assumed as a non-linear one. The concern of this study is the non-linear flow.

Some of the significant research work based on biomagnetic fluid published in different journals. Haik et al. (1996) first developed biomagnetic model. As far as the BFD flow over a stretching sheet is concerned the first work has been carried out by Tzirtzilakis and Kafoussias (2003) which was the study of a biomagnetic fluid flow over a stretching sheet

with nonlinear temperature-dependent magnetization. Moreover, Tzirtzilakis and Tanoudis (2003) have presented a numerical method for the study of laminar incompressible two-dimensional biofluid over a stretching sheet with heat transfer. Flows of biomagnetic viscoelastic fluids in different situations were investigated theoretically by Misra and Shit (2009a, 2009b). These studies reveal that the presence of external magnetic field bears the potential of influencing the flow behaviour of biomagnetic viscoelastic fluids quite appreciably. Several problems of flow and heat transfer on sheets/channels under the action of external magnetic/electric fields that have applications to physiological fluid dynamics have been treated mathematically among others (Misra and Sinha (2013), Sinha and Misra (2014), Misra and Chandra (2013), Misra and Adhikary (2016, 2017), Misra et al. (2015, 2017, 2018)).

1.6 Magnetohydrodynamics (MHD)

Magnetohydrodynamics (MHD) is the academic discipline concerned with the dynamics of electrically conducting fluids in the present of a magnetic field. On another way, Magnetohydrodynamics (MHD) is the branch of physics that's deals with the motion of electrically conducting fluids in the presence of magnetic field, especially where currents established in the matter of induction modify the field (Jackson (1998), Griffiths (1999)). The field of MHD was initiated by the Swedish Physicist Hannes Alfven, who received the Nobel Prize in Physics in 1970 for fundamental work and discovered in Magnetohydrodynamics with fruitful applications in different parts of plasma physics by Cambel (1963).

First historically documented MHD experiment was performed by Michael Faraday in 1832. He carried out experiments with the flow of mercury in glass tubes placed between poles of a magnet, and discovered that a voltage was induced across the tube due to the motion of mercury across the magnetic fields, perpendicular to the direction of flow and to the magnetic field. He observed that the current generated by this induced voltage interacted with the magnetic field to slow down the motion of the fluid, and this current produced its own magnetic field, and that obeyed Ampere's right hand law and thus, in turn distorted the magnetic field.

Alfven (1942) discovered the MHD waves in the sun. These wave are produce by disturbances which propagate simultaneously in the conducting fluid and the magnetic field. The current trend for the application of magneto fluid dynamics is toward a strong magnetic field and towards a low density of the gas.

The motion of the conducting fluid moved across the magnetic field, there arises an interaction between the flow field and the magnetic field by Davidson (2001). The magnetic field exerts a force on the fluid due to induced currents and these induce currents creates forces on the fluid and also modify the original magnetic field. The action of magnetic field on these currents give rise to mechanical forces, which modify the fluid. MHD covers those phenomena, where, in an electrically conducting fluid, the velocity field **V** and magnetic field **B** are coupled, which arises partially as a result of the Ampere laws and Faraday laws, and partially because of the Lorentz force experience by a current carrying body. This situation can comfortably be described splitting the process into three parts

(i) According to the Faraday laws the electromagnetic force $V \times B$ produced due to the movement of a conducting fluid and a magnetic field. In general, electrical currents will ensue, the current density being of order $\sigma(V \times B, \sigma)$ being the electrical conductivity.

(ii) These induced currents must, according to Ampere's law, give rise to a second magnetic field. This adds to the original magnetic field and the change is such that the fluid appears to 'drag' the magnetic field lines along with it.

(iii) The magnetic field (imposed and induced) interacts with the induced electric currents density **J** in the moving conducted fluid, to give rise to a Lorentz force $J \times B$. This acts on the conductor and is generally directed so as to inhibit the relative movement of the magnetic field and the fluid.

(iv) The electrical field, which may be characterized by E is of the same order of magnitude as the induced electric field. For electromagnetic problems, an equation, namely the law of conduction is added to the Maxwell's equation. This equation is known as Ohm's law, and is given by $J = \sigma(E + u \times B)$

The coupling requires the study of the fluid and the electromagnetic problems, making MHD a couple, complex and interdisciplinary problem. The set of equations which describes MHD flows, the equation involves are Navier-Stokes equations of fluid dynamics and Maxwell’s equation of electromagnetism through Ohm’s law.

The most widespread application of MHD in engineering is the use of electromagnetic stirring. Here the liquid metal, which is to be stirred, is placed in a rotating magnetic field. The resulting effect is an induction motor. This is regularly used in casting operation to homogenize the liquid zone of a partial ingot. In another casting operations, magnetic fields

are used to dampen the motion of liquid metal. Since the magnetic field is static here, so, it can convert kinetic energy into heat via Joule dissipation. The magnetic levitation or confinement relies on the fact that a high-frequency induction coil repels conducting material by inducing opposite currents in any adjacent conductor. MHD is also important in electrolysis, particularly in those electrolysis cells used to reduce aluminium oxide to aluminium. This process is highly energy intensive. This is due to the fact that electrolyte is high electrical resisting. For example, in the USA, around 3% of all generated electricity is used for aluminium production. There are many other applications of MHD in engineering and metallurgical industry by Cramer and Pai (1973). Theses includes electromagnetic casting of aluminium, vacuum-arc remelting of titanium and nickel-based super alloys, electromagnetic removal of non-metallic inclusions from melts, electromagnetic launchers and the so-called 'cold-crucible' induction melting process in which the melt is protected from the crucible walls by a thin solid crust of its own material. This latter technology is currently finding favour in the nuclear waste. MHD is using in military arena as a propulsion mechanism for submarine. All in all, it would seem that MHD has now found a substantial and permanent place in the world of material processing. MHD principles are using in medical sciences, particularly for the treatment of those diseases, which are related with the blood flow. Hence Biomathematics is the branch of science in which MHD principles would be used for the days to come by Murray (1993), Anderson et al. (1999), Misra (2006).

1.7 Ferrohydrodynamics (FHD)

Ferrohydrodynamics (FHD) is the mechanics of fluid motion influenced by strong forces of magnetic polarization and in this branch. The importance of Ferro hydrodynamics (FHD) was realized, because of large potential application in various fields. We study the interaction of magnetic fields with non-conducting ferromagnetic fluids. Many physicists and engineers gave great contributions (theoretical and experimental) to Ferrohydrodynamics and its applications.

Ferrofluids were first discovered at National Aeronautics and Space Administration (NASA) Research Center in mid 1960‟s. The scientists at NASA found that they could make to flow this amazing ferrofluid by varying the external magnetic field. After the discovery of ferrofluid, not only original publications in journals and conferences have been released, but some textbooks like “Ferrohydrodynamics” by Rosensweig (1985), “Magnetic Fluids: Engineering Applications” by Berkovsky et al. (1993), “Magnetic Fluids and Applications

Handbook" by Berkovsky and Bastovoy (1996), "Magnetic Fluids" by Blums et al. (1997), "Magnetoviscous Effects in Ferrofluids" by Odenbach (2002) etc. also have been published in this area to supplement the basis for its engineering applications.

These fluids have variety of applications in the field of sciences and engineering like instrumentation, electrical and electronics engineering etc. which are being commercialized. Ferrofluids are widely used in sealing of computer hard disk drives, rotating X-ray tubes, rotating shafts, rods and sink-float systems for separation of materials. These are used as lubricants in bearing and dumpers. They are also used as heat controller in electric motors and hi-fi speaker systems without the need of change in their geometrical shape (Hathaway 1979). Ferrofluids are being greatly used in many magnetic fluid based scientific devices like sensors, densimeters, accelerometer, pressure transducers etc. and are also used in actuating machines like electromechanical converters, energy converters etc.(Raj and Moskowitz 1990). One special application of ferrofluids is their use as magnetic ink for high-speed, inexpensive and silent printers (Maruno et al. 1983).

They are also found to be very useful in the field of biomedicine due to magnetically targeted drug delivery (anti-cancer agents such as radio-nuclides, cancer specific antibodies, genes etc.) (Ruuge and Rusetski 1999) to a certain area of human body, targeted destruction of tumors, in-vivo monitoring of chemical activity in the brain and toxin removal from the body for cancer treatment (Goodwin et al. 1999, Pulfer and Gallo 2000, Kim et al. 2001). Due to its viscous action, in a non-uniform magnetic field, a drop of magnetic fluid can move as a whole fluid body. Magnetic nanoparticles can reach even the smallest capillaries of the body, which are 5-6 μm in diameter. Magnetic fluids are also used in the contrast medium in X-ray examinations (Papisov et al. 1993) and for positioning tamponade for retinal detachment repair in eye surgery (Dailey et al. 1999). A potential application of ferrofluids is found in the subsurface environmental engineering, in which externally applied magnetic fields are used to direct and control the flow of ferrofluids.

1.8 Force due to magnetic field

In this study, we considered when blood flow under the influence of a magnetic field, two major force will act upon it. The first one is magnetization force due to the tendency of the RBC (erythrocyte) to orient with magnetic field, and second one is Lorentz force arising from electric current which generate the moving ions in the plasma. In the presence of an external magnetic field, the ferromagnetic colloidal particles suspended in the carrier liquid of

a ferrofluid become magnetized and produce attractive forces on each particle that produce a body force on the liquid. The magnetic (Kelvin) force F on ferrofluid per unit volume is given by $F = (M \bullet \nabla)B = \mu_0 (M \bullet \nabla)H$ where μ_0 is magnetic permeability of free space, M is magnetization, ***H*** is magnetic field strength of the external magnetic field. The body force in FHD is due to polarization force.

The expression for the electromagnetic forces:

$F = J \times B$, where, current density $J = \sigma(V \times B)$

The magnetic (Kelvin) force F on ferrofluid per unit volume is

$$F = (M \bullet \nabla)B = \mu_0 (M \bullet \nabla)H = \mu_0 \frac{M}{H}(H \bullet \nabla)H$$

$$= \mu_0 \frac{M}{H}\left(\frac{1}{2}\nabla(H \bullet H) - H \times (\nabla \times H)\right)$$

$$= \mu_0 \frac{M}{H}\frac{1}{2}\nabla H^2 - \mu_0 \frac{M}{H}(H \times J), \text{ where induce current } J = \nabla \times H$$

$$= \mu_0 M \nabla H - \frac{M}{H}(B \times J), \quad B = \mu_0 H$$

$$= \mu_0 M \nabla H + \frac{M}{H}(J \times B)$$

Thus the magnetization force along with Lorentz force is

$$= \mu_0 M \nabla H + \frac{M}{H}(J \times B) + (J \times B)$$

$$= \mu_0 M \nabla H + \left(\frac{M}{H} + 1\right)(J \times B)$$

For strong magnetic field $H >> M$ thus $\frac{M}{H} << 1$ and the total force due to impose magnetic field is finally by Tzirtzilakis (2005)

$$\mu_0 M \nabla H + (J \times B)$$

1.9 Biomagnetic Fluid Dynamics

Biomagnetic fluid dynamics (BFD) has emerged as a new area of research in the study of a certain class of biological/physiological problems from fluid mechanics under the action of a magnetic fluid. Biomagnetic fluid is a fluid that exists in a leaving creature and its flow is influenced by the present of a magnetic field. In this thesis, we adopts the biomagnetic fluid model in representing the blood flow. Blood is one of the fluid that has characteristic of biomagnetic fluid and is considered a magnetic fluid. The characteristics of blood which indicate the nature of a magnetic fluid due to the complex interaction of the cell membrane, intercellular protein and the hemoglobin molecule which is a form of iron oxides that exist at a uniquely high concentration in the mature red blood cells. Blood has been recorded to have different magnetic susceptibility values depending on its oxygenation state. Deoxygenated blood, such as that which travels in veins towards the heart, behaves as a paramagnetic solution and has a magnetic susceptibility of 3.5×10^{-6}. Oxygenated blood, which is found in arteries and is pumped from the heart, has diamagnetic properties, with a magnetic susceptibility of 6.67×10^{-7}. The BFD flow studies have been attracted many researchers in recent years due to its wide range of applications in bioengineering and medical sciences.

Biomagnetic fluid mechanics is the study of a certain class of biological problems from fluid mechanics point of view. For an organism, biomechanics helps us to understand its normal function, predict changes due to alteration, and propose methods of artificial intervention. Thus diagnosis, surgery, and prosthesis are closely associated with biomechanics. Different mathematical models, using the principle of fluid mechanics have been developed with a view to understand the complex phenomena associated with the dynamics of blood flow. These mathematical models are currently being used for diagnosis of various arterial diseases, appraisal of newly found treatment procedures like drug delivery, developing and designing various artificial organs, Kleinstreure (2006), Goyal (2013), Schneck (2013).

1.10 Applications of Biomagnetic Fluid

This study will have an important due to to its wide range of applications in biomedical engineering sciences, in particular, it is directed towards finding and developing the solutions to some of the human body related diseases and disorders such as designing artificial organs, creating nan-robots for surgery and developing advanced imaging and signal processing techniques for cancer, tumor, magnetic drug targeting, accelerating blood flow, measuring blood flow and other life threating diseases. These research works can have a direct real

world impact such as in the field of medical imaging based diagnostics (MRI, CT scan, ultrasound etc.) will possess the expertise to work with medical practitioners on interpreting clinical data. It has also important applications in the development ofmagnetic devices for cell separation, targeted transport of magnetic particles as drug carriers, cancer tumor treatment causing magnetic hyperthermia, provocation of occlusion of the feeding vessels of cancer tumors and the development of magnetic tracers. So study of blood flow is very important not only for understanding of blood flow characteristics through the arteries but also for taking prevention measures or curing many diseases which occurs in the blood vessels.

1.10.1 Nanotechnology and drug delivery

Nanotechnology has applications in several areas which include drug delivery, tissue engineering, biosensors, microfluidic, microarrays and bioengineering. The nano technology based drug delivery system has emerged as mainstream research in advance medical diagnosis and treatment. Corporate investment on nanotechnology for drug delivery diagnostic increased year by year nanotechnology based drug delivery has already been commercialized by many reputed companies (Safari and Zarnegar (2014)). Nanotechnology based drug delivery has many advantages and provides the insight for solving problems associated with conventional drug delivery systems. It has control over delivery of drugs to specific sites and to certain cells only, without affecting neighbouring normal cells. Different types of carrier particles are used in the targeting of nanotechnology based drug delivery systems, some of them are PH-sensitive carrier, thermally responsive carrier, ultrasound-medicated drug delivery and targeting.

1.10.2 Magnetic drug targeting

Magnetic targeting is one of the major drug delivery methods which are used for treatment in different parts of our circulatory system. The therapy is very fruitful because it helps in the development of functional magnetic nanoparticles that are designed to target a specified tissue and it also reduces side effects. Magnetic carrier particles with surface bound drug molecules are injected into the vascular system upstream from the malignant tissue, are capture at the tumor via a local applied magnetic field. Upon achieving a sufficient concentration, the drug molecules are released from the carrier by changing many physiological conditions such as pH, temperature or different enzymatic activity, which help in realising a drug molecules from the carrier particles. Sometimes higher dosage can be

applied for more effective treatment as the therapeutic agents are localized to regions of diseases tissue (Speziale, 2008).

1.10.3 Magnetic resonance imaging (MRI)

Magnetic resonance imaging (MRI) is a medical imaging technique used in radiology to form pictures of the anatomy and physiological processes of the specific part of the body in both health and diseases. The major components of an MRI required a magnetic field which is both strong and uniform, magnetic field gradients and radio waves to generate images of the organs of the body. The field strength of magnetic field is measured in tesla and while the majority of systems operate at 1.5 T, commercial system are available between 0.2T and 7 T. Most clinical magnets are superconducting magnets, which required liquid helium. . Lower field strengths can be achieved with permanent magnets, which are often used in "open" MRI scanners for claustrophobic patients (Sassaki (1990)). MRI has a wide range of applications in medical diagnosis and more than 25,000 scanners are estimated to be in use worldwide (Kolka et al. (2013)). MRI affects diagnosis and treatment in many specialties although the effect on improved health outcomes is uncertain (Hollingworth et al. (2000)).

1.10.4 Magnetic hyperthermia in cancer therapy

Magnetic hyperthermia is a term used to describe the generation of heat by magnetic particles in response to the application of an external magnetic field. It is one of the many possible applications of biomagnetic fluid in the treatment of cancer and infectious diseases. Tumour vasculature has been shown to possess distinctive anatomical and biochemical characteristics arising from a lack of adequate perfusion leading to the generation of hypoxia and acidosis rending cancerous cells thermally sensitive (Baillie, et al.(1995), Fenton et al., (1999)). Tumour growth can be halted by heating cells to 40°C for 30 min or more; however, it is difficult to raise whole body temperature without also promoting adverse biochemical side effects. In 2010, Balivada et al. demonstrated the production of a localized thermo-ablative effect that did not induce systemic hyperthermia in vivo. Here, the researchers reported an increase of 11°C–12°C in C57/BL6 mice mediated by the accumulation and subsequent activation of MNPs. In addition, Balivada et al. (2010) demonstrated that as the iron concentration of the magnetic nanocomposites increased from 5 μg/ml to 25 μg/ml, the number of viable tumour cells decreased from approximately 480 000 to 150 000 indicating the increase in iron concentration had an in vivo cytolytic action. Yanase et al. (1998) suggest

that the used of magnetic hyperthermia in the treatment of cancers may be more technically demanding.

1.11 Governing Equations

The physical aspects of any fluid are governed by three fundamental principles, i.e., conservation of (i) mass, (ii) momentum and (iii) energy. These fundamental physical principles can be expressed in terms of basic mathematical equations known as equation of continuity, equations of momentum or motion and equation of energy respectively.

The continuity equation for a viscous compressible electrically conducting fluid in vector form is

$$\frac{\partial \rho}{\partial t} + \nabla \bullet (\rho q) = 0$$

Where ρ is the density of the fluid; $q = (u, v, w)$ is the fluid velocity vector in three dimensional Cartesian coordinates system and u, v and w are x, y and z component of flow velocity respectively.

For incompressible fluid ($\rho =$ constant) the equation yields

$$\nabla \bullet q = 0$$

i.e. $$\frac{\partial u}{\partial x} + \frac{\partial v}{\partial y} + \frac{\partial w}{\partial z} = 0$$

The momentum equations for viscous incompressible fluid in vector form are:

$$\frac{\partial q}{\partial t} + (q \bullet \nabla) q = F - \frac{1}{\rho} \nabla P + \nu \nabla^2 q$$

Where F the body force per unit mass, P is the fluid pressure, ν is the kinematic viscosity.

when a fluid flow under the influence of a magnetic field, two major force will act upon it. The first one is magnetization force due to the tendency of the RBC (erythrocyte) to orient with magnetic field, and second one is Lorentz force arising from electric current which generate the moving ions in the plasma.

$$\frac{\partial q}{\partial t} + (q \bullet \nabla) q = F - \frac{1}{\rho} \nabla P + \nu \nabla^2 q + \frac{1}{\rho} \mu_0 (M \bullet \nabla) H + \frac{1}{\rho} (J \times B)$$

H is the magnetic field strength, B is the magnetic induction, J is the current density, M is the magnetization. The term $(J \times B)$ represent the Lorentz force per unit volume and the term $\mu_0 (M \bullet \nabla) H$ represent the components of the magnetic force per unit volume.

Now $q \bullet \nabla = \left(\hat{i}u + \hat{j}u + \hat{k}w\right) \bullet \left(\hat{i}\frac{\partial}{\partial x} + \hat{j}\frac{\partial}{\partial y} + \hat{k}\frac{\partial}{\partial z}\right) = u\frac{\partial}{\partial x} + v\frac{\partial}{\partial y} + w\frac{\partial}{\partial z}$

$$(q \bullet \nabla)q = \left(u\frac{\partial}{\partial x} + v\frac{\partial}{\partial y} + w\frac{\partial}{\partial z}\right)\left(\hat{i}u + \hat{j}v + \hat{k}w\right)$$

$$= \left(u\frac{\partial u}{\partial x} + v\frac{\partial u}{\partial y} + w\frac{\partial u}{\partial z}\right)\hat{i} + \left(u\frac{\partial v}{\partial x} + v\frac{\partial v}{\partial y} + w\frac{\partial v}{\partial z}\right)\hat{j} + \left(u\frac{\partial w}{\partial x} + v\frac{\partial w}{\partial y} + w\frac{\partial w}{\partial z}\right)\hat{k}$$

$$\nabla P = \left(\hat{i}\frac{\partial P}{\partial x} + \hat{j}\frac{\partial P}{\partial y} + \hat{k}\frac{\partial P}{\partial z}\right)$$

$$\nabla^2 q = \left(\frac{\partial^2}{\partial x^2} + \frac{\partial^2}{\partial y^2} + \frac{\partial^2}{\partial z^2}\right)\left(\hat{i}u + \hat{j}u + \hat{k}w\right)$$

$$= \left(\frac{\partial^2 u}{\partial x^2} + \frac{\partial^2 u}{\partial y^2} + \frac{\partial^2 u}{\partial z^2}\right)\hat{i} + \left(\frac{\partial^2 v}{\partial x^2} + \frac{\partial^2 v}{\partial y^2} + \frac{\partial^2 v}{\partial z^2}\right)\hat{j} + \left(\frac{\partial^2 w}{\partial x^2} + \frac{\partial^2 w}{\partial y^2} + \frac{\partial^2 w}{\partial z^2}\right)\hat{k}$$

From the Maxwell equation we have

$$\nabla \bullet B = 0$$

Which gives $\frac{\partial B}{\partial y} = 0$

i.e. $B_y = \text{constant} = B_0$

thus $B = (0, B_0, 0)$.

In MHD phenomenon the current density (J) is composed of two terms: external electric field (E) and induced current field $(u \times B)$. In this study there is no external electric field; therefore, the current density equation is as follows from the MHD generalized Ohm's law we have

$$J = \sigma(q \times B) = \sigma \begin{vmatrix} \hat{i} & \hat{j} & \hat{k} \\ u & 0 & 0 \\ 0 & B_0 & 0 \end{vmatrix} = \sigma B_0 u \hat{k}$$

Hence $J = (0,\ 0,\ \sigma B_0 u)$ and where σ is the conductivity of the material.

Now from Lorentz's force, we have

$$J \times B = \sigma \begin{vmatrix} \hat{i} & \hat{j} & \hat{k} \\ 0 & 0 & \sigma B_0 u \\ 0 & B_0 & 0 \end{vmatrix} = -\sigma B_0^2 u \hat{i}$$

Therefore, the x component of Lorentz's force is $(J \times B)_x = -\sigma B_0^2 u$

Therefore, the x momentum equation is

$$\frac{\partial u}{\partial t}+u\frac{\partial u}{\partial x}+v\frac{\partial u}{\partial y}+w\frac{\partial u}{\partial z}=-\frac{1}{\rho}\frac{\partial P}{\partial x}+\nu\left(\frac{\partial^2 u}{\partial x^2}+\frac{\partial^2 u}{\partial y^2}+\frac{\partial^2 u}{\partial z^2}\right)+\mu_0 M\frac{\partial H}{\partial x}-\frac{1}{\rho}\sigma B_0^2 u$$

Energy equation.

In the mathematical model, the energy equation containing the temperature T of the fluid. This equation can be written as

$$\rho c_p\left(\frac{DT}{Dt}\right)+\mu_o T\frac{\partial M}{\partial T}(q\bullet\nabla)H-\frac{J\bullet J}{\sigma}=K\nabla^2 T$$

where $\frac{D}{Dt}=\frac{\partial}{\partial t}+q\bullet\nabla$, ρ is the density of the fluid; $q=(u,v,w)$ is the fluid velocity vector in three dimensional Cartesian coordinates system and u, v and w are x, y and z component of flow velocity respectively. The term $\mu_o T\frac{\partial M}{\partial T}(q\bullet\nabla)H$ is a magneto caloric effect and represent the thermal power per unit volume. This term arises due to the FHD, whereas the term $\frac{J\bullet J}{\sigma}$ represent magnetohydrodynamic effect and known as joule heating and arises due to the MHD.

Now $q\bullet\nabla=\left(\hat{i}u+\hat{j}u+\hat{k}w\right)\bullet\left(\hat{i}\frac{\partial}{\partial x}+\hat{j}\frac{\partial}{\partial y}+\hat{k}\frac{\partial}{\partial z}\right)=u\frac{\partial}{\partial x}+v\frac{\partial}{\partial y}+w\frac{\partial}{\partial z}$

$$(q\bullet\nabla)T=\left(u\frac{\partial}{\partial x}+v\frac{\partial}{\partial y}+w\frac{\partial}{\partial z}\right)T=u\frac{\partial T}{\partial x}+v\frac{\partial T}{\partial y}+w\frac{\partial T}{\partial z}$$

$$(q\bullet\nabla)H=\left(u\frac{\partial}{\partial x}+v\frac{\partial}{\partial y}+w\frac{\partial}{\partial z}\right)H=u\frac{\partial H}{\partial x}+v\frac{\partial H}{\partial y}+w\frac{\partial H}{\partial z}$$

$$J=\sigma(q\times B)=\sigma\begin{vmatrix}\hat{i}&\hat{j}&\hat{k}\\u&0&0\\0&B_0&0\end{vmatrix}=\sigma B_0 u\hat{k}$$

$$J\bullet J=\sigma B_0 u\hat{k}\bullet\sigma B_0 u\hat{k}=\sigma^2 B_0^2 u^2$$

$$\nabla^2 T=\left(\frac{\partial^2}{\partial x^2}+\frac{\partial^2}{\partial y^2}+\frac{\partial^2}{\partial z^2}\right)T=\left(\frac{\partial^2 T}{\partial x^2}+\frac{\partial^2 T}{\partial y^2}+\frac{\partial^2 T}{\partial z^2}\right)$$

Therefore, the energy equation is

$$\rho c_p\left(\frac{\partial T}{\partial t}+u\frac{\partial T}{\partial x}+v\frac{\partial T}{\partial y}+w\frac{\partial T}{\partial z}\right)+\mu_o T\frac{\partial M}{\partial T}\left(u\frac{\partial H}{\partial x}+v\frac{\partial H}{\partial y}+w\frac{\partial H}{\partial z}\right)$$
$$-\sigma B_0^2 u^2=k\left(\frac{\partial^2 T}{\partial x^2}+\frac{\partial^2 T}{\partial y^2}+\frac{\partial^2 T}{\partial z^2}\right)$$

1.12 Lie Symmetry Analysis for Differential Equations

Here, we present some basics of Lie symmetry methods for solving differential equations, Olver (1986), Ovsiannikov (1982), Bluman and Kumei (1991).

1.12.1 Symmetry transformations of differential equations

A transformation under which a differential equation remains invariant (unchanged) is called a symmetry transformation of the differential equation.

Consider a kth order $(k \geq 1)$ system of differential equations

$$F^{\alpha}(x, u, u_{(1)}, ..., u_{(k)}) = 0; \ \alpha = 1, ..., m \tag{1.1}$$

where $u = (u^1, ..., u^m)$ called the dependent variable, is a function of the independent variable $x = (x^1, ..., x^n)$ and $u_{(1)}, u_{(2)}$ upto $u_{(k)}$ are the collection of all first, second, up to kth - order derivatives of u.

A transformation of the variable x and u, viz.

$$\bar{x}^i = f^i(x, u), \ \bar{u}^{\alpha} = g^{\alpha}(x, u), \ \ i = 1, ..., n; \ \ \alpha = 1, ..., m. \tag{1.2}$$

is called a symmetry transformation of the system (1.1) if (1.1) is form-invariant in the new variables $\bar{x}$ and $\bar{u}$, that is

$$F^{\alpha}(\bar{x}, \bar{u}, \bar{u}_{(1)}, ..., \bar{u}_{(k)}) = 0; \ \alpha = 1, ..., m \tag{1.3}$$

whenever

$$F^{\alpha}(x, u, u_{(1)}, ..., u_{(k)}) = 0; \ \alpha = 1, ..., m \tag{1.4}$$

1.12.2 Lie symmetry method for partial differential equations

Here we discuss the classical Lie symmetry method to obtain all possible symmetries of a system of partial differential equations.

Let us consider a p-th order system of partial differential equations in n independent variables $x = (x^1, ..., x^n)$ and m dependent variable $u = (u^1, ..., u^m)$, viz.

$$E(x, u, u_{(1)}, ..., u_{(p)}) = 0; \tag{1.5}$$

where $u_{(k)}$, $1 \leq k \leq p$ denotes the set of all kth order derivative of u; with respect to the independent variables defined by

$$u^{\alpha}_{(k)} = \frac{\partial^k u}{\partial x_{i1}, ..., \partial x_{ik}} \tag{1.6}$$

With $1 \le i_1, i_2, ..., i_k \le n$ (1.7)

For finding the symmetries of Eq. (1.5), we first construct the group of invertible transformations depending on the real parameter a; that leaves Eq. (1.5) invariant, namely

$$\bar{x}_1 = f^1(x,u,a),\ ...,\bar{x}_n = f^n(x,u,a),\ \ \bar{u}^\alpha = g^\alpha(x,u,a)\,. \tag{1.8}$$

The above transformations have the closure property, are associative, admit inverses and identity transformation and are said to form a one-parameter group.

Since a is a small parameter, the transformations (1.8) can be expanded in terms of a series expansion as

$$\bar{x}_1 = \bar{x} + a\xi_1(x,u) + O(a^2), ..., \bar{x}_n = \bar{x} + a\xi_n(x,u) + O(a^2)$$

$$\bar{u}_1 = \bar{u} + a\xi_1(x,u) + O(a^2), ..., \bar{u}_n = \bar{u} + a\xi_n(x,u) + O(a^2) \tag{1.9}$$

The transformations (2.32) are the infinitesimal transformations and the finite transformations are found by solving the Lie equations

$$\xi_1(\bar{x},\bar{u}) = \frac{d\bar{x}_1}{da}, ..., \xi_n(\bar{x},\bar{u}) = \frac{d\bar{x}_n}{da},\ \eta(\bar{x},\bar{u}) = \frac{d\bar{u}}{da} \tag{1.10}$$

with the initial conditions

$$\bar{x}_1(\bar{x},\bar{u},a)\big|_{a=0} = x_1, ...,\ \bar{x}_n(\bar{x},\bar{u},a)\big|_{a=0} = x_n$$

$$\bar{u}_1(\bar{x},\bar{u},a)\big|_{a=0} = u_1, ...,\ \bar{u}_n(\bar{x},\bar{u},a)\big|_{a=0} = u_m \tag{1.11}$$

Where $\bar{x} = (\bar{x}^1, ..., \bar{x}^n)$ and $\bar{u} = (\bar{u}^1, ..., \bar{u}^n)$

1.13 Survey of Literature

Biofluid dynamics may be considered as the discipline of biological engineering or biomedical engineering in which the fundamental principles of fluid dynamics are used to explain the mechanisms of biological flows and their interrelationships with physiological processes, in health and in diseases/disorder. It can be considered as the conjuncture of mechanical engineering and biological engineering. It spans from cells to organs, covering aspects of functionality of systemic physiology, including cardiovascular, reproductive, urinary, musculoskeletal and neurological system etc. Biofluid dynamics and its simulations through computational fluid dynamics (CFD) apply to both internal and external flows. Internal flow such as cardiovascular blood flow and respiratory airflow and external flow such as flying and aquatic locomotion. Biological fluid dynamics involves the study of the motion of biological fluids. It can be either circulatory system or respiratory system. The

study of biofluid dynamics is also directed towards finding solutions to some of the human body related diseases and disorders. The usefulness of the subject can can also be understood by seeing the use of biofluid dynamics in the areas of physiology in order to explain how living thing work and about their motions, in developing an understanding of the origins and development of various diseases related to human body and diagnosing them, in finding the cure for the diseases related to cardiovascular and pulmonary system. Observations also derived from related investigation are useful in the design and development of magnetic devices for cell separation, reduction of blood flow during surgery, targeted transport of drugs through the use of magnetic particles as drug carriers, magnetic resonance imaging (MRI) of specific parts of the human body, electromagnetic hyperthermia in cancer treatment etc., as mentioned in earlier communications

Heat is continuously generated in the human body by metabolic processes and exchanged with the environment and among internal organ through a complex combination of conduction, convection, evaporation and radiation. Transport of heat by the circulatory system makes heat transfer in the body. Heat transfer in biological systems is relevant in many diagnostic and therapeutic applications that involve changes in temperature. As we know, the cardiovascular system is sensitive to change in the environment, and flow characteristics of blood are modified to satisfy changing demands of the orgasm. In addition to transporting of oxygen, metabolites and other dissolved substance to and from the tissue, blood flow alter heat transfer within the body.

Heat transfer of blood flow is an important subject of research, because it has got significant applications in biomedical engineering and several medical treatment, particularly in thermal therapeutic procedures. It is also used in the treatment of muscle pumps, myalgia (muscle pain), chronic wide-spreed pain (in medical term, fibromyalgia), permanent shortening of muscle (medically called as contracture) and also used in the treatment of bursitis, that is, inflammation of the fluid-filled sac that lies between tendon and bone, or between tendon and skin. Several experimental investigations have been carried out by some researchers (Kobu (1999), Nishimoto et al. (2006)) to examine the effects of infrared radiation on blood flow. The effect of radiative heat transfer on blood flow in a stenosis artery was studied by Prakash and Makinde (2011). He et al. (2006) discussed the effect of temperature on blood flow in human breast tumor under laser irradiation. While flowing through the arterial tree, blood carries a large quantity of heat to different parts of the body. On the skin surface, the transfer of heat can take place by any of the four processes: radiation, evaporation, conduction and convection. It is known that in the case of radiative heat transfer,

energy is transferred through space by means of electromagnetic wave propagation. There are several determinants for the quantity of heat that blood can carry with it, namely, (1) heat transfer coefficient of blood, (2) density of blood, (3) velocity of blood flow, (4) radius of the artery and (5) temperature of the tissues that surround the artery. Out of these, since Reynolds number is related to the velocity and density of blood as well as the arterial radius, the quantity of heat carried by blood can be regarded as dependent only on Reynolds number and heat transfer coefficient of blood, and the temperature of the tissues surrounding the artery.

The effect of a magnetic field on blood flow has been analyzed theoretically. Chen (1985) treating blood as an electrically conducting fluid. Tzirtzilakis and Tanoudis (2003) studied the biomagnetic fluid flow over a stretching sheet. Pulsed magnetic fields have been used to treat various conditions, such as soft-tissue injury by Wilson (1974), chronic pelvic pain by Varcaccio et al. (1995). Keeping all these in mind, presence of an external magnetic field has been paid due consideration in the present study.

Two major functions that blood performs while flowing in the circulatory system are to carry nutrients and to supply heat to body tissues. The exchange of materials mainly takes place at the capillary level. However, there exists evidence to support that materials are also transported across the permeable walls of arteries (and veins) by Caro et al. (1978). The transport of water across the arterial wall is of interest in the study of metabolism and pathology of an artery. The nourishment of the arterial wall depends predominantly on the transport of materials from the arterial lumen. This transport can, sometimes, cause the genesis and the progression of arterial diseases such as atherosclerosis, atherogenesis, atheroma. Oka and Murata (1970) discussed the steady flow of blood through a permeable capillary wall.

Since blood is an electrically conducting fluid, in the presence of a magnetic field, its flow exhibits magnetohydrodynamic (MHD) behaviour. Misra, et al. (1998) investigated the steady MHD flow of an electrically conducting fluid (with particular reference to blood flow in arteries) in a slowly varying channel in the presence of a uniform transverse magnetic field. Misra and Shit (2009) developed a mathematical model of the flow of a biomagnetic viscoelastic fluid over a stretching sheet. Misra et al. (2008) also investigated the flow and heat transfer of an MHD viscoelastic fluid in a channel with stretching walls. All these investigations carried out by Misra and his research group have been recognized as benchmark contributions in the field of physiological fluid dynamics.

Cardiovascular disease is now the leading global cause of death. During a heart attack, a clot forms in an artery that supplies blood to the heart and blocks blood flow to the area of

heart muscle supplied by that artery. The portion of the heart muscle deprived of blood carrying the needed oxygen begins to become damaged. This is called a "myocardial infarction," more commonly known as a heart attack. The amount of lasting damage to the heart muscle depends on a number of factors—the size of the clot, the location of the clot, and how long the clot blocks blood flow to the muscle. The longer the heart muscle is without blood and oxygen, the more extensive the damage to the muscle and the greater the size of the heart attack. There are other kinds of diseases which are concerned with narrowing of blood vessels such as peripheral artery disease, vascular diseases, atherosclerosis etc. Peripheral artery disease is a common circulatory problem in which narrowed arteries reduce blood flow to human limbs. Arteries carry oxygen-rich blood from the heart to nourish every part of the body, including the brain, kidneys, intestines, arms, legs, and heart itself. When peripheral artery disease (PAD) is developed, extremities such as legs don't receive enough blood flow to keep up with body demand. Vascular disease is an abnormal condition of the blood vessels which commonly occurs where turbulent blood flow takes place, such as when the direction of blood flow in the arteries changes abruptly. Atherosclerosis is the narrowing and / or blockage of the blood vessels that supply the heart, due to fat deposit built up in the artery walls. Hereby the inevitable usefulness of the study of blood flow in a narrow blood vessel. This study uses the extract of Biofluid Dynamics (BFD), Magnetohydrodynamics (MHD) and Ferrohydrodynamics (FHD). Biofluid Dynamics studies the fundamental principles of fluid dynamics that are used to explain the mechanisms of biological flows and their interrelationships with physiological processes, in health and in diseases. Magnetohydrodynamicsis the study of the magnetic properties of electrically conducting fluids and Ferrohydrodynamics treats the flow of strongly magnetized fluid media.

Unsteady fluid flow hinges upon time dependent flow properties: velocity, pressure, temperature etc. This type of fluid flow can be observed in human body due to much impulsive body movement, vibration, unintentional abrupt body acceleration while riding any vehicle or in various kinds of physical competition. In addition, this type of flow might occur in a cardiovascular disease: the leading global cause of death. According to the World Health Organization (WHO), an estimated 17.7 million people died from cardiovascular diseases in 2015, representing 31% of all global deaths. Of these deaths, an estimated 7.4 million were due to coronary heart disease and 6.7 million were due to stroke. A great deal of work has been carried out on biological fluids. Among them the most important and characteristic one is blood. Also some extensive amounts of works have been along with the effects of magnetic field and heat transfer.

A symmetry group of a system of differential equation is a group of transformations, which maps any solution to another solution of system. According to Lie‘s (1875) frame work such a group depends on continuous parameters and consist of either point transformation (point symmetry) acting on a systems space of independent and dependent variables, or more generally, contact transformations (contact symmetry) acting on the space including all first order derivatives of dependent variables. Elementary examples of Lie groups include translation, rotation and scaling and autonomous system of first order ordinary differential equation essentially defines one parameter Lie group of point transformation. Whereas discrete groups of point transformation, acting on the space of its dependent and independent variables that can be determine by Lie‘s algorithm. Mathematicians have studied the theory of continuous transformation of group extensively since the late of nineteenth century. First, it was Sophus Lie (1842-1899), the Russian mathematician, who has introduced the notations continuous groups, known as Lie groups, in order to unify and extend various specialized solution methods for the ordinary differential equations. Lie show then, one can reduce the order of ordinary differential equation, constructively, if the said differential equation is invariant under a one-parameter Lie group of point transformation.

Lie’s work systematically relates miscellany of topics in ordinary differential equations including integrating factor, separable equation, homogeneous equation, reduction of order of an equation, method of undetermined coefficient and the method of variation of parameter for linear equation, Euler‘s equation and the use of Laplace transform. Further Lie has also indicated that linear partial differential equation invariant under a group, so called Lie group, leads directly to superposition of solutions in terms of transformations.

In the recent past, several researchers are focused on obtaining the similarity solutions of the convective transport phenomena problems arising in fluid dynamics, aerodynamics, plasma physics, meteorology, and some branches of engineering by using different procedures. One such procedure is Lie group analysis. The concept of Lie group analysis also called symmetry analysis is developed by Sophius Lie 1976 to determine transformations which map a given differential equation to itself and it unifies almost all known exact integration techniques, Ovsiannikov (1982), Olver (1993), Bluman and Kumei (1991). Lie group analysis used to find the similarity reduction of the non-linear differential equations. In such analysis, one reduces the number of variable governing the partial differential equations. This reduction of variables changes the system of partial differential equations to self-similar system of the ordinary differential equations. Lie group analysis has been used to analyze convective phenomena under various flow configurations that arise in various branch of

science and engineering. It provides a potent, sophisticated, and systematic tool for generating the invariant solutions of the system of nonlinear partial differential equations (PDEs) with relevant initial or boundary conditions. A special form of Lie group transformations, known as the scaling group, has been suggested by various researchers to study convection flows of different flow phenomena (see Ferdows et al. (2013), Aziz et al. (2012), Prabhu et al. (2009), . Rashidi et al. (2014) etc.; they are worth observing).

1.14 Research Objectives

The main objectives of this thesis is a theoretical investigation of boundary layer flow of a biomagnetic fluid and heat transfer on a stretching/shrinking sheet in the presence of a magnetic dipole. Here we have examined the cases of (i) Hydrodynamic, (ii) Pure MHD, (iii) Pure FHD, and (iv) BFD. For all the cases, the specific aims of the study are as follows:

- To investigate the blood flow patterns considering a two/three dimensional steady/unsteady, laminar, incompressible and in the presence of magnetic dipole.
- To incorporating both magnetization and electrical conductivity into BFD model.
- To use the temperature dependent magnetization.
- To construct the mathematical and physical model.
- The problem has been treated mathematically by using Lie group transformation.
- To solve the systems of transformed equations with boundary conditions through the use of finite difference method/ bvp4c function available in FORTRAN/MATLAB software.
- To analyze the features of the dual solutions.
- To perform the stability analysis that determine which solution is stable that can be physically realistic and which is not.
- To determine the effects of the flow control parameters on fluid velocity, temperature, pressure and relative pressure distributions.
- To show the behavior of the physical quantities such as the skin friction coefficient, rate of heat transfer and relative pressure against the flow parameters.

1.15 Structure of the thesis

In the thesis, we have constructed the mathematical models for steady-unsteady, linear-nonlinear, stretching-shrinking sheet for biomagnetic fluid flow and heat transfer has been analyzed for various boundary conditions. The work contained in the thesis has adequately met the objectives outlined above. The main body of the thesis consists of **eight** chapters and the conclusion. In each chapter a specific problem is investigated. In **chapter 1**, we shall build up a strong structure in logical manner to provide knowledge of very basic concepts of biofluid dynamics. It is the essential part of study to have better understanding of behavior of particle in flow. This chapter deals with definitions and a brief discussion of bio fluids and its important applications, magnetohydrodynamic, ferrodydrodynamic, Lie group analysis, magnetization, magnetic field and other related research area of biomagnetic fluid dynamics. Clearly, this chapter provides strong foundation for next coming chapters.

In **chapter 2,** the solution techniques have been described in details. The solution techniques are involving the Finite difference method (FDM), Efficient Numerical Technique of two point boundary value problem based on the common finite difference method with central differencing, a tridiagonal matrix manipulation and an iterative procedure. And finally the boundary value problem solver, bvp4c function technique in MATLAB are discussed here.

The mathematical models developed to meet the specific objectives are presented in the eight subsequent chapters, from Chapter 3 to Chapter 9. In **Chapter 3**, we investigate the Biomagnetic Fluid Flow (BFD) (blood) over a stretching sheet in the presence of a magnetic field. For the mathematical formulation of the problem both magnetization and electrical conductivity of blood are taken into account and consequently both principles of Magnetohydrodynamics (MHD) and FerroHydroDynamics (FHD) are adopted. The physical problem is described by a coupled, nonlinear system of ordinary differential equations subject to appropriate boundary conditions. This solution is obtained numerically by applying an efficient numerical technique based on finite differences method. The obtained results are presented graphically for different values of the parameters entering into the problem under consideration, Murtaza et al. (2017).

A study of three dimensional time dependent biomagnetic fluid flow and heat transfer over a stretching/shrinking sheet has been carried out in **Chapter 4**. In this chapter, impact of unsteadiness parameter, ferromagnetic interaction parameter, stretching parameter and other involved parameters on bio-fluid velocity, temperature and pressure as well as skin friction

coefficient, rate of heat transfer and wall pressure has been investigated, Murtaza et al. (2018).

Chapter 5 deals with the time-dependent two-dimensional biomagnetic fluid (blood) flow (BFD) over a stretching sheet under the action of strong magnetic field. In this chapter we discuss the stability and convergence analysis of this problem. The stability and convergence analysis have been used for measuring the restriction of the useful parameters and this restrictions. The explicit finite difference methods (EFDM) have been used to solve the transform equations. To obtained results are presented graphically and discuss for different values of the dimensionless parameter entering into it.

A study of BFD flow and heat transfer over a non-linearly stretching sheet with variable thickness has been carried out in **Chapter 6**. The governing PDEs are transformed into a system of couple non-linear ODEs subject to appropriate boundary conditions. The numerical solution is obtained by an efficient numerical technique based on common finite differences method. The effect of various governing parameters on the flow, pressure and temperature profile as well as skin friction coefficient, rate of heat transfer and wall pressure are presented graphically and briefly discussed.

A study of temperature dependent viscosity and thermal diffusivity on BFD boundary layer flow and heat transfer over a stretching sheet has been carried out in **Chapter 7**. It was assumed that the thermal conductivity varies linearly with temperature, whereas fluid viscosity varies inversely with temperature and also assume that wall temperature are varies in the (x, y) plane. The influence of various parameters namely the viscosity parameter, thermal conductivity parameter, ferromagnetic interaction parameter on the velocity and temperature fields have been discussed and presented in Chapter eight through graphs.

Chapter 8 and 9 deal with a theoretical and numerical investigation of stability and dual solutions of a biomagnetic fluid flow. It was assumed that the stretching velocity and temperature are vary as a power of the distance from the origin. The problem has been treated mathematically by using Lie group transformation. Lie group analysis used to find the similarity reduction of the non-linear differential equations. In such analysis, one reduces the number of variable governing the partial differential equations. This reduction of variables changes the system of partial differential equations to self-similar system of the ordinary differential equations. Existence of dual solutions (stable or unstable) has been reported in this chapter. A stability analysis has also been carried out and presented in the chapter. This enables one to determine which solution is stable that can be realized physically, and which is

not. The numerical solution is done by using bvp4c function available in Matlab software. The effect of various physical parameter on the velocity and temperature profiles as well as skin friction coefficient and rate of heat have been drawn and adequate discussion.

Finally, the overall conclusions are summarized in **Chapter 10.**

All references of this thesis are listed in the bibliography section just after Chapter 10.

Chapter 2
Numerical Technique

The world is defined by structure in space and time, and it is forever changing in complex ways that can't be solved exactly. Therefore the numerical solution of partial differential equations leads to some of the most important, and computationally intensive, tasks in all of numerical analysis. Many physical phenomena in applied science and engineering when formulated into mathematical models fall into a category of systems known as non-linear coupled partial differential equations. Most of these problems can be formulated as second order partial differential equations. A system of non-linear coupled partial differential equations with the boundary conditions are very difficult to solve analytically. For obtaining the solution of such problems advanced numerical methods have been employed. Hence two numerical procedures have been adopted to obtain solutions. The governing equations are transformed by usual transformation into a non-dimensional system of non-linear coupled partial differential equations with initial and boundary conditions. Hence the solution of our problem would be based on advanced numerical methods. The Explicit as well as Implicit Finite Difference Method will be used for solving the obtained non-similar coupled partial differential equations. Then we discuss a simple and efficient approximate numerical technique of two-point boundary value similarity problems which is based on the common finite difference method with central differencing, a tridiagonal matrix manipulation and an iterative procedure. After that we discuss the boundary value problem solver bvp4c in Matlab.

2.1 Finite Difference Methods (FDM)

We use the finite difference methods to solve the boundary value problem by discretizing the continuous solution domain and approximating the exact derivatives by finite difference approximation and substitute into the boundary value problem to obtain the finite difference equation.

The finite difference techniques are based upon the approximations that permit replacing differential equation by finite difference equation by Strikwerda (1989), Mitchell and Griffiths (1980). There finite difference approximations are algebraic in form, and the

solutions are related to grid points. Thus, a finite difference solution basically involves three steps:-

1) Dividing the solution into grids of notes.

2) Approximating the given differential equation by finite difference equivalence that relates the solutions to grid points.

3) Solving the difference equations subject to the prescribed boundary conditions and/or initial conditions.

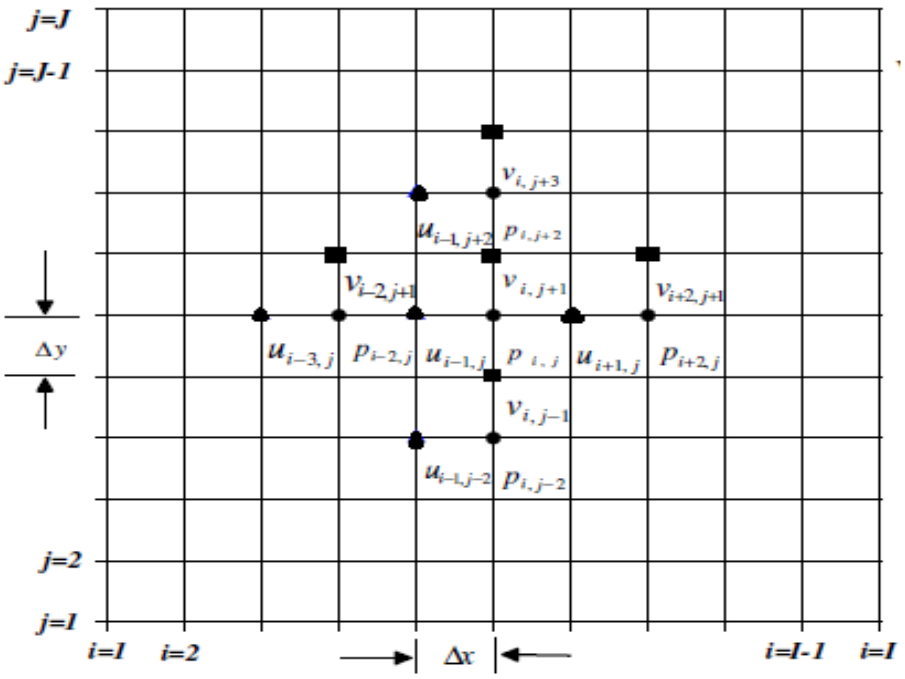

Fig. 2.1 Finite difference space grid

We now construct common finite difference approximations to common partial derivatives. For simplicity we suppose that U is a function of two special coordinates x, y and time t. We adopt the following notation. Let the subscripts i and j represent x and y coordinates and superscript n represents time. Let the mesh spacing in x and y directions are denoted by Δx and Δy also the time step by Δt. We will approximate the partial derivatives of U with respect to x. As t and y are held constant U is effectively a function of the single variable x, so we can use Taylor's formula, where the ordinary derivative terms are partial derivatives and the arguments are (t, x, y) instead of x. Finally we will replace the step size h by Δx to indicate the change of x, so that we have

$$U(t, x_0 + \Delta x, y_0) = U(t, x_0, y_0) + \Delta x U_x(t, x_0, y_0) + \frac{\Delta x^2}{2!} U_{xx}(t, x_0, y_0) + \ldots + \frac{\Delta x^{n-1}}{(n-1)!} U_{(n-1)}(t, x_0, y_0) + O(\Delta x^n) \quad (2.1)$$

Now with truncating error of order $O(\Delta x^2)$ then we have

$$U(t, x_0 + \Delta x, y_0) = U(t, x_0, y_0) + \Delta x U_x(t, x_0, y_0) + O(\Delta x^2) \quad (2.2)$$

Rearranging the equation (2.2), we get

$$U_x(t, x_0, y_0) = \frac{U(t, x_0 + \Delta x, y_0) - U(t, x_0, y_0)}{\Delta x} - \frac{O(\Delta x^2)}{\Delta x}$$

$$U_x(t, x_0, y_0) = \frac{U(t, x_0 + \Delta x, y_0) - U(t, x_0, y_0)}{\Delta x} - O(\Delta x) \quad (2.3)$$

Equation (2.3) holds at any points (t, x_0). In numerical schemes for solving PDEs we are restricted to a grid of discrete x values, $x_1, x_2, x_3 \ldots, x_N$ and discrete t levels $t_1, t_2, t_3 \ldots, t_N$. We will assume a constant grid spacing Δx in x, so that $x_{i+1} = x_i + \Delta x$. Evaluating equation (2.3) for a point (t_n, x_i), on the grid gives,

$$U_x(t_n, x_i, y_j) = \frac{U(t_n, x_{i+1}, y_j) - U(t_n, x_i, y_j)}{\Delta x} - O(\Delta x) \quad (2.4)$$

We will use common subscript/superscript notation,

$$U_{i,j}^n = U(t_n, x_i, y_j) \quad (2.5)$$

So the dropping the $O(\Delta x$ term, equation (2.4) becomes,

$$U_x(t_n, x_i, y_j) = \frac{U_{i+1,j}^n - U_{i,j}^n}{\Delta x} \quad (2.6)$$

Equation (2.6) is the first order forward difference approximation to $U_x(t_n, x_i, y_j)$.

We now derive another FD approximation to $U_x(t_n, x_i, y_j)$. Replacing Δx by $-\Delta x$ in (2.2), we get

$$U(t, x_0 - \Delta x) = U(t, x_0) - \Delta x U_x(t, x_0) + O(\Delta x^2) \quad (2.7)$$

Evaluating (2.7) at (t_n, x_i, y_j) and rearranging as previously gives,

$$U_x(t_n, x_i, y_j) = \frac{U_{i.j}^n - U_{i-1,j}^n}{\Delta x} \quad (2.8)$$

Equation (2.8) is the first order backward difference approximation to $U_x(t_n, x_i, y_j)$.

Our first two FD approximations are first order in x but we can increase the order by taking more terms in the Taylor's series as follows. Truncating (2.2) to $O(\Delta x^2)$, then replacing Δx by $-\Delta x$ and subtracting this new expression from (2.2) evaluating at (t_n, x_i) gives, after some calculation, we have

$$U_x(t_n, x_i, y_j) = \frac{U^n_{i+1,j} - U^n_{i-1,j}}{2\Delta x} \tag{2.9}$$

Equation (2.9) is the first order central difference approximation to $U_x(t_n, x_i, y_j)$.

Many PDEs contain second order or higher order partial derivatives, so we need to derive approximations to them. Equation (2.1) becomes

$$\begin{aligned} U(t, x_0 + \Delta x, y_0) = U(t, x_0, y_0) + \Delta x U_x(t, x_0, y_0) + \frac{\Delta x^2}{2!} U_{xx}(t, x_0, y_0) \\ + \frac{\Delta x^3}{3!} U_{xxx}(t, x_0, y_0) + O(\Delta x^4) \end{aligned} \tag{2.10}$$

replacing Δx by $-\Delta x$ in (2.10), we get

$$\begin{aligned} U(t, x_0 - \Delta x, y_0) = U(t, x_0, y_0) - \Delta x U_x(t, x_0, y_0) + \frac{\Delta x^2}{2!} U_{xx}(t, x_0, y_0) \\ - \frac{\Delta x^3}{3!} U_{xxx}(t, x_0, y_0) + O(\Delta x^4) \end{aligned} \tag{2.11}$$

Adding (2.10) and (2.11), we get

$$U(t, x_0 + \Delta x, y_0) + U(t, x_0 - \Delta x, y_0) = 2U(t, x_0, y_0) + \Delta x^2 U_{xx}(t, x_0, y_0) + O(\Delta x^4)$$

Using our discrete notation at the point (t_n, x_i, y_j) and dropping the $O(\Delta x^4)$ term, we have

$$U_{xx}(t_n, x_i, y_j) = \frac{U^n_{i+1,j} - 2U^n_{i,j} + U^n_{i-1,j}}{\Delta x^2} \tag{2.12}$$

Equation (2.12) is the second order central difference approximation to $U_{xx}(t_n, x_i, y_j)$.

The expressions for mixed derivatives can be obtained by differentiating with respect to each variable in turn. Thus for example,

$$U_{xy}(t_n, x_i, y_j) = \frac{U^n_{i+1,j+1} - U^n_{i+1,j-1} - U^n_{i-1,j+1} + U^n_{i-1,j-1}}{4\Delta x \Delta y} \tag{2.13}$$

Proceeding in a similar manner, approximation can be obtained even to higher order derivatives.

2.2 Efficient Numerical Technique for two point boundary value problem

Here we described a simple and efficient approximate numerical technique for solving a wide class of two-point boundary value similarity problems in fluid mechanics **(**Kaffaussias and Williams (1993). This numerical technique is based on the common finite difference method with central differencing, a tridiagonal matrix manipulation and an iterative procedure. So, it can be programmed and applied easily. The whole numerical scheme is stable, accurate and rapidly converging. These facts suggest this is a powerful and accurate method suitable for application to a wide class of two-point boundary value similarity problems in fluid mechanics (Tzirtzilakis and Kafoussias (2010)).

First we consider the flow and heat transfer of two dimensional, steady, laminar, viscous and incompressible fluid over a stretching sheet. Assume that the boundary layer problem is governed by the following set of partial differential equations

$$\frac{\partial u}{\partial x}+\frac{\partial v}{\partial y}=0 \tag{2.14}$$

$$u\frac{\partial u}{\partial x}+v\frac{\partial u}{\partial y}=-\frac{1}{\rho}\frac{\partial P}{\partial x}+\nu\frac{\partial^2 u}{\partial x^2} \tag{2.15}$$

$$u\frac{\partial T}{\partial x}+v\frac{\partial T}{\partial y}=k\frac{\partial^2 T}{\partial y^2} \tag{2.16}$$

The boundary conditions for the velocity and temperature field are given by the following:

$$y=0:\quad u=cx,\quad v=0,\quad T=T_w$$

$$y\to\infty:\quad u=0,\quad T=T_c,\quad p+1/2\rho q^2=const \tag{2.17}$$

Using the suitable similarity variable and dimensionless temperature and stream function,

$$\xi(x)=\left(\frac{c\rho}{\mu}\right)^{\frac{1}{2}}x,\ \eta(x)=\left(\frac{c\rho}{\mu}\right)^{\frac{1}{2}}y,\ \psi(\xi,\eta)=\left(\frac{\mu}{\rho}\right)\xi\, f(\eta), \tag{2.18}$$

The governing equations reduced to the following ordinary differential equations

$$f'''+ff''-f'^2+2P=0 \tag{2.19}$$

$$\theta''+\Pr f\theta'-4\lambda f'^2=0 \tag{2.20}$$

and the boundary conditions are transformed to:

$$\eta=0:\quad f'=1,\quad f=0,\ \theta=1$$

$$\eta\to\infty:\quad f'\to 0,\quad \theta\to 0, P_1\to -P_\infty \tag{2.21}$$

To calculate the numerical solution of a class of similarity problems. Now we demonstrate this technique by solving the system of equations (2.19)-(2.20) with associated boundary conditions (2.21).
The Equation (2.19) can be written as

$$f'''+ff''-f'^2=-2P \tag{2.22}$$

The above equations can be considered as a second order linear differential equation by setting $y(x)=f'(\eta)$ provided that P and $f(\eta)$ are considered known functions. In this case equation (2.22) can be written as

$$(f')''+f(f')'-(f')f'=-2P$$

which is of the form

$$P(x)y''(x)+Q(x)y'(x)+R(x)y(x)=S(x) \tag{2.23}$$

where $P(x)=1,\ Q(x)=f(\eta),\ R(x)=-f'(\eta),\ S(x)=-2P$

In an analogous manner all equations of the system can be reduced in this form of equation (2.23). Equation (2.22) can be solved by a common finite difference method, based on central differencing and tridiagonal matrix manipulation.

To start the solution procedure, we assume initial guesses (distribution curves) for $f'(\eta)$ and $P(\eta)$ between $\eta=0$ and $\eta=\eta_\infty(\eta\to\infty)$ which satisfy the boundary conditions (2.21). For this problem indicative initial guesses are

$$f'(\eta)=1-\frac{\eta}{\eta_\infty},\quad \theta_1(\eta)=1-\frac{\eta}{\eta_\infty}$$

The $f(\eta)$ distribution is obtained by the integration from $f'(\eta)$ curve. The next step is to consider the f, P, θ known and to determine a new estimation for $f'(\eta)$, $f'_{new}(\eta)$ by solving the non-linear equation (2.23) using the above method. The distribution is updated by the integration of new $f'(\eta)$ curve. These new profiles of $f'(\eta)$ and $f(\eta)$ are then used for new inputs and so on. In this way the momentum equation (2.19) is solved iteratively until convergence up to a small quantity ε is attained.

After $f(\eta)$ is obtained the solution of the energy equation (2.20) with boundary condition (2.21) is solved by using the same algorithm, but without iteration now as for as equation (2.20) is linear. Equation (2.20) is

$$\theta''+\mathrm{Pr}\ f\theta'-4\lambda f'^2=0$$

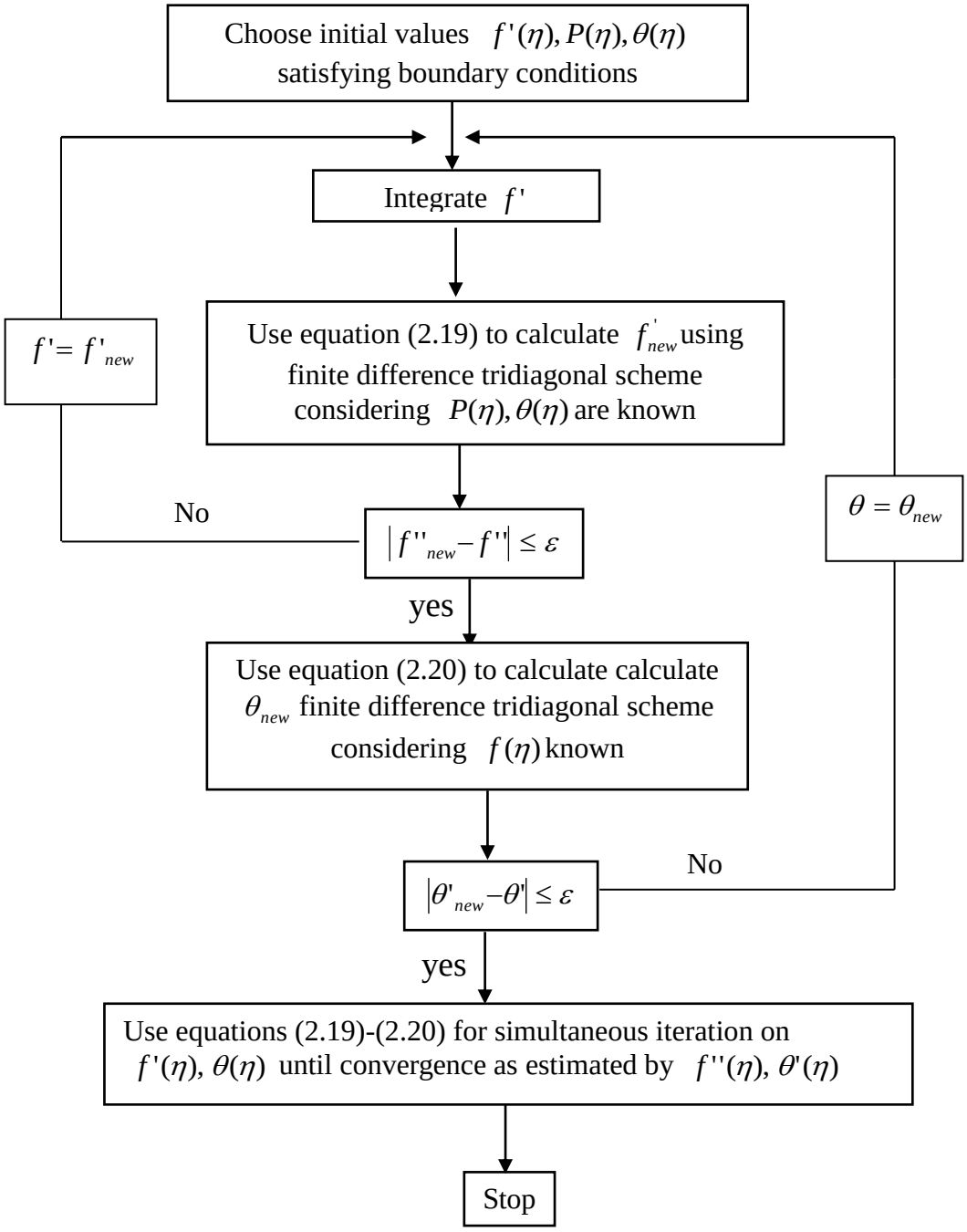

Fig 2.2. Flow chart of the computer program for the approximation numerical technique

This equation can be written as

$$\theta'' + \Pr f\theta' = 4\lambda f'^2 \tag{2.24}$$

Equation (2.24) is a second order linear differential equation in setting $y(\eta) = \theta(\eta)$ which is of the form

$$P(x)y''(x)+Q(x)y'(x)+R(x)y(x)=S(x) \tag{2.25}$$

where $P(x)=1,\ Q(x)=\Pr f,\ R(x)=0,\ S(x)=4\lambda f'^{2}$

Considering $f(\eta), f'(\eta)$ are known, we obtain a new approximation θ_{new} for θ and this process is continue until convergence up to a small quantity ε is attained and finally we obtain θ.

2.3 Boundary value problem solver bvp4c in Matlab

The system of nonlinear ordinary differential equations (ODEs) have been solved numerically by using the boundary value problem solver, bvp4c function technique in MATLAB by Shampine et al. (2000). To obtain the solution we need three necessary conditions: (i) first order ODEs which are to be solved (ii) their associated boundary conditions and (iii) initial guesses for these functions.

Since the transformed governing equation (2.19) and (2.20) are of third and second order we reduce them to a system of first order differential equations. New variables are now defined by the equations $f=y_1, f'=y_2, f''=y_3, \theta=y_4, \theta'=y_5$. Thus, the two coupled higher order differential equations and the corresponding boundary conditions, can be transformed to five equivalent first ODEs subject to corresponding boundary conditions. The system of first order ODEs is:

$$\begin{aligned} f' &= y_2 \\ y_2' &= y_3 \\ f''' = y_3' &= -y_1y_3+y_2^2+2P \\ \theta' &= y_5 \\ \theta'' = y_5' &= -\Pr y_1y_5+4\lambda y_2^2 \end{aligned}$$

The above equation is then integrated numerically as an initial valued problem to a given terminal point. All these simplifications are done for using the MATLAB package.

The numerical procedure of bvp4c followed is:

- Nonlinear PDEs are reduced to 1st order ODEs .
- The solution is returned by bvp4c as a structure called *sol*
- Mesh selection is generated and returned in the field *sol.x*
- Solution can be fetch from array *sol.y* corresponding to *sol.x*
- let $y(0)$ be the left boundary, $y(\infty)$ be the right boundary.

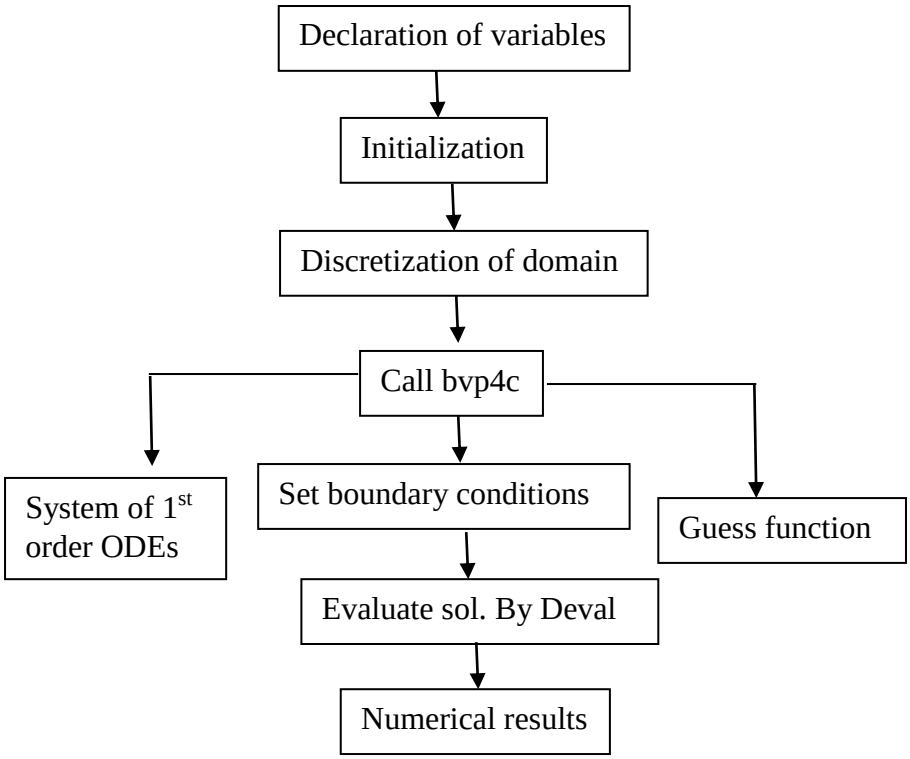

Fig. 2.3 Algorithm of bvp4c routine in MATLAB

Chapter 3

Effect of electrical conductivity and magnetization on the biomagnetic fluid flow over a stretching sheet

The aim of this chapter is to investigate the Biomagnetic Fluid Flow (BFD) (blood) over a stretching sheet in the presence of magnetic field. For the mathematical formulation of the problem both magnetization and electrical conductivity of blood are taken into account and consequently both principles of Magnetohydrodynamics (MHD) and FerroHydroDynamics (FHD) are adopted. The physical problem is described by a coupled, nonlinear system of ordinary differential equations subject to appropriate boundary conditions. This solution is obtained numerically by applying an efficient numerical technique based on finite differences method. The obtained results are presented graphically for different values of the parameters entering into the problem under consideration. Emphasis is given to the study of the effect of the MHD and FHD interaction parameters on the flow field. It is apparent that both parameters effect significantly on various characteristics of the flow and consequently neither electrical conductivity nor magnetization of blood could be neglected by Murtaza et al. (2017).

3.1 Introduction

Biomagnetic fluid dynamics (BFD) is a relatively new area of fluid mechanics. Numerous applications have been proposed in bioengineering and medical science, and some of them include cancer tumor treatment by using magnetic hyperthermia or development of magnetic devices for cell separation, Alimohamadi and Sadeghy (2015), Misra et al. (2010), Haik et al. (1999). BFD is the study of the effect of an applied magnetic field on biological fluid flow. An initial model of BFD was developed by Haik et al. (1996) and is actually based on the principles of Ferrohydrodynamics (FHD). According to this information, blood is considered as an electrically non-conducting magnetic fluid and the flow is affected by the magnetization of the fluid in the magnetic field.

Thus, the arising force is due to magnetization and depends on the existence of a spatially varying magnetic field. However, blood also possesses properties of an electrically

conducting fluid due to the ions in the plasma. The flowing ions produce a slight electric current which interacts with magnetic fields. The formulation of electrically conducting fluids is made by adopting the principles of the well-known magnetohydrodynamics (MHD) which in contrast to FHD ignores the effect of polarization and magnetization, Rosensweig (1987). In order to formulate the entire magnetic properties of blood, i.e., electrical conductivity along with polarization an extended BFD model was developed by Tzirtzilakis (2005). This model is consistent with the properties of MHD as well as with those of FHD and also includes the energy equation.

The shear-driven flow over a stretching sheet constitutes a classical physical problem first studied by Crane (1970) for a Newtonian fluid. Later, Anderson (1995) derived an exact similarity solution for velocity and pressure of the magnetohydrodynamic flow past a stretching sheet. The study of MHD flow over a stretching sheet still constitutes a topic of current ongoing research. The radiation effects on the MHD flow near the stagnation point of a stretching sheet were studied by Jat and Chaudhary (2010) and Pop et al. (2011). Das et al. (2015) studied the unsteady MHD flow of nanofluids over an accelerating convectively heated stretching sheet in the presence of a transverse magnetic field with heat source/sink. The MHD flow of a viscous liquid film over a stretching sheet under different nonlinear stretching velocities was studied by Dandapat et al. (2010). Finally, a characteristic study concerning applications of MHD flow problems to hemodynamics is that of the steady incompressible viscoelastic and electrically conducting fluid flow and heat transfer in a parallel plate channel with stretching walls in the presence of a magnetic field, Misra et al. (2008).

Furthermore, analogous FHD flows over a stretching sheet have been investigated as well. A classical study flow of a heated ferrofluid over a stretching sheet in the presence of a magnetic dipole is that of Anderson and Valnes (1998). Recently, Zeeshan et al. (2015) studied the effect of thermal radiation and heat transfer on the flow of ferromagnetic fluid on a stretching sheet. The appropriate combination of nonmagnetic viscous base fluid, magnetic solid and surfactant composes magnetic fluid in the presence of magnetic dipole. Finally, Tzirtzilakis and Kafoussias (2010) studied the three-dimensional laminar and steady boundary layer flow of an electrically non-conducting and incompressible magnetic fluid, with low Curie temperature and moderate saturation magnetization, over an elastic stretching sheet. It was also assumed that the magnetization of the fluid varied with the magnetic field strength H and the temperature T.

As far as the BFD flow over a stretching sheet is concerned the first work has been carried out by Tzirtzilakis and Kafoussias (2003) which was the study of a biomagnetic fluid flow over a stretching sheet with nonlinear temperature-dependent magnetization. Moreover, Tzirtzilakis and Tanoudis (2003) have presented a numerical method for the study of laminar incompressible two-dimensional biofluid over a stretching sheet with heat transfer. It was assumed that the magnetization of the fluid varied with the magnetic field strength *H* and the temperature *T*. Recently, Misra and Shit (2009) studied the BFD flow of a non-Newtonian viscoelastic fluid over a stretching sheet under the influence of an applied magnetic field generated by a magnetic dipole. The magnetization of the fluid is considered to vary linearly with temperature as well as the magnetic field intensity.

To the authors' knowledge all the above-mentioned BFD flows over a stretching sheet have been studied using either the formulation consistent with the principles of FHD or the formulation consistent with the principles of MHD. So, the present study concerns the flow of biomagnetic fluid over a stretching sheet, in the present of an applied magnetic field using the extended BFD model incorporating both FHD and MHD formulations. The magnetization is considered to vary with the temperature and the magnetic field strength intensity, and the biofluid is treated as an electrically conducting magnetic fluid which also exhibits magnetization. The formulation of the problem is obtained by an analogous manner presented in previous studies by Anderson and Valnes (1998) and Tzirtzilakis and Kafoussias (2003), and the numerical solution is obtained by applying an efficient numerical technique based on the common finite difference method which have been presented by Kafoussias and Williams (1993). The obtained results for critical flow characteristics like velocity, pressure and temperate as well as rate of heat transfer, skin friction or pressure on the stretching sheet are presented graphically for specific parameters entering into the problem under consideration. Special detailed analysis is performed for the variation of these physical quantities with the FHD and MHD interaction parameters which formulate the forces arising due to magnetization and the electrical conductivity, respectively.

3.2 Mathematical Formulation

Let us consider the viscous, steady, two-dimensional, laminar flow of an incompressible and electrically conducting biomagnetic fluid past a flat elastic sheet which is stretched with a velocity proportional to distance $i.e.\ u = cx$, where c is a dimensional constant. The temperature of the stretched sheet is kept at fixed T_w and the temperature of the

fluid far away from the sheet is T_c, where $T_c > T_w$. The fluid is confined to the half space $(y > 0)$ above the sheet, and magnetic dipole is located at distance d below the sheet, giving rise to a magnetic field of sufficient strength to saturate the biomagnetic fluid. The flow configuration is shown schematically at Fig. 3.1.

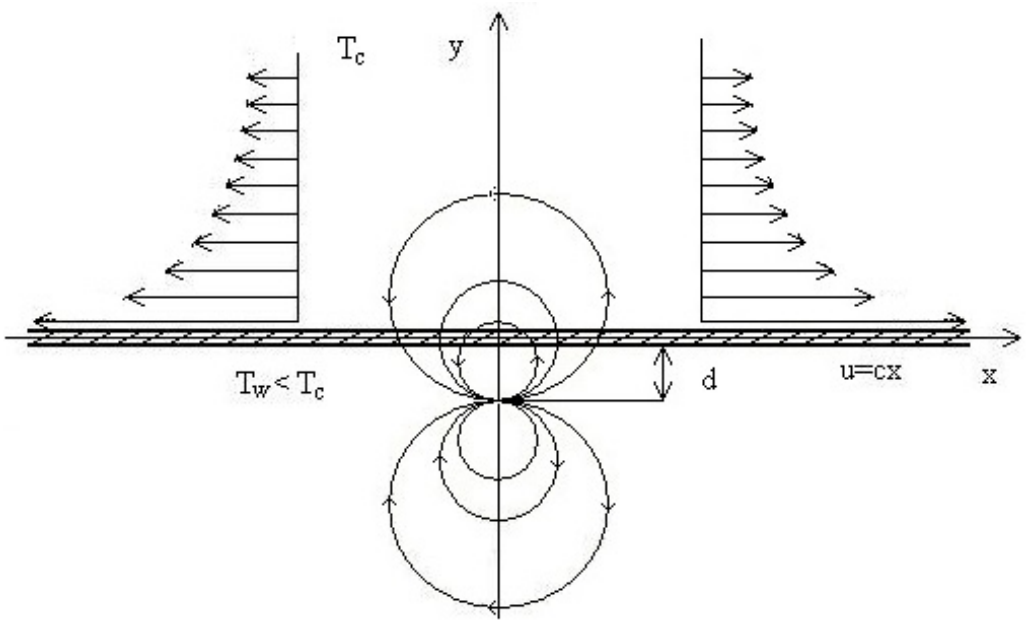

Fig. 3.1. Flow configuration of the flow field

Under the above assumptions the equations governing the flow under consideration are, Rosensweig (1987) and Tzirtzilakis and Xenos (2013):

Continuity equation:

$$\frac{\partial u}{\partial x} + \frac{\partial \mathrm{v}}{\partial \mathrm{y}} = 0 \tag{3.1}$$

Momentum equation:

$$\rho\left(u\frac{\partial u}{\partial x} + v\frac{\partial u}{\partial y}\right) = -\frac{\partial p}{\partial x} + \mu_0 M\frac{\partial H}{\partial x} - \sigma B_y^2 u + \sigma B_x B_y v + \mu\left(\frac{\partial^2 u}{\partial x^2} + \frac{\partial^2 u}{\partial y^2}\right) \tag{3.2}$$

$$\rho\left(u\frac{\partial v}{\partial x} + v\frac{\partial v}{\partial y}\right) = -\frac{\partial p}{\partial y} + \mu_0 M\frac{\partial H}{\partial y} - \sigma B_x^2 v + \sigma B_x B_y u + \mu\left(\frac{\partial^2 v}{\partial x^2} + \frac{\partial^2 v}{\partial y^2}\right) \tag{3.3}$$

Energy equation:

$$\begin{aligned}\rho C_p\left(u\frac{\partial T}{\partial x} + v\frac{\partial T}{\partial y}\right) + \mu_0 T\frac{\partial M}{\partial T}\left(u\frac{\partial H}{\partial x} + v\frac{\partial H}{\partial y}\right) - \sigma B^2 u^2 = k\left(\frac{\partial^2 T}{\partial x^2} + \frac{\partial^2 T}{\partial y^2}\right) \\ + \mu\left[2\left[\left(\frac{\partial u}{\partial x}\right)^2 + \left(\frac{\partial v}{\partial y}\right)^2\right] + \left(\frac{\partial v}{\partial x} + \frac{\partial u}{\partial y}\right)^2\right]\end{aligned} \tag{3.4}$$

with boundary conditions:

$$y = 0: \quad u = cx, \quad v = 0, \quad T = T_w \tag{3.5}$$

$$y \to \infty: \quad u = 0, \quad T = T_c, \quad p + 1/2\rho q^2 = const. \tag{3.6}$$

In the above equations $q = (u, v)$ the dimensional velocity, p is the pressure, ρ is the biomagnetic fluid density, σ is the electrical conductivity, μ is the dynamic viscosity, C_p the specific heat at constant pressure and k the thermal conductivity, μ_0 is the magnetic permeability and $H = (H_x, H_y)$ s the magnetic field strength, B is the magnetic induction $(B = \mu_0 H \Rightarrow (B_x, B_y) = \mu_0 (H_x, H_y))$.

The terms $-\sigma B_y^2 u + \sigma B_x B_y v$ and $-\sigma B_x^2 v + \sigma B_x B_y u$ in (3.2) and (3.3), respectively, represent the Lorentz force per unit volume towards the x and y directions respectively, whereas the term $-\sigma B^2 u^2$ in the energy equation (3.4) represents the Joule heating. These terms arise due to the electrical conductivity of the fluid and are known in MHD, Rosensweig (1987), Das et al. (2015), Misra et al. (2008). The terms $\mu_0 M \dfrac{\partial H}{\partial x}$ and $\mu_0 M \dfrac{\partial H}{\partial y}$ in (3.2) and (3.3), respectively, represent the components of the magnetic force per unit volume and depend on the existence of the magnetic gradient on the corresponding x and y directions. The second term on the left-hand side of the energy equation (3.4), accounts for heating due to the adiabatic magnetization. These terms are known from FHD, Rosensweig (1987), Tzirtzilaki (2005), Tzirtzilakis and Kafoussias, (2003, 2010).

The magnetic dipole gives rise to a magnetic field, sufficiently strong to saturate the biofluid, and its scalar potential is given by Andersson and Valnes (1998)

$$V(x, y) = \frac{\alpha}{2\pi} \frac{x}{x^2 + (y + d)^2} \tag{3.7}$$

Thus, the magnitude $\|H\| = H$ of the magnetic field intensity by

$$H(x, y) = \left(H_x^2 + H_y^2\right)^{\frac{1}{2}} = \frac{\gamma}{2\pi} \frac{x}{x^2 + (y + d)^2} \tag{3.8}$$

where $\gamma = \alpha$ and H_x, H_y are the component of the magnetic field $\overrightarrow{H} = (H_x, H_y)$ given by

$$H_x(x,y) = -\frac{dv}{dx} = \frac{\gamma}{2\pi}\frac{x^2 - (y+d)^2}{\left(x^2 + (y+d)^2\right)^2} \tag{3.9}$$

$$H_y(x,y) = -\frac{dv}{dy} = \frac{\gamma}{2\pi}\frac{2x(y+d)}{\left(x^2 + (y+d)^2\right)^2} \tag{3.10}$$

Following analogous manipulations to previous studies by Andersson and Valnes (1998), Tzirtzilaki (2005), Tzirtzilakis and Kafoussias (2003, 2010) the gradients of the magnetic field strength can be obtained from Eq. (3.8) after having expanded in powers of x and retained terms up to x^2, thus

$$\begin{cases} \dfrac{\partial H}{\partial x} \approx -\dfrac{\gamma}{2\pi}\dfrac{2x}{(y+d)^4} \\ \dfrac{\partial H}{\partial y} \approx \dfrac{\gamma}{2\pi}\left[\dfrac{2}{(y+d)^3} + \dfrac{4x^2}{(y+d)^5}\right] \end{cases} \tag{3.11}$$

The magnetic field intensity H can be expressed by analogous manner, as

$$H(x,y) = \frac{\gamma}{2\pi}\left[\frac{1}{(y+d)^2} - \frac{x^2}{(y+d)^4}\right] \tag{3.12}$$

The above relations of the magnetic field strength H and its gradients, i.e., (3.12) and (3.11), respectively, are valid close to region where $x = 0$ and are used for the further transformation of the system of the governing equations.

Moreover, under the assumption that the applied magnetic field $\overrightarrow{H}$ is sufficiently strong to saturate the biomagnetic fluid, the magnetization M is generally determined by the fluid temperature and magnetic field intensity H. There is a variety of equations that can be used for the variation of the magnetization under the equilibrium assumption. In this study the relation derived experimentally is adopted by Matsuki et al. (1977). This relation expresses the magnetization as a function of the magnetic field strength intensity H and the temperature of the fluid T.

$$M = KH(T_c - T) \tag{3.13}$$

where K is a constant called pyromagnetic coefficient and T_c is the Curie temperature. The above relation for the magnetization M has also proposed for the formulation of BFD by Tzirtzilakis (2005) and used for stretching sheet flow problems, Tzirtzilakis and Kafoussias, (2003a, 2003b, 2010).

3.3 Mathematical Analysis

Following Anderson and Valnes (1998) we introduce the following non-dimensional coordinates

$$\begin{cases} \xi(x) = \left(\dfrac{c\rho}{\mu}\right)^{\frac{1}{2}} x, \\ \eta(y) = \left(\dfrac{c\rho}{\mu}\right)^{\frac{1}{2}} y \end{cases} \tag{3.14}$$

and the dimensionless variables

$$\psi(\xi,\eta) = \left(\frac{\mu}{\rho}\right)\xi\, f(\eta), \tag{3.15}$$

$$p(\xi,\eta) = \frac{P}{c\mu} = -P_1(\eta) - \xi^2 P_2(\eta) \tag{3.16}$$

$$\theta(\xi,\eta) = \frac{T_c - T}{T_c - T_w} = \theta_1(\eta) + \xi^2\theta_2(\eta) \tag{3.17}$$

where $\psi(\xi,\eta), \theta(\xi,\eta)$ and $p(\xi,\eta)$ are the dimensionless stream function, temperature and pressure respectively.

The velocity components can be calculate as

$$\begin{cases} u = \dfrac{\partial\psi}{\partial y} = \dfrac{\partial\psi}{\partial\eta}\dfrac{\partial\eta}{\partial y} + \dfrac{\partial\psi}{\partial\xi}\dfrac{\partial\xi}{\partial y} = \left(\dfrac{\mu}{\rho}\right)\xi f'\left(\dfrac{c\rho}{\mu}\right)^{\frac{1}{2}} = \left(\dfrac{\mu}{\rho}\right)\left(\dfrac{c\rho}{\mu}\right)^{\frac{1}{2}} xf'\left(\dfrac{c\rho}{\mu}\right)^{\frac{1}{2}} = cxf'(\eta) \\ v = -\dfrac{\partial\psi}{\partial x} = \dfrac{\partial\psi}{\partial\xi}\dfrac{\partial\xi}{\partial x} + \dfrac{\partial\psi}{\partial\eta}\dfrac{\partial\eta}{\partial x} = -\left(\dfrac{\mu}{\rho}\right) f\left(\dfrac{c\rho}{\mu}\right)^{\frac{1}{2}} + 0 = -\left(\dfrac{\mu}{\rho}\right) f\left(\dfrac{c\rho}{\mu}\right)^{\frac{1}{2}} \end{cases} \tag{3.18}$$

Substituting the above equations into the momentum equations in (3.2) and (3.3), we get

$$c^2 x\rho\left[f'^2 - ff'' - f'''\right] = 2c^2\rho x P_2 - \frac{\gamma}{2\pi}\frac{\gamma}{2\pi} K\mu_0 (T_c - T_w)(\theta_1 + \xi^2\theta_2)\left(\frac{2x}{(y+d)^6} - \frac{2x^3}{(y+d)^8}\right)$$

$$- \sigma\mu_0^2 H_y^2 cxf' + \sigma\mu_0^2 H_x H_y\left(-\frac{\mu}{\rho}\right) f\left(\frac{c\rho}{\mu}\right)^{\frac{1}{2}}$$

Divided by $c^2 x\rho$ on both side, we get

$$f'^2 - ff'' - f''' = 2P_2 - \frac{1}{c^2\rho}\frac{\gamma}{2\pi}\frac{\gamma}{2\pi}K\mu_0(T_c - T_w)(\theta_1 + \xi^2\theta_2)\left(\frac{2}{(\eta+\alpha)^6\left(\frac{\mu}{c\rho}\right)^3} - \frac{2\xi^2\left(\frac{\mu}{c\rho}\right)}{(\eta+\alpha)^8\left(\frac{\mu}{c\rho}\right)^4}\right)$$

$$-\frac{\sigma\mu_0^2 H_y^2 f'}{c\rho} - \frac{\sigma\mu_0^2 H_x H_y}{c^2\xi\left(\frac{\mu}{c\rho}\right)^{\frac{1}{2}}\rho}\left(\frac{c\mu}{\rho}\right)^{\frac{1}{2}} f$$

Equate the coefficient of ξ^0, we get

$$f'^2 - ff'' - f''' = 2P_2 - \frac{\gamma}{2\pi}\frac{KH(0,0)\mu_0(T_c - T_w)\rho}{\mu^2}\alpha^2\left(\frac{2}{(\eta+\alpha)^6}\right)\theta_1 - \frac{\sigma\mu_0^2 H_y^2 f'}{c\rho}$$

$$\Rightarrow f''' + f'' - f'^2 + 2P_2 - \frac{2\alpha^2\beta\theta_1}{(\eta+\alpha)^6} - Mf' = 0$$

Again from equation (3.3), we get

$$c\mu ff'\left(\frac{c\rho}{\mu}\right)^{\frac{1}{2}} = c\mu\left(P_1' + \xi^2 P_2'\right)\left(\frac{c\rho}{\mu}\right)^{\frac{1}{2}} + \mu_0 K\left(\frac{T_c - T}{T_c - T_w}\right)(T_c - T_w)\frac{\gamma}{2\pi}\frac{\gamma}{2\pi}\left[\frac{1}{(y+d)^2} - \frac{x^2}{(y+d)^4}\right]$$

$$\left[-\frac{2}{(y+d)^3} + \frac{4x^2}{(y+d)^5}\right] + \mu\left(-cf''\left(\frac{c\rho}{\mu}\right)^{\frac{1}{2}}\right) - \sigma\mu_0^2 H_x^2\left(-\frac{\mu}{\rho}\right)f\left(\frac{c\rho}{\mu}\right)^{\frac{1}{2}} + \sigma\mu_0^2 H_x H_y cxf'$$

Divided both side by $c\mu\left(\frac{c\rho}{\mu}\right)^{\frac{1}{2}}$, we get

$$\Rightarrow ff' = \left(P_1' + \xi^2 P_2'\right) - f'' + \frac{1}{c\mu\left(\frac{c\rho}{\mu}\right)^{\frac{1}{2}}}\mu_0 K(\theta_1 + \xi^2\theta_2)(T_c - T_w)\frac{\gamma}{2\pi}\frac{\gamma}{2\pi}\left[\frac{1}{(\eta+\alpha)^2\left(\frac{\mu}{c\rho}\right)} - \frac{\xi^2\left(\frac{\mu}{c\rho}\right)}{(\eta+\alpha)^4\left(\frac{\mu}{c\rho}\right)^2}\right]$$

$$\left[-\frac{2}{(\eta+\alpha)^3\left(\frac{\mu}{c\rho}\right)^{3/2}} + \frac{4\xi^2\left(\frac{\mu}{c\rho}\right)}{(\eta+\alpha)^5\left(\frac{\mu}{c\rho}\right)^{5/2}}\right] - \frac{\sigma\mu_0^2 H_x^2}{c\rho}f + \frac{\sigma\mu_0^2 H_x H_y c\xi\left(\frac{\mu}{c\rho}\right)^{1/2} f'}{c\mu\left(\frac{c\rho}{\mu}\right)^{\frac{1}{2}}}$$

Equate the coefficient of ξ^o, we have

$$\Rightarrow P_1^{'} - f''- ff'- \frac{\gamma}{2\pi}\frac{\mu_0 KH(0,0)(T_c - T_w)\rho}{\mu^2}\frac{\gamma}{2\pi}\alpha^2\left[\frac{2}{(\eta+\alpha)^5}\right]\theta_1 - \frac{\sigma\mu_0^2 H_x^2}{c\rho} f = 0$$

$$\Rightarrow P_1^{'} - f''- ff'- \frac{2\alpha^2\beta\theta_1}{(\eta+\alpha)^5} - Mf' = 0$$

Equate the coefficient of ξ^2, we have

$$\Rightarrow P_2^{'} + \frac{\gamma}{2\pi}\frac{\mu_0 KH(0,0)(T_c - T_w)\rho}{\mu^2}\left[\frac{6\theta_1}{(\eta+\alpha)^7} - \frac{2\theta_2}{(\eta+\alpha)^5}\right]\alpha^2 = 0$$

$$\Rightarrow P_2^{'} + \left[\frac{6\alpha^2\beta\theta_1}{(\eta+\alpha)^7} - \frac{2\alpha^2\beta\theta_2}{(\eta+\alpha)^5}\right] = 0$$

and equation (3.4) we have

$$\Rightarrow \rho c_p\left[-2c\xi^2 f'.(T_c - T_w)\theta_2 + cf(T_c - T_w)(\theta_1^{'} + \xi^2\theta_2^{'})\right] + \mu_0\left[(T_c - (T_c - T_w)(\theta_1 + \xi^2\theta_2))K\frac{\gamma}{2\pi}\frac{\gamma}{2\pi}\right.$$

$$\left(\frac{2c\xi^2\frac{\mu}{c\rho}f'}{(\eta+\alpha)^6\left(\frac{\mu}{c\rho}\right)^3} - \frac{2c\xi^4\left(\frac{\mu}{c\rho}\right)^2 f'}{(\eta+\alpha)^8\left(\frac{\mu}{c\rho}\right)^4} + \frac{\mu}{\rho}f\left(\frac{c\rho}{\mu}\right)^{\frac{1}{2}}\left(-\frac{2}{(\eta+\alpha)^5\left(\frac{\mu}{c\rho}\right)^{5/2}} + \frac{6\xi^2\frac{\mu}{c\rho}}{(\eta+\alpha)^7\left(\frac{\mu}{c\rho}\right)^{7/2}}\right.\right.$$

$$\left.\left.\left.\left.-\frac{4\xi^4\left(\frac{\mu}{c\rho}\right)^2}{(\eta+\alpha)^9\left(\frac{\mu}{c\rho}\right)^{9/2}}\right)\right)\right] = -k\left[2.\left(\frac{c\rho}{\mu}\right)(T_c - T_w)\theta_2 + \left(\frac{c\rho}{\mu}\right)(T_c - T_w)(\theta_1^{''} + \xi^2\theta_2^{''})\right] +$$

$$\mu\left[4c^2 f'^2 + c^2\xi^2\frac{\mu}{c\rho}f''^2\left(\frac{c\rho}{\mu}\right)\right]$$

Divided both side by $\frac{kc\rho(T_c - T_w)}{\mu}$ and equate the coefficient of ξ^0, we get

$$\Rightarrow \Pr f'\theta_1^{'} + \frac{\gamma}{2\pi}\frac{\mu_0 KH(0,0)(T_c - T_w)}{\mu^2}\times\frac{c\mu^2}{\rho k(T_c - T_w)}\left[(\theta_1 - T_\varepsilon)\left(f\frac{2}{(\eta+\alpha)^5}\right)\alpha^2\right] = -2\theta_2 - \theta_2^{''} + 4\lambda f'^2$$

$$\Rightarrow \theta_2^{''} + \Pr f'\theta_1^{'} + \frac{2\alpha^2\beta\lambda(\theta_1 - T_\varepsilon)f}{(\eta+\alpha)^5} + 2\theta_2 - 4\lambda f'^2 = 0$$

and equating the coefficient of ξ^2 we have

$$\theta_2^{''} - \lambda f''^2 - \Pr\left(2f'\theta_2 - f\theta_2^{'}\right) - 2\beta\lambda\alpha^2\left(\theta_1 - T_\varepsilon\right)\left(\frac{f'}{(\eta+\alpha)^6} + \frac{3f}{(\eta+\alpha)^7}\right)$$
$$+ \frac{2\beta\lambda\alpha^2\left(\theta_2 - T_\varepsilon\right)f}{(\eta+\alpha)^5} + M\lambda f'^2 = 0$$

Finally, we get the following system of differential equations

$$f''' + ff'' - f'^2 + 2P_2 - \frac{2\alpha^2\beta\theta_1}{(\eta+\alpha)^6} - Mf' = 0 \tag{3.19}$$

$$P_1^{'} - f'' - ff' - \frac{2\alpha^2\beta\theta_1}{(\eta+\alpha)^5} - Mf = 0 \tag{3.20}$$

$$P_2^{'} + \frac{6\alpha^2\beta\theta_1}{(\eta+\alpha)^7} - \frac{2\alpha^2\beta\theta_2}{(\eta+\alpha)^5} = 0 \tag{3.21}$$

$$\theta_1^{''} + \Pr f\theta_1^{'} + \frac{2\alpha^2\beta\lambda\left(\theta_1 - T_\varepsilon\right)f}{(\eta+\alpha)^5} + 2\theta_2 - 4\lambda f'^2 = 0 \tag{3.22}$$

$$\theta_2^{''} - \lambda f''^2 - \Pr\left(2f'\theta_2 - f\theta_2^{'}\right) - 2\alpha^2\beta\lambda\left(\theta_1 - T_\varepsilon\right)\left(\frac{f'}{(\eta+\alpha)^6} + \frac{3f}{(\eta+\alpha)^7}\right)$$
$$+ \frac{2\alpha^2\beta\lambda\left(\theta_2 - T_\varepsilon\right)}{(\eta+\alpha)^5} + M\lambda f'^2 = 0 \tag{3.23}$$

and the boundary conditions (3.5) and (3.6) are transformed to:

$$\eta = 0: \ f' = 1, \ f = 0, \ \theta_1 = 1, \ \theta_2 = 0. \tag{3.24}$$

$$\eta \to \infty: \ f' \to 0, \ \theta_1 \to 0, \ \theta_2 \to 0, P_1 \to -P_\infty, \ P_2 \to 0. \tag{3.25}$$

The dimensional parameters appearing in the above governing equations are:

$\Pr = \frac{\mu c_p}{k}$ Prandtl number

$T_\varepsilon = \frac{T_c}{T_c - T_w}$ Dimensionless temperature parameter

$\lambda = \frac{c\mu^2}{\rho k\left(T_c - T_w\right)}$ Viscous dissipation parameter

$$\beta = \frac{\gamma}{2\pi}\frac{\mu_0 KH(0,0)\left(T_c - T_w\right)}{\mu^2}$$ Ferromagnetic interaction parameter

$$M = \frac{\sigma\mu_0^2 H^2}{c\rho}$$ Magnetohydrodynamic interaction parameter

$$\alpha = \left(\frac{c\rho}{\mu}\right)^{\frac{1}{2}} d$$ Dimensionless distance.

The ferromagnetic interaction parameter arises in the governing equations due to the magnetization (polarization) of the fluid and is consistent to the FHD properties. If one set $M \neq 0$ and $\beta = 0$ to the governing equations (3.19)-(3.23) then the polarization is "switched off" and the governing equations along with the corresponding boundary conditions correspond to the MHD flow over a stretching sheet. On the other hand the Magnetohydrodynamic interaction parameter arises in the governing equations due to the electrical conductivity of the biofluids. If now one set $M = 0$ and $\beta \neq 0$ then the electrical conductivity is omitted and the governing equations along with the corresponding boundary conditions formulate the pure FHD flow over a stretching sheet. It is clear that if $M = \beta = 0$ then the set of equations corresponds to a pure hydrodynamic flow.

The system of equations (3.19)-(3.23) subject to the boundary conditions (3.24) and (3.25), constitute a six parameter $\left(\alpha, \beta, \lambda, M, \text{Pr}, T_\varepsilon\right)$ coupled and non-linear system of ordinary differential equations, describing the BFD flow over a stretching sheet when the fluids exhibits both electrical conductivity and magnetization which is given as a function of temperature T and the magnetic field strength H.

3.4 Numerical Method

For the numerical solution of the problem under consideration we apply an approximate technique that has better stability characteristics than classical Runge-Kutta combined with a shooting method, is simple, accurate and efficient. The essential features of this technique are the following: (i) It is based on the common finite difference method with central differencing (ii) on a tridiagonal matrix manipulation and (iii) on an iterative procedure. This numerical method is described in detail in Kafoussias and Williams (1993). For reasons of completeness of this study we demonstrate the application of this methodology

for the numerical solution of the system of equations (3.19), (3.22) and (3.23), subject to the boundary conditions (3.24) and (3.25).

The momentum Equation (3.19) can be written as

$$f'''+ff''-f'^{2}-Mf'=\frac{2\alpha^{2}\beta\theta_1}{(\eta+\alpha)^{6}}-2P_2 \tag{3.26}$$

The above equations can be considered as a second order linear differential equation by setting $y(x)=f'(\eta)$ provided that P_2 and $f(\eta)$ are considered known functions. In this case equation (3.26) can be written as

$$(f')''+f(f')'-(f'+M)f'=\frac{2\alpha^{2}\beta\theta_1}{(\eta+\alpha)^{6}}-2P_2$$

which is of the form

$$P(x)y''(x)+Q(x)y'(x)+R(x)y(x)=S(x) \tag{3.27}$$

where $P(x)=1,\ Q(x)=f(\eta),\ R(x)=-f'(\eta)-M,\ \ S(x)=\frac{2\alpha^{2}\beta\theta_1}{(\eta+\alpha)^{6}}-2P_2$

In an analogous manner all equations of the system can be reduced in this form of equation (3.27) except for equation (3.20) and (3.21) which are already first order differential equations. Equation (3.26) can be solved by a common finite difference method, based on central differencing and tridiagonal matrix manipulation.

To start the solution procedure, we assume initial guesses (distribution curves) for $f'(\eta)$ and $P_2(\eta)$ between $\eta=0$ and $\eta=\eta_\infty(\eta\to\infty)$ which satisfy the boundary conditions (3.24) and (3.25). For this problem indicative initial guesses are

$$f'(\eta)=1-\frac{\eta}{\eta_\infty},\ \ \theta_1(\eta)=1-\frac{\eta}{\eta_\infty},\ \theta_2(\eta)=0.5\left(\frac{\eta}{\eta_\infty}\right)\left(1-\frac{\eta}{\eta_\infty}\right)$$

The $f(\eta)$ distribution is obtained by the integration from $f'(\eta)$ curve. The next step is to consider the f, P_2, θ_1 known and to determine a new estimation for $f'(\eta)$, $f'_{new}(\eta)$ by solving the non-linear equation (3.27) using the above method. The distribution is updated by the integration of new $f'(\eta)$ curve. These new profiles of $f'(\eta)$ and $f(\eta)$ are then used for new inputs and so on. In this way the momentum equation (3.26) and consequently (3.19) is solved iteratively until convergence up to a small quantity ε is attained.

After $f(\eta)$ is obtained the solution of the energy equation (3.22) with boundary condition (3.24) and (3.25) is solved by using the same algorithm, but without iteration now as for as equation (3.22) is linear. Equation (3.22) is

$$\theta_1'' + \Pr\, f\theta_1' + \frac{2\alpha^2\beta\lambda(\theta_1 - T_\varepsilon)f}{(\eta+\alpha)^5} + 2\theta_2 - 4\lambda f'^2 = 0$$

This equation can be written as

$$\theta_1'' + \Pr\, f\theta_1' + \frac{2\alpha^2\beta\lambda f}{(\eta+\alpha)^5}\theta_1 = \frac{2\alpha^2\beta\lambda T_\varepsilon f}{(\eta+\alpha)^5} - 2\theta_2 + 4\lambda f'^2 \tag{3.28}$$

Equation (3.28) is a second order linear differential equation in setting $y(\eta) = \theta_1(\eta)$

which is of the form

$$P(x)y''(x) + Q(x)y'(x) + R(x)y(x) = S(x) \tag{3.29}$$

where $P(x) = 1,\ Q(x) = \Pr f,\ R(x) = \frac{2\alpha^2\beta\lambda f}{(\eta+\alpha)^5},\ S(x) = \frac{2\alpha^2\beta\lambda T_\varepsilon f}{(\eta+\alpha)^5} - 2\theta_2 + 4\lambda f'^2$

Considering $f(\eta), f'(\eta)$ and θ_2 known, we obtain a new approximation θ_{1new} for θ_1 and this process is continue until convergence up to a small quantity ε is attained and finally we obtain θ_1

Hereafter the energy equation (3.23) with boundary condition (3.24) and (3.25) is solved. Equation (3.23) can be written as

$$\theta_2'' - \lambda f''^2 - \Pr\left(2f'\theta_2 - f\theta_2'\right) - 2\alpha^2\beta\lambda(\theta_1 - T_\varepsilon)\left(\frac{f'}{(\eta+\alpha)^6} + \frac{3f}{(\eta+\alpha)^7}\right)$$

$$+ \frac{2\alpha^2\beta\lambda(\theta_2 - T_\varepsilon)}{(\eta+\alpha)^5} + M\lambda f'^2 = 0$$

$$\theta_2'' + \Pr\, f\theta_2' + \left(\frac{2\alpha^2\beta\lambda f}{(\eta+\alpha)^5} - 2\Pr f'\right)\theta_2 = 2\alpha^2\beta\lambda(\theta_1 - T_\varepsilon)\left(\frac{f'}{(\eta+\alpha)^6} + \frac{3f}{(\eta+\alpha)^7}\right) + \lambda f''^2$$

$$+ \frac{2\alpha^2\beta\lambda T_\varepsilon f}{(\eta+\alpha)^5} - M\lambda f'^2 \tag{3.30}$$

Equation (3.30) is a second order linear differential equation by setting $y(\eta) = \theta_2(\eta)$ which is of the form (3.27) with

$$P(x)=1,\ Q(x)=\Pr f,\ R(x)=\left(\frac{2\alpha^2\beta\lambda f}{(\eta+\alpha)^5}-2\Pr f'\right),$$

$$S(x)=2\alpha^2\beta\lambda(\theta_1-T_\varepsilon)\left(\frac{f'}{(\eta+\alpha)^6}+\frac{3f}{(\eta+\alpha)^7}\right)+\lambda f''^2+\frac{2\alpha^2\beta\lambda T_\varepsilon f}{(\eta+\alpha)^5}-M\lambda f'^2$$

Considering f, f', f'' and θ_1 known we calculate the new approximation $\theta_{2(new)}$ for θ_2 and continue this iteration until convergence up to a small quantity ε is attained and finally we obtain θ_2. Considering now θ_1 and θ_2 known, we obtained a new estimate for P_1 and P_2 (Eqs. (3.20)-(3.21)). Next the computational procedure reverts to its starting point using the most current distribution of of f', *P, and* θ_1 as inputs. This process is continuing until final convergence of the solution is attained.

In order to apply to our numerical computation a proper step size $h=\Delta\eta=0.01$ and appropriate η_∞ value as $(y\to\infty)$ must be determined. By "trial and error" we set $\eta_\infty=6$, $\Delta\eta=0.01$ and the tolerance between the iterations is set at $\varepsilon=10^{-4}$ defined as $\varepsilon=\max_{i=1,N}\left(\left|\frac{f_{old}(i)-f_{new}(i)}{f_{old}(i)}\right|\right)$. Computations were also performed for $\Delta\eta=0.001$ and no significant differences were found.

3.5 Results and Discussion

For the derivation of the numerical solution it is necessary to assign some numerical values to the parameters involved in the problem under consideration. In this study we adopt case scenarios also discussed in previous study by Tzirtzilakis (2008, 2015) according to which the fluid is blood with density $\rho=1050\ kgm^{-3}$ and viscosity $\mu=3.2\times10^{-3}kgm^{-1}s^{-1}$. The electrical conductivity of blood is $\sigma=0.8sm^{-1}$. The temperature of the plate is $T_w=37^0C=310K$ whereas the temperature of the fluid is $T_c=41^0C=314K$. Although the viscosity μ, the specific heat under constant pressure C_p and thermal conductivity k of any fluid and hence of the fluid is blood, are temperature dependent the Prandtl number can be considered constant. Thus, for the temperature range considered in this problem $C_p=3.9\times10^3\,Jkg^{-1}K^{-1}$ and $k=0.5Jm^{-1}s^{-1}K^{-1}$.

For the definition of ferromagnetic parameter and magnetohydrodynamic parameter, we have

$$\beta = \frac{\gamma}{2\pi}\frac{\mu_0 KH(0,0)(T_c - T_w)\rho}{\mu^2}, \qquad M = \frac{\sigma\mu_0^2 H^2}{c\rho} \tag{3.31}$$

For magnetization, we have

$$M = KH(T_c - T) \tag{3.32}$$

magnetic field intensity is $H(x,y) = \frac{\gamma}{2\pi}\left[\frac{1}{(y+d)^2} - \frac{x^2}{(y+d)^4}\right]$ (3.33)

and the magnetic induction is $B = \mu_0 H$ (3.34)

Let us consider the magnetization very close to the wall at the point $(0,0)$. then the magnetization equation becomes $M_0 = KH(0,0)(T_c - T_w)$, magnetic intensity becomes $H(0,0) = \frac{\gamma}{2\pi}\left[\frac{1}{d^2}\right]$ and magnetic induction is $B_0 = \mu_0 H(0,0)$.

Using the above relation, equation (3.31) becomes

$$\beta = \frac{\gamma}{2\pi}\frac{\mu_0 KH(0,0)(T_c - T_w)\rho}{\mu^2} = \frac{M_0 B_0 d^2 \rho}{\mu^2}$$

and $M = \frac{\sigma\mu_0^2 H^2(0,0)}{c\rho} = \frac{\sigma B_0^2 d^2}{\alpha^2 \mu}$

Where $\alpha = \left(\frac{c\rho}{\mu}\right)^{\frac{1}{2}} d \Rightarrow \alpha^2 = \left(\frac{c\rho}{\mu}\right) d^2 \Rightarrow c\rho = \frac{\alpha^2 \mu}{d^2}$

For these values, the dimensionless temperature number is

$$T_\varepsilon = \frac{T_c}{T_c - T_w} = \frac{314}{314 - 310} = \frac{314}{4} = 78.5$$

and the viscous dissipation number is $\lambda = \frac{c\mu^2}{\rho K(T_c - T_w)}$

$$= \frac{1.28 \times 10^{-5} \times \left(3.2 \times 10^{-3}\right)^2}{1050 \times 0.5 \times (314 - 310)}$$

$$= 6.4 \times 10^{-14}.$$

Prandtl number $\Pr = \frac{\mu c_p}{k} = \frac{3.2\times10^{-3}\times3.9\times10^{3}}{0.5} \cong 25$

If we take $d = 5\times10^{-4}$ and $\alpha = 3.5\times10^{-4}$ then the ferromagnetic parameter is

$$\beta = \frac{B_0 M_0 \rho d^2}{\mu^2} = \frac{1\times40\times1050\times0.00005^2}{\left(3.2\times10^{-3}\right)^2} \cong 10$$

and magnetohydrodynamic parameter is

$$M = \frac{\sigma B_0^2 d^2}{\alpha^2 \mu} = \frac{0.8\times1\times0.00005^2}{0.00035^2\times3{,}2\times10^{-3}} \cong 5$$

As far as the values of the magnetic parameters M and β are concerned there exist extended discussions in various studies among them are Tzirtzilakis (2005, 2008, 2015) and Misra et al. (2008). Especially the biomagnetic interaction parameter can take a quite large range of values depending by the magnetic field gradient. For β in the present study we adopt values in the range of 0-10 used also in the studies of Tzirtzilakis and Kafoussias (2003), Tzittzilakis and Tanoudis (2003), Misra and Shit (2009). For the magnetic parameter M the range that could be adopted is also large and could reach the value of 600 for very strong magnetic fields used by Misra et al. (2008). In this study we perform calculations for the range 0-10 for M. The above ranges of the magnetic parameters albeit correspond to low values of the magnetic field strength we will see that result to considerable changes in the flow field comparable to the hydrodynamic case which is given for $M = \beta = 0$.

As far as the relevance of this flow case with a realistic situation with blood as the fluid is concerned, the studies Tzirtzilakis (2005, 2008, 2015) contain discussion of general flow conditions and corresponding parameter values for blood. For this specific physical problem, one could say that these parameters are corresponding to a flow problem of heated blood ($41^0 C$) over a stretched tissue (at $37^0 C$) during a hyperthermia treatment. However, it is admitted that this type of flow is investigated as a basic BFD flow problem for the understanding of the influence of the magnetic field on blood flow possessing properties of a magnetic material rather than a very realistic physical problem.

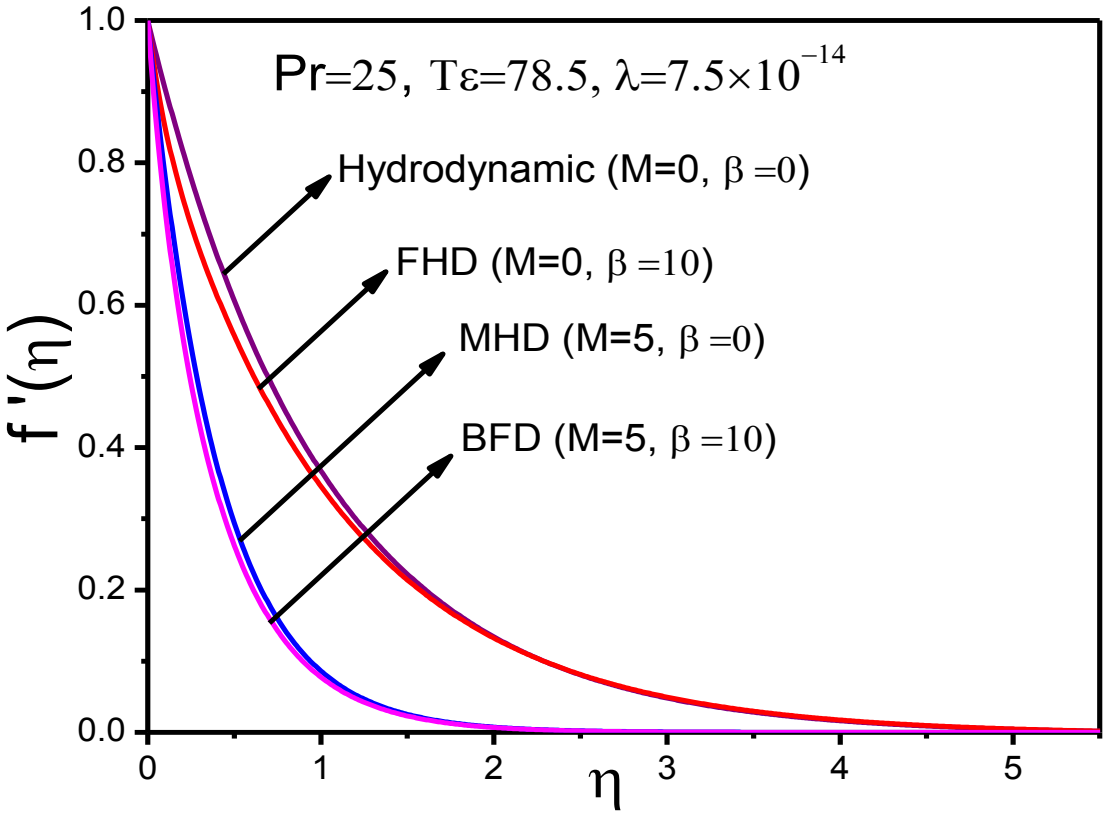

Fig. 3.2. Variation of the dimensionless velocity component $f'(\eta)$

In order to compare the obtained numerical results with others documented in the literature, computations were carried out by setting $M = 0$ and for $\beta = 0$, 2 and 5. The results are identical with those obtained by Tzirtzilakis and Tanoudis (2003) as well as with those obtained by Tzirtzilakis and Kafoussias (2003) for the values of the critical exponent $\delta = 0$ and $\beta = 0$, 5, and the corresponding values of the parameters refereed in that study. It is noted that the results obtained by Tzirtzilakis and Tanoudis (2003) have been also validated with results obtained by Anderson and Valnes (1998) and are in accordance with the hydrodynamic case ($M = \beta = 0$) with the results obtained by Crane (1970).

Furthermore, additional comparisons were performed for the MHD case with analytical results provided by Anderson for the dimensionless stream function f , for $\beta = 0$ and $M = 5$. It is found that the absolute difference at all the points of calculation between the theoretical and numerical estimated value is less than 5×10^{-5}. It is noted that the Lorentz force at the study of Anderson is risen only due to the *u*-velocity component, whereas, in the present study, both velocity components are taken into account (see Eqs. 3.2, 3.3). This accordance between the present results and the analytical ones presented by Anderson indicate an interesting matter as far as the physical problem is concerned. The consideration of both

velocity components in the Lorentz force does not significantly alter the flow field, and Eqs. (3.2) and (3.3) can be simplified. This is justified due to the fact that the *u* velocity component is dominant to the boundary layer flow field and the *v*-velocity component is insignificant to cause further changes in the Lorentz force. Moreover, the above results indicate that the simplification made in the energy equation concerning the joule heating term, i.e., the consideration that only the *u*-velocity component gives rise to the joule heating, is valid.

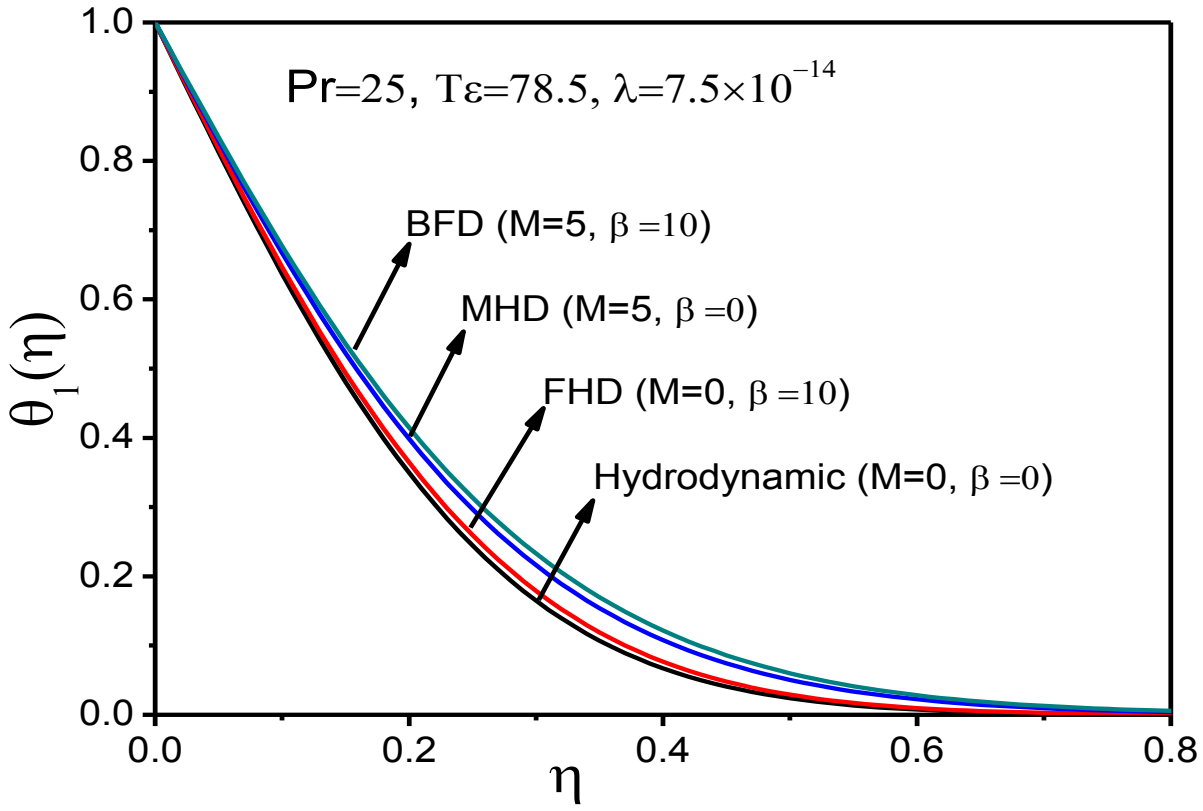

Fig. 3.3. Variation of the dimensionless temperature $\theta_1(\eta)$

From relation (3.18) it is apparent that $f'(\eta) = u/cx$. The function $f'(\eta)$ is called dimensionless velocity component and its variation is pictured at Fig. 3.2. The curves are plotted for $M = \beta = 0$ which corresponds to pure hydrodynamic flow, $M = 0$, $\beta = 10$ which corresponds to pure FHD flow, $M = 5$, $\beta = 0$ which corresponds to pure MHD flow and finally for $M = 5$, $\beta = 10$ which correspond to the mixed FHD and MHD flow of the extended BFD model. It is observed that the dimensionless velocity is reduced considerably with the increment of β or M. Increment of β causes reduction of the dimensionless velocity. However, the major reduction of the velocity is observed with the increment of M and the differences by increasing β is negligible comparable to those occur by the increment of M.

Figure 3.3 shows the variation of the dimensionless temperature $\theta_1(\eta)$ for the same values of M and β as with the dimensionless velocity above. Generally, the temperature in the flow field increases with the increment of the magnetic parameters M or β. Again the greater increment of θ_1 occurs with the increment of M and when β increases smaller increments are noticed. The higher temperature distribution is similar to the corresponding one obtained in previous studies by Tzirtzilakis and Tanoudis (2003) and Tzirtzilakis and Kafoussias (2003). The calculations show that the dimensionless temperature $\theta(\xi,\eta)$ is represented only by the function $\theta_1(\eta)$, whereas $\theta_2(\eta)$ is negligible. Namely, the calculated absolute values of the distribution of θ_2 were $<10^{-5}$ which is well below the accuracy of the numerical method used, and thus θ_2 is practically zero.

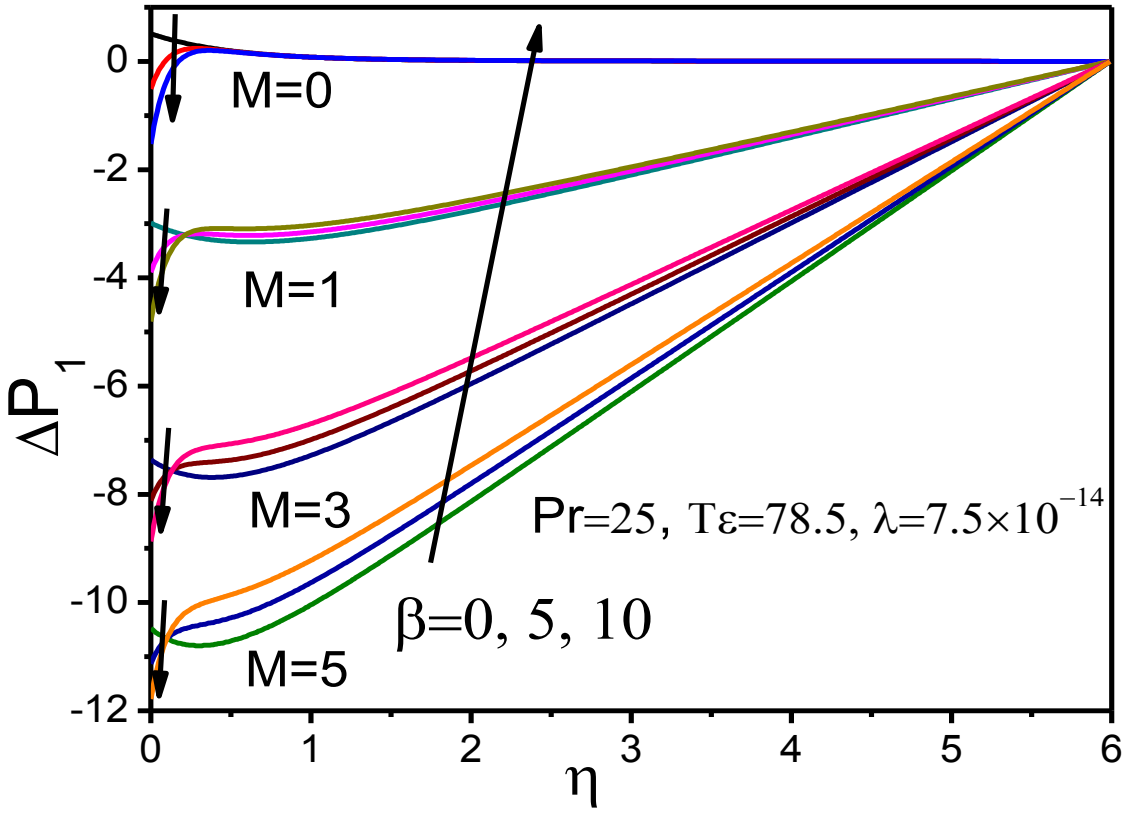

Fig. 3.4. Variation of the dimensionless relative pressure $\Delta P_1(\eta)$

The dimensionless pressure P_1 is estimated from integration of Eq. (3.20) under the boundary condition (3.25), i.e., $P_1 \rightarrow -P_\infty$. It is noted that this equation is not coupled to the rest of the system of the governing equations and is solved once at the end of the procedure. The boundary condition is derived from the initial set of the equations and the Bernoulli equation at conditions (3.6) holding far away from the stretching sheet. If one consider the

relative pressure $\Delta P_1 = P_1 - P_\infty$ then Eq. (3.20) can be integrated for unknown function the relative pressure ΔP_1 under the boundary condition $\Delta P_1 \to 0$ as $\eta \to \infty$.

The variation of the relative pressure ΔP_1 for various numbers M and β is shown at Fig. 3.4. It is obtained that the determining factor of the reduction of the relative pressure is the parameter M. The arrows point increases, for a specific value of M, it is observed that the relative pressure also increases almost all over the flow field except a region close to the stretching sheet $(0 \le \eta \le 0.2)$ where the opposite happens. The decrement of the relative dimensionless P_1 is almost one order of magnitude for M = 5 close to the area of magnetic field.

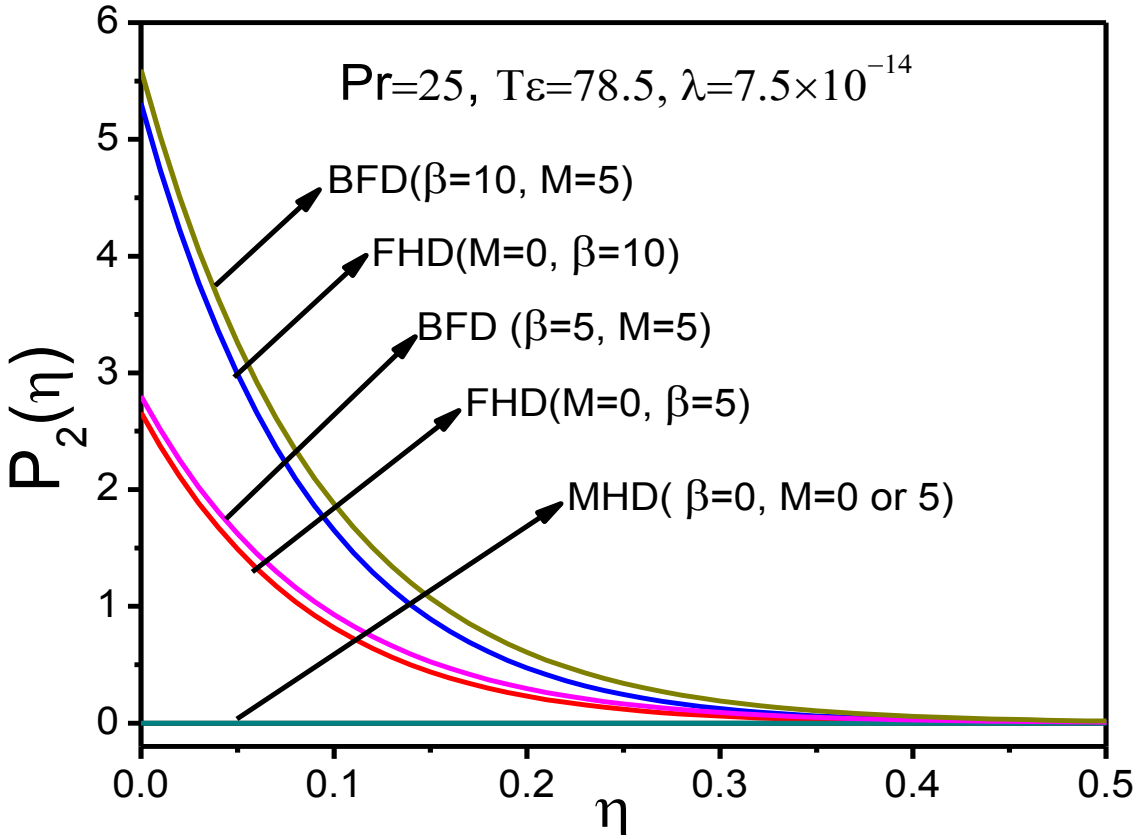

Fig. 3.5. Variation of the dimensionless pressure $P_2(\eta)$

Indeed, the results for ΔP_1 and consequently for P_1 seem to be dependent on the choice of the integration domain and this could be explained by the following reasons. First, from the problem formulation the boundary condition of P_1 lay at the end of the physical domain. If for example P_∞ is the atmospheric pressure, then ΔP_1 corresponds to the relative pressure and the integration starts from the outer region of the boundary layer toward to the plate $(\eta = 0)$.

On the other hand, the integration domain, i.e., length of η, corresponds to the physical thickness of the boundary layer. This thickness cannot be determined without experimental data and seems that the appearance of MHD effect $(M \neq 0)$, plays role in the distribution of the relative pressure which is not asymptotically tends to 0. Nevertheless, due to the fact that Eq. (3.20) under the boundary condition (3.25) from which P_1 is estimated is uncoupled from the rest of the system of the governing equations, the observed domain dependency is of minor importance.

Figure 3.5 shows the variation of the dimensionless pressure P_2 with the magnetic parameters M and β. A general observation is that the variations of P_2 are limited close to the stretching sheet and for $0 \leq \eta \leq 0.5$. It is obtained that this time the important parameter for the increment of P_2 is β. For a specific value of β increment of M results to further small increment of P_2. The curve for M = 0, β = 5 is similar to the corresponding one obtained in the aforementioned previous studies by Tzirtzilakis and Tanoudis (2003) and Tzirtzilakis and Kafoussias (2003).

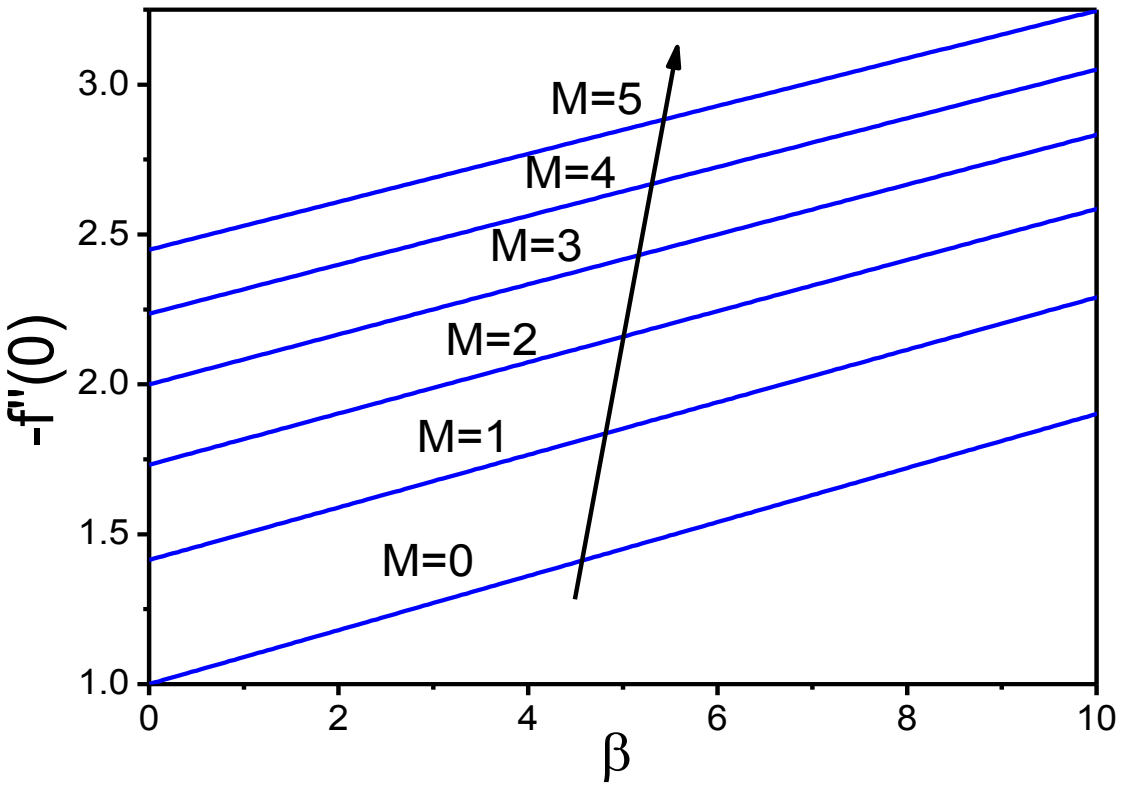

Fig. 3.6 (a) Variation of the dimensionless wall shear parameter $-f''(0)$ with β.

Another important parameters investigated in stretching sheet problems are the dimensionless wall shear parameter $f''(0)$ and the dimensionless wall heat transfer

parameter $\theta^*(0)$. These parameters are related to the local skin friction coefficient and the local rate of heat transfer respectively by Tzirtzilakis and Kafoussias (2003). The variation of $-f''(0)$ is shown at Fig. 3.6(a), 3.6(b). The increment of β leads to linear increment of $-f''(0)$. The line for M = 0 is similar to corresponding one obtained in previous studies of Tzirtzilakis and Tanoudis (2003) and Tzirtzilakis and Kafoussias (2003). Moreover, further increment is observed if M increases for a specific value of β. The increment of $-f''(0)$ with M is not linear and is depicted at Fig. 3.6(b). Increment of either M or β results to almost equivalent significant increment of $-f''(0)$.

Figure 3.7(a) and 3.7(b) shows the variation of the dimensionless relative wall pressure $\Delta P_1(0)$ with β and various values of M and with M for β = 0, 5 and 10, respectively. The relative wall pressure $\Delta P_1(0)$ reduces linearly with the increment of β. It is apparent from Fig. 3.7(b) that the reduction of $\Delta P_1(0)$ is much greaterwith the increment of M than that caused by the increment of β.

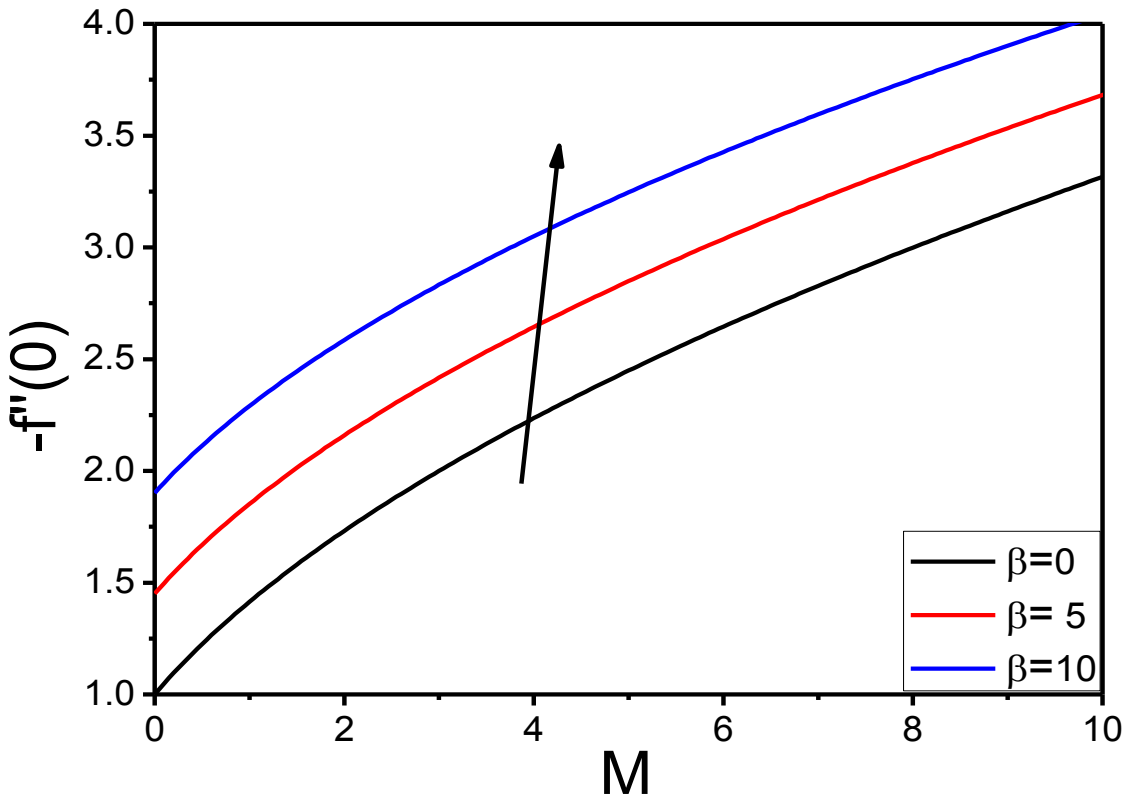

Fig. 3.6 (b) Variation of the dimensionless wall shear parameter $-f''(0)$ with M.

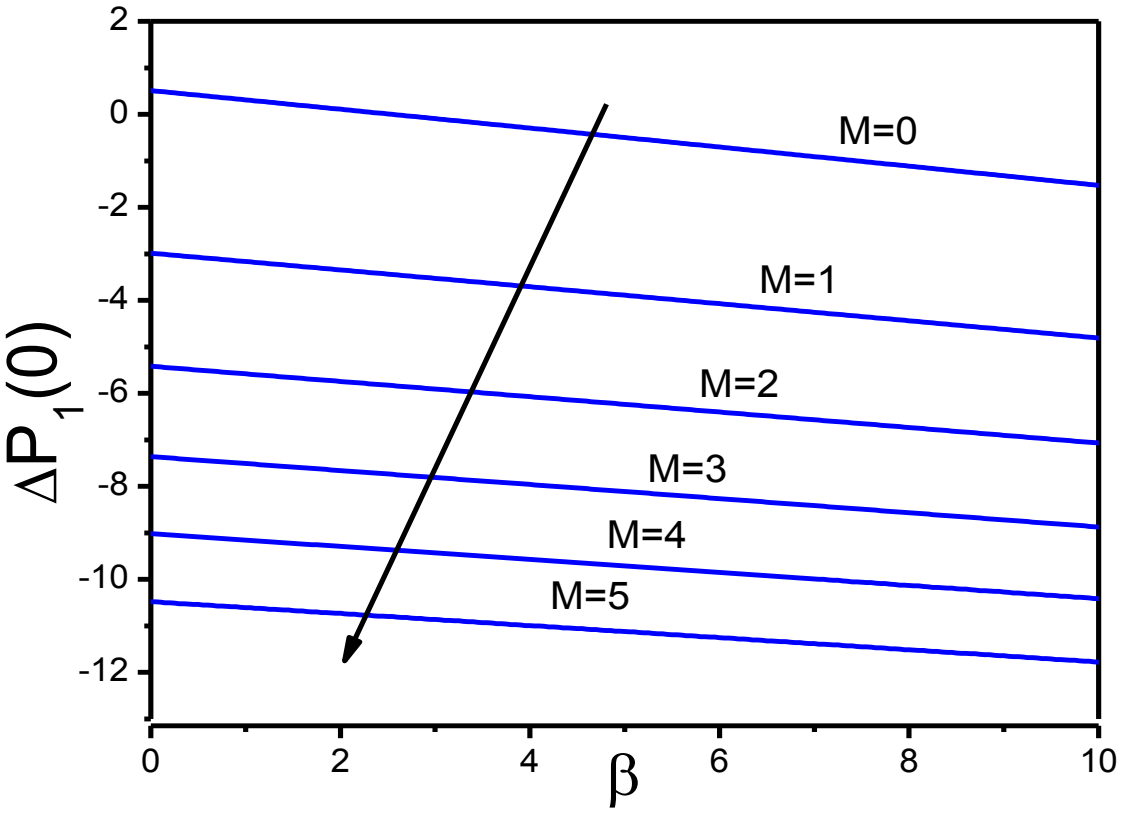

Fig. 3.7 (a). Variation of the dimensionless relative wall pressure $\Delta P_1(0)$ with β

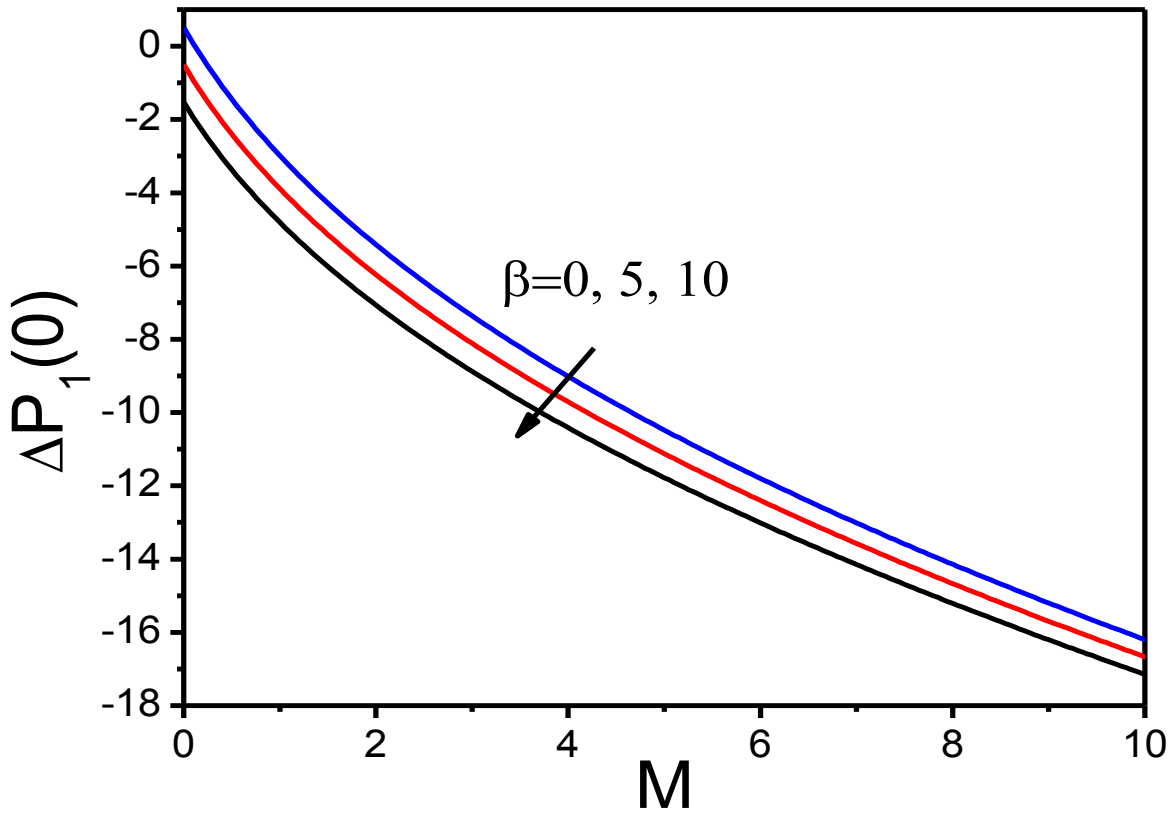

Fig. 3.7(b). Variation of the dimensionless relative wall pressure $\Delta P_1(0)$ with M.

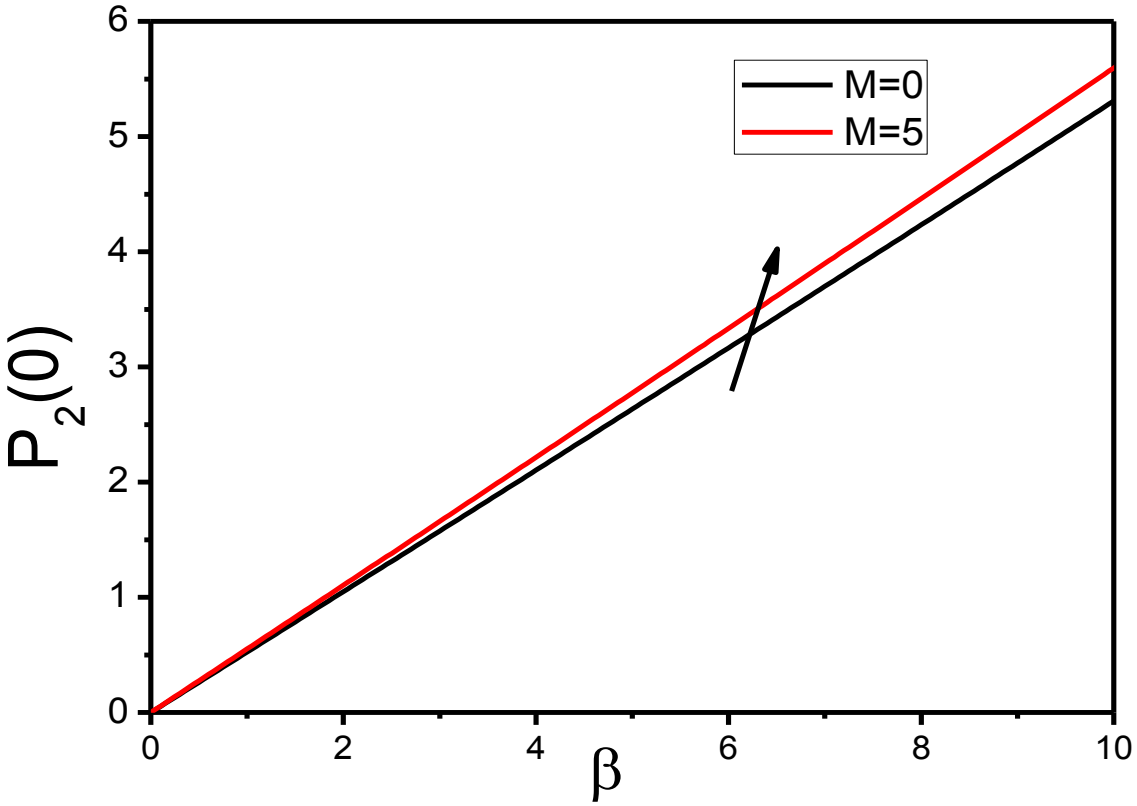

Fig. 3.8. Variation of the dimensionless wall pressure $P_2(0)$ with β.

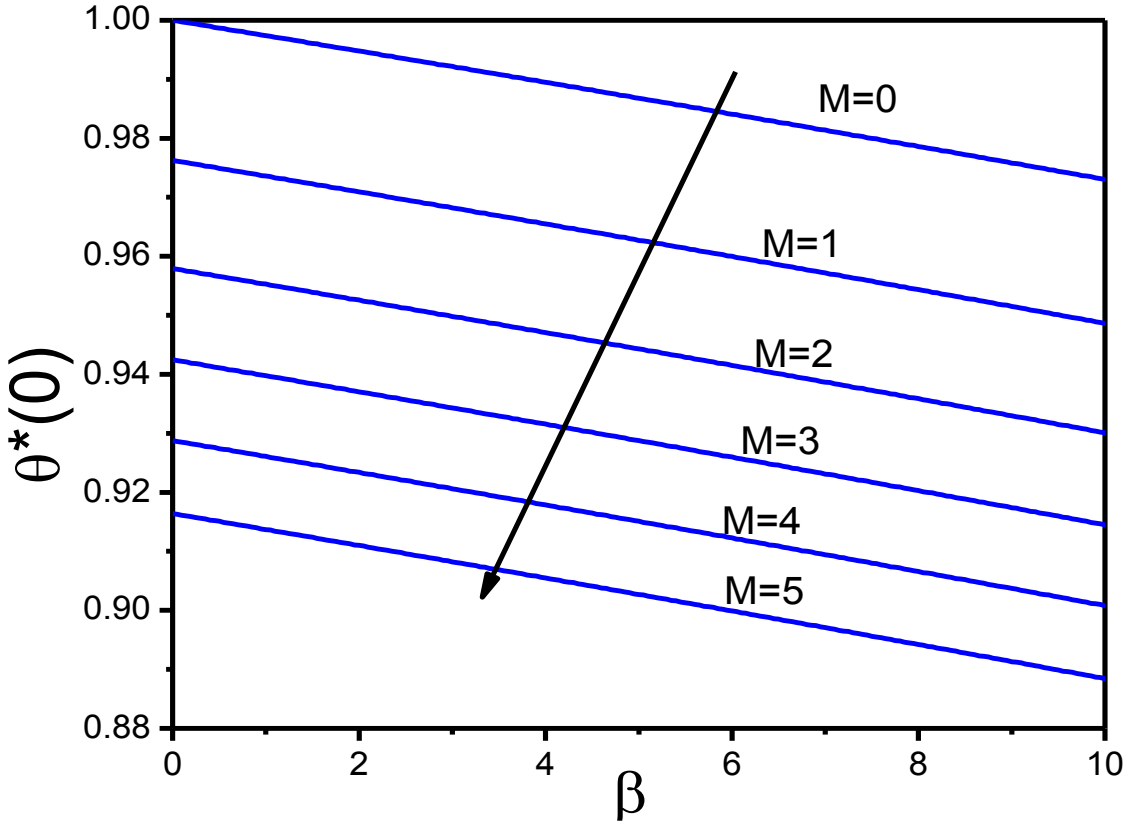

Fig. 3.9 (a).Variation of the wall heat transfer parameter $\theta^*(0)$ with β.

On the other hand from Fig. 3.8 it is obtained that the dimensionless wall pressure $P_2(0)$ increases linearly with the increment of β and the increment of M does not have significant effects in the flow field. The line for M = 0 is similar to the corresponding one obtained in the aforementioned previous studies of Tzirtzilakis and Tanoudis, (2003) and Tzirtzilakis and Kafoussias (2003).

Another interesting parameter for the study of the thermal problem is the so-called coefficient of the heat transfer rate at the wall (sheet) which is independent of the distance ξ and is defined by the ratio $\theta^*(0) = \dfrac{\theta_1'(0)}{\theta_1'(0)\big|_{M=\beta=0}}$. The variation of the wall heat transfer parameter $\theta^*(0)$ with β and M is shown at Fig. 3.9(a) and 3.9(b). For the case of the variation with β pictured at Fig. 3.9(a), $\theta^*(0)$ reduces linearly. The reduction is greater comparable to the hydrodynamic case ($M = \beta = 0$) as M increases.

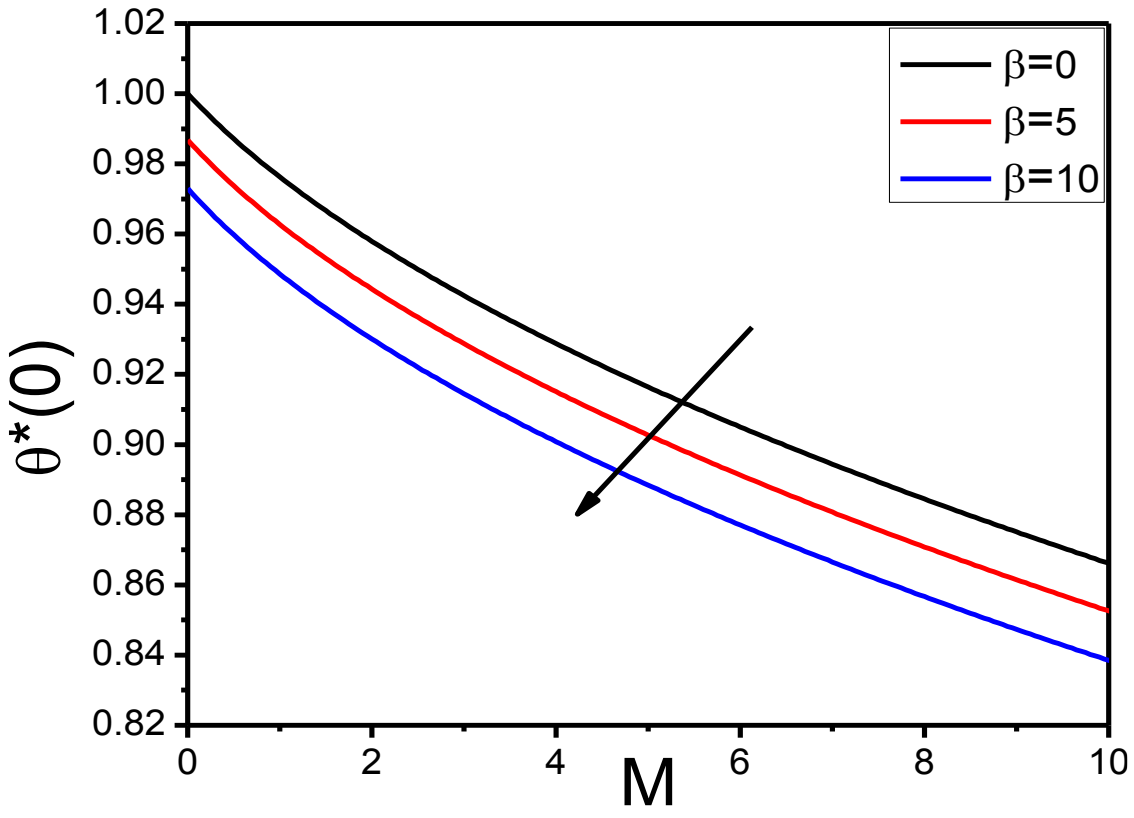

Fig. 3.9(b).Variation of the wall heat transfer parameter $\theta^*(0)$ with M.

Figure 3.9(b) shows the variation of $\theta^*(0)$ with M which for this case is not linear. It is generally obtained that the increment of M or β results to similar amount of reduction for this parameter. The maximum rate of heat transfer at the wall is attained for β = 10 and M =

5. The line for M = 0 at Fig. 3.9(a) is similar to the corresponding one obtained in previous study of Tzirtzilakis and Tanoudis (2003) and Tzirtzilakis and Kafoussias (2003).

3.6 Summary of the chapter

For the problem of the BFD flow over a stretching sheet it is concluded that the electrical conductivity and the polarization of the fluid are both determining factors of the flow field. The dimensionless velocity of the fluid over the stretching sheet is reduced by the application of the magnetic field. This reduction is caused almost exclusively from the electrical conductivity whereas the reduction caused by the polarization is negligible. Analogous behavior is observed for the dimensionless temperature θ_1. The effect of the electrical conductivity of the fluid prevails over the one caused by the polarization effect on the values of the dimensionless relative pressure ΔP_1 whereas the opposite is true for the dimensionless pressure P_2.

As far as the very important characteristics of the flow on the stretching sheet are concerned the dimensionless wall shear parameter $-f''(0)$ is almost equally affected by the variation of M or β. Increment of β results to increment of $-f''(0)$. On the other hand the electrical conductivity plays the dominant role in the variation of dimensionless relative wall pressure $\Delta P_1(0)$ which reduces as M increases. Moreover, the dimensionless wall pressure P_2 is not affected by the increment of M and increases linearly with the increase of β. The coefficient of the heat transfer rate at the wall (sheet) $\theta^*(0)$ decreases with the increase of β and/or M. The polarization has less, nonetheless significant effect on the variation of $\theta^*(0)$ than the electrical conductivity of the biofluid.

Overall, the adoption of the extended BFD model combining the principles of MHD and FHD is necessary to be adopted for the study of stretching sheet problems since for the values of the parameters used both electrical conductivity and polarization play important role in the formation of the flow field.

Chapter 4

Numerical solution of three dimensional unsteady biomagnetic flow and heat transfer through stretching/shrinking sheet using temperature dependent magnetization

The problem of biomagnetic fluid flow and heat transfer in three-dimensional unsteady stretching/shrinking sheet is examined in this chapter. Our model is the version of biomagnetic fluid dynamics (BFD) which is consistent with the principles of ferrohydrodynamics (FHD). Our main contribution is the study of three dimensional time dependent BFD flow which has not been considered yet to our best knowledge. The physical problem is described by a coupled, nonlinear system of ordinary differential equations subject to appropriate boundary conditions. The solution is obtained numerically by applying an efficient numerical technique based on finite differences method. Computations are performed for a wide range of the governing parameters such as ferromagnetic interaction parameter, unsteadiness parameter, stretching parameter and other involved parameters. The effect of these parameters on the velocity and the temperature field are examined. We observed that for decelerated flow, the velocity profile overlap with increasing unsteadiness parameter and we also found that skin friction coefficient is decreased for shrinking sheet whereas, opposite behavior is shown for the stretching sheet. We also monitored the rate of heat transfer coefficient with ferromagnetic interaction parameter and showed opposite behavior for stretching and shrinking sheet (Murtaza et al. (2018)).

4.1 Introduction

When the human body is moving to the various environments, such as travelling or any hard working then the body accelerated or decelerated with time and space as well as flow behavior of blood and temperature are also changes in time. In this situation the blood flow of artery is not normal and heat transfer from surface of skin or body loses heat by sweating or conducting. Most of the author's analysis biomagnetic fluid is steady state. The most

common example of biomagnetic fluid is blood and this type of fluid is a living creature. Since the body always moving in various position in time, so the unsteady state condition analysis is an important of that flow problem.

The influence of the magnetic field on biofluid flow has been extensively investigated for bioengineering and medical applications, Rusetski et al. (1999), Lauva et al. (1993), particularly by controlling blood flow for surgery, cancer treatment, drug targeting, Haik et al. (1999). The mathematical model of ferrofluid over a stretching sheet was used by Andersson and Valnes (1998) and found that the flow has significantly affected in the presence of magnetic dipole. Yasmeen et al. (2016) investigated the flow and heat transfer of ferrofluid over a stretched surface and reported that the velocity profile decreases due to the increases in magnetic number. Zeeshan et al. (2016) studied ferrofluid over stretching sheet and shows the effect of magnetic dipole on flow behavior. Majeed et al. (2016) studied the ferromagnetic flow in unsteady stretching sheet with prescribe heat flux. Abbasbandy and Roohani (2013) studied the MHD viscous flow by using Hankel-Pade method over a shrinking sheet. Rosca et al. (2016) analyzed the fluid flow over a stretching/shrinking sheet with convective boundary condition. Pop et al. (2016) investigated the MHD flow over a stretching / shrinking sheet with electrical conductivity.

Many authors have investigated their several works on blood flow and heat transfer under the action of external magnetic field. Haik et al. (1999) first introduced the mathematical model of BFD. This model is based on the principles of FHD, Rosensweig (1985, 1987). On the base of FHD Tzirtzilakis and Tanoudis (2003) studied the biomagnetic fluid flow over a stretching sheet using Chebyshev pseudospectral method. Further an extended BFD mathematical model was developed by Tzirtzilakis (2005) and this model was based on both the principle of FHD and MHD.

The magnetic field H which is generated by magnetic dipole is affecting on the fluid flow and the magnetization M is attained when the magnetic field is sufficiently strength to saturate the biomagnetic fluid. There are various magnetization equations describing the variation of *M.* Anderson and valnes (1998) considered the magnetization equation varying linearly with temperature dependent whereas Tzirtzilakis and Kafoussia (2010) considered the nonlinear magnetization equation.

Further, mathematical models have been developed for blood flow and many authors assumed blood as Newtonian fluid. Eldesoky (2012) studied the MHD blood flow of unsteady parallel plate in the presence heat source. Misra and Sinha (2013) studied the MHD

flow of blood in a capillary with lumen being porous and wall permeable. Tzirtzilakis et al. (2010) investigated the magnetic fluid over a three dimensional stretching sheet.

Singh and Rathee (2010) studied the blood flow through an artery in the presence of magnetic field with variable blood viscosity. Under the periodic body movement, the MHD pulsatitle flow presented by Das and Saha (2009). Dulal and Ananda (2010) investigated the blood flow through an artery in the presence of magnetic field. Unsteady MHD blood flow through a parallel plate studied by Ali et al. (2015).

Most of the researchers studied steady flow of stretching sheet problems. However the interest of the unsteady flow over a shrinking sheet has considerably increased among researchers. Bachok et al. (2010, 2012) and Fang et al. (2009) studied the unsteady fluid flow over a stretching/shrinking sheet and they emphasized the deviation in flow behaviour's for an unsteady shrinking sheet compared with an unsteady stretching sheet. Further the problems of steady and unsteady stretching/shrinking sheets were also considered by several authors; namely, Nik long et al. (2011), Naramgari et al. (2016), Thumma et al. (2017) etc.

This chapter analyze the BFD flow and heat transfer in case of blood flow along a stretching/shrinking sheet. In the present analysis, the sheet is unsteady and the flow is influenced by the magnetic field. The governing equations are shown to be controlled by several thermophysical parameters governing the physics of the problem under consideration together with the boundary conditions. For the numerical solution we use common finite differences technique together with central difference schemes. Furthermore comparison is performed within some limitations through existing results.

4.2 Mathematical Formulation

We consider an unsteady three dimensional incompressible, viscous, laminar biomagnetic fluid past a stretching/shrinking sheet whose flow direction in the coordinate system is taking place in the (x, y, z) plane with velocities $U(x,t) = U_w(x,t)$, $V(y,t) = V_w(y,t)$ and $w(z,t) = 0$ whereas, z is perpendicular to the (x, y) plane (Fig 4.1). Assume that the fluid occupies the upper half plane $z \geq 0$. The flow field is subject to the presence of a magnetic field generated by a magnetic wire which is located below the sheet at a distance d. The temperature of the sheet T_w is kept fixed and T_c is the temperature far away from the sheet, with $T_w < T_c$.

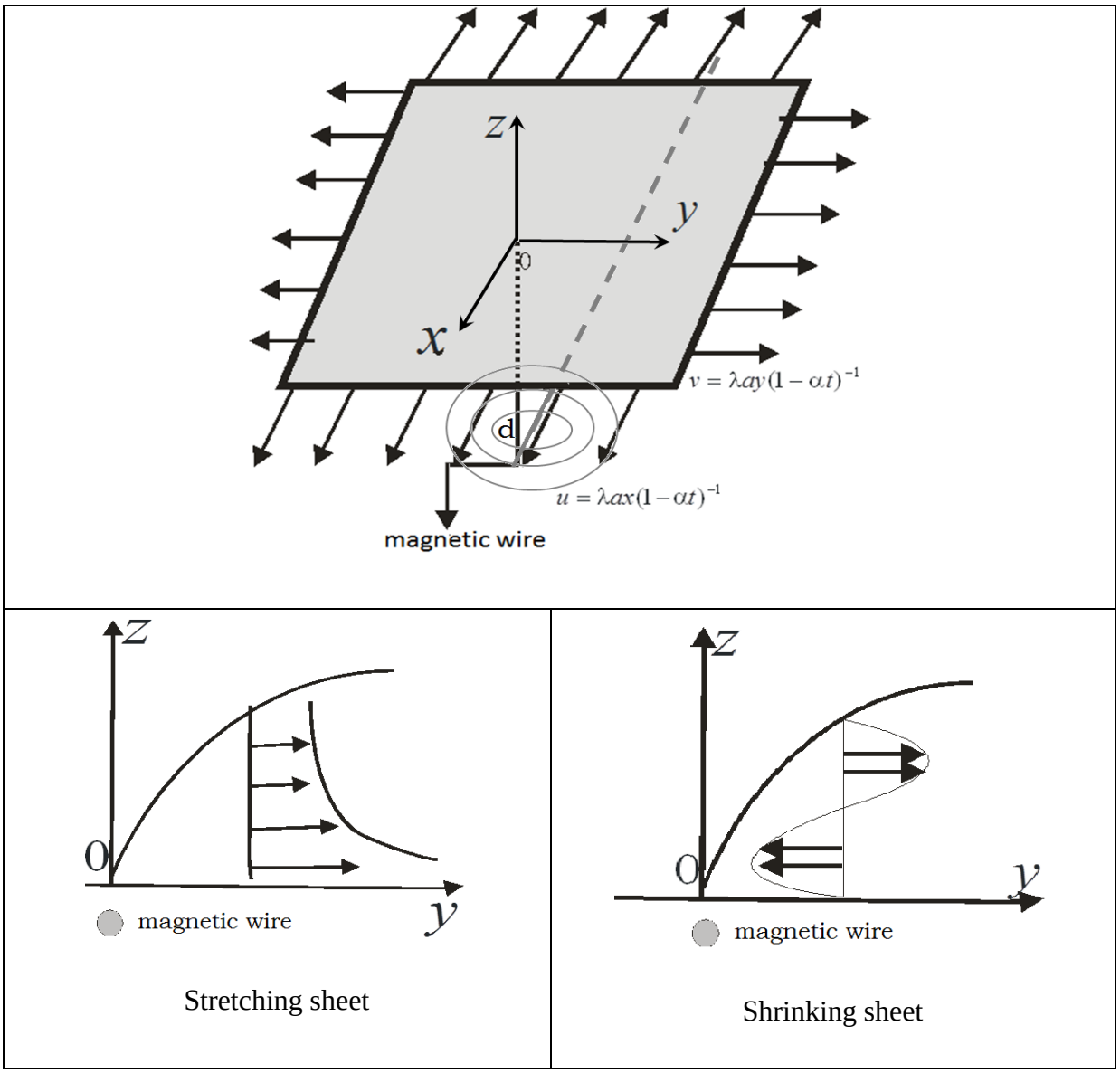

Fig 4.1 Geometry of the model

The governing equations of the unsteady three-dimensional flow of viscous incompressible biomagnetic fluid and heat transfer equations under the influence of magnetic field are Tzirtzilakis and Tanoudis (2003), Tzirtzilakis (2005, 2010), Hafizuddin (2014):

Continuity equation:

$$\frac{\partial \mathrm{u}}{\partial \mathrm{x}} + \frac{\partial \mathrm{v}}{\partial \mathrm{y}} + \frac{\partial w}{\partial \mathrm{z}} = 0 \tag{4.1}$$

Momentum equation:

$$\frac{\partial \mathrm{u}}{\partial \mathrm{t}} + u\frac{\partial \mathrm{u}}{\partial \mathrm{x}} + v\frac{\partial u}{\partial \mathrm{y}} + w\frac{\partial \mathrm{u}}{\partial \mathrm{z}} = -\frac{1}{\rho}\frac{\partial p}{\partial x} + \nu\frac{\partial^2 u}{\partial \mathrm{z}^2} \tag{4.2}$$

$$\frac{\partial \mathrm{v}}{\partial \mathrm{t}} + u\frac{\partial \mathrm{v}}{\partial \mathrm{x}} + v\frac{\partial v}{\partial \mathrm{y}} + w\frac{\partial \mathrm{v}}{\partial \mathrm{z}} = -\frac{1}{\rho}\frac{\partial p}{\partial y} + \frac{1}{\rho}\mu_0 M\frac{\partial H}{\partial y} + \nu\frac{\partial^2 v}{\partial \mathrm{z}^2} \tag{4.3}$$

$$\frac{\partial \mathrm{w}}{\partial \mathrm{t}} + w\frac{\partial \mathrm{w}}{\partial \mathrm{z}} = -\frac{1}{\rho}\frac{\partial p}{\partial \mathrm{z}} + \frac{1}{\rho}\mu_0 M\frac{\partial H}{\partial \mathrm{z}} + \nu\frac{\partial^2 w}{\partial \mathrm{z}^2} \tag{4.4}$$

Energy equation:

$$\rho C_p\left(\frac{\partial T}{\partial t} + u\frac{\partial T}{\partial x} + v\frac{\partial T}{\partial y} + w\frac{\partial T}{\partial z}\right) + \mu_0 T\frac{\partial M}{\partial T}\left(v\frac{\partial H}{\partial y} + w\frac{\partial H}{\partial z}\right) = k\left(\frac{\partial^2 T}{\partial x^2} + \frac{\partial^2 T}{\partial y^2} + \frac{\partial^2 T}{\partial z^2}\right) + \mu\varphi \tag{4.5}$$

Where φ is dissipation function and is given by the expression mentioned in Tzirtzilakis and Kafoussias (2010)

$$\varphi = 2\left[\left(\frac{\partial u}{\partial x}\right)^2 + \left(\frac{\partial v}{\partial y}\right)^2 + \left(\frac{\partial w}{\partial z}\right)^2\right] + \left[\left(\frac{\partial v}{\partial z}\right)^2 + \left(\frac{\partial u}{\partial z}\right)^2\right] \tag{4.6}$$

The initial and boundary conditions for the velocity, temperature and pressure are:

$$t < 0:\ u(x,y,z) = 0,\ v(x,y,z) = 0,\ w(x,y,z) = 0 \text{ for any } x, y, z$$

$$t \le 0:\ u = u_w(x,t) = \lambda a x(1-\alpha t)^{-1},\ v = v_w(y,t) = \lambda a y(1-\alpha t)^{-1},\ w = 0,\ T = T_w \text{ at } z = 0 \tag{4.7}$$

$$u \to 0,\ v \to 0,\ T \to T_c,\ p + \frac{1}{2}\rho q^2 = p_\infty = const \text{ as } z \to \infty \tag{4.8}$$

Here $q=(u,v,w)$ are the velocity of the fluid in x, y and z axis, respectively. t is the time, a is positive constants, p, ρ, μ, ν , α, λ, μ_0, C_p, k, M are the pressure, density, dynamic viscosity, kinematic viscosity, unsteadiness parameter, stretching parameter, magnetic permeability, specific heat at constant pressure, thermal conductivity and magnetization respectively. Note that for $\lambda>0$ the sheet is stretching whereas for $\lambda<0$ the sheet is shrinking.

The terms $\mu_0 M\dfrac{\partial H}{\partial y}$ and $\mu_0 M\dfrac{\partial H}{\partial z}$ in (4.3) and (4.4), respectively, represent the magnetic force in y and z direction which is known as Kelvin forces and the term $\mu_0 T\dfrac{\partial M}{\partial T}\left(v\dfrac{\partial H}{\partial y}+w\dfrac{\partial H}{\partial z}\right)$ in (4.5) represents the Joule heating and the thermal power per unit volume.

The magnetic wire is located below the sheet at a distance d which generates the magnetic field whose components are given by Tzirtzilakis and Kafoussias (2010)

$$H_y(y,z)=-\frac{\gamma}{2\pi}\frac{z+d}{y^2+(z+d)^2} \text{ and } H_z(y,z)=\frac{\gamma}{2\pi}\frac{y}{y^2+(z+d)^2}$$

Therefore, the magnitude $\|H\|=H$ of the magnetic field is given by

$$H(x,y,z)=H(y,z)=\left[H_y^2+H_z^2\right]^{1/2}=\frac{\gamma}{2\pi}\frac{1}{\sqrt{y^2+(z+d)^2}} \tag{4.9}$$

The flow behavior of the biofluid is affected by the magnetic field which is described by the magnetization M. In this analysis, we consider that the magnetization varies with the magnetic field intensity H and temperature T and use the magnetization equation which proposed by Tzirtzilakis and Tanoudis (2003) and Matsuki et al. (1977).

$$M=KH(T_c-T) \tag{4.10}$$

4.3. Mathematical Analysis

We introducing the following non-dimensional variables and velocity as Hafidzuddin et al. (2014) and Tzirtilakis (2010).

$$\left.\begin{aligned}\xi(x) &= \sqrt{\frac{a}{\nu(1-\alpha t)}}\; x\\ \zeta(y) &= \sqrt{\frac{a}{\nu(1-\alpha t)}}\; y\\ \eta(z) &= \sqrt{\frac{a}{\nu(1-\alpha t)}}\; z\end{aligned}\right\} \tag{4.11}$$

$$u = \frac{ax}{1-\alpha t} f'(\eta),\; v = \frac{ay}{1-\alpha t} g'(\eta),\; w = -\sqrt{\frac{a\nu}{1-\alpha t}}\left(f(\eta)+g(\eta)\right). \tag{4.12}$$

where primes denote derivative with respect to η. The continuity equation (4.1) is satisfied using the similarity variables (4.12). The dimensionless pressure $P(\xi,\zeta,\eta)$ and temperature $\theta(\xi,\zeta,\eta)$ of the magnetic fluid are given by the following expressions:

$$P(\xi,\zeta,\eta) = \frac{p}{\frac{a\mu}{1-\alpha t}} = P_1(\eta) + \xi P_2(\eta) + \xi^2 P_3(\eta) + \zeta P_4(\eta) + \zeta^2 P_5(\eta) \tag{4.13}$$

$$\theta(\xi,\zeta,\eta) = \frac{T_c - T}{T_c - T_w} = \theta_1(\eta) + \xi\theta_2(\eta) + \xi^2\theta_3(\eta) + \zeta\theta_4(\eta) + \zeta^2\theta_5(\eta) \tag{4.14}$$

The dimensionless form of the equation (4.9) is

$$H(\zeta,\eta) = \frac{\gamma}{2\pi}\sqrt{\frac{a}{\nu(1-\alpha t)}}\left[\frac{1}{\eta+\delta} - \frac{1}{2}\frac{\zeta^2}{(\eta+\delta)^3}\right] \tag{4.15}$$

where δ is the dimensionless distance of the dipole from the $\xi-$axis $\delta = d\sqrt{\frac{a}{\nu(1-\alpha t)}}$

we also have $\frac{\partial H}{\partial \zeta} = -\frac{\gamma}{2\pi}\frac{a}{\nu(1-\alpha t)}\frac{\zeta}{(\eta+\delta)^3}$ (4.16)

and $\frac{\partial H}{\partial \eta} = \frac{\gamma}{2\pi}\frac{a}{\nu(1-\alpha t)}\left[-\frac{1}{(\eta+\delta)^2} + \frac{3}{2}\frac{\zeta^2}{(\eta+\delta)^4}\right]$ (4.17)

Now substituting all the above expression into the momentum equation (4.2), we have

$$\Rightarrow \frac{a^{\frac{3}{2}}\nu^{\frac{1}{2}}}{(1-\alpha t)^{\frac{3}{2}}}\xi\left[\frac{\alpha}{a}f'+\frac{1}{2}\frac{\alpha}{a}\eta f''+f'^2-(f+g).f''-f'''\right]=-\frac{a^{\frac{3}{2}}\nu^{\frac{1}{2}}}{(1-\alpha t)^{\frac{3}{2}}}(P_2+2\xi P_3)$$

Dividing both side by $\frac{a^{\frac{3}{2}}\nu^{\frac{1}{2}}}{(1-\alpha t)^{\frac{3}{2}}}$ and equate the coefficient of ξ , we get

$$\Rightarrow \frac{\alpha}{a}f'+\frac{1}{2}\frac{\alpha}{a}\eta f''+f'^2-(f+g).f''-f'''=-2P_3$$

$$f'''+(f+g)f''-f'^2-2P_3-A(f'+\frac{\eta}{2}f'')=0$$

Again from momentum equation (4.3), we have

$$\Rightarrow \frac{a^{\frac{3}{2}}}{(1-\alpha t)^{\frac{3}{2}}}\left[\frac{\alpha}{a}g'+\frac{1}{2}\frac{\alpha}{a}\eta g''+g'^2-(f+g).g''-g'''\right]\zeta=-\frac{a^{\frac{3}{2}}\nu^{\frac{1}{2}}}{(1-\alpha t)^{\frac{3}{2}}}(P_4+2\zeta P_5)+$$

$$\frac{\mu_0}{\rho}K(T_c-T_w)(\theta_1+\xi\theta_2+\xi^2\theta_3+\zeta\theta_4+\zeta^2\theta_5)\left(-\frac{\gamma^2}{4\pi^2}\right)\frac{a^{\frac{3}{2}}\nu^{\frac{1}{2}}}{(1-\alpha t)^{\frac{3}{2}}}\left[\frac{\zeta}{(\eta+\delta)^4}-\frac{1}{2}\frac{\zeta^3}{(\eta+\delta)^6}\right]$$

Dividing both sides by $\frac{a^{\frac{3}{2}}\nu^{\frac{1}{2}}}{(1-\alpha t)^{\frac{3}{2}}}$ and equate the coefficient of ζ , we get

$$g'''+(f+g)g''-g'^2-2P_5-A(g'+\frac{\eta}{2}g'')-\frac{\gamma^2}{4\pi^2}\frac{\mu_0 K(T_c-T_w)\rho}{\mu^2}\theta_1\left[\frac{1}{(\eta+\delta)^4}\right]=0$$

$$g'''+(f+g)g''-g'^2-2P_5-A(g'+\frac{\eta}{2}g'')-\frac{\beta\theta_1}{(\eta+\delta)^4}=0$$

From the momentum equation (4.4), we have

$$\Rightarrow -\frac{1}{2}\frac{\alpha}{a}[(f+g)+\eta(f'+g')]+(f+g)(f'+g')+(f''+g'')=(P_1'+\xi P_2'+\xi^2 P_3'+\zeta P_4'+\zeta^2 P_5')+$$

$$\frac{\mu_0}{\rho\nu^2}K(T_c-T_w)(\theta_1+\xi\theta_2+\xi^2\theta_3+\zeta\theta_4+\zeta^2\theta_5)\left(\frac{\gamma^2}{4\pi^2}\right)\left[-\frac{1}{(\eta+\delta)^3}+\frac{2\zeta^2}{(\eta+\delta)^5}-\frac{3}{4}\frac{\zeta^4}{(\eta+\delta)^7}\right]$$

Equating the coefficients of equal power of $\xi^0, \xi^2,$ *and* ζ^2, we get

$$\Rightarrow P_1' + f''+g''+(f+g)(f'+g') - \frac{1}{2}A\left[(f+g)+\eta(f'+g')\right] - \frac{\gamma^2}{4\pi^2}\frac{\mu_0 K(T_c - T_w)}{\rho\nu^2}\frac{1}{(\eta+\delta)^3} = 0$$

$$\Rightarrow P_1' + f''+g''+(f+g)(f'+g') - \frac{1}{2}A\left[(f+g)+\eta(f'+g')\right] - \frac{\gamma^2}{4\pi^2}\frac{\mu_0 K(T_c - T_w)\rho}{\rho\mu^2}\frac{1}{(\eta+\delta)^3} = 0$$

$$\Rightarrow P_1' + f''+g''+(f+g)(f'+g') + \frac{\beta\theta_1}{(\eta+\delta)^3} - \frac{A}{2}\left[(f+g)+\eta(f'+g')\right] = 0$$

Equating the coefficients of equal power of ξ^2, we get

$$P_3' + \frac{\beta\theta_3}{(\eta+\delta)^3} = 0$$

Equating the coefficients of equal power of ζ^2, we get

$$P_5' + \frac{\beta\theta_5}{(\eta+\delta)^3} - \frac{2\beta\theta_5}{(\eta+\delta)^5} = 0$$

Now from energy equation, we have

$$T = T_c - (T_c - T_w)\left(\theta_1(\eta) + \xi\theta_2(\eta) + \xi^2\theta_3(\eta) + \zeta\theta_4(\eta) + \zeta^2\theta_5(\eta)\right)$$

From the energy equation (4.4) and equating the coefficients of equal power of $\xi, \xi^2, \zeta, \zeta^2$, we get the following system of equations.

$$\theta_1'' + P_r\left[(f+g) - \frac{1}{2}A\eta\right]\theta_1' + 2(\theta_3+\theta_5) - \frac{\delta^2\beta\lambda_a(\varepsilon-\theta_1)}{(\eta+\delta)^3}(f+g) - 4\delta^2\lambda_a\left(f'^2+g'^2+f'g'\right) = 0$$

$$\theta_3'' + P_r\left[(f+g) - \frac{1}{2}A\eta\right]\theta_3' - P_r(A+2f')\theta_3 + \frac{\delta^2\beta\lambda_a}{(\eta+\delta)^3}(f+g)\theta_3 - \delta^2\lambda_a f''^2 = 0$$

$$\theta_5'' + P_r\left[(f+g) - \frac{1}{2}A\eta\right]\theta_5' - P_r(A+2g')\theta_5 +$$

$$\delta^2\beta\lambda_a\left[\left(\frac{g'}{(\eta+\delta)^4} + 2\frac{f+g}{(\eta+\delta)^5}\right)(\varepsilon-\theta_1) + \frac{f+g}{(\eta+\delta)^3}\theta_5\right] - \delta^2\lambda_a g''^2 = 0$$

By substituting equation (4.10) and all the above expressions (4.11)-(4.17) into the momentum equations (4.2)-(4.4) and energy equation (4.5), and equating the coefficients of equal power of $\xi, \xi^2, \zeta, \zeta^2$, we get the following system of equations.

$$f'''+(f+g)f''-f'^2-2P_3-A(f'+\frac{\eta}{2}f'')=0 \tag{4.18}$$

$$g'''+(f+g)g''-g'^2-2P_5-A(g'+\frac{\eta}{2}g'')-\frac{\beta\theta_1}{(\eta+\delta)^4}=0 \tag{4.19}$$

$$P_1'+f''+g''+(f+g)(f'+g')+\frac{\beta\theta_1}{(\eta+\delta)^3}-\frac{A}{2}\left[(f+g)+\eta(f'+g')\right]=0 \tag{4.20}$$

$$P_3'+\frac{\beta\theta_3}{(\eta+\delta)^3}=0 \tag{4.21}$$

$$P_5'+\frac{\beta\theta_5}{(\eta+\delta)^3}-\frac{2\beta\theta_5}{(\eta+\delta)^5}=0 \tag{4.22}$$

$$\theta_1''+P_r\left[(f+g)-\frac{1}{2}A\eta\right]\theta_1'+2(\theta_3+\theta_5)-\frac{\delta^2\beta\lambda_a(\varepsilon-\theta_1)}{(\eta+\delta)^3}(f+g)-4\delta^2\lambda_a\left(f'^2+g'^2+f'g'\right)=0 \tag{4.23}$$

$$\theta_3''+P_r\left[(f+g)-\frac{1}{2}A\eta\right]\theta_3'-P_r(A+2f')\theta_3+\frac{\delta^2\beta\lambda_a}{(\eta+\delta)^3}(f+g)\theta_3-\delta^2\lambda_a f''^2=0 \tag{4.24}$$

$$\begin{aligned}&\theta_5''+P_r\left[(f+g)-\frac{1}{2}A\eta\right]\theta_5'-P_r(A+2g')\theta_5+\\&\delta^2\beta\lambda_a\left[\left(\frac{g'}{(\eta+\delta)^4}+2\frac{f+g}{(\eta+\delta)^5}\right)(\varepsilon-\theta_1)+\frac{f+g}{(\eta+\delta)^3}\theta_5\right]-\delta^2\lambda_a g''^2=0\end{aligned} \tag{4.25}$$

Also, the boundary conditions (4.7) and (4.8) become

$$f'=\lambda,\ g'=\lambda,\ \theta_1=1,\ \theta_3=\theta_5=0,\ f=g=0 \quad \text{at } \eta=0 \tag{4.26}$$

$$f'\to 0, g'\to 0, P_1\to P_\infty,\ P_3=P_5=0 \text{ as } \eta\to\infty \tag{4.27}$$

The dimensionless parameters are:

$P_r=\frac{\mu c_p}{k}$ Prandtl number

$\lambda_a=\frac{\mu^3}{\rho^2 k(T_c-T_w)d^2}$ viscous dissipation parameter

$\varepsilon = \dfrac{T_c}{T_c - T_w}$ dimensionless Curie temperature

$\beta = \dfrac{\gamma^2}{4\pi^2}\dfrac{K\mu_0(T_c - T_w)\rho}{\mu^2}$ ferromagnetic interaction parameter

$\delta = d\sqrt{\dfrac{a}{\nu(1-\alpha t)}}$ dimensionless distance

$A = \dfrac{\alpha}{a}$ dimensionless unsteadiness parameter

For the present work, when $(A > 0)$ we have the case of the accelerated flow whereas for $(A < 0)$ we have decelerated flow.

4.4 Numerical Method

The essential features of the numerical technique used in the present paper are the following: (i) It is based on the common finite difference method with central differencing (ii) on a tridiagonal matrix manipulation and (iii) on an iterative procedure. This methodology developed by Kafoussias and Williams (1993). The equations (4.18)-(4.19) are highly nonlinear. So first we consider the first momentum equation and reduce it to a second order linear differential equation by considering

$$F(x) = f'(\eta),\ F'(x) = f''(\eta),\ F''(x) = f'''(\eta)$$

Now we rewrite the equation (4.18) as follows

$$\Rightarrow F''(x) + (f+g)F'(x) - f'F(x) - 2P_3 - A(F(x) + \frac{\eta}{2}F'(x)) = 0$$

$$\Rightarrow F''(x) + ((f+g) - \frac{\eta}{2}A)F'(x) - (f'+A)F(x) - 2P_3 = 0$$

which is of the form

$$P(x)F''(x) + Q(x)F'(x) + R(x)F(x) = S(x) \tag{4.28}$$

where $P(x) = 1,\ \ Q(x) = f + g - \dfrac{\eta}{2}A,\ \ R(x) = -(f'+A),\ \ S(x) = 2P_3$

In an analogous manner all equations of the system can be reduced in this form of equation (4.28) except equations (4.20)-(4.22) which are already first order differential equations. Equation (4.18) and (4.19) can be solved by two point boundary value problem which execute the following steps: (i) based on central differencing (ii) tridiagonal matrix manipulation and (iii) iteration procedure. This method is detail in Kaffoussias and Williams (1993).

To start the solution procedure we first have to set initial guesses for $f'(\eta)$, $g'(\eta)$, $\theta_1(\eta)$, $\theta_3(\eta)$, $\theta_5(\eta)$ between $\eta = 0$ and $\eta = \eta_\infty (\eta_\infty \to \infty)$ which should obviously satisfy the boundary conditions (4.26) and (4.27). For the present problem we insert the following initial guesses: $f'(\eta) = g'(\eta) = \left(\lambda - \frac{\eta}{\eta_\infty}\right)$, $\theta_1(\eta) = \left(1 - \frac{\eta}{\eta_\infty}\right)$, $\theta_3(\eta) = \theta_5 = 0.5\left(\frac{\eta}{\eta_\infty}\right)\left(1 - \frac{\eta}{\eta_\infty}\right)$.

By integration of $f'(\eta)$ we determine the value of $f(\eta)$. Hereafter we assume that f, g, P_3, P_5, θ_1 are known and calculate new estimations for $f'(\eta), f'_{new}(\eta)$ *and* $g'(\eta), g'_{new}(\eta)$. These values are used for new inputs, the profiles are updated and so on. Finally, the solution is achieved iteratively until the criterion of convergence is satisfied.

After $f'(\eta)$ is obtained the solution of the energy equation (4.23) with boundary conditions (4.26) and (4.27) is solved by using the same algorithm, but without iteration now as far as Eq. (4.23) is linear. Equation (4.23) is

$$\theta_1'' + P_r\left[(f+g) - \frac{1}{2}A\eta\right]\theta_1' + 2(\theta_3 + \theta_5) - \frac{\delta^2\beta\lambda_a(\varepsilon - \theta_1)}{(\eta+\delta)^3}(f+g) - 4\delta^2\lambda_a\left(f'^2 + g'^2 + f'g'\right) = 0$$

which can be written as

$$\theta_1'' + P_r\left[(f+g) - \frac{1}{2}A\eta\right]\theta_1' + \frac{\delta^2\beta\lambda_a}{(\eta+\delta)^3}(f+g)\theta_1 = -2(\theta_3 + \theta_5) + \frac{\delta^2\beta\lambda_a\varepsilon}{(\eta+\delta)^3}(f+g) + 4\delta^2\lambda_a\left(f'^2 + g'^2 + f'g'\right)$$

By setting $y(\eta) = \theta_1(\eta)$ is again a second-order linear differential equation of the form

$$P(x)F''(x) + Q(x)F'(x) + R(x)F(x) = S(x)$$

Where $P(x) = 1,\ Q(x) = P_r\left[(f+g) - \frac{1}{2}A\eta\right],\ R(x) = \frac{\delta^2\beta\lambda_a}{(\eta+\delta)^3}(f+g),$

$$S(x) = -2(\theta_3 + \theta_5) + \frac{\delta^2 \beta \lambda_a \varepsilon}{(\eta + \delta)^3}(f + g) + 4\delta^2 \lambda_a \left(f'^2 + g'^2 + f'g'\right)$$

Considering $f, f', g, g', \theta_3, \theta_5$ known, we obtain a new approximation θ_{1new} for θ_1 and this process continues until convergence is attained up to a small quantity ε and finally we obtain θ_1.

In this problem we use discretization step $\Delta\eta = 0.01$ and by trial and error we consider the value of $\eta_\infty = 6,$ and convergence criterion $\varepsilon = 10^{-4}$ defined as $\varepsilon = \max_{i=1,N}\left(\left|\frac{f_{old}(i) - f_{new}(i)}{f_{old}(i)}\right|\right)$. The process is repeated until the results are corrected up to a desired accuracy.

4.5 Results and Discussion

In this chapter, unsteady biomagnetic fluid flow along a three dimensional stretching/shrinking sheet under the action of a magnetic field has been investigated numerically. The governing parameters such as unsteadiness parameter A, Stretching parameter λ, Prandtle number P_r, and ferromagnetic interaction parameter β have a significant impact on flow and heat transfer. As far as the values of the magnetic parameters are concerned, there have been extended discussions in various studies for the possible case scenarios corresponding to plausible physical problems, Tzirtzilakis (2005, 2008), Tzirtzilakis and Xenos (2013), Loukopoulos and Tzirtzilakis (2004). Especially the biomagnetic interaction parameter β can take a quite large range of values depending by the magnetic field gradient. So, for the fluid which is considered to be blood we have that: $\rho = 1050\, kg/m^3$, $\mu = 3.2\times10^{-3}\, kgm^{-1}s^{-1}$, $\sigma = 0.8 sm^{-1}$, $C_p = 14.65\, JKg^{-1}.K^{-1}$, $k = 2.2\times10^{-3}\, Jm^{-1}s^{-1}k^{-1}$ by Tzirtzilakis (2013) and hence $P_r = \frac{\mu C_p}{k} = 21$, for a human body temperature by Loukopoulos and Tzirtzilakis (2004) $T_w = 37^0 C$ whereas the body curie temperature is $T_c = 41^0 C$, hence the dimensionless temperature is $\varepsilon = 78.5$.

The ferromagnetic number β, is defined as $\beta = \frac{I^2}{4\pi^2}\frac{K\mu_0(T_c - T_w)\rho}{\mu^2} = \frac{M_s B_s \rho d^2}{\mu^2}$

where $M_s = KH(0,0)(T_c - T_w)$, $B_s = \mu_0 H(0,0)$, $H(0,0)$ are the magnetization, the magnetic field induction and the magnetic field strength intensity at the wall, respectively.

For magnetic field 1T to 10T, the blood has reached magnetization of $40 Am^{-1}$ by Tzirtzilakis (2005). Ferromagnetic interaction parameter is calculated from the above relation and the corresponding range is from $\beta = 1\times10^3 \; to \; 1\times10^5$. Note that $\beta = 0.0$ corresponds to hydrodynamic flow.

In order to verify the accuracy of the present method, the values of skin frictions $f''(0), g''(0)$ compared with the results in Hafizuddin et al. (2014) and Surma Devi et al. (1986) for $\beta = 0 \; and \; f'(0) = 1, \; g'(0) = 0.5$. The comparison indicates excellent agreement with previous data.

Table 4.1. The value of skin friction coefficients $f''(0), g''(0)$ varying with unsteadiness parameter.

Unsteadiness Parameter	Present result		Hafizuddin et al. (2014)		Surma Devi et al. (1986)	
A	$-f''(0)$	$-g''(0)$	$-f''(0)$	$-g''(0)$	$-f''(0)$	$-g''(0)$
-1.0	0.79127	0.29566	0.7912	0.2956	0.7912	0.2956
-0.75	0.86731	0.33839	0.8673	0.3384	0.8673	0.3384
-0.5	0.94301	0.38092	0.9430	0.3809	0.9430	0.3809
0.25	1.01833	0.42325	1.0183	0.4232	1.0183	0.4232
0.0	1.09323	0.46533	1.0931	0.4652	1.0931	0.4652
0.25	1.16753	0.50706	1.1674	0.5059	1.1674	0.5059
0.5	1.24074	0.54806	1.2407	0.5480	1.2407	0.5480
0.75	1.31217	0.58784	1.3122	0.5878	1.3122	0.5878
1.0	1.38132	0.62604	1.3814	0.6261	1.3814	0.6261

Fig. 4.2-4.4 show the effect of unsteadiness parameter on velocity and temperature profiles in reducing mode (A < 0) and accelerated mode (A>0).

In Fig. 4.2, we observe the velocity profiles for the variation of unsteady parameter for the stretching/shrinking sheet respectively. For decelerated flow (A<0), the fluid velocity increases with the increment of the unsteadiness parameter A and this behavior is happening approximately near the wall within the region (η<1.2) whereas, far away from the wall this behavior is reversed. On the other hand, for accelerated flow (A>0), the velocity is decreased with the increment of the unsteadiness parameter A in whole region.

Fig. 4.3 shows that velocity profile $g'(\eta)$ for y axis. It is evident from the plots that for decelerated flow (A<0), the velocity decreases with the increment of the unsteadiness parameter near the wall and the opposite behaviour is observed away from the boundary. For accelerated flow, increment of the unsteadiness parameter results to the decrement of the boundary layer thickness in the whole region.

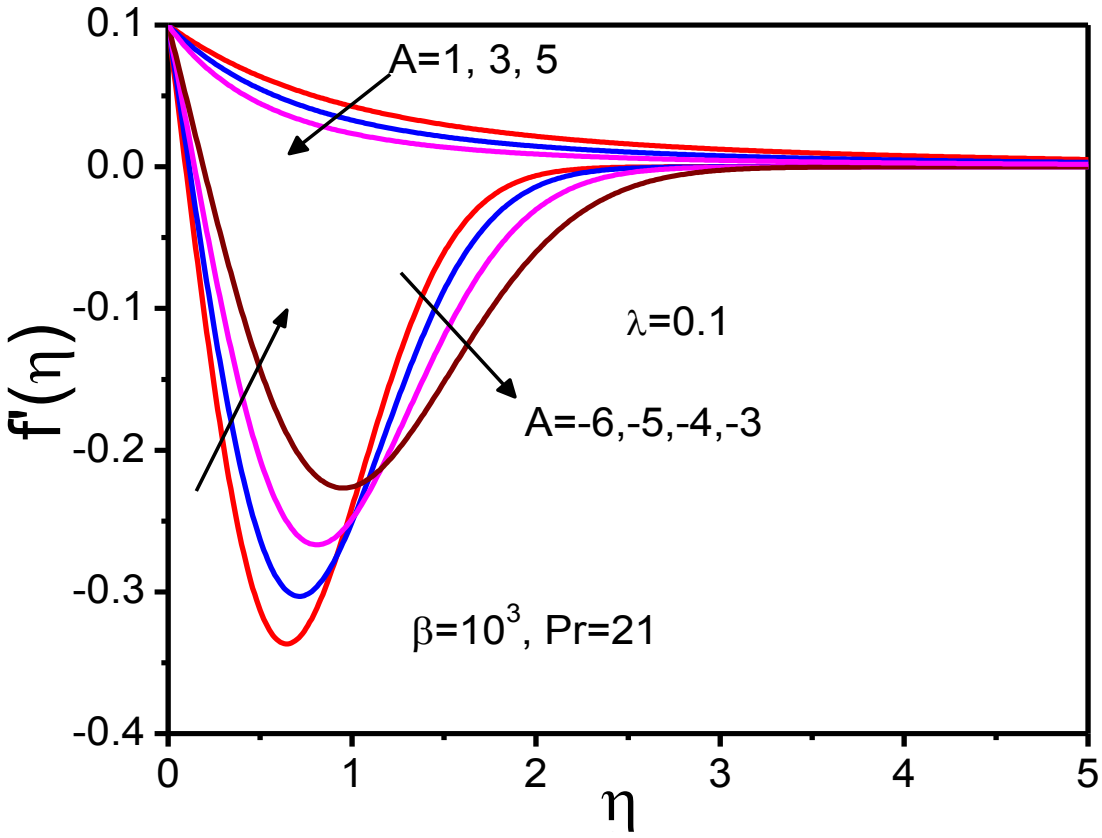

Fig. 4.2: The velocity profile $f'(\eta)$ for different values of unsteadiness parameter A

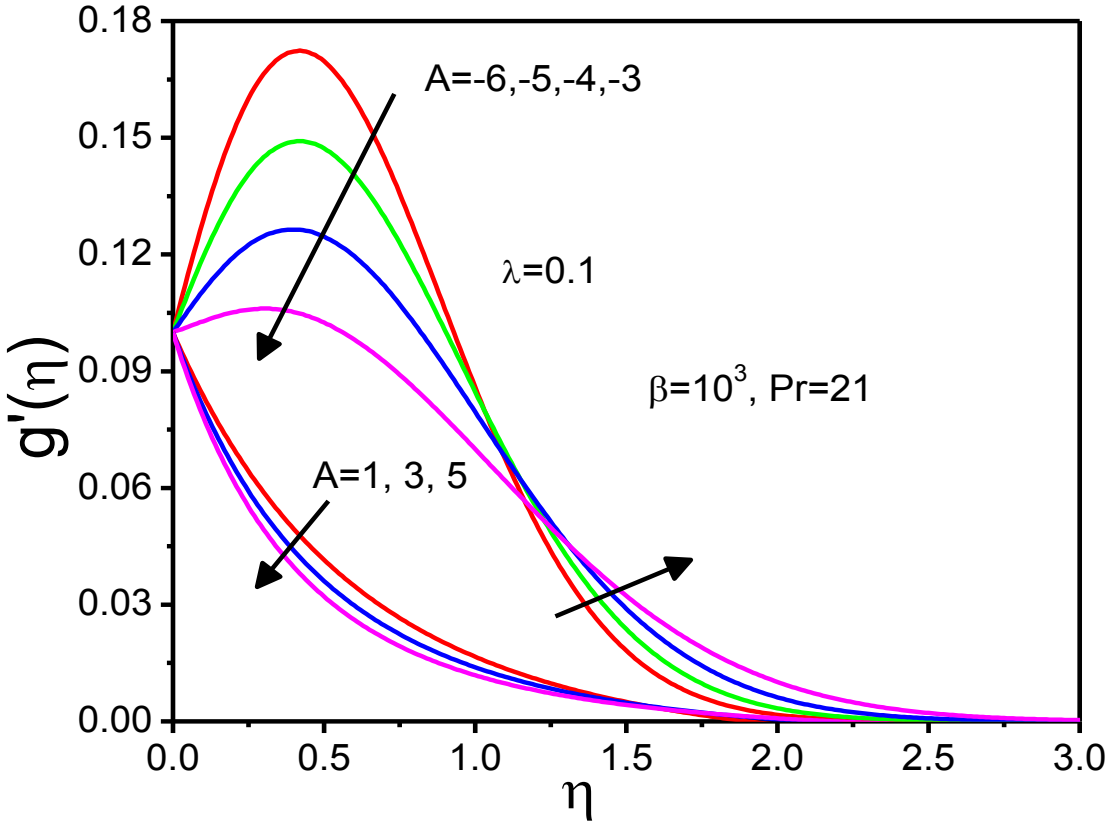

Fig. 4.3: The velocity profile $g'(\eta)$ for different values of unsteadiness parameter A

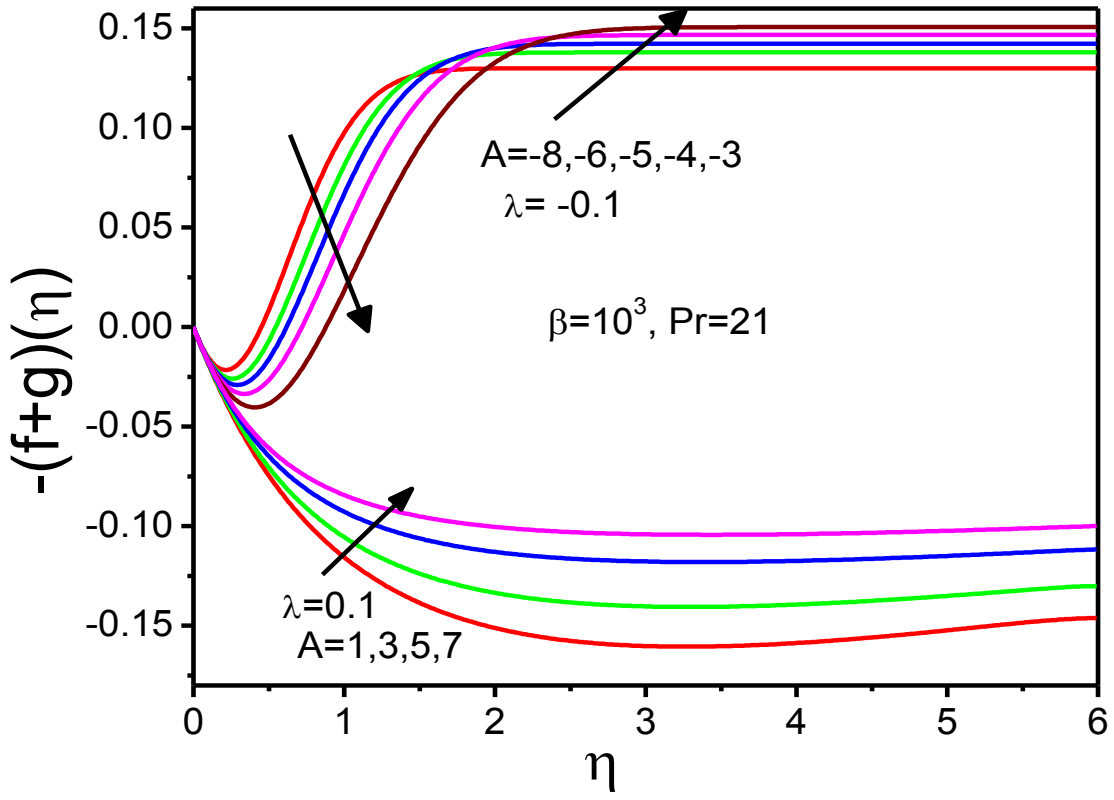

Fig 4.4: The velocity profile for $-(f(\eta)+g(\eta))$ for different values of unsteadiness parameter A

Figure 4.4 present the velocity profile $-(f(\eta)+g(\eta))$ for the z axis. We observe that for A<0, the velocity is found to decrease with the increment of the unsteadiness parameter near the wall and the reverse trend is observed at $\eta_{appro}=2.0$. For the accelerated flow the boundary layer thickness decreases monotonically with the increment of the unsteadiness parameter A.

Fig. 4.5 demonstrates the temperature profiles $\theta_1(\eta)$, for various values of the unsteadiness parameter for decelerated flow. The temperature profile $\theta_1(\eta)$ is increased with the increment of the unsteadiness parameter.

Figs.4.6-4.13 show the combine impact of stretching and shrinking sheet for various parameters. In fig. 4.6 we see that for a stretching sheet, the velocity profile decreases with the increment of the unsteady parameter but this result is reversed for the shrinking sheet. Hence we conclude that for stretching sheet, increment of the unsteady parameter results to resistant of the flow i.e. reduction the momentum boundary layer thickness.

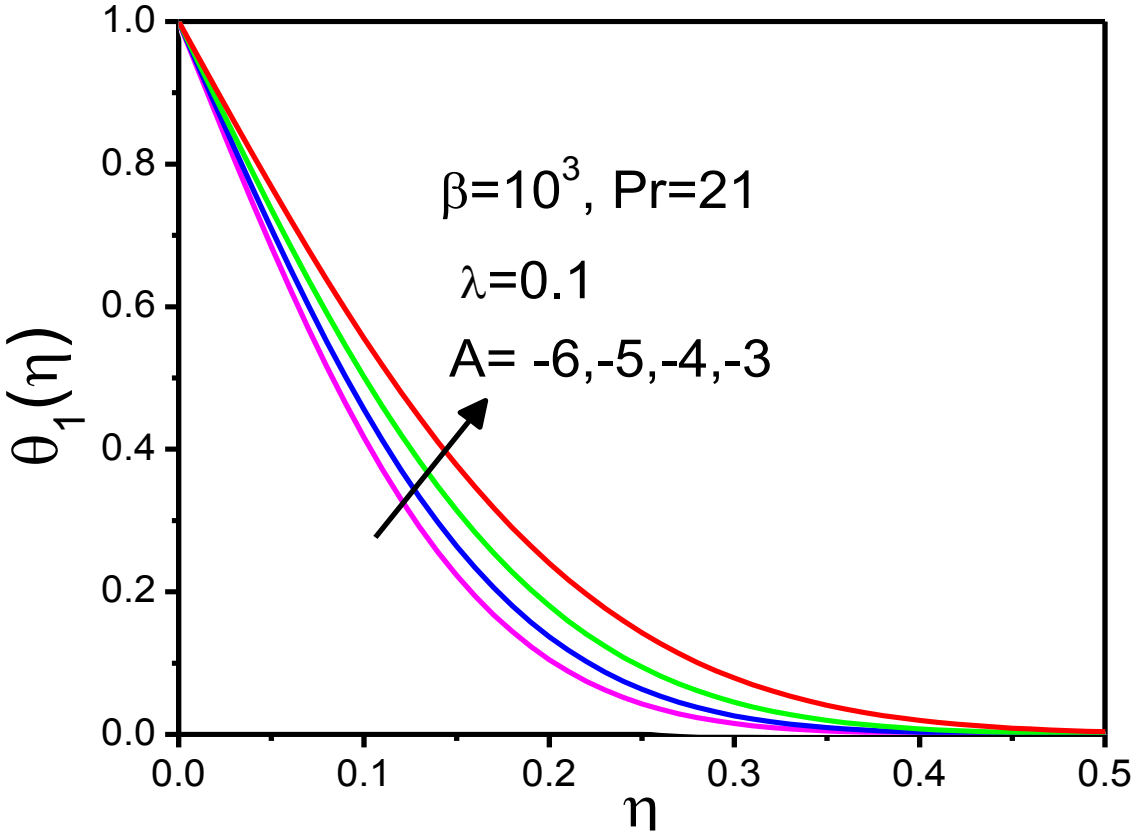

Fig 4.5: The temperature profile $\theta_1(\eta)$ for different values of unsteadiness parameter A

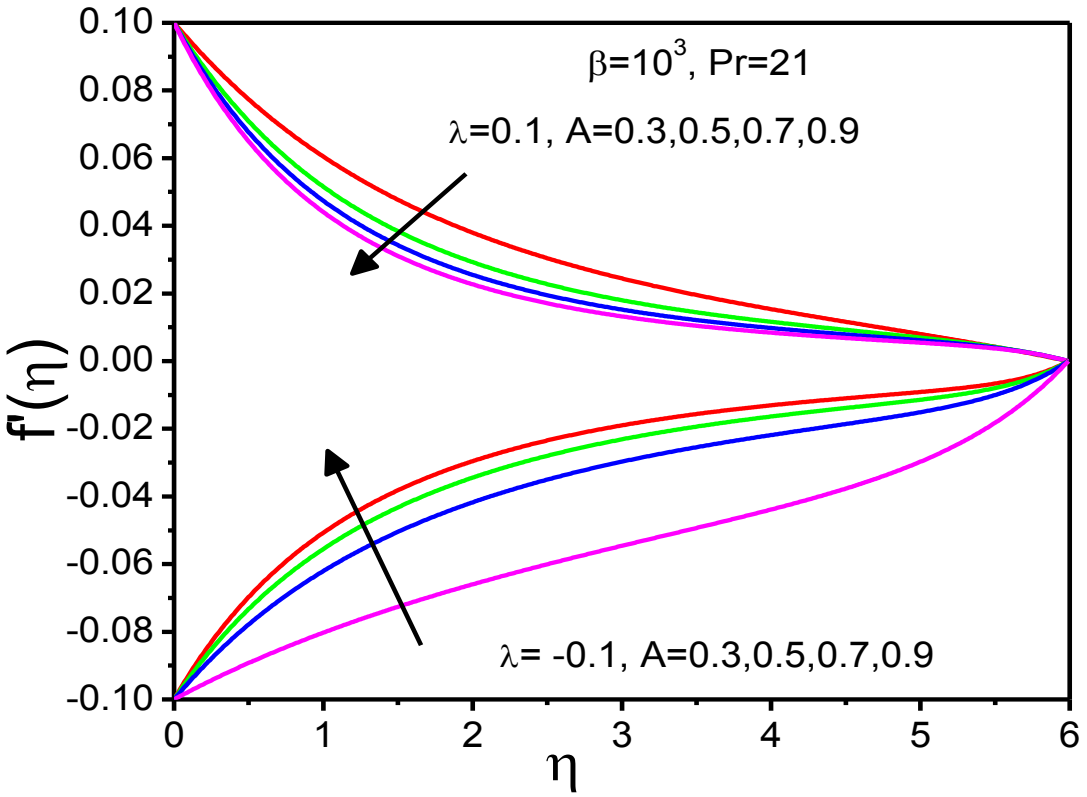

Fig 4.6: The velocity profile for $f'(\eta)$ for different values of unsteadiness parameter A with stretching/shrinking sheet.

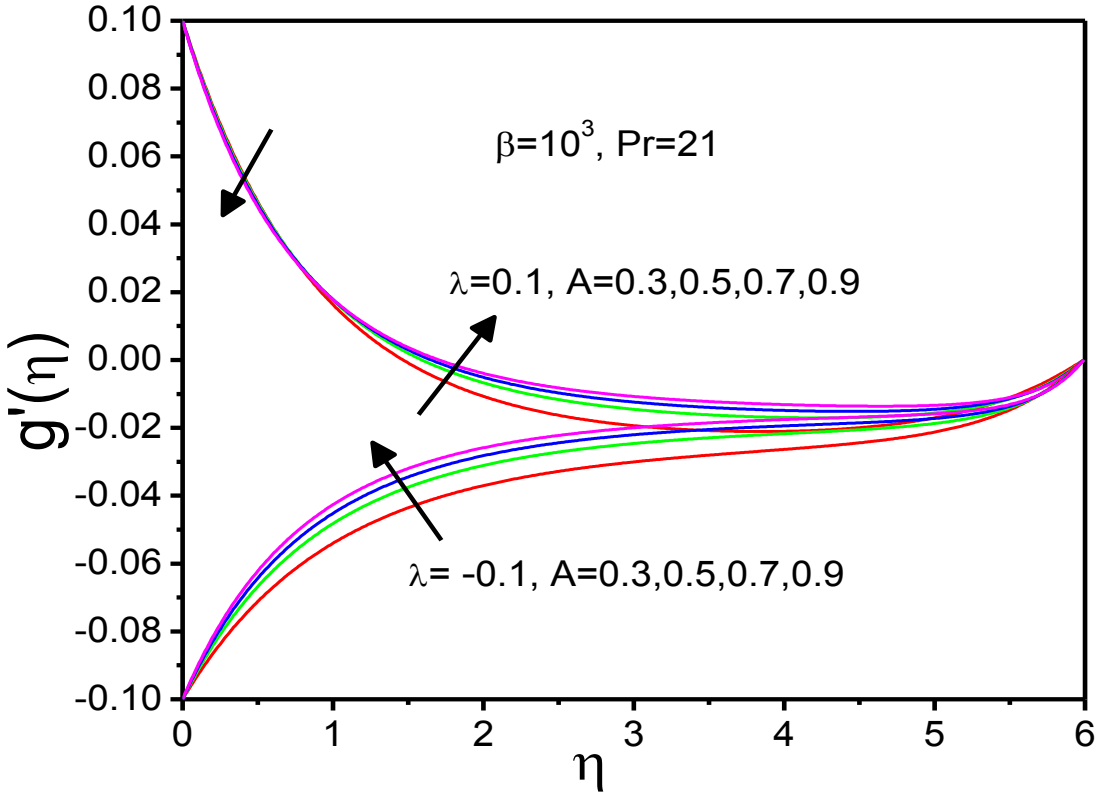

Fig 4.7: The velocity profile for $g'(\eta)$ for different values of unsteadiness parameter A with stretching/shrinking sheet.

From Fig. 4.7, we observe that increasing the unsteadiness parameter results to the increment of the velocity profile $g'(\eta)$ for both stretching and shrinking case.

On the other hand, Fig. 4.8 shows that the increasing of the unsteadiness parameter results to decrement of the distribution of the velocity profile $-(f(\eta)+g(\eta))$ for the shrinking case whereas, the opposite occurs for the stretching case. The temperature profile $\theta_1(\eta)$ is pictured at Fig. 4.9. We observe that the increment of the unsteadiness parameter results to the increment of the temperature profile for both stretching and shrinking case. In all cases the effect of unsteadiness parameter is more effective in shrinking sheet than the stretching one.

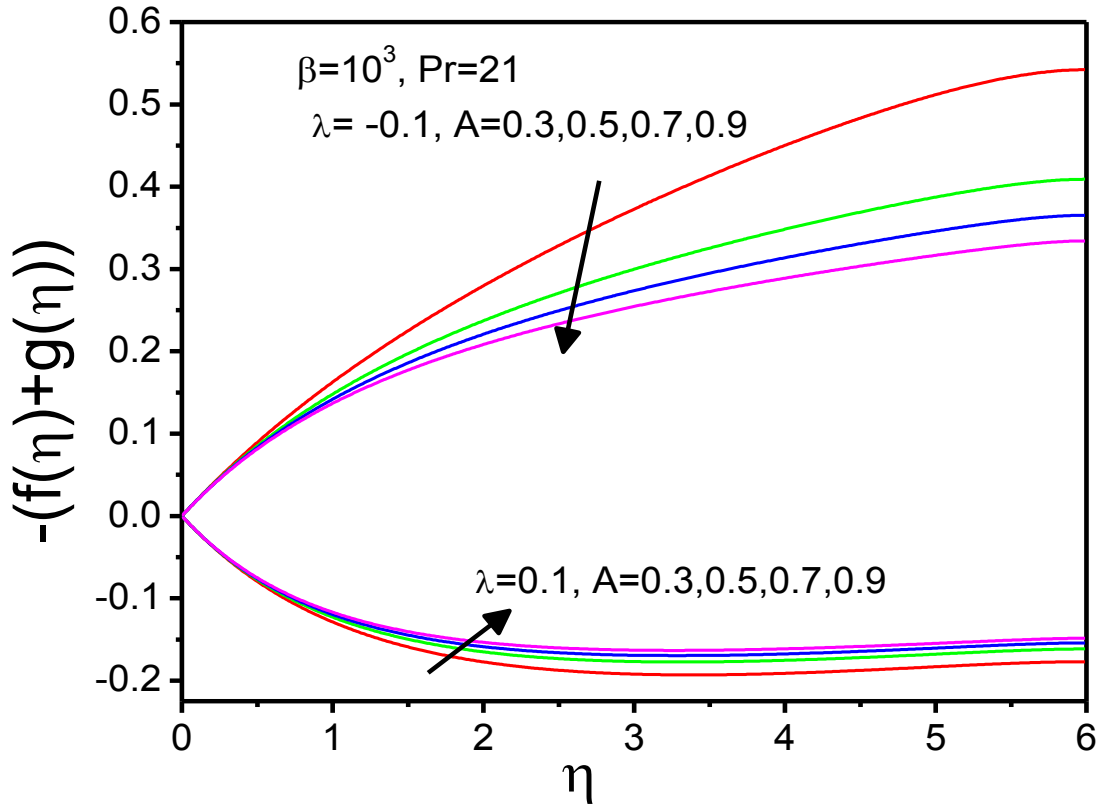

Fig 4.8: The velocity profile for $-(f(\eta)+g(\eta))$ for different values of unsteadiness parameter A with stretching/shrinking sheet.

Fig. 4.10-4.12 exhibit the impact of the magnetic field on velocity profiles for stretching and shrinking cases, respectively. We observe that for stretching sheet, $f'(\eta)$ and $g'(\eta)$ exhibit the reverse behavior as the magnetic field is increased. From Fig. 4.10 it is observed that $f'(\eta)$ is greater than that of the corresponding hydrodynamic case and is increased with the increment of the magnetic parameter for the stretching case. The opposite is happening for the shrinking case.

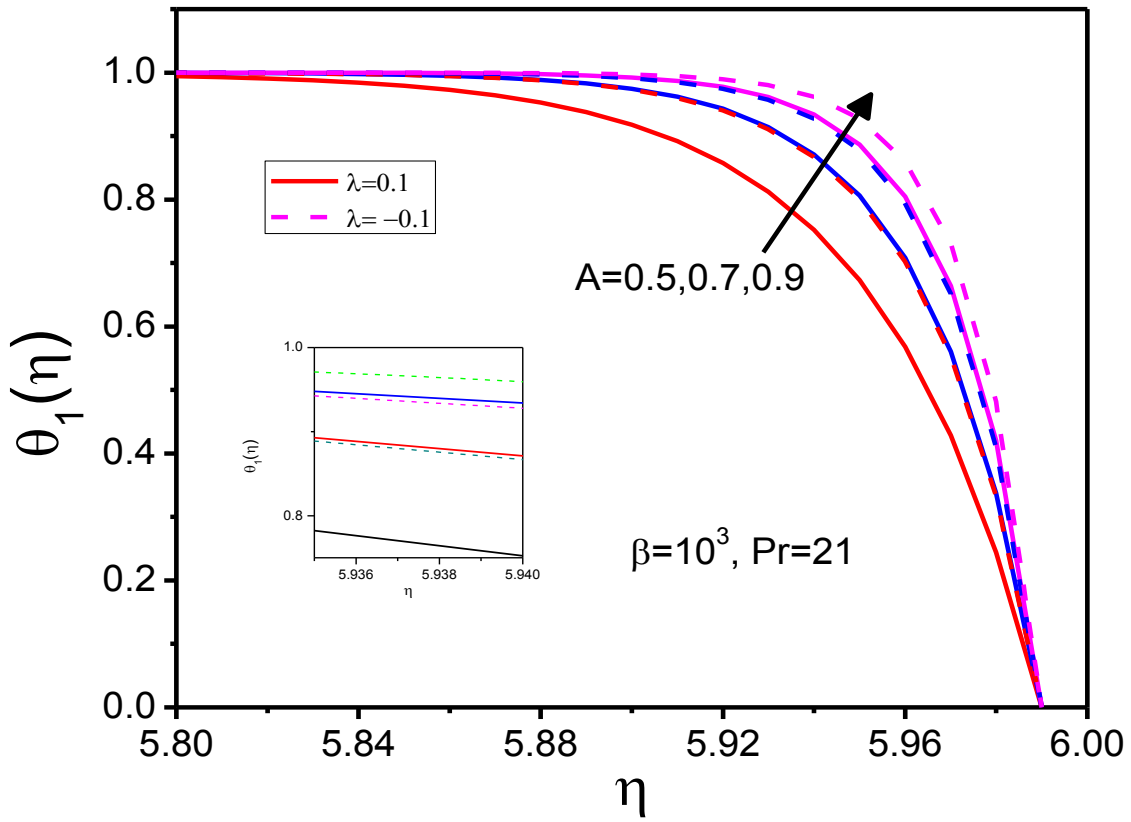

Fig 4.9: The temperature profile $\theta_1(\eta)$ for different values of unsteadiness parameter A with stretching/shrinking sheet.

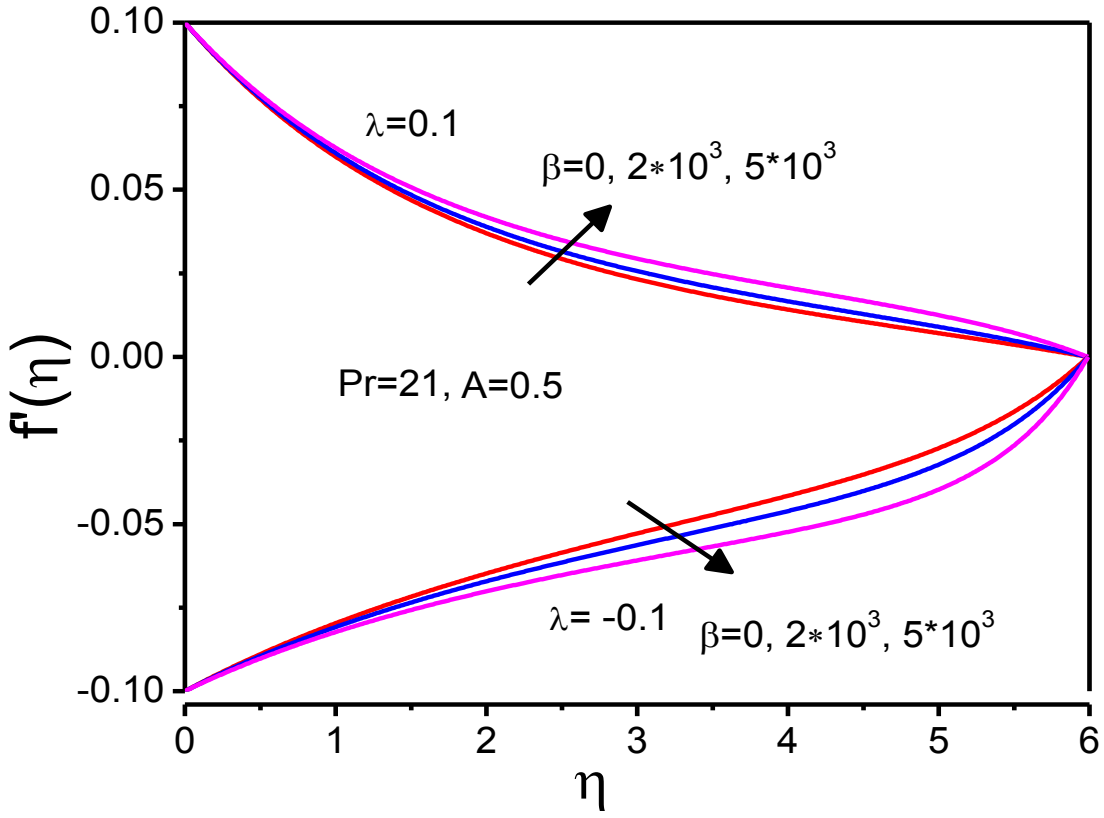

Fig. 4.10 The velocity profile $f'(\eta)$ of stretching/shrinking sheet with different ferromagnetic parameter β

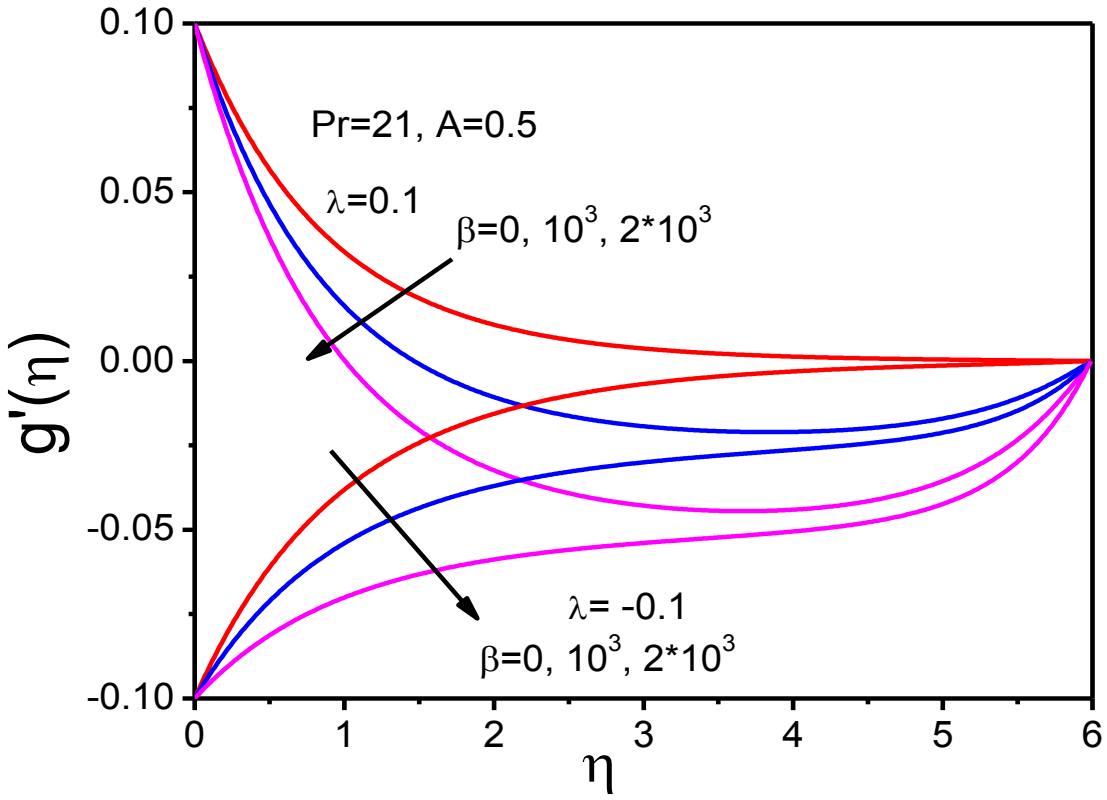

Fig 4.11 The velocity profile for $g'(\eta)$ of stretching/shrinking sheet with different ferromagnetic parameter β

The behavior of $g'(\eta)$ is pictured at Fig 4.11. The distribution of $g'(\eta)$ is reduced with the increment of the magnetic parameter for the shrinking and the stretching sheet as well. The opposite is observed for the distributions of $-(f(\eta)+g(\eta))$ pictured at Fig. 4.12. This is happening because the Kelvin force acts on the sheet towards the y and z axis.

Fig. 4.13 depicts the impact of magnetic field on temperature profiles for stretching/shrinking cases respectively. From this figure it is apparent that the temperature profiles are increased in both stretching and shrinking case with the increment of the magnetic field parameter. The reason of this behavior is that the increment in magnetic field results to the reduction of the boundary layer thickness and enhances the thermal conductivity of the fluid in the stretching/shrinking sheet. This effect is more intense for the shrinking case compared to the one of the stretching case.

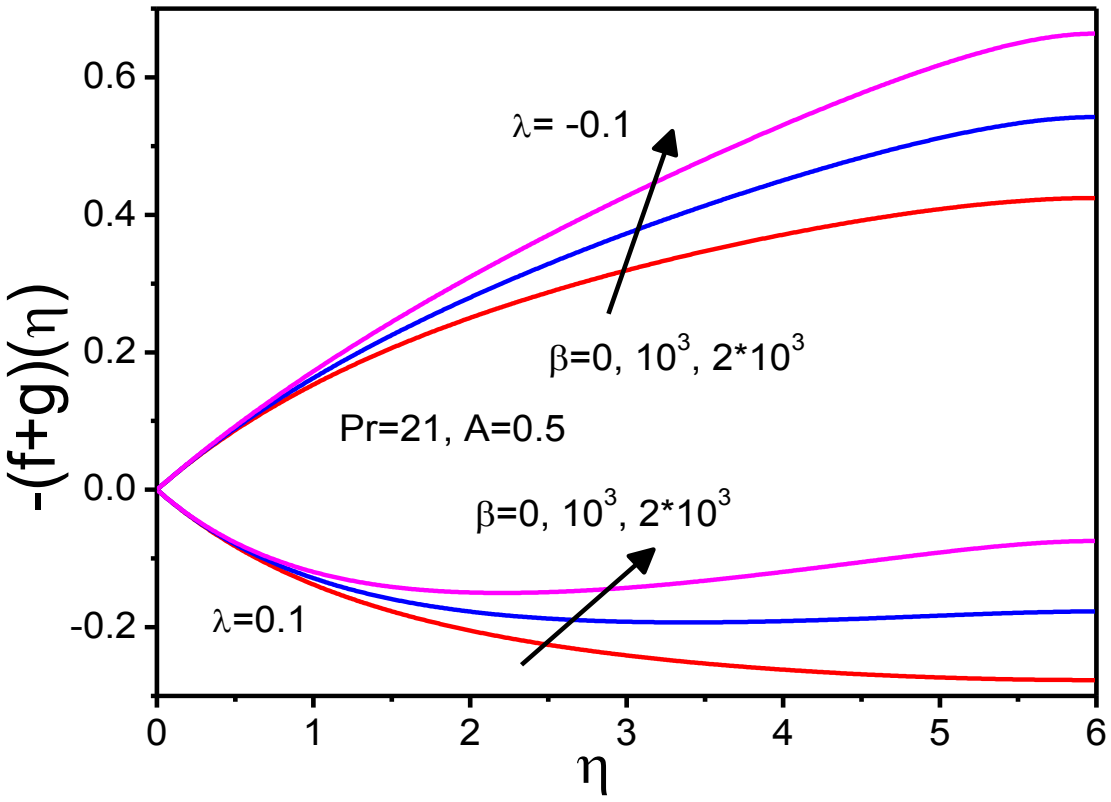

Fig. 4.12: The velocity profile $-(f(\eta)+g(\eta))$ for different values of ferromagnetic parameter β with stretching/shrinking sheet.

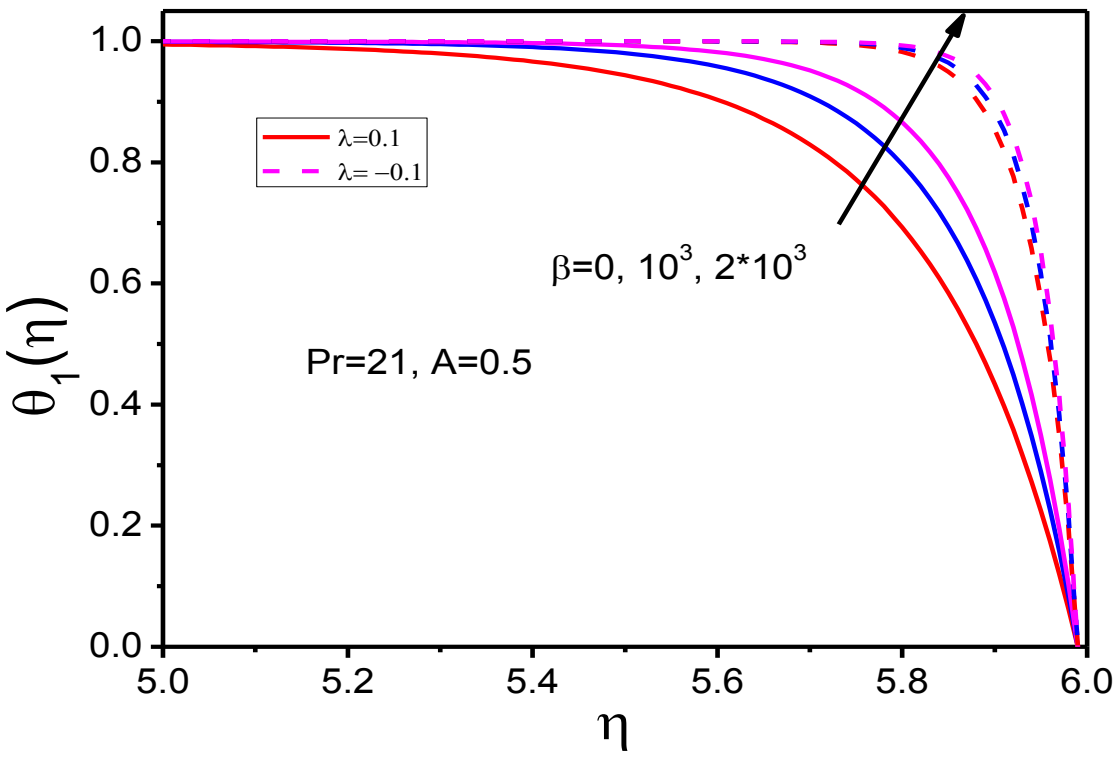

Fig 4.13: The temperature profile $\theta_1(\eta)$ for different values of ferromagnetic β with stretching/shrinking sheet.

Figs. 4.14 and 4.15 depict the skin friction coefficients ($f''(0)$, $g''(0)$) with respect to the parameter λ for various values of A. It is noted that as the unsteadiness parameter A is increased, the velocity gradients near the wall are decreased for shrinking sheet whereas are increased for the stretching one.

Figs. 4.16-4.17 depict the skin friction coefficient $(-g''(0))$ with respect to the unsteadiness parameter A and shrinking/stretching parameter λ for different values of ferromagnetic parameter β. It is observed that the skin friction coefficient increases with the increment of the magnetic parameter β. Finally, Fig 4.18 shows that the wall temperature gradient is increased with the increment of the ferromagnetic field parameter β in the shrinking region whereas is reduced in the stretching region.

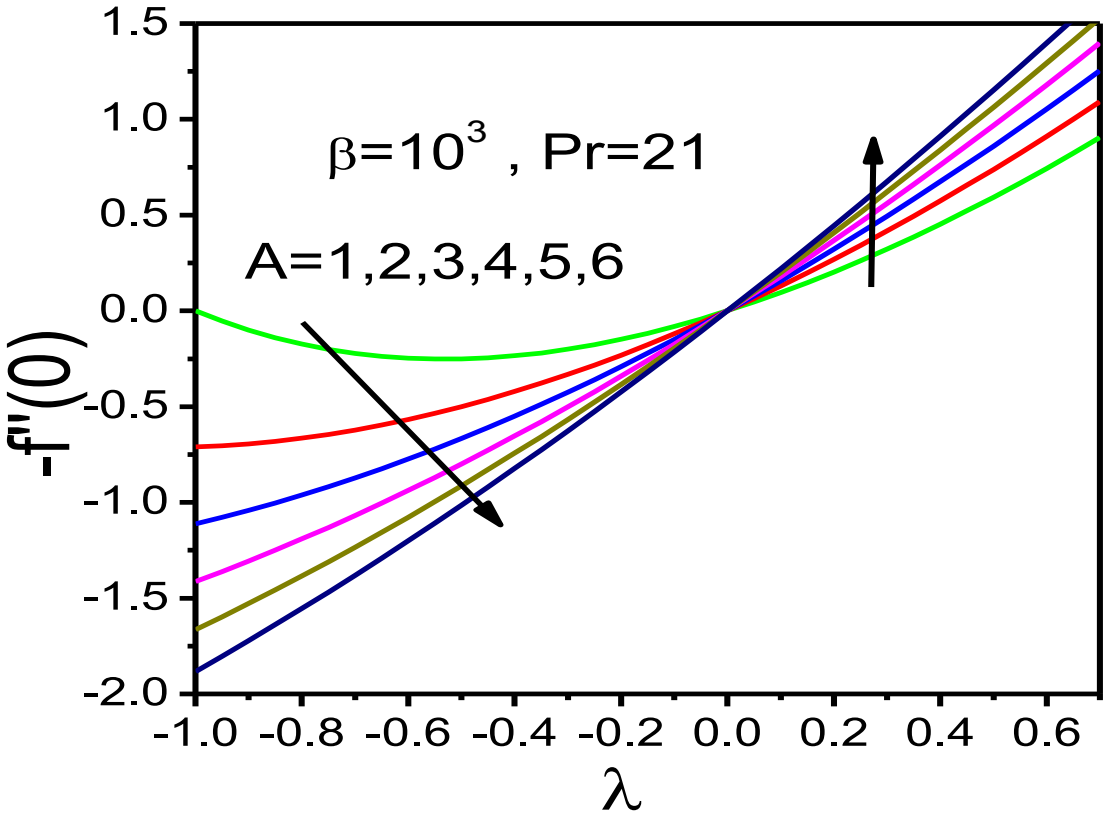

Fig 4.14: Skin friction coefficient $-f''(0)$ with λ for different values of A

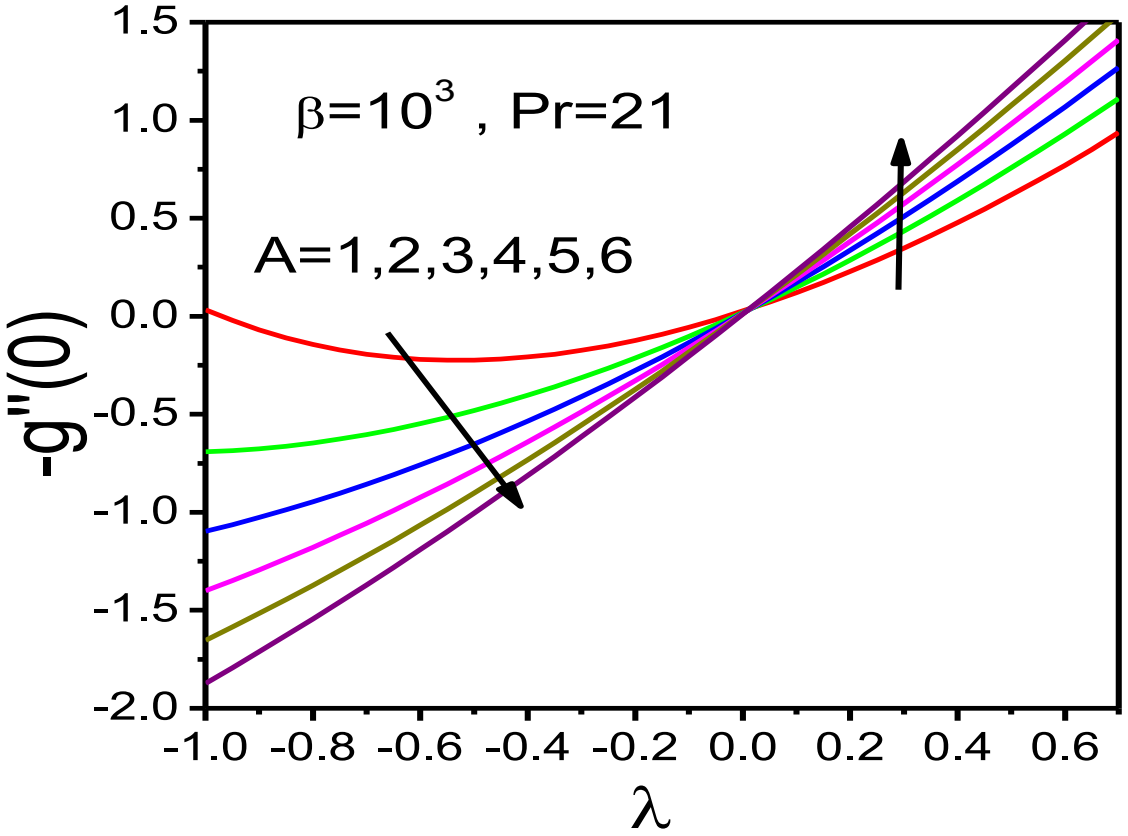

Fig 4.15: Skin friction coefficient $-g''(0)$ with λ for different values of A

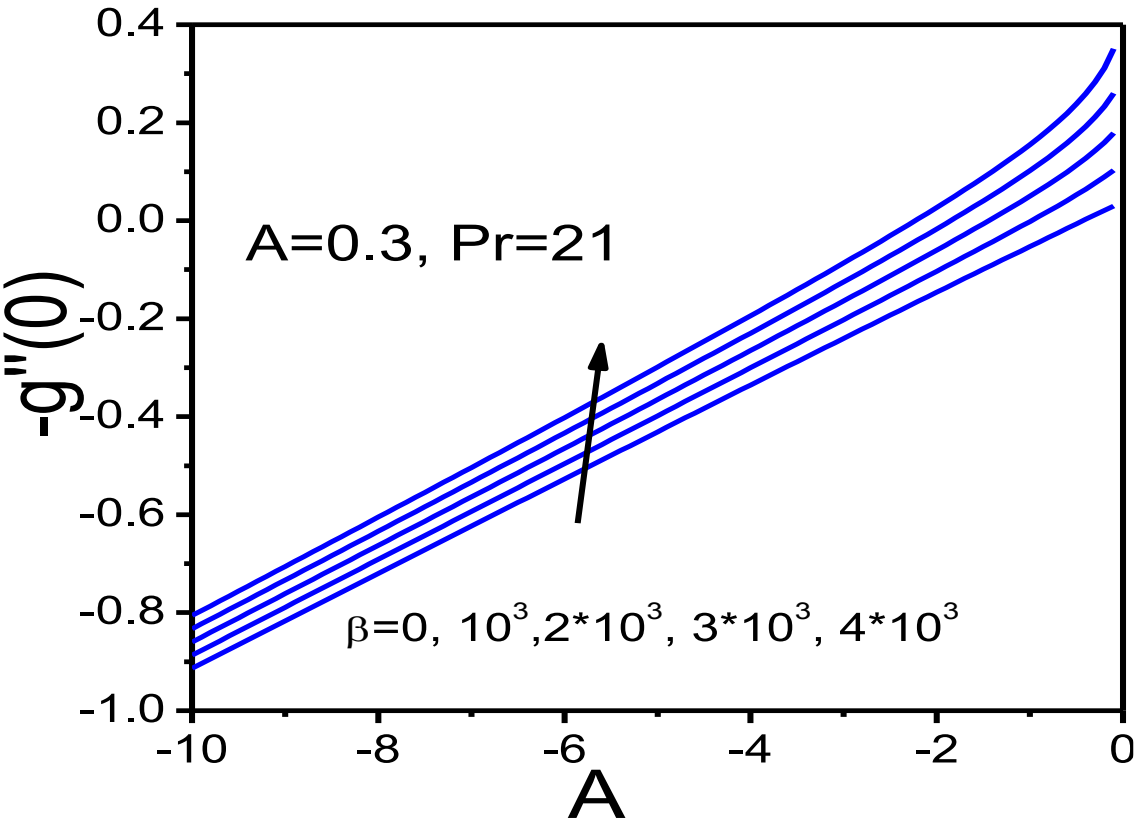

Fig 4.16: Skin friction coefficient $-g''(0)$ with A for different values of β

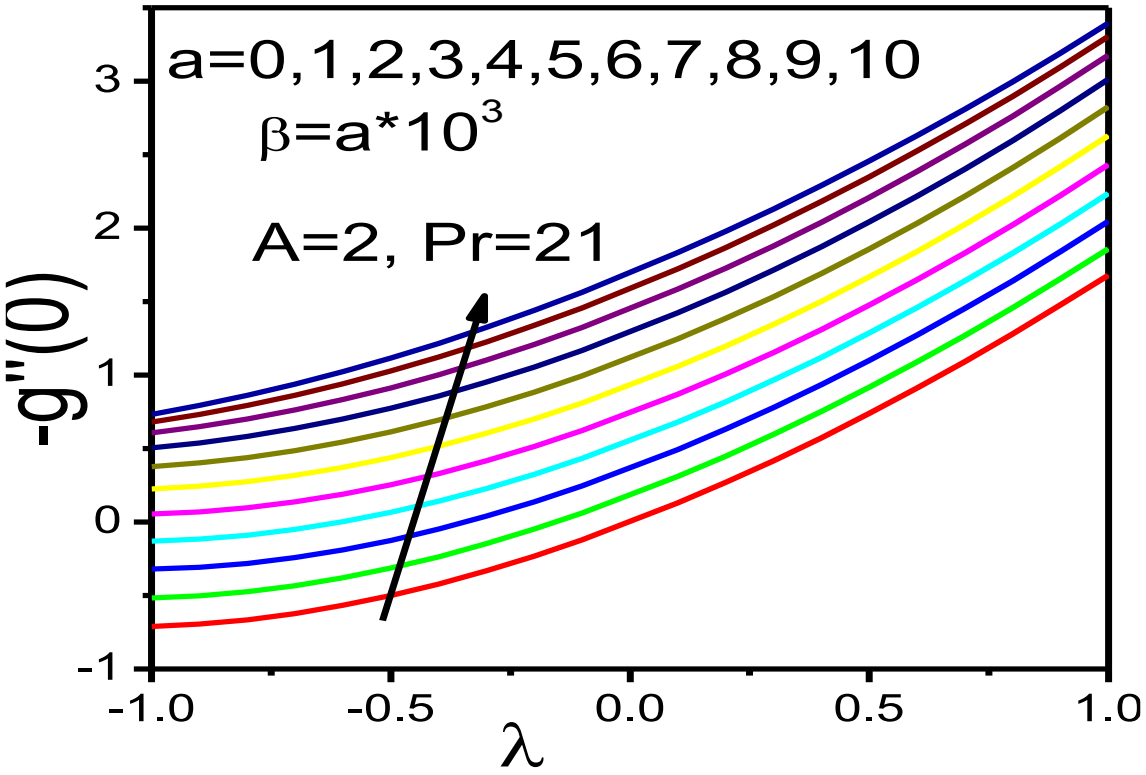

Fig 4.17: Skin friction coefficien $-g''(0)$ with λ for different values of β

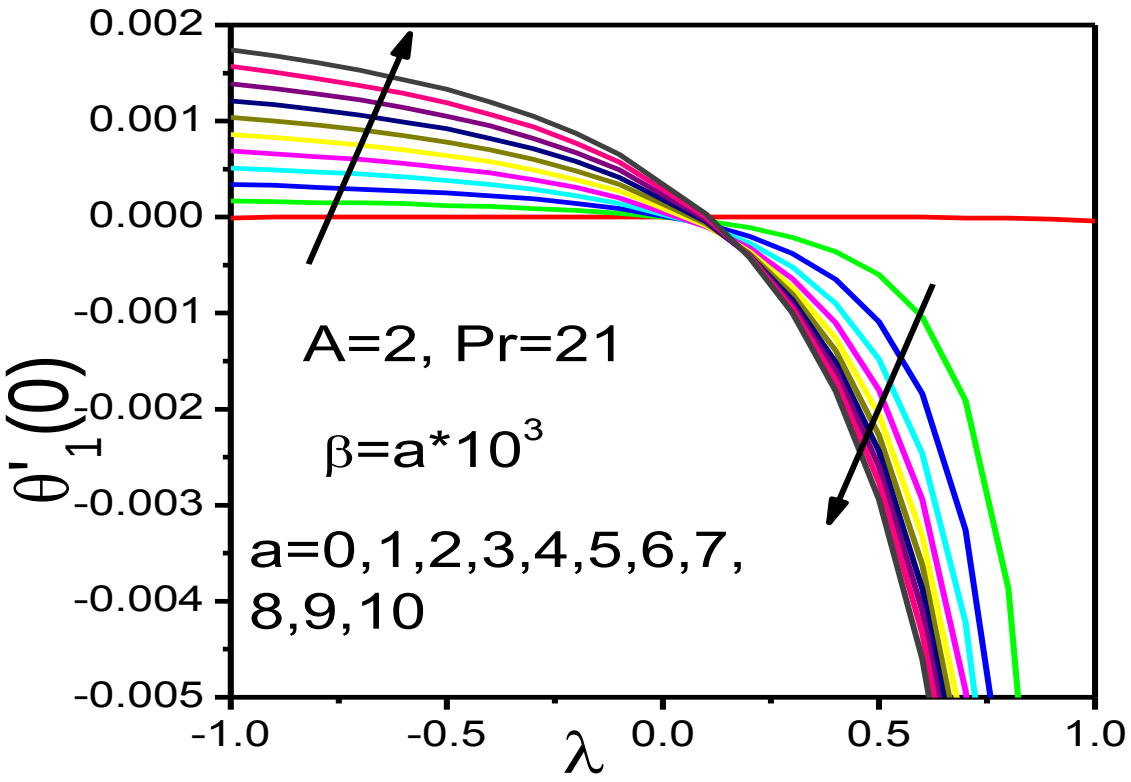

Fig 4.18: Local Nusselt number $-\theta'_1(0)$ with λ for different values of ferromagnetic parameter β.

4.6 Summary of the chapter

In this work, three dimensional biomagnetic fluid flow past unsteady stretching/shrinking sheet has been investigated numerically. The results indicate the following:

1) For accelerated flow, the velocity profile $f'(\eta)$ decreases with the increment of the unsteadiness parameter over a stretching sheet and the opposite behavior shown for the shrinking sheet. On the other hand the velocity profile $g'(\eta)$ is decreased for both stretching and shrinking sheet (Fig. 4.7) with the increment of the unsteadiness parameter.
2) For decelerated flow, we observed that all the flow profile has a cross flow, i.e, near the wall initially the flow motion is decreased and far away from the wall is increased and the reverse is true.
3) For the effect of magnetic parameter, the velocity profile $f'(\eta)$ is increased with the increment of the magnetic number in stretching sheet but this observation is reversed for the shrinking sheet. On the other hand the velocity profiles $g'(\eta)$ and $-(f(\eta)+g(\eta))$ are decreased with the increment of the magnetic number in both stretching and shrinking sheet.
4) The thermal boundary layer thickness is increased in both stretching and shrinking sheet with the increment of the unsteady parameter and magnetic number. Note that the profile is higher in shrinking sheet than that of the stretching one.
5) Skin friction coefficient is decreased/increased with the increment of the unsteady parameter for the shrinking/stretching sheet, respectively. Also skin friction is increased with the increment of the ferromagnetic number β in both sheets.
6) Wall temperature gradient is increased/decreased with the increase of the unsteady parameter for the shrinking/stretching sheet, respectively.

This study is intended to constitute an initial inside for all kinds of applications that deal with blood flow aiming to control the flow rate and rate of heat transfer such as magnetic drug targeting or/and magnetic hyperthermia.

Chapter 5

Stability and Convergence analysis of biomagnetic fluid flow over a stretching sheet in the presence of magnetic field

The aim of this chapter is to investigate the time-dependent two-dimensional biomagnetic fluid (blood) flow (BFD) over a stretching sheet under the action of strong magnetic field. Blood is considered as a biomagnetic fluid which is homogeneous and Newtonian and is treated as an electrical conducting magnetic fluid is also exhibits magnetization. To obtain the transform non-similar coupled non-linear momentum and energy equation, usual non-dimensional variable have been used. The explicit finite difference methods (EFDM) have been used to solve the transform equations. A detailed stability and convergence analysis is also conducted. The stability and convergence analysis have been used for measuring the restriction of the useful parameters and this restrictions are $\Pr \geq 0.733$, $M_F \leq 1.73\times10^{8}$ and $M_M \leq 2.1\times10^{4}$. The combine effect of Magnetohydrodynamics number (M_M) and Ferromagnetic number (M_F) are studied here. The obtained results are presented graphically and discussed for different values of the dimensionless parameter entering into it. The flow and temperature distribution are found to be increased as the values (M_F) and (M_M) are increasing. With the progression in time, flow profile and temperature distribution are increased. This study will have an important bearing for a high targeting efficiency; a high magnetic field is required in the targeted body compartment.

5.1 Introduction

Nowadays, the study of Biomagnetic Fluid Dynamics (BFD) exhibits interest due to potential biomedical applications. Several applications in bio engineering and medical science have been proposed by several researchers. Among them is the development of magnetic device for cell separation (Plavins et al. (1993), Haik et al. (1999)), delivery system for anticancer agents in localized tumor therapy (Ruuge and Rusetski (1993), Voltairas et al. (2002)), magnetic wound or cancer tumor treatment causing magnetic hyperthermia (Fiorentini and Szasa (2006), Misra et al. (2008)).

The biofluids, the flow of which is affected by the application of magnetic field, are called biomagnetic fluids. The most characteristic biomagnetic fluid is blood, which possesses properties of a magnetic fluid because of the red blood cells which contain in high concentration the hemoglobin molecule, a form of iron oxides. This iron oxide molecule constitute a magnetic dipole which is affected by the application of a magnetic field. Thus, it is verified that blood could be considered as a magnetic fluid with the red blood cells playing the role of the magnetic dipoles in a fluid carrier i.e. the plasma. The behavior of a biomagnetic fluid is basically determined by the magnetization force which is the measure of the how much the magnetic field is affecting the magnetic fluid. In general, Magnetization is a function of magnetic field intensity (H) and the temperature (T).

The effect of the magnetic field on the flow behavior of blood has been studied by several researchers. The first formulation of BFD, for the investigation of the flow of a biofluid under the influence of an applied magnetic field has been developed by Haik et al (1996). This BFD model is consistent with the principles of Ferrohydrodynamics (FHD) which deals with no induced electric current and considers that the isothermal flow is affected by the magnetization of the fluid in the magnetic field (Rosensweig (1985), Bashtovoy et al. (1988)). However, blood also possesses properties of an electrically conducting fluid due to the ions in the plasma. The flowing blood due to the plasma ions produce a slight electric current which interacts with magnetic fields. The inclusion in the formulation of the electrical conductivity of the fluid is made by adopting the principles of the MagnetoHydroDynamics (MHD). Thus, an extended mathematical model of BFD, taking into account the electrical conductivity of blood, has been proposed in Tzirtzilakis (2005). This model is derived by adopting the properties of both MHD and FHD considering both magnetization and electrical conductivity of blood and, in addition, includes the energy equation for the investigation of biomedical applications like magnetic hyperthermia.

Crane in 1970, studied for the first time the classical physical problem of a shear-driven flow over a stretching sheet for a Newtonian fluid. Another classical study is that of MHD stretching sheet flow of a heated ferrofluid in the presence of a magnetic dipole of Anderson and Valnes (1998). Recently, Zeeshan et al. (2016) studied the effect of thermal radiation and heat transfer on the flow of ferromagnetic fluid on a stretching sheet. Tzirtzilakis and Kafoussias (2003) analyzed the mathematical model of the flow of a heated ferrofluid over a linearly stretching sheet under the action of a magnetic field which is generated by a magnetic dipole. Tzirtzilakis and Tanoudis (2003) have presented a numerical method for the study of laminar incompressible two dimensional biofluid over a stretching sheet with heat transfer with the magnetization given as a function of both magnetic field strength intensity H and temperature T.

Murtaza et al. (2017) studied the flow of biomagnetic fluid over a stretching sheet, in the present of an applied magnetic field using the extended BFD model incorporating both FHD and MHD formulations. The magnetization was considered to vary with the temperature and the magnetic field strength intensity, and the biofluid was treated as an electrically conducting magnetic fluid which also exhibits magnetization. Finally, Ali et al. (2011) studied the MHD stagnation point flow, taking into account the effects of the induced magnetic field.

The study of unsteady stretching sheet flow constitutes also a topic of ongoing research. More specifically, Das et al. (2015) studied the unsteady MHD flow of nanofluids over an accelerating convectively heated stretching sheet in the presence of a transverse magnetic field with heat source/sink. Hayat et al. (2016) studied the unsteady MHD stretching sheet flow which was also investigated in three-dimensions considering velocity and thermal slip boundary conditions. Finally, a characteristic study concerning applications of MHD flow problems to hemodynamics is that of the steady incompressible viscoelastic and electrically conducting fluid flow and heat transfer in a parallel plate channel with stretching walls in the presence of a magnetic field by Misra et al. (2008).

In the present chapter we study the unsteady biomagnetic fluid flow over a stretching sheet with the influence of magnetic field. The present study, as far as the physical problem is concerned, is similar to the one studied before Murtaza et al. (2017) with the consideration of the time dependency. Moreover, in the present chapter the mathematical problem is solved by numerical treatment of the initial set of partial differential equations in conjunction with the previous study by Murtaza et al. (2017) where, a similarity problem governed by a system of

ordinary differential equations subject to corresponding boundary conditions, was solved numerically. The explicit finite difference methods (EFDM) have been used to solve the transformed equations presented by Mitchell and Griffiths (1980) and Charnahan et al. (1969). A detailed stability and convergence analysis is also conducted. The stability and convergence analysis have been used for measuring the restriction values of important flow parameters. The present study is hoped to have an important bearing for a high targeting efficiency; a high magnetic field is required in the targeted body compartment.

5.2. Mathematical Formulation

Let us consider the time-dependent (unsteady) two-dimensional laminar flow of an incompressible viscous and electrically conducting biomagnetic fluid past a stretching sheet with a velocity proportional to distance i.e. $u = cx$, where c is a dimensional constant. The temperature of the stretched sheet is kept at fixed T_w and the temperature of the fluid far away from the sheet is T_c, where $T_c > T_w$. The fluid is confined to the half space $y > 0$ above the sheet and magnetic dipole is located at distance d below the sheet, giving rise to a magnetic field of sufficient strength to saturate the biomagnetic fluid. The flow configuration is shown schematically at figure 5. 1.

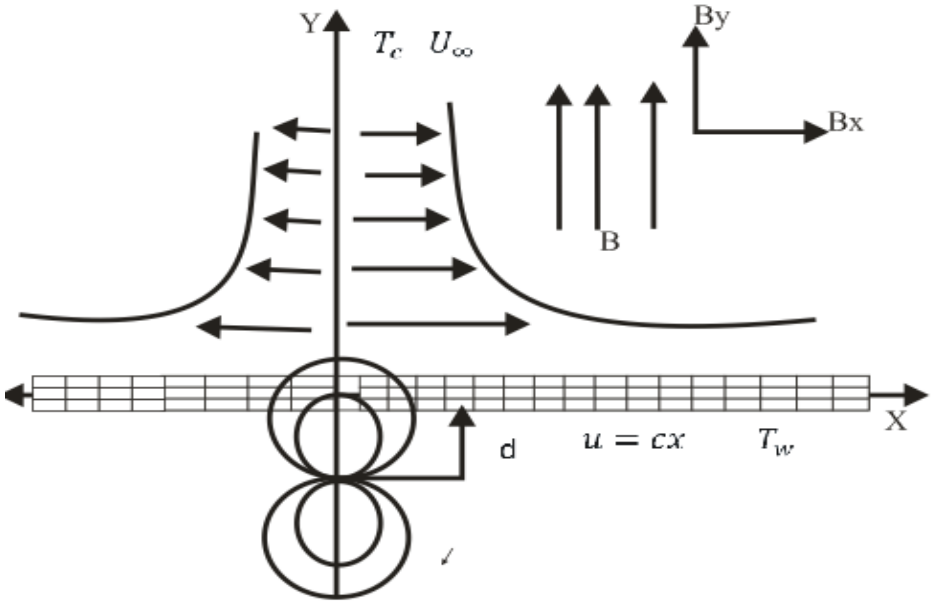

Figure 5.1. Flow configuration of the flow field

Under the above assumptions the flow governing equations are the valid one of the extended BFD model, (Tzirtzilakis (2005), Tzirtzilakis and Xenos (2013), Murtaza et al. (2017)) i.e:

Continuity equation:

$$\frac{\partial \mathrm{u}}{\partial \mathrm{x}} + \frac{\partial \mathrm{v}}{\partial \mathrm{y}} = 0 \tag{5.1}$$

Momentum equation:

$$\frac{\partial u}{\partial t} + u\frac{\partial u}{\partial x} + v\frac{\partial u}{\partial y} = -\frac{1}{\rho}\frac{\partial p}{\partial x} + \frac{1}{\rho}\mu_0 M\frac{\partial H}{\partial x} - \frac{1}{\rho}\sigma B_y^2 u + \frac{1}{\rho}\sigma B_x B_y v + \frac{1}{\rho}\mu\left(\frac{\partial^2 u}{\partial x^2} + \frac{\partial^2 u}{\partial y^2}\right) \tag{5.2}$$

$$\frac{\partial v}{\partial t} + u\frac{\partial v}{\partial x} + v\frac{\partial v}{\partial y} = -\frac{1}{\rho}\frac{\partial p}{\partial y} + \frac{1}{\rho}\mu_0 M\frac{\partial H}{\partial y} - \frac{1}{\rho}\sigma B_x^2 v + \frac{1}{\rho}\sigma B_x B_y u + \frac{1}{\rho}\mu\left(\frac{\partial^2 v}{\partial x^2} + \frac{\partial^2 v}{\partial y^2}\right) \tag{5.3}$$

Energy equation:

$$\begin{aligned}\rho C_p\left(\frac{\partial T}{\partial t} + u\frac{\partial T}{\partial x} + v\frac{\partial T}{\partial y}\right) + \mu_0 T\frac{\partial M}{\partial T}\left(u\frac{\partial H}{\partial x} + v\frac{\partial H}{\partial y}\right) - \sigma B^2 u^2 &= k\left(\frac{\partial^2 T}{\partial x^2} + \frac{\partial^2 T}{\partial y^2}\right) \\ &+ \mu\left[2\left[\left(\frac{\partial u}{\partial x}\right)^2 + \left(\frac{\partial v}{\partial y}\right)^2\right] + \left(\frac{\partial v}{\partial x} + \frac{\partial u}{\partial y}\right)^2\right]\end{aligned} \tag{5.4}$$

subject to the following initial and boundary conditions:

$$t = 0:\ u = 0,\ \ v = 0,\ \ T = T_c \qquad \text{everywhere} \tag{5.5}$$

$$t > 0:\ u = 0,\ v = 0,\ \ T = T_c \qquad \text{at } x = 0$$

$$u = U_0 = cx,\ \ v = 0,\ T = T_w \qquad \text{at } y = 0$$

$$u = 0,\ v = 0,\ \ T = T_c \qquad \text{as } y \to \infty \tag{5.6}$$

In the above equations $q = (u, v)$ is the dimensional velocity, p is the pressure, ρ is the biomagnetic fluid density, σ is the electrical conductivity, μ is the dynamic viscosity, C_p the specific heat at constant pressure and k the thermal conductivity, μ_0 is the magnetic permeability and $H = (H_x, H_y)$ is the magnetic field strength, B is the magnetic induction $(B = \mu_0 H \Rightarrow (B_x, B_y) = \mu_0 (H_x, H_y))$

The terms $-\sigma B_y^2 u + \sigma B_x B_y v$ and $-\sigma B_x^2 v + \sigma B_x B_y u$ in (5.2) and (5.3), respectively, represent the Lorentz force per unit volume towards the x and y directions respectively,

whereas the term $-\sigma B^2 u^2$ in the energy equation (5.4) represents the Joule heating. Clearly, for the energy equation only the primary velocity u is considered for the generation of the Joule heating term. The aforementioned terms arise due to the electrical conductivity of the fluid and are known in MHD. The terms $\mu_0 M \frac{\partial H}{\partial x}$ and $\mu_0 M \frac{\partial H}{\partial y}$ in (5.2) and (5.3), respectively, represent the components of the magnetic force per unit volume and depend on the existence of the magnetic gradient on the corresponding x and y directions, respectively. The second term on the left-hand side of the energy equation (5.4), accounts for heating due to the adiabatic magnetization. These terms are known from FHD (Rosensweig (1985)).

The magnetic dipole gives rise to a magnetic field, sufficiently strong to saturate the biofluid, and its scalar potential is given by Andersson and Valnes (1998)

$$V(x,y) = \frac{\alpha}{2\pi} \frac{x}{x^2 + (y+d)^2} \tag{5.7}$$

Thus the magnitude $\|H\| = H$ of the magnetic field intensity by

$$H(x,y) = \left(H_x^2 + H_y^2\right)^{\frac{1}{2}} = \frac{\gamma}{2\pi} \frac{x}{x^2 + (y+d)^2} \tag{5.8}$$

where $\gamma = \alpha$ and H_x, H_y are the component of the magnetic field $\overrightarrow{H} = \left(H_x, H_y\right)$ given by

$$H_x(x,y) = -\frac{dv}{dx} = \frac{\gamma}{2\pi} \frac{x^2 - (y+d)^2}{\left(x^2 + (y+d)^2\right)^2} \tag{5.9}$$

$$H_y(x,y) = -\frac{dv}{dy} = \frac{\gamma}{2\pi} \frac{2x(y+d)}{\left(x^2 + (y+d)^2\right)^2} \tag{5.10}$$

and the gradients are given by

$$\frac{\partial H}{\partial x} = -\frac{\gamma}{2\pi} \frac{2x}{(y+d)^4} \quad \text{and} \quad \frac{\partial H}{\partial y} = \frac{\gamma}{2\pi}\left(-\frac{2}{(y+d)^3} + \frac{4x^2}{(y+d)^5}\right) \tag{5.11}$$

The magnetic field intensity H, can be expressed by analogous manner, as

$$H(x,y)=\frac{\gamma}{2\pi}\left(\frac{1}{(y+d)^2}-\frac{x^2}{(y+d)^4}\right) \tag{5.12}$$

Under the assumption that the applied magnetic field H is sufficiently strong to saturate the biomagnetic fluid, the magnetization M is generally determined by the fluid temperature and magnetic field intensity H. There is a variety of equations that can be used for the variation of the magnetization under the equilibrium assumption by Tzirtzilakis (2005). In this study the relation of Matsuki et al. (1977) derived experimentally is adopted. This relation expresses the magnetization as a function of the magnetic field strength intensity H and the temperature of the fluid T

$$M=KH(T_c-T) \tag{5.13}$$

where K is a constant called pyromagnetic coefficient is and T_c is the Curie temperature. The above relation for the magnetization M has also proposed in Tzirtzilakis (2005) and used in Murtaza et al. (2017).

5.3. Mathematical Analysis

Since the solution of the governing equations (5.1) to (5.4) under the initial and boundary conditions (5.5) to (5.6) will be based on the finite difference method, it is required to make the said equations dimensionless. For this purpose we now introduce the following dimensionless quantities;

$$X=\frac{xU_0}{\nu},\ Y=\frac{yU_0}{\nu},\ U=\frac{u}{U_0},\ V=\frac{v}{U_0},\ P=\frac{p}{\rho U_0^2},\ \overline{H}=\frac{H}{H_0}$$

$$\overline{H_x}=\frac{H_x}{H_0},\ \overline{H_y}=\frac{H_y}{H_0},\ \overline{T}=\frac{T_c-T}{T_c-T_w},\ \tau=\frac{tU_0^2}{\nu}$$

From the above dimensionless variable we have

$$x=\frac{X\nu}{U_0},\ y=\frac{Y\nu}{U_0},\ u=UU_0,\ v=VU_0,\ p=\rho PU_0^2,\ H=\overline{H}H_0$$

$$H_x=\overline{H}_xH_0,\ H_y=\overline{H}_yH_0,\ t=\frac{\tau\nu}{U_0^2},\ T=T_c-\overline{T}(T_c-T_w)$$

Now after using dimensionless quantities into the equations (5.1) to (5.4), the following nonlinear coupled partial differential equations in terms of dimensionless variables are obtained as:

$$\frac{\partial U}{\partial X}+\frac{\partial V}{\partial Y}=0 \tag{5.14}$$

$$\frac{\partial U}{\partial \tau}+U\frac{\partial U}{\partial X}+V\frac{\partial U}{\partial Y}=-\frac{\partial P}{\partial X}+\left(\frac{\partial^2 U}{\partial X^2}+\frac{\partial^2 U}{\partial Y^2}\right)+M_F\overline{H}\overline{T}\frac{\partial \overline{H}}{\partial X}-M_M\overline{H}_y^2U+M_M\overline{H}_x\overline{H}_yV \tag{5.15}$$

$$\frac{\partial V}{\partial \tau}+U\frac{\partial V}{\partial X}+V\frac{\partial V}{\partial Y}=-\frac{\partial P}{\partial Y}+\left(\frac{\partial^2 V}{\partial X^2}+\frac{\partial^2 V}{\partial Y^2}\right)+M_F\overline{H}\overline{T}\frac{\partial \overline{H}}{\partial Y}-M_M\overline{H}_x^2V+M_M\overline{H}_x\overline{H}_yU \tag{5.16}$$

$$\frac{\partial \overline{T}}{\partial \tau}+U\frac{\partial \overline{T}}{\partial X}+V\frac{\partial \overline{T}}{\partial Y}+M_FE_c\overline{H}\left(\varepsilon-\overline{T}\right)\left(U\frac{\partial \overline{H}}{\partial X}+V\frac{\partial \overline{H}}{\partial Y}\right)+M_ME_c\overline{H}^2U^2=\left(\frac{1}{P_r}\right)\left(\frac{\partial^2 \overline{T}}{\partial X^2}+\frac{\partial^2 \overline{T}}{\partial Y^2}\right)$$

$$-E_c\left[2\left\{\left(\frac{\partial U}{\partial X}\right)^2+\left(\frac{\partial V}{\partial Y}\right)^2\right\}+\left(\frac{\partial V}{\partial X}+\frac{\partial U}{\partial Y}\right)^2\right] \tag{5.17}$$

The non-dimensional boundary conditions are:

$$\tau\le 0:\ U=0,\ V=0,\ \overline{T}=0 \qquad \text{everywhere} \tag{5.18}$$

$$\tau>0:\ U=0,\ V=0,\ \overline{T}=0 \ \text{ at } X=0$$

$$U=1,\ V=0,\ \overline{T}=1 \quad \text{at } Y=0$$

$$U=0,\ V=0,\ \overline{T}=0 \quad \text{as } Y\to\infty \tag{5.19}$$

where $P_r=\frac{\mu c_p}{k}$ is Prandtl number, $E_c=\frac{U_0^2}{c_p(T_c-T_w)}$ is Eckert number, $\varepsilon=\frac{T_c}{T_c-T_w}$ is dimensionless temperature parameter, $M_F=\frac{\mu_0 kH_0^2(T_c-T_w)}{\rho U_0^2}$ is Ferromagnetic (FHD) parameter and $M_M=\frac{\sigma\mu_0^2H_0^2\nu}{\rho U_0^2}$ is Magnetohydrodynamic (MHD) parameter.

The most important parameters entering to the problems of BFD are the two magnetic parameters, M_F and M_M, which is defined above. Especially, the M_M parameter is the square of the widely known in MHD Hartmann number. Increment of the above mentioned

dimensionless parameters, for specific fluid $(\mu, \sigma, \mu_0 = const)$ and for a specific flow problem $(h = const)$ means increment of the magnetic field strength induction B_0.

It is worth mention here, that when these magnetic parameters $M_F = M_M = 0$ the problem is a common hydrodynamic fluid flow with heat transfer. For a specific Reynolds number and temperature difference, an increase the value of these magnetic parameters means a corresponding increase in the value of the magnetic field strength H_0.

5.5. Numerical Method

In this section, the non-linear equations (5.14)-(5.17) subject to the initial and boundary conditions (5.18) and (5.19) are solved numerically for the velocity and temperature using the explicit finite differences scheme of Callahan and Marner (1976) technique which is conditionally stable.

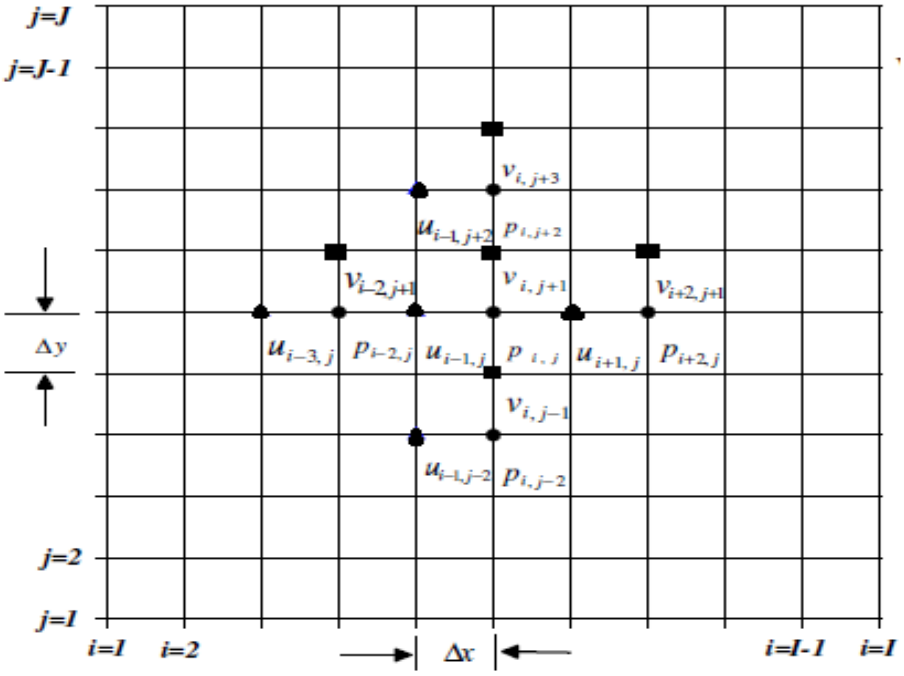

Figure: 5.2. Finite difference space grid

From the concept of above discussion, for simplicity the explicit finite difference method has been used to solve equations (5.14) to (5.17) subject to the conditions given by (5.18) and (5.19).To obtained the difference equation the region of the flow is divided into a grid or mesh of lines parallel to X and Y axes where *x*-axis is taken along the plate and y-axis is normal to the plate.

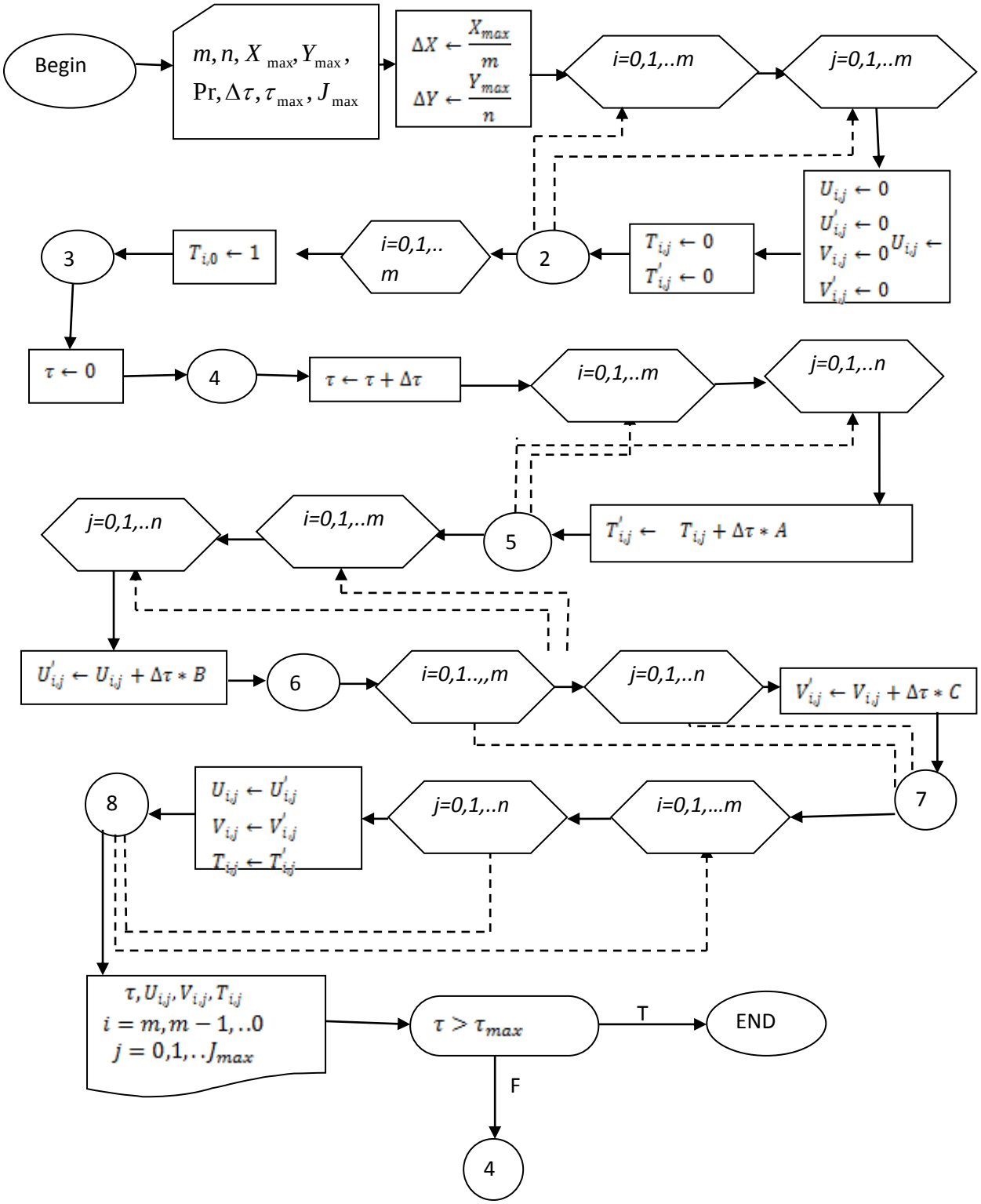

Fig. 5.3 Algorithm of finite difference procedure.

Here the plate height $X_{\max}(=100)$ i.e. X varies from 0 to 100 and regard $Y_{\max}(=10)$ as corresponding to $Y \to \infty$ i.e. Y varies from 0 to 10. There are $m = 600$ and $n = 600$ grid spacing in the X and Y directions respectively as shown figure 5.2.

It is assumed that $\Delta X, \Delta Y$ are constant mesh sizes along X and Y directions respectively and taken as follows

$$\Delta X = 0.166 \left(0 < X < 100\right)$$

$$\Delta Y = 0.016 \left(0 < Y < 10\right)$$

with the smaller time step $\Delta\tau = 0.0001$.

Let U', V' and T' denote the values of U, V and T at the end of time step respectively. Using the explicit finite difference approximation, the following relation obtained,

$$\left(\frac{\partial U}{\partial \tau}\right)_{i,j} = \frac{U'_{i,j} - U_{i,j}}{\Delta\tau}, \left(\frac{\partial U}{\partial X}\right)_{i,j} = \frac{U_{i,j} - U_{i-1,j}}{\Delta X}, \left(\frac{\partial U}{\partial Y}\right)_{i,j} = \frac{U_{i,j+1} - U_{i,j}}{\Delta Y}$$

$$\left(\frac{\partial V}{\partial \tau}\right)_{i,j} = \frac{V'_{i,j} - V_{i,j}}{\Delta\tau}, \left(\frac{\partial V}{\partial X}\right)_{i,j} = \frac{V_{i,j} - V_{i-1,j}}{\Delta X}, \left(\frac{\partial V}{\partial Y}\right)_{i,j} = \frac{V_{i,j+1} - V_{i,j}}{\Delta Y}$$

$$\left(\frac{\partial T}{\partial \tau}\right)_{i,j} = \frac{\overline{T}'_{i,j} - \overline{T}_{i,j}}{\Delta\tau}, \left(\frac{\partial T}{\partial X}\right)_{i,j} = \frac{\overline{T}_{i,j} - \overline{T}_{i-1,j}}{\Delta X}, \left(\frac{\partial T}{\partial Y}\right)_{i,j} = \frac{\overline{T}_{i,j+1} - \overline{T}_{i,j}}{\Delta Y}$$

$$\left(\frac{\partial^2 T}{\partial X^2}\right)_{i,j} = \frac{\overline{T}_{i+1,j} - 2\overline{T}_{i,j} + \overline{T}_{i-1,j}}{(\Delta X)^2}, \left(\frac{\partial^2 T}{\partial Y^2}\right)_{i,j} = \frac{\overline{T}_{i,j+1} - 2\overline{T}_{i,j} + \overline{T}_{i,j-1}}{(\Delta Y)^2}$$

$$\left(\frac{\partial^2 U}{\partial X^2}\right)_{i,j} = \frac{U_{i+1,j} - 2U_{i,j} + U_{i-1,j}}{(\Delta X)^2}, \left(\frac{\partial^2 U}{\partial Y^2}\right)_{i,j} = \frac{U_{i,j+1} - 2U_{i,j} + U_{i,j-1}}{(\Delta Y)^2},$$

$$\left(\frac{\partial^2 V}{\partial X^2}\right)_{i,j} = \frac{V_{i+1,j} - 2V_{i,j} + V_{i-1,j}}{(\Delta X)^2}, \left(\frac{\partial^2 V}{\partial Y^2}\right)_{i,j} = \frac{V_{i,j+1} - 2V_{i,j} + V_{i,j-1}}{(\Delta Y)^2},$$

From the system of partial differential equations (5.14) to (5.17) by substituting the above relations into the corresponding differential equations, an appropriate set of finite difference equations is obtained as:

$$\frac{U_{i,j}-U_{i-1,j}}{\Delta X}+\frac{V_{i,j+1}-V_{i,j}}{\Delta Y}=0 \tag{5.20}$$

$$\frac{U'_{i,j}-U_{i,j}}{\Delta\tau}+U_{i,j}\frac{U_{i,j}-U_{i-1,j}}{\Delta X}+V_{i,j}\frac{U_{i,j+1}-U_{i,j}}{\Delta Y}=-P_1+\left(\frac{U_{i+1,j}-2U_{i,j}+U_{i-1,j}}{(\Delta X)^2}+\frac{U_{i,j+1}-2U_{i,j}+U_{i,j-1}}{(\Delta Y)^2}\right)+M_F\overline{H}\frac{\partial\overline{H}}{\partial X}\overline{T}'_{i,j}-M_M\overline{H}_y^2U_{i,j}+M_M\overline{H}_x\overline{H}_yV_{i,j} \tag{5.21}$$

$$\frac{V'_{i,j}-V_{i,j}}{\Delta\tau}+U_{i,j}\frac{V_{i,j}-V_{i-1,j}}{\Delta X}+V_{i,j}\frac{V_{i,j+1}-V_{i,j}}{\Delta Y}=-P_2+\left(\frac{V_{i+1,j}-2V_{i,j}+V_{i-1,j}}{(\Delta X)^2}+\frac{V_{i,j+1}-2V_{i,j}+V_{i,j-1}}{(\Delta Y)^2}\right)+M_F\overline{H}\frac{\partial\overline{H}}{\partial Y}\overline{T}'_{i,j}-M_M\overline{H}_x^2V_{i,j}+M_M\overline{H}_x\overline{H}_yU_{i,j} \tag{5.22}$$

$$\frac{T'_{i,j}-T_{i,j}}{\Delta\tau}+U_{i,j}\frac{T_{i,j}-T_{i-1,j}}{\Delta X}+V_{i,j}\frac{T_{i,j+1}-T_{i,j}}{\Delta Y}+\varepsilon M_FE_c\overline{H}\left(U_{i,j}\frac{\partial\overline{H}}{\partial X}+V_{i,j}\frac{\partial\overline{H}}{\partial Y}\right)-M_ME_c\overline{H}^2U_{i,j}^2$$
$$-M_FE_c\overline{H}\overline{T}_{i,j}\left(U_{i,j}\frac{\partial\overline{H}}{\partial X}+V_{i,j}\frac{\partial\overline{H}}{\partial Y}\right)=\frac{1}{P_r}\left(\frac{\overline{T}_{i+1,j}-2\overline{T}_{i,j}+\overline{T}_{i-1,j}}{(\Delta X)^2}+\frac{\overline{T}_{i,j+1}-2\overline{T}_{i,j}+\overline{T}_{i,j-1}}{(\Delta Y)^2}\right)$$

$$-E_c\left[2\left\{\left(\frac{U_{i,j}-U_{i-1,j}}{\Delta X}\right)^2+\left(\frac{V_{i,j+1}-V_{i,j}}{\Delta Y}\right)^2\right\}+\left(\frac{V_{i,j}-V_{i-1,j}}{\Delta X}+\frac{U_{i,j+1}-U_{i,j}}{\Delta Y}\right)^2\right] \tag{5.23}$$

with initial and boundary conditions

$$U_{i,j}^0=V_{i,j}^0=\overline{T}_{i,j}^0=0 \tag{5.24}$$

$$U_{0,j}^n=V_{0,j}^n=\overline{T}_{0,j}^n=0$$

$$U_{i,0}^n=1,\ V_{i,0}^n=0,\ \overline{T}_{i,0}^n=1$$

$$U_{i,l}^n=0,\ V_{i,l}^n=0,\ \overline{T}_{i,l}^n=0 \quad \text{where} \quad l\to\infty \tag{5.25}$$

Here the subscripts i and j designate the grid points with x and y coordinates respectively and the subscript n represent the value of time, $\tau=n\Delta\tau$ where $n=0,1,2,....$ From the initial condition (5.24) The value of U, V *and* $\overline{T}$ are known at $\tau=0$. During any one time step, the coefficients $U_{i,j}$ and $V_{i,j}$ appearing the equations (5.20) to (5.23) are treated as constants. Then at the end of any time step $\Delta\tau$, the new temperature $\overline{T}'$, the new

velocity U' and V' at all interior nodal points may be obtained by successive applications of (5.23), (5.21), (5.22) and (5.20) respectively. This process is repeated in time and provided the time step is sufficiently small, U, V *and* $\overline{T}$ should eventually converge to values which approximate the steady state solution of equations (5.20) –(5.23).

5.5. Stability and Convergence Analysis

Since the explicit procedure is being used, so we need to discuss the stability and convergence of the finite difference scheme. For a constant mesh sizes the stability criteria of the scheme may be established as follows:

The equation (5.20) will be ignored since $\Delta\tau$ does not appear in it. The general terms of the Fourier expansion for U, V *and* $\overline{T}$ at a time arbitrary called $\tau = 0$ are all $e^{i\alpha X} e^{i\beta Y}$, apart from a constant, where $i = \sqrt{-1}.$ At a time τ, these terms becomes

$$\left.\begin{aligned} U &: \psi_1(\tau) e^{i\alpha X} e^{i\beta Y} \\ V &: \psi_2(\tau) e^{i\alpha X} e^{i\beta Y} \\ \overline{T} &: \theta(\tau) e^{i\alpha X} e^{i\beta Y} \end{aligned}\right\} \tag{5.26}$$

After time step these terms will become

$$\left.\begin{aligned} U &: \psi_1'(\tau) e^{i\alpha X} e^{i\beta Y} \\ V &: \psi_2'(\tau) e^{i\alpha X} e^{i\beta Y} \\ \overline{T} &: \theta'(\tau) e^{i\alpha X} e^{i\beta Y} \end{aligned}\right\} \tag{5.27}$$

Substituting (5.26) and (5.27) in equation (5.21)-(5.23), regarding the coefficients U and V as constant over any time step, the following equations upon simplification obtained:

$$\frac{\psi_1'(\tau) - \psi_1(\tau)}{\Delta\tau} + U\psi_1(\tau)\frac{1 - e^{-i\alpha\Delta X}}{\Delta X} + V\psi_1(\tau)\frac{e^{i\beta\Delta Y} - 1}{\Delta Y} = -P_1 e^{-i\alpha X} e^{-i\beta Y} + M_F \overline{H}\frac{\partial \overline{H}}{\partial X}\theta'(\tau) +$$

$$2\psi_1(\tau)\left(\frac{\cos\alpha\Delta X - 1}{(\Delta X)^2} + \frac{\cos\beta\Delta Y - 1}{(\Delta Y)^2}\right) - \psi_1(\tau) M_M \overline{H}_y^2 + \psi_2(\tau) M_M \overline{H}_x \overline{H}_y \tag{5.28}$$

$$\frac{\psi_2'(\tau) - \psi_2(\tau)}{\Delta\tau} + U\psi_2(\tau)\frac{1 - e^{-i\alpha\Delta X}}{\Delta X} + V\psi_2(\tau)\frac{e^{i\beta\Delta Y} - 1}{\Delta Y} = -P_2 e^{-i\alpha X} e^{-i\beta Y} + M_F \overline{H}\frac{\partial \overline{H}}{\partial Y}\theta'(\tau) +$$

$$2\psi_2(\tau)\left(\frac{\cos\alpha\Delta X - 1}{(\Delta X)^2} + \frac{\cos\beta\Delta Y - 1}{(\Delta Y)^2}\right) - \psi_2(\tau) M_M \overline{H}_x^2 + \psi_1(\tau) M_M \overline{H}_x \overline{H}_y \tag{5.29}$$

$$\frac{\theta'(\tau)-\theta(\tau)}{\Delta\tau}+U\theta(\tau)\frac{1-e^{-i\alpha\Delta X}}{\Delta X}+V\theta(\tau)\frac{e^{-i\beta\Delta Y}-1}{\Delta Y}+M_F E_c\overline{H}\varepsilon\left(\psi_1(\tau)\frac{\partial\overline{H}}{\partial X}+\psi_2(\tau)\frac{\partial\overline{H}}{\partial Y}\right)-$$

$$M_F E_c\overline{H}\theta(\tau)\left(U\frac{\partial\overline{H}}{\partial X}+V\frac{\partial\overline{H}}{\partial Y}\right)+M_M E_c\overline{H}^2U\psi_1(\tau)=\frac{2}{P_r}\theta(\tau)\left(\frac{\cos\alpha\Delta X-1}{(\Delta X)^2}+\frac{\cos\beta\Delta Y-1}{(\Delta Y)^2}\right)-$$

$$E_c\left[2U\psi_1(\tau)\left(\frac{1-e^{-i\alpha\Delta X}}{\Delta X}\right)^2+2V\psi_2(\tau)\left(\frac{e^{i\beta\Delta Y}-1}{\Delta Y}\right)^2+V\psi_2(\tau)\left(\frac{1-e^{-i\alpha\Delta X}}{\Delta X}\right)^2+\right.$$

$$\left.U\psi_1(\tau)\left(\frac{e^{i\beta\Delta Y}-1}{\Delta Y}\right)^2+2U\psi_2(\tau)\left(\frac{1-e^{-i\alpha\Delta X}}{\Delta X}\right)\left(\frac{e^{i\beta\Delta Y}-1}{\Delta Y}\right)\right] \tag{5.30}$$

The equations (5.28)-(5.30) can be written in the following form

$$\psi_1^{'}=A_1\psi_1+B_1\psi_2+C_1\theta' \tag{5.31}$$

$$\psi_2^{'}=A_2\psi_1+B_2\psi_2+C_2\theta' \tag{5.32}$$

$$\theta'=A_3\psi_1+B_3\psi_2+C_3\theta \tag{5.33}$$

Again using equation (5.33) in (5.31) and (5.32), we get

$$\psi_1^{'}=A_4\psi_1+B_4\psi_2+C_4\theta$$

$$\psi_2^{'}=A_5\psi_1+B_5\psi_2+C_5\theta$$

Here, $A_4=A_1+C_1A_3,\ \ B_4=B_1+C_1B_3,\ \ C_4=C_1C_3$

and $A_5=A_2+C_2A_3,\ \ B_5=B_2+C_2B_3,\ \ C_5=C_2C_3$

where

$$A_4=1-\frac{U\Delta\tau}{\Delta X}\left(1-e^{-i\alpha\Delta X}\right)-\frac{V\Delta\tau}{\Delta Y}\left(e^{i\beta\Delta Y}-1\right)+\left[\frac{2\Delta\tau}{(\Delta X)^2}\left(\cos\alpha\Delta X-1\right)+\frac{2\Delta\tau}{(\Delta Y)^2}\left(\cos\beta\Delta Y-1\right)\right.$$

$$\left.-M_M\overline{H}_y^2\Delta\tau-M_F\overline{H}\frac{\partial\overline{H}}{\partial X}\left[M_M E_c\overline{H}^2U+\varepsilon M_F E_c\overline{H}\frac{\partial\overline{H}}{\partial X}+E_c\left(\frac{2U}{(\Delta X)^2}\left(1-e^{-i\alpha\Delta X}\right)^2+\right.\right.\right.$$

$$\frac{U}{(\Delta Y)^2}\left(e^{i\beta\Delta Y}-1\right)^2\Bigg)\Bigg](\Delta\tau)^2\Bigg] \tag{5.34}$$

$$B_4=\left(M_M\overline{H}_x\overline{H}_y-\frac{P_1}{V}\right)\Delta\tau-M_F\overline{H}\frac{\partial\overline{H}}{\partial X}\Bigg[\varepsilon M_F E_c\overline{H}\frac{\partial\overline{H}}{\partial Y}+E_c\Bigg(\frac{V}{(\Delta X)^2}\left(1-e^{-i\alpha\Delta X}\right)^2+$$

$$\frac{2V}{(\Delta Y)^2}\left(e^{i\beta\Delta Y}-1\right)^2\Bigg)+\frac{2U}{(\Delta X.\Delta Y)}\left(1-e^{-i\alpha\Delta X}\right)\left(e^{i\beta\Delta Y}-1\right)\Bigg](\Delta\tau)^2 \tag{5.35}$$

$$C_4=\Big[M_F\overline{H}\frac{\partial\overline{H}}{\partial X}\Bigg(1-\frac{U\Delta\tau}{\Delta X}\left(1-e^{-i\alpha\Delta X}\right)-\frac{V\Delta\tau}{\Delta Y}\left(e^{i\beta\Delta Y}-1\right)+M_F E_c\overline{H}\Bigg(U\frac{\partial\overline{H}}{\partial X}+V\frac{\partial\overline{H}}{\partial Y}\Bigg)\Delta\tau+$$

$$\frac{1}{P_r}\Bigg(\frac{2\Delta\tau}{(\Delta X)^2}\left(\cos\alpha\Delta X-1\right)+\frac{2\Delta\tau}{(\Delta Y)^2}\left(\cos\beta\Delta Y-1\right)\Bigg)\Bigg]\Delta\tau \tag{5.36}$$

$$A_5=\left(M_M\overline{H}_x\overline{H}_y-\frac{P_2}{U}\right)\Delta\tau-M_F\overline{H}\frac{\partial\overline{H}}{\partial Y}\Bigg(M_M E_C\overline{H}^2U+\varepsilon M_F E_C\overline{H}\frac{\partial\overline{H}}{\partial X}\Bigg)(\Delta\tau)^2$$

$$-M_F\overline{H}\frac{\partial\overline{H}}{\partial Y}\Bigg(E_C\Bigg(\frac{2U}{(\Delta X)^2}\left(1-e^{-i\alpha\Delta X}\right)^2+\frac{U}{(\Delta Y)^2}\left(e^{i\beta\Delta Y}-1\right)^2\Bigg)\Bigg)(\Delta\tau)^2 \tag{5.37}$$

$$B_5=1-\frac{U\Delta\tau}{\Delta X}\left(1-e^{-i\alpha\Delta X}\right)-\frac{V\Delta\tau}{\Delta Y}\left(e^{i\beta\Delta Y}-1\right)+\Bigg[\frac{2\Delta\tau}{(\Delta X)^2}\left(\cos\alpha\Delta X-1\right)+\frac{2\Delta\tau}{(\Delta Y)^2}\left(\cos\beta\Delta Y-1\right)\Bigg]-$$

$$M_M\overline{H}_x^2\Delta\tau-M_F\overline{H}\frac{\partial\overline{H}}{\partial Y}\Bigg(\varepsilon M_F E_C\overline{H}\frac{\partial\overline{H}}{\partial Y}\Bigg)(\Delta\tau)^2-M_F\overline{H}\frac{\partial H}{\partial Y}\Bigg[E_c\Bigg(\frac{V}{(\Delta X)^2}\left(1-e^{-i\alpha\Delta X}\right)^2+$$

$$\frac{2V}{(\Delta Y)^2}\left(e^{i\beta\Delta Y}-1\right)^2\Bigg)+\frac{2U}{\Delta X\Delta Y}\left(1-e^{-i\alpha\Delta X}\right)\left(e^{i\beta\Delta Y}-1\right)\Bigg](\Delta\tau)^2 \tag{5.38}$$

$$C_5=M_F\overline{H}\frac{\partial\overline{H}}{\partial Y}\Bigg(1-\frac{U\Delta\tau}{\Delta X}\left(1-e^{-i\alpha\Delta X}\right)-\frac{V\Delta\tau}{\Delta Y}\left(e^{i\beta\Delta Y}-1\right)+M_F E_c\overline{H}\Bigg(U\frac{\partial\overline{H}}{\partial X}+V\frac{\partial\overline{H}}{\partial Y}\Bigg)\Delta\tau\Bigg)\Delta\tau$$
$$+M_F\overline{H}\frac{\partial\overline{H}}{\partial Y}\Bigg(\frac{1}{P_r}\Bigg(\frac{2\Delta\tau}{(\Delta X)^2}\left(\cos\alpha\Delta X-1\right)+\frac{2\Delta\tau}{(\Delta Y)^2}\left(\cos\beta\Delta Y-1\right)\Bigg)\Bigg)\Delta\tau \tag{5.39}$$

$$A_3=-\Bigg(M_F E_c\overline{H}^2U+\varepsilon M_F E_c\overline{H}\frac{\partial\overline{H}}{\partial X}+E_C\Bigg(\frac{2U}{(\Delta X)^2}\left(1-e^{-i\alpha\Delta X}\right)^2+\frac{U}{(\Delta Y)^2}\left(e^{i\beta\Delta Y}-1\right)^2\Bigg)\Bigg)\Delta\tau \tag{5.40}$$

$$B_3 = -\left(\varepsilon M_F E_C \overline{H} \frac{\partial \overline{H}}{\partial Y} + \left[E_c \left(\frac{V}{(\Delta X)^2} \left(1 - e^{-i\alpha\Delta X}\right)^2 + \frac{2V}{(\Delta Y)^2} \left(e^{i\beta\Delta Y} - 1\right)^2 \right) + \right.\right.$$

$$\left.\left. \frac{2U}{\Delta X \Delta Y} \left(1 - e^{-i\alpha\Delta X}\right)\left(e^{i\beta\Delta Y} - 1\right) \right] \right) \Delta\tau \qquad (5.41)$$

$$C_3 = 1 - \frac{U\Delta\tau}{\Delta X}\left(1 - e^{-i\alpha\Delta X}\right) - \frac{V\Delta\tau}{\Delta Y}\left(e^{i\beta\Delta Y} - 1\right) + M_F E_c \overline{H} \left(U \frac{\partial \overline{H}}{\partial X} + V \frac{\partial \overline{H}}{\partial Y} \right) \Delta\tau +$$

$$\frac{1}{P_r} \left(\frac{2\Delta\tau}{(\Delta X)^2} \left(\cos\alpha\Delta X - 1\right) + \frac{2\Delta\tau}{(\Delta Y)^2} \left(\cos\beta\Delta Y - 1\right) \right) \qquad (5.42)$$

Hence the equations (5.31), (5.32) and (5.33) can be expressed in matrix notation and these equations are

$$\begin{bmatrix} \psi_1' \\ \psi_2' \\ \theta' \end{bmatrix} = \begin{bmatrix} A_4 & B_4 & C_4 \\ A_5 & B_5 & C_5 \\ A_3 & B_3 & C_3 \end{bmatrix} \begin{bmatrix} \psi_1 \\ \psi_2 \\ \theta \end{bmatrix}$$

That is $\eta' = T\eta$

Where $\eta' = \begin{bmatrix} \psi_1' \\ \psi_2' \\ \theta' \end{bmatrix}$, $T = \begin{bmatrix} A_4 & B_4 & C_4 \\ A_5 & B_5 & C_5 \\ A_3 & B_3 & C_3 \end{bmatrix}$ and $\eta = \begin{bmatrix} \psi_1 \\ \psi_2 \\ \theta \end{bmatrix}$

For obtaining the stability condition, it is necessary to find out eigenvalues of the amplification matrix *T*, but this study is very difficult because it is a third order square matrix and all element are nonzero. For this explicit finite difference solution the dimensionless time difference $\Delta\tau$ is very small that is tends to zero.

Under this consideration,

$B_4 \to 0,\ C_4 \to 0,\ A_5 \to 0,\ C_5 \to 0,\ A_3 \to 0,\ B_3 \to 0$

and the amplification matrix becomes

$$T = \begin{bmatrix} A_4 & 0 & 0 \\ 0 & B_5 & 0 \\ 0 & 0 & C_3 \end{bmatrix}$$

After simplification of the matrix T, we get the following eigenvalues,

$$\lambda_1 = A_4, \quad \lambda_2 = B_5, \quad \lambda_3 = C_3$$

For stability each eigenvalues $\lambda_1, \lambda_2, \lambda_3$ must not exceed unity in modulus. Hence the stability condition is

$$|A_4| \le 1, |B_5| \le 1, \ |C_3| \le 1 \quad \text{for all } a \text{ and } b.$$

Now consider that U is everywhere non-negative and V is everywhere non-positive.

Let $a = U\frac{\Delta\tau}{\Delta X}, \ b = |V|\frac{\Delta\tau}{\Delta Y}, \ c = 2\frac{\Delta\tau}{(\Delta X)^2}, \ d = 2\frac{\Delta\tau}{(\Delta Y)^2}$,

Thus

$$A_4 = 1 - 2\left(a + b + (c+d) + \frac{1}{2}M_M \overline{H}_y^2 \Delta\tau + \frac{1}{2}M_F \overline{H}\frac{\partial \overline{H}}{\partial X}\left[M_M E_c \overline{H}^2 U + \varepsilon M_F E_c \overline{H}\frac{\partial \overline{H}}{\partial X} + E_c\left(\frac{8U}{(\Delta X)^2} + \frac{4U}{(\Delta Y)^2} \right) \right] (\Delta\tau)^2 \right)$$

$$B_5 = 1 - 2\left(a + b + c + d + \frac{1}{2}M_M \overline{H}_x^2 \Delta\tau + \frac{1}{2}M_F \overline{H}\frac{\partial \overline{H}}{\partial Y}\left[\varepsilon M_F E_C \overline{H}\frac{\partial \overline{H}}{\partial Y} + E_c\left(\frac{8V}{(\Delta Y)^2} + \frac{4V}{(\Delta X)^2} - \frac{8U}{\Delta X \Delta Y} \right) \right] (\Delta\tau)^2 \right)$$

$$C_3 = 1 - 2\left(a + b + \frac{1}{P_r}(c+d) - \frac{1}{2}M_F E_c \overline{H}\left(U\frac{\partial \overline{H}}{\partial X} + V\frac{\partial \overline{H}}{\partial Y} \right)\Delta\tau \right)$$

The coefficient a, b, c are real and non-negative. Demonstrated that the maximum modulus of A_4, B_5 *and* C_3 occurs when $\alpha\Delta X = m\pi$ and $\beta\Delta Y = n\pi$, m and n are integer and hence A_4, B_5 *and* C_3 are real. The value of $|A_4|, |B_5|$ *and* $|C_3|$ is greater when both m and n are odd integers.

To satisfy the condition $|C_3| \le 1$, the most negative allowable value is $C_3 = -1$ therefore the first stability condition is

$$2\left(a+b+\frac{1}{P_r}(c+d)-\frac{1}{2}M_F E_c \overline{H}\left(U\frac{\partial \overline{H}}{\partial X}+V\frac{\partial \overline{H}}{\partial Y}\right)\Delta\tau \le 2\right)$$

That is $U\frac{\Delta\tau}{\Delta X}+|V|\frac{\Delta\tau}{\Delta Y}+\frac{2}{P_r}\left(\frac{\Delta\tau}{(\Delta X)^2}+\frac{\Delta\tau}{(\Delta Y)^2}\right)-\frac{1}{2}M_F E_c \overline{H}\left(U\frac{\partial \overline{H}}{\partial X}+V\frac{\partial \overline{H}}{\partial Y}\right)\Delta\tau \le 1$

Likewise, the second and third conditions are $|A_4| \le 1, |B_4| \le 1$ required that

$$U\frac{\Delta\tau}{\Delta X}+|V|\frac{\Delta\tau}{\Delta Y}+2\left(\frac{\Delta\tau}{(\Delta X)^2}+\frac{\Delta\tau}{(\Delta Y)^2}\right)+\frac{1}{2}M_M \overline{H}_y^2\Delta\tau+\frac{1}{2}M_F \overline{H}\frac{\partial \overline{H}}{\partial X}\left[M_M E_c \overline{H}^2 U+\varepsilon M_F E_c \overline{H}\frac{\partial \overline{H}}{\partial X}\right.$$
$$\left.+E_c\left(\frac{8U}{(\Delta X)^2}+\frac{4U}{(\Delta Y)^2}\right)\right](\Delta\tau)^2 \le 1$$

And

$$U\frac{\Delta\tau}{\Delta X}+|V|\frac{\Delta\tau}{\Delta Y}+2\left(\frac{\Delta\tau}{(\Delta X)^2}+\frac{\Delta\tau}{(\Delta Y)^2}\right)+\frac{1}{2}M_M \overline{H}_x^2\Delta\tau+\frac{1}{2}M_F \overline{H}\frac{\partial \overline{H}}{\partial Y}\left[\varepsilon M_F E_c \overline{H}\frac{\partial \overline{H}}{\partial Y}\right.$$
$$\left.+E_c\left(\frac{8V}{(\Delta Y)^2}+\frac{4V}{(\Delta X)^2}-\frac{8U}{\Delta X.\Delta Y}\right)\right](\Delta\tau)^2 \le 1$$

Therefore, the stability conditions of the method are:

$$U\frac{\Delta\tau}{\Delta X}+|V|\frac{\Delta\tau}{\Delta Y}+\frac{2}{P_r}\left(\frac{\Delta\tau}{(\Delta X)^2}+\frac{\Delta\tau}{(\Delta Y)^2}\right)-\frac{1}{2}M_F E_c \overline{H}\left(U\frac{\partial \overline{H}}{\partial X}+V\frac{\partial \overline{H}}{\partial Y}\right)\Delta\tau \le 1 \qquad (5.43)$$

$$U\frac{\Delta\tau}{\Delta X}+|V|\frac{\Delta\tau}{\Delta Y}+2\left(\frac{\Delta\tau}{(\Delta X)^2}+\frac{\Delta\tau}{(\Delta Y)^2}\right)+\frac{1}{2}M_M \overline{H}_y^2\Delta\tau+\frac{1}{2}M_F \overline{H}\frac{\partial \overline{H}}{\partial X}\left[M_M E_c \overline{H}^2 U+\right.$$
$$\left.\varepsilon M_F E_c \overline{H}\frac{\partial \overline{H}}{\partial X}+E_c\left(\frac{8U}{(\Delta X)^2}+\frac{4U}{(\Delta Y)^2}\right)\right](\Delta\tau)^2 \le 1 \qquad (5.44)$$

$$U\frac{\Delta\tau}{\Delta X}+|V|\frac{\Delta\tau}{\Delta Y}+2\left(\frac{\Delta\tau}{(\Delta X)^2}+\frac{\Delta\tau}{(\Delta Y)^2}\right)+\frac{1}{2}M_M \overline{H}_x^2\Delta\tau+\frac{1}{2}M_F \overline{H}\frac{\partial \overline{H}}{\partial Y}\left[\varepsilon M_F E_c \overline{H}\frac{\partial \overline{H}}{\partial Y}\right.$$
$$\left.+E_c\left(\frac{8V}{(\Delta Y)^2}+\frac{4V}{(\Delta X)^2}-\frac{8U}{\Delta X.\Delta Y}\right)\right](\Delta\tau)^2 \le 1 \qquad (5.45)$$

Using the initial condition, $U = V = \overline{T} = 0$ at $\tau = 0$, we have the stability and convergence criteria of the method to be $\Pr \ge 0.733$, $M_F \le 1.73\times10^8$ and $M_M \le 2.1\times10^4$.

5.6 Results and Discussion:

5.6.1 Justification of grid space:

To verify the effects of space grid for m and n, the code is run with different space grid such as $m = n = 200$, $m = n = 300$, $m = n = 400$, $m = n = 500$, $m = n = 600$, $m = n = 700$ and $m = n = 750$. It is seen that there is a little change between $m = n = 600$ and $m = n = 750$ which are shown in Fig. 5.4. According to this solution the result of velocity and temperature have been carried out for $m = n = 600$.

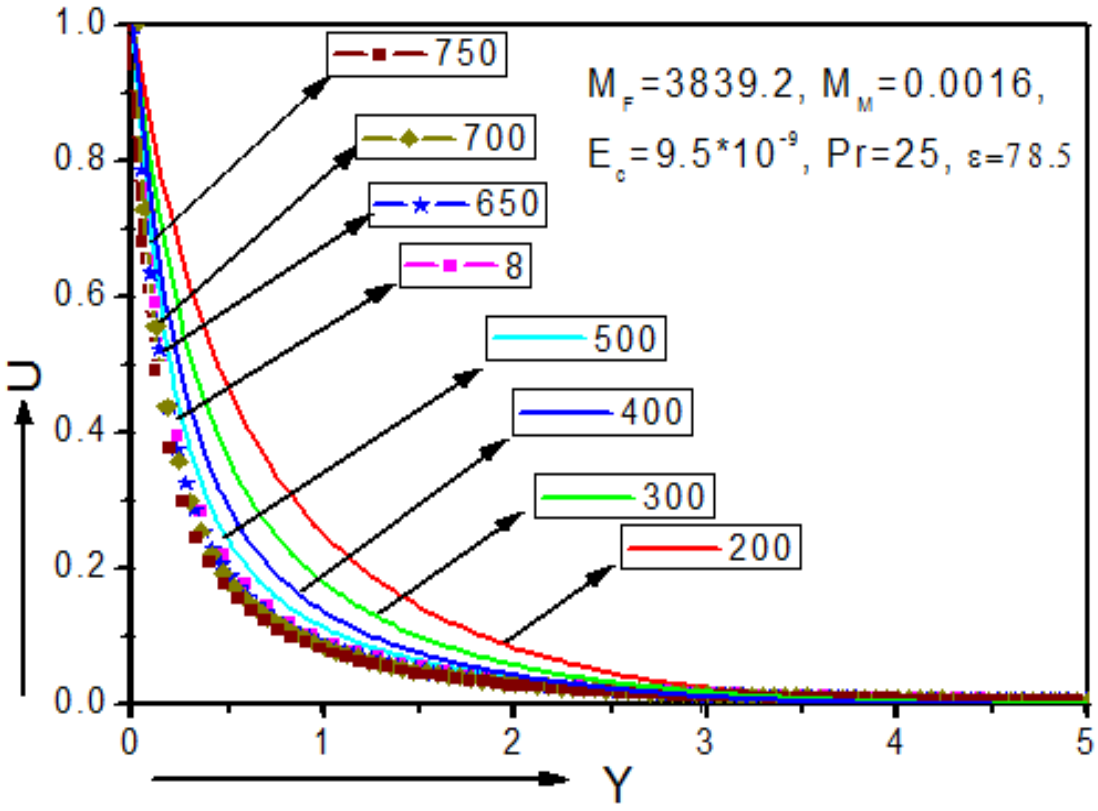

Fig 5.4: Velocity profile for different grid space

5.6.2 Steady state solution:

The computation has been carried out up to dimensionless time $\tau = 25$. The results of the computation however, show graphical changes in the below mentioned quantities to time $\tau = 25$ have been reached and after this at $\tau = 10$ *to* 25. The primary velocity do not exhibit any subsequent variation. Thus the solution for dimensionless time $\tau = 25$ for steady-state

solution for this problem. The figure 5.5 shows the solution for different time step. Therefore the steady state numerical results have been obtained for $\tau = 25,\ m = 600,\ n = 600$.

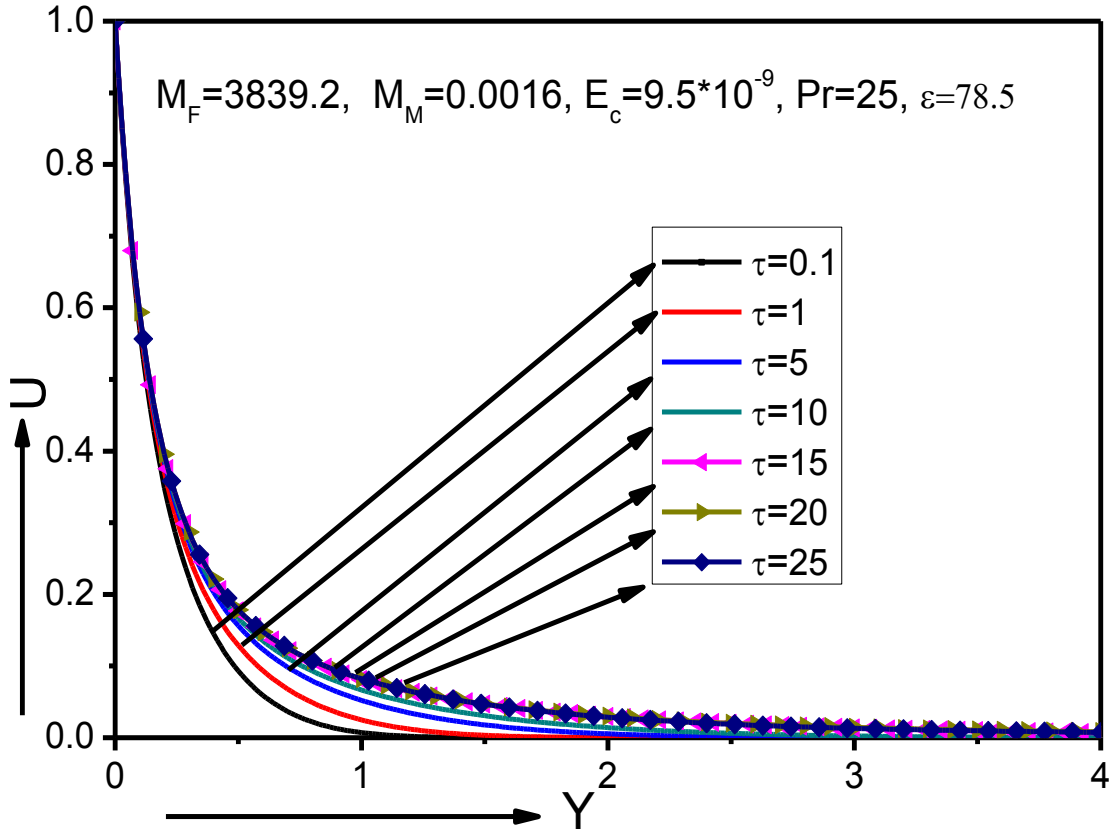

Fig 5.5: Steady case analysis for different time step

5.6.3 Estimation of Parameters:

For the numerical solution it is necessary to assign some numerical values in the dimensionless parameters entering into the problem under consideration. For these values, in order to be realistic, a similar case scenario is adopted with the one in (Tzirtzilakis (2003), (2005), Murtaza et al. (2017)) according to which the fluid is blood with density $\rho = 1050\, kg\, m^{-3}$ and viscosity $\mu = 3.2 \times 10^{-3}\, kg\, m^{-1} s^{-1}$, flowing with maximum velocity $U_0 = 1.22 \times 10^{-2}\, m\sec^{-1}$. The electrical conductivity of blood is $\sigma = 0.8 sm^{-1}$. The temperature of the plate is $T_w = 37^0 c$ whereas the temperature of the fluid is $T_c = 41^0 c$. For these values the temperature number ε is equal to 78.5. Although the viscosity μ, the specific heat under constant pressure C_p and thermal conductivity *k* of any fluid and hence of the fluid is blood, are temperature dependent the prandtl number can be considered constant.

Thus, for the temperature range considered in this problem $C_p = 3.9 \times 10^3 \, JKg^{-1}K^{-1}$ and $k = 0.5 \, Jm^{-1}s^{-1}K^{-1}$ and hence $\Pr = 25.$

The magnetic parameter M_F can be written as

$$M_F = \frac{\mu_0 k H_0^2 (T_c - T_w)}{\rho U_0^2} = \frac{\mu_0 H_0 k H_0 (T_c - T_w)}{\rho U_0^2} = \frac{BM}{\rho U_0^2} \text{ and } M_M = \frac{\sigma \mu_0^2 H_0^2 \nu}{\rho U_0^2} \tag{5.46}$$

Where *B* and *M* are the magnetic induction and magnetization respectively. For magnetic field equal to 6*T* to 10*T*, the blood has reached magnetization of $60 Am^{-1}$ by Misra et al. (2013)

Thus, for the problem under consideration M_F and M_M is determined from equation (5.46) which is given in the following table 5.1

Table 5.1: Magnetic field induction and corresponding values of M_F and M_M.

Magnetic induction (B)	Magnetohydrodynamics Number (M_M)	Ferromagnetic number (M_F)
6 T	0.00054	2303
8 T	0.00096	3071.2
9 T	0.0013	3455.1
10 T	0.0016	3839.2

In order to discuss the results of the problem, the numerical solutions are computed by the explicit method. For analyzing the physical situation of the model, we have the steady-state numerical value of the non-dimensional primary velocity *U*, secondary velocity *V* and temperature $\overline{T}$ for Eckert number, $E_c = 9.5 \times 10^{-9}$, Prandtl number, $\Pr = 25$, Magnetohydrodynamic (MHD) parameter, $M_M = 0, 0.0016, 0.0013, 0.00094, 0.00054$ and Ferromagnetic (FHD) parameter, $M_F = 0, 3839.2, 3455.1, 3071.2, 2303$.

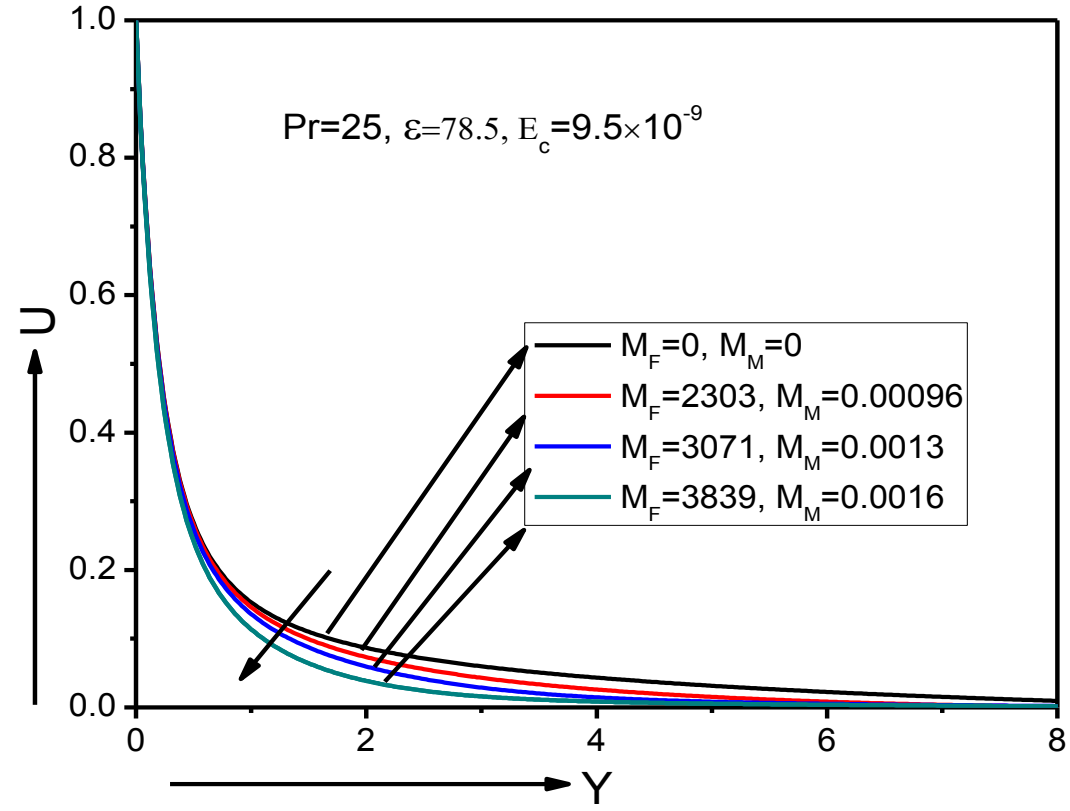

Fig 5.6: Primary velocity for different value of M_M and M_F

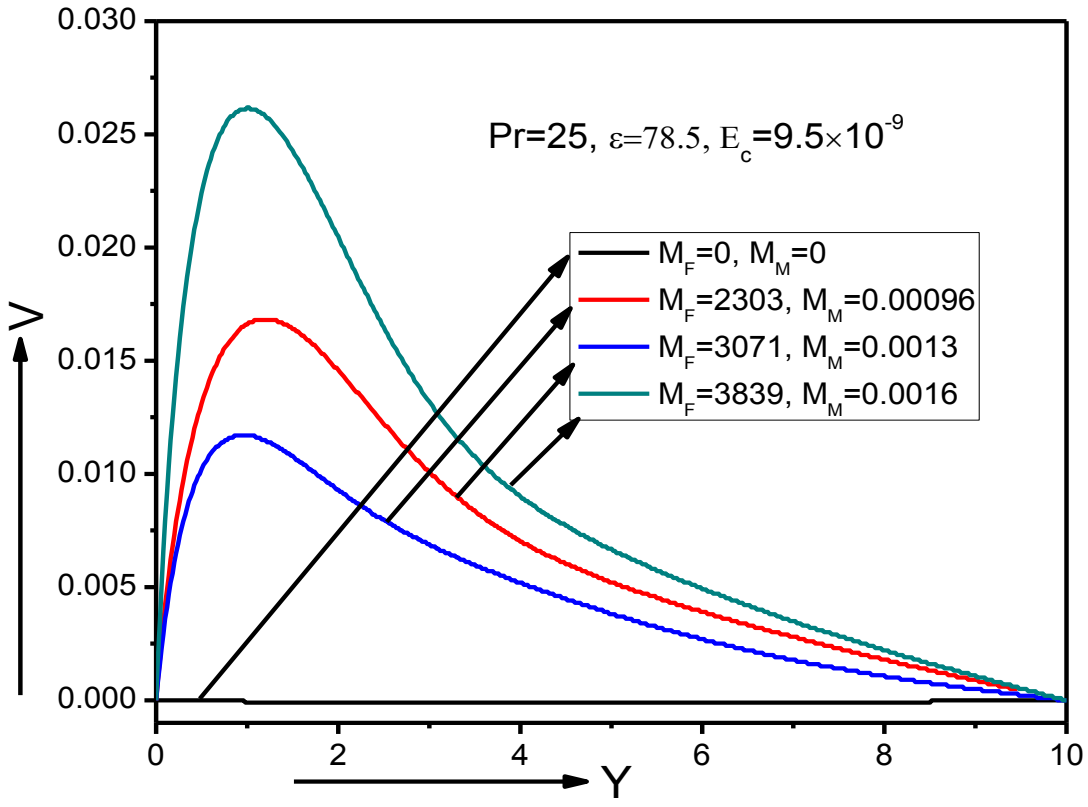

Fig 5.7: Secondary velocity for different value of M_M and M_F

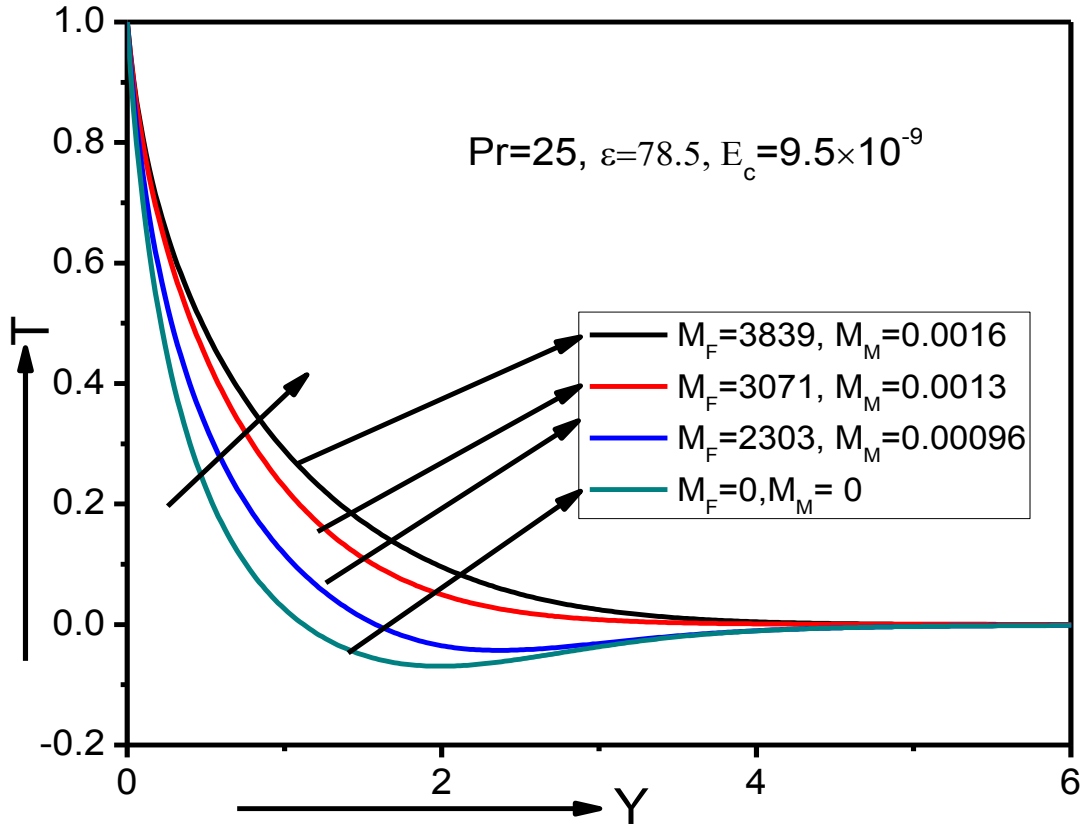

Fig 5.8: Temperature profile for different value of M_M and M_F

The effect of Magnetohydrodynamic (MHD) parameter and ferromagnetic parameter on the primary velocity, secondary velocity and temperature distributions have been shown in figures 5.6-5.8. We observed from these figures, fluid primary velocity decreases but secondary velocity and temperature distribution increases with increase of MHD and FHD parameter which is represented at fig. 5.6, 5.7 and 5.8, respectively.

Figure 5.9 shows the stream function contour for the value of the above mentioned parameters and for M_M and M_F numbers are 0.0, 0.00054, 0.00096 ,0.0016 and 0, 2303, 3071.2, 3839.2, respectively.

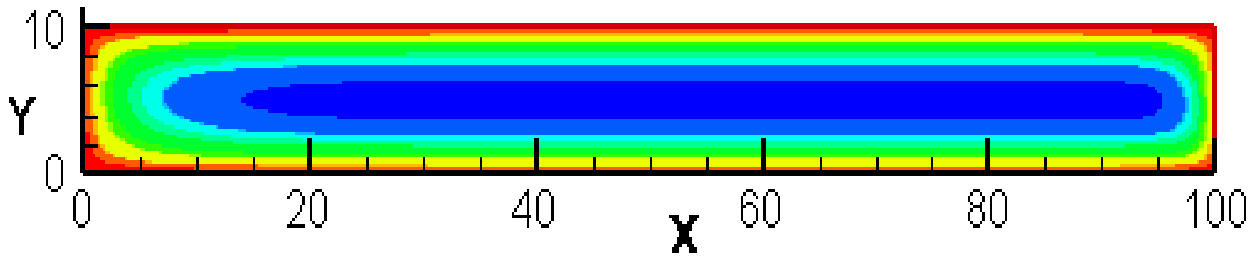

$B = 0T, M_M = 0, M_F = 0$

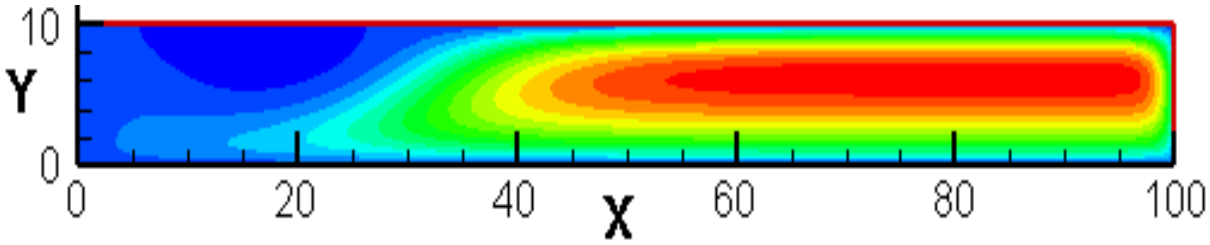

$B = 6T, M_M = 0.00054, M_F = 2303$

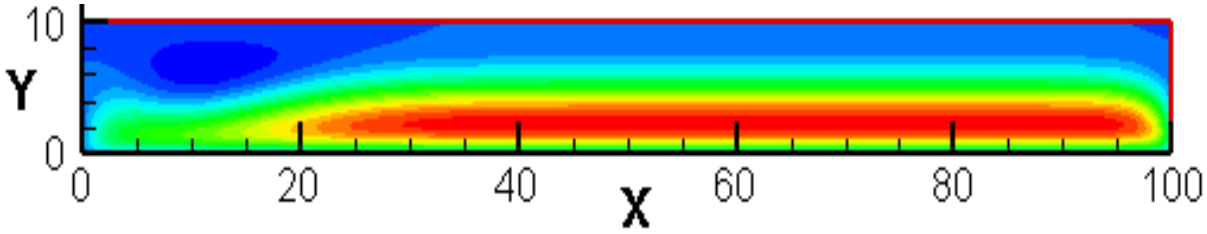

$B = 8T, M_M = 0.00094, M_F = 3071.2$

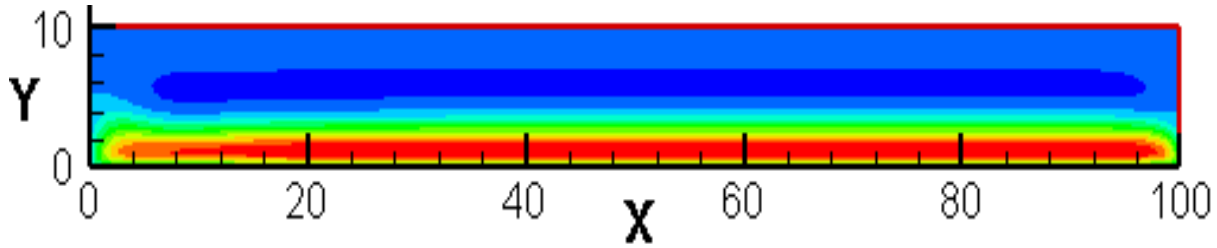

$B = 10T, M_M = 0.0016, M_F = 3839.2$

Fig. 5.9 Stream function contours for different value of M_F and M_M

5.7 Summary of the chapter

A mathematical model with mixed FHD and MHD unsteady fluid flow of the extended BFD has been studied.

The boundary layer equations have been non-dimensionalized by using non-dimensional variable. The non-dimensional boundary layer equations are non-linear partial differential equations. These equations are solved by using an explicit finite difference method (EFDM), details of the stability and convergence characteristics are also included. A detailed study of the effect of several key parameters controlling the flow characteristics has been conducted. The computations have shown that:

The primary velocity and secondary velocity and temperature profile is increased with the increase of Magnetic number arising from MHD and FHD.

With grater elapse of time (τ), velocity and temperature profiles found to be enhance subsequently.

Chapter 6

Influence of magnetic field on biomagnetic fluid over a nonlinearly stretching sheet with variable thickness

The aim of this chapter is to investigate the fundamental problem of biomagnetic fluid flow over a new dimension in the field of stretching sheet with variable thickness in the presence of applied magnetic field. The model used takes into account both magnetization and electrically conductivity arising in a magnetic fluid. The governing PDEs are transformed into a system of couple non-linear ODEs subject to appropriate boundary conditions. The numerical solution is obtained by an efficient numerical technique based on common finite differences method. The effect of wall thickness parameter α, ferromagnetic parameter β, magnetohydrodynamic parameter M_n, velocity index parameter m on the flow, pressure and temperature profile are presented graphically for specific values of dimensionless parameters entering into the problem under consideration. It is interesting to note that all over the sheet the skin friction coefficient, rate of heat transfer and wall pressure are increased linearly as the ferromagnetic parameter increases but are increased nonlinearly with the increment of the magnetohydrodynamic and velocity power index parameter. It is also noted that a dominant factor for the formation of the BFD flow field is m along with the magnetic parameters β and M_n .

6.1 Introduction

Biomagnetic fluid dynamics (BFD) is the investigation of biological fluid and the flows which are affected by the influence of external magnetic field. A fluid that is present in a living creature is known as a biomagnetic fluid. Blood is one of the fluids that has characteristic of biomagnetic fluid and is considered a magnetic fluid.

Many research works have been done on the biomagnetic fluids in theoretical and experimental due to the applications of medical and bioengineering since the last decades. The investigation of the effect of magnetic field on fluids is valuable because there are many applications in a wide range of fields. There are numerous applications on BFD study in

medicine and bioengineering research work. The magnetic devices development for cell separation, high-gradient magnetic separation, reduction of blood flow during surgeries, targeted transport of drugs using magnetic particles as drug carries, treatment of cancer tumor causing magnetic hyperthermia and magnetic wound treatment and development of magnetic tracers, (Haik et al. (1999), Fiorentini and Szasz (2006), Andra and Nowak (1998), Voltaira and Fotiadis (2002), Misra et al. (2011), Ruuge and Rusetski (1993)).

Based on the mathematical model of BFD, the flow of biofluid under the effect of magnetic field consider both principles of ferrohydrodynamics (FHD) and magnetohydrodynamics (MHD). Usually, FHD is considered for the formulation of electrically non-conducting magnetic fluids and the flow is influenced by the fluid magnetization in the magnetic field. On the other hand, MHD is considered for conducting fluids and ignores the effect of polarization and magnetization. The magnetization property M is the behavior of a biological fluid when it is exposed to magnetic field. This measures how much the magnetic field is affecting the fluid in various aspects. There are various equations describing the dependence of M. Another variable important to BFD problems, is the temperature field as well as the heat transfer on the walls. These flow characteristics are of interest for problems investigating the possible influence of the application of the magnetic field during a hyperthermia treatment, (Andersson and Valnes (1998), Tzirtzilakis and Kafaussias (2003), Tzirtzilakis and Tanoudis (2003), Higashi et al. (1993)).

In general, biological systems are affected by an application of external magnetic field on blood flow through human arterial system. Many mathematical models have already been investigated by several research workers to explore the nature of blood flow under the influence of an external magnetic field. The flow of BFD, mathematical model has been developed first Haik el al. (1999). This model is conformed with the principles of FHD, Rosensweig (1985, 1987). For a full description of blood flow, the contribution of the Lorentz force due to the induced electric current of MHD should be taken into account. Therefore, an extended BFD mathematical model, which include the Lorentz force was developed by Tzirtzilakis (2005). He studied the mathematical model of biomagnetic fluid dynamics (BFD), suitable for the description of the Newtonian blood flow under the action of magnetic field. This model is consistent with the principles of ferrodynamics and magnetohydrodynamics and takes into account both magnetization and electrical conductivity of blood. Ramamurthy and Shanker

(1994) studied magnetohydrodynamic effects on blood flow through a porous channel. They considered the blood as a Newtonian and electrically conducting fluid.

The problem of biomagnetic fluid flow under the action of a spatially varying magnetic field was developed by Nursalasawati (2012). She assumed that the magnetization force was due to FHD interaction. From her investigation, the results regarding the velocity showed that the presence of magnetic field appreciably influenced the flow field. In addition, she considered the Lorentz forces due to MHD and FHD interaction only. The Lorentz force just gives a small influence to the flow behaviors.

Tzirtzilakis and Kafoussias (2003) analyzed the mathematical model of the flow of a heated ferrofluid over a linearly stretching sheet under the action of a magnetic field which is generated by a magnetic dipole. Tzirtzilakis and Tanoudis (2003) presented a numerical method for the study of laminar incompressible two dimensional biofluid over a stretching sheet with heat transfer. It was assumed that the magnetization of the fluid varied with the magnetic field strength H and the temperature T. Tzirtzilakis et al. (2006) further analyzed a problem of a turbulent biomagnetic fluid flow in a rectangular channel under the action of localized magnetic field. Misra and Shit (2009) investigated the biomagnetic viscoelastic fluid flow over a stretching sheet.

Many investigators were studied the influence of a uniform magnetic field on the flow and heat transfer of an electrically conducting fluid past a stretching sheet/surface. Pavlov (1974) obtained a closed form solution for the velocity field, within the boundary layer approximation. He investigated the effect of a magnetic field on the viscous flow of an electrically conducting fluid past a stretching sheet. The same solution was shown by Andersson (1995) to be an exact solution of the Navier-Stokes equations. Andersson (2002), Ishak et al. (2006, 2009, 2010) were also made to examine the flow characteristic over a stretching sheet under the influences of magnetic field. Further Anderson (1992) investigated the MHD flow of a viscoelastic fluid past a stretching surface. He consider the combined effects of viscoelasticity and a magnetic field and concluded that an increase of the magnetic field has the same influence on the flow field as increased viscoelasticity. El-Mistikawy (2016) studied the MHD flow due to a linearly stretching sheet with induced magnetic field. Ali et al. (2011) examined MHD boundary layer flow and heat transfer over a stretching sheet with induced magnetic field. They found that the external magnetic field affects the flow and heat transfer. Further Ali et al. (2011) also studied

numerically the MHD mixed convection boundary layer flow towards a stagnation point flow on a vertical surface with the effect of induced magnetic field. Their study indicates that the induced field is most affected by the reciprocal of the magnetic Prandtl number when compared with the skin friction and heat transfer coefficients. Devi and Thiyagarajan (2006) solved the steady nonlinear MHD flow of an incompressible, viscous and electrically conducting fluid with heat transfer over a surface of variable temperature stretching with a power law velocity in the presence of variable transverse magnetic field. Their study shows that the surface velocity gradient and heat transfer increase with an increase in magnetic.

Most of the researchers studied the biomagnetic fluid flow over a linearly stretching sheet. First Fang et al. (2012) examined the fluid flow using a special form of non-linear stretching sheet which is called a stretching sheet with variable thickness. It was found that the adoption of vartiable thickness leads to significantly different results for the boundary layer development, comparable to those obtained for the plain stretching sheet. After then Lee (1967) studied the boundary layer flow over a slender body with variable thickness. Ishak et al. (2007) examined the boundary layer flow over a horizontal thin needle. Khader and Megahed (2015), Prasad et al. (2016) and Vajravelu et al (2017) explained the effects of various physical parameters on the flow and heat transfer by considering the special form of stretching sheet (i.e. stretching sheet with variable thickness).

Therefore, the objective of this chapter is to study the biomagnetic fluid flow over a stretching sheet with variables thickness in the presence of an applied magnetic field. Various methodologies for numerical solutions are adopted in order to solve the biomagnetic fluid flow problem. For the present study, this model is solved by applying and efficient numerical technique based on the common finite difference method described by Kafoussias and Williams (1993). The obtained results for critical flow characteristics like velocity, pressure and temperate as well as rate of heat transfer, skin friction or pressure on the stretching sheet are presented graphically for specific parameters entering into the problem under consideration.

6.2 Mathematical Formulation

We consider a steady, two-dimensional boundary layer flow of an incompressible and electrical conducting biomagnetic fluid over a non-linear stretching sheet with variable thickness. The origin of the Cartesian system is located at a slit, through which the sheet is drawn through the fluid medium. The sheet moves with the non-uniform velocity $U_w = U_0(x+b)^m$, U_0 is the reference velocity, b is the physical parameter related to the stretching sheet, x is the coordinates measured along the stretching surface. The flow is confined to the region $y \geq 0$, where y is the coordinate measured normal to the stretching surface.

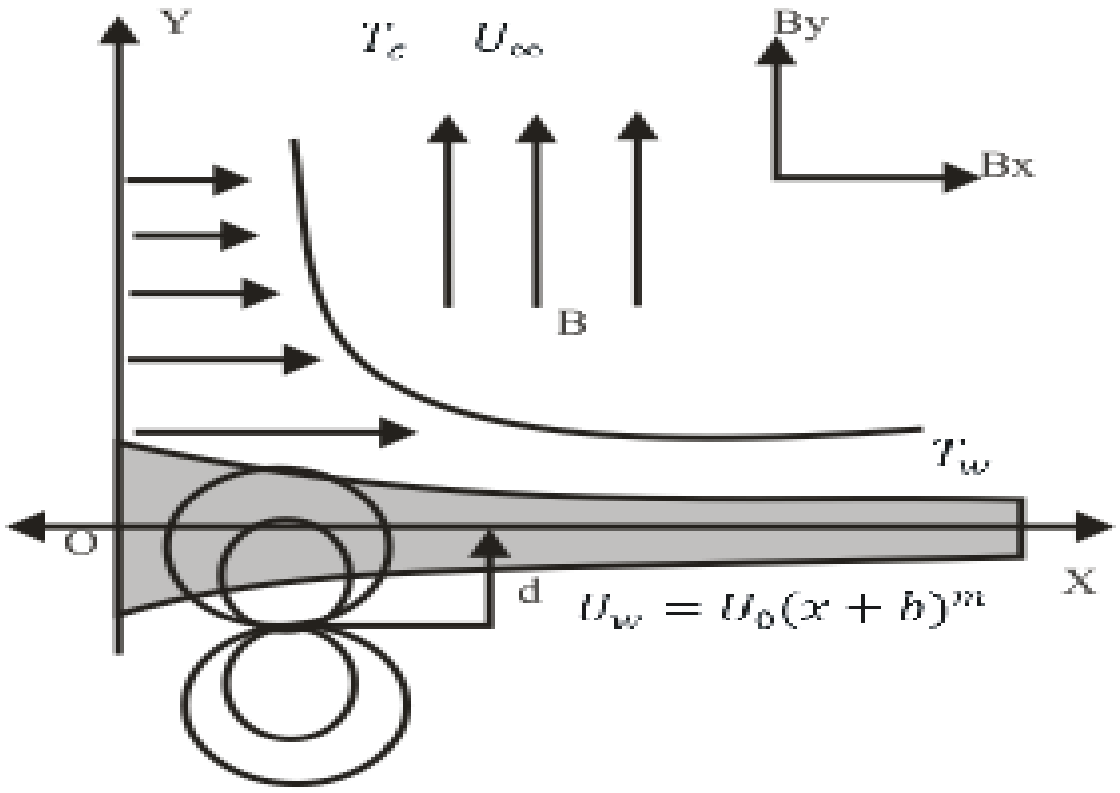

Fig.6.1 Schematic diagram of the stretching sheet with variable thickness

We assume that the sheet is not flat and its thickness is defined by $A(x+b)^{\frac{1-m}{2}}$, where A is a very small constant so that the sheet is sufficiently thin and m is the nonlinear parameter. Since the sheet is not flat so we must observe that our problem is valid for $m \neq 1$ because for $m = 1$ the problem is reduced to that of a flat sheet. Also, the fluid is electrically conducted due

to an applied magnetic field normal to the stretching sheet. We consider a non-uniform heat source/ sink applied to the flow. Let the wall temperature T_w assumed constant at the stretching surface, while far away from the sheet temperature is T_c, where $T_c > T_w$ Here the magnetic dipole is located at the distance d below the sheet which gives rise to a magnetic field of sufficient strength to saturate the biomagnetic fluid. The coordinate system and the flow model are shown in Fig. 6.1

Under the boundary layer approximation and the assumptions that the basic equations of continuity, momentum and energy are given by, (Haik et al. (1999), Tzirtzilakis (2005), Tzirtzilakis and Xenos (2013))

Continuity equation:

$$\frac{\partial \mathrm{u}}{\partial \mathrm{x}} + \frac{\partial \mathrm{v}}{\partial \mathrm{y}} = 0 \tag{6.1}$$

Momentum equation:

$$\rho\left(u\frac{\partial \mathrm{u}}{\partial \mathrm{x}} + v\frac{\partial u}{\partial \mathrm{y}} \right) = -\frac{\partial p}{\partial x} + \mu_0 M\,\frac{\partial H}{\partial x} - \sigma B_y^2 u + \sigma B_x B_y v + \mu\frac{\partial^2 u}{\partial y^2} \tag{6.2}$$

$$\rho\left(u\frac{\partial \mathrm{v}}{\partial \mathrm{x}} + v\frac{\partial v}{\partial \mathrm{y}} \right) = -\frac{\partial p}{\partial y} + \mu_0 M\,\frac{\partial H}{\partial y} - \sigma B_x^2 v + \sigma B_x B_y u + \mu\frac{\partial^2 v}{\partial y^2} \tag{6.3}$$

Energy equation:

$$\rho C_p\left(u\frac{\partial T}{\partial x} + v\frac{\partial T}{\partial y} \right) + \mu_0 T\frac{\partial M}{\partial T}\left(u\frac{\partial H}{\partial x} + v\frac{\partial H}{\partial y} \right) = k\frac{\partial^2 T}{\partial y^2} + q''' \tag{6.4}$$

The relevant boundary conditions at the sheet $y = A(x+b)^{\frac{1-m}{2}}$ is

$$u(x,y) = U_w = U_0(x+b)^m,\ v(x,y) = 0,\ T(x,y) = T_w = T_c + D\left(\frac{x+b}{l}\right)^{2m-1} \tag{6.5}$$

Whereas, the boundary conditions infinitely far away from the sheet, i.e. as $y \to \infty$

$$u(x,y) \to 0,\quad T \to T_c,\quad p + \frac{1}{2}q^2 = const \tag{6.6}$$

where u and v are the velocity components in x and y directions, respectively. ρ and k are the fluid density and thermal conductivity respectively. T is the temperature of the fluid and c_p is the specific heat at constant pressure, μ is the fluid viscosity, σ is the electrical conductivity, μ_0 is the magnetic permeability, q''' is the space and temperature dependent internal heat generation / absorption (non-uniform heat source/sink) and $H=(H_x,H_y)$ is the magnetic field strength, B is the magnetic induction where $B=\mu_0 H$

Here, the second terms on the right-hand side of the ferrohydromagnetic momentum equations (6.2) and (6.3) represent the magnetic body force per unit volume $\mu_o M\nabla H$, and the second term on the left-hand side of the thermal energy equation (6.4) accounts for heating due to adiabatic magnetization. These two terms arise due to the principles of FHD. Also, the terms known in MHD $-\sigma B_y^2 u+\sigma B_x B_y v$ and $-\sigma B_x^2 v+\sigma B_x B_y u$ in (6.2) and (6.3), respectively, represent the Lorentz force per unit volume towards the x and y directions respectively.

An important flow characteristic is expressed by the term q''' which is the space and temperature dependent internal heat generation/absorption (non-uniform heat source/sink) which can be express in simplest form as Abel and Mahesha (2008), Abel et al. (2007)

$$q'''=\frac{kU_w(x)}{(x+b)^m \nu}\left[A^*\left(T_w-T_c\right)f'+B^*\left(T-T_c\right)\right] \tag{6.7}$$

Where A^* and B^* are the coefficient of space and temperature dependent heat source/ sink, respectively. The value of A^* and B^* are arise two cases (i) $A^*>0$ and $B^*>0$ which corresponds to internal heat generation and (ii) $A^*<0$ and $B^*<0$ which corresponds to internal heat absorption.

We consider that the components H_x, H_y of the magnetic field $\overline{H}=(H_x,H_y)$ due to the electric current following through the wire with intensity γ, are given by

$$H_x=\frac{\gamma}{2\pi}\frac{(x+b)^2-(y+d)^2}{\left[(x+b)^2+(y+d)^2\right]^2}$$

$$H_y = \frac{\gamma}{2\pi} \frac{2(x+b)(y+d)}{\left[(x+b)^2 + (y+d)^2\right]^2}$$

Thus, the magnitude $\|H\| = H$ of the magnetic field intensity by

$$H(x,y) = \left(H_x^2 + H_y^2\right)^{\frac{1}{2}} = \frac{\gamma}{2\pi} \frac{1}{(x+b)^2 + (y+d)^2}$$

and the gradient are given by

$$\frac{\partial H}{\partial x} = -\frac{\gamma}{2\pi} \frac{2(x+b)}{(y+d)^4} \quad \text{and} \quad \frac{\partial H}{\partial y} = \frac{\gamma}{2\pi}\left[-\frac{2}{(y+d)^3} + \frac{4(x+b)^2}{(y+d)^5}\right]$$

According to FHD the magnetization M, under the equilibrium assumption, is generally a function of the magnetic field strength H, temperature T and fluid density ρ. In the present formulation of BFD, the blood is actually considered as a electrically non-conducting magnetic fluid. Thus, for the variation of the magnetization M with the magnetic field intensity H and temperature T, the following relation derived experimentally by Matsuki et al. (1977) and also used in Tzirtzilakis (2008, 2015) is

$$M = KH(T_c - T) \tag{6.8}$$

where K is a constant and T_c is the Curie temperature.

6.3 Mathematical Analysis

The mathematical analysis of the problem is simplified by introducing the following non-dimensionless variables, (Fang et al. (2012), Khader and Megahed (2015), Vajravelue et al. (2017))

$$\eta_1 = y\sqrt{\frac{m+1}{2}\frac{U_0(x+b)^{m-1}}{\nu}}, m \neq 1 \tag{6.9}$$

$$\psi(x,y) = F(\eta_1)\sqrt{\frac{2}{m+1}\nu U_0(x+b)^{m+1}} \tag{6.10}$$

$$\theta(\eta_1) = \frac{T - T_c}{T_w - T_c} \tag{6.11}$$

$$P(\eta_1) = U_0 \nu \frac{m+1}{2} \frac{U_0 (x+b)^{m+1}}{\nu} \tag{6.12}$$

Where η_1 is the dimensionless similarity variable, $\psi(x, y)$ is the dimensionless stream function and $\theta(\eta_1)$ is the dimensionless temperature distribution.

The velocity components can be defined as

$$u = \frac{\partial \psi}{\partial y} = U_0 (x+b)^m F'(\eta_1) = U_w F'(\eta_1) \text{ and}$$

$$v = -\frac{\partial \psi}{\partial x} = -\sqrt{\nu \frac{m+1}{2} U_0 (x+b)^{m-1}} \left(F(\eta_1) + \eta_1 \frac{m-1}{m+1} F'(\eta_1) \right)$$

In the present work, it is assumed that $m > -1$ for the validity of the similarity transformations. Substituting equations (6.9)-(6.12), into equations (6.2)-(6.4), the non-dimensional governing equations become

$$F''' + FF'' - \frac{2m}{m+1} F'^2 + \frac{(m+1)^2}{2} P - (m+1) \frac{\delta^2 \beta \theta}{(\eta_1 + \delta)^6} - M_n F' = 0 \tag{6.13}$$

$$P' + \frac{6\delta^2 \beta \theta}{(\eta_1 + \delta)^7} = 0 \tag{6.14}$$

$$\theta'' - P_r \left[\frac{2(2m-1)}{m+1} F' \theta - F \theta' \right] + \frac{2\delta^2 \lambda \beta (\theta - \varepsilon)}{(\eta_1 + \delta)^5} F + A^* F' + B^* \theta = 0 \tag{6.15}$$

Subject to the following boundary conditions:

$$F(\alpha) = \alpha \left(\frac{1-m}{1+m} \right),\ F'(\alpha) = 1,\ F'(\infty) \to 0,\ \theta(\alpha) = 1 \text{ and } \theta(\infty) \to 0. \tag{6.16}$$

where $\alpha = A \sqrt{\frac{m+1}{2} \frac{U_0}{\nu}}$ is a parameter related to the thickness of the wall and $\alpha = \eta_1 = A \sqrt{\frac{m+1}{2} \frac{U_0}{\nu}}$ indicates the plate surface. In order to proceed to the numerical computations, we define $F(\eta_1) = F(\eta - \alpha) = f(\eta)$ and $\theta(\eta_1) = \theta(\eta - \alpha) = \Theta(\eta)$ and $P(\eta_1) = P(\eta - \alpha) = p(\eta)$

Then the similarity equations (6.13), (6.14) and (6.15) along with associated corresponding boundary conditions (6.16) become:

$$f'''+ff''-\frac{2m}{m+1}f'^{2}+\frac{(m+1)^2}{2}p-(m+1)\frac{\delta^2\beta\theta}{(\eta+\delta)^6}-M_n f'=0 \tag{6.17}$$

$$p'+\frac{6\delta^2\beta\Theta}{(\eta+\delta)^7}=0 \tag{6.18}$$

$$\Theta''-P_r\left[\frac{2(2m-1)}{m+1}f'\Theta-f\Theta'\right]+\frac{2\delta^2\lambda\beta(\Theta-\varepsilon)}{(\eta+\delta)^5}f+A^*f'+B^*\Theta=0 \tag{6.19}$$

$$f(0)=\alpha\left(\frac{1-m}{1+m}\right),\ f'(0)=1,\ f'(\infty)\to 0,\ \Theta(0)=1,\ \Theta(\infty)\to 0.\ and\ \ p(\infty)\to 0 \tag{6.20}$$

The non-dimensional parameters entering now into the problem under consideration are

Where $P_r=\frac{\mu C_p}{k}$ Prandtl number

$M_n=\frac{\sigma\mu_0^2H}{U_0\rho}$ Magnetohydrodynamic interaction parameter

$\lambda=\frac{U_0\mu^2}{\rho k(T_c-T_w)}$ Viscous dissipation parameter.

$\beta=\frac{\gamma}{2\pi}\frac{\mu_0KH(0,0)(T_c-T_w)\rho}{\mu^2}$ Ferromagnetic number.

$\varepsilon=\frac{T_w}{T_c-T_w}$ Dimensionless temperature parameter.

$\delta=\left(\frac{U_0\rho}{\mu}\right)^{\frac{1}{2}}d$ Dimensionless distance

The physical quantities of primary interest are the local skin friction coefficient C_{fx} and the local Nusselt number N_u which are defined as

$$C_{fx}=-2\sqrt{\frac{m+1}{2}}R_e^{-\frac{1}{2}}f''(0)\ \text{ and }\ N_u=-\sqrt{\frac{m+1}{2}}R_e^{-\frac{1}{2}}\Theta'(0)$$

where $R_e=\frac{u_w(x+b)}{\nu}$ is the local Reynolds numbers.

6.4 Numerical Method

For the numerical solution of the problem under consideration we apply an approximate technique that has better stability characteristics than classical Runge-Kutta combined with a shooting method, is simple, accurate and efficient. The essential features of this technique are the following: (i) It is based on the common finite difference method with central differencing (ii) on a tridiagonal matrix manipulation and (iii) on an iterative procedure. This numerical method is described in detail in Kafoussias and Williams (1993). For reasons of completeness of this study we demonstrate the application of this methodology for the numerical solution of the system of equations (6.17) and (6.19), subject to the boundary conditions (6.20).

The momentum Equation (6.17) can be written as

$$f'''+ff''-\frac{2m}{m+1}f'^{2}-M_n f'=(m+1)\frac{\delta^2\beta\theta}{(\eta+\delta)^6}-\frac{(m+1)^2}{2}p \qquad (6.21)$$

The above equations can be considered as a second order linear differential equation by setting $y(x)=f'(\eta)$ provided that P and $f(\eta)$ are considered known functions. In this case equation (6.21) can be written as

$$(f')''+f(f')'-\left(\frac{2m}{m+1}f'+M_n\right)f'=(m+1)\frac{\delta^2\beta\theta}{(\eta+\alpha)^6}-\frac{(m+1)^2}{2}P$$

which is of the form

$$P(x)y''(x)+Q(x)y'(x)+R(x)y(x)=S(x) \qquad (6.22)$$

where $P(x)=1,\ Q(x)=f(\eta),\ R(x)=\left(\frac{2m}{m+1}f'+M_n\right),\ S(x)=m+1)\frac{\delta^2\beta\theta}{(\eta+\alpha)^6}-\frac{(m+1)^2}{2}P$

In an analogous manner all equations of the system can be reduced in this form of equation (6.22) except for equation (6.18) which are already first order differential equations. Equation (6.22) can be solved by a common finite difference method, based on central differencing and tridiagonal matrix manipulation.

To start the solution procedure, we assume initial guesses (distribution curves) for $f'(\eta)$ and $P(\eta)$ between $\eta=0$ and $\eta=\eta_\infty(\eta\to\infty)$ which satisfy the boundary condition (6.20). For this problem indicative initial guesses are

$$f(\eta)=\alpha\left(\frac{1-m}{1+m}\right)-\frac{\eta}{\eta_\infty},\ f'(\eta)=1-\frac{\eta}{\eta_\infty},\ \theta(\eta)=1-\frac{\eta}{\eta_\infty}.$$

The $f(\eta)$ distribution is obtained by the integration from $f'(\eta)$ curve. The next step is to consider the f, P, θ known and to determine a new estimation for $f'(\eta)$, $f'_{new}(\eta)$ by solving the non-linear equation (6.22) using the above method. The distribution is updated by the integration of new $f'(\eta)$ curve. These new profiles of $f'(\eta)$ and $f(\eta)$ are then used for new inputs and so on. In this way the momentum equation (6.21) and consequently (6.17) is solved iteratively until convergence up to a small quantity ε is attained.

After $f(\eta)$ is obtained the solution of the energy equation (6.19) with boundary condition (6.20) is solved by using the same algorithm, but without iteration now as for as equation (6.19) is linear. Equation (6.19) is

$$\Theta''-P_r\left[\frac{2(2m-1)}{m+1}f'\Theta-f\Theta'\right]+\frac{2\delta^2\lambda\beta(\Theta-\varepsilon)}{(\eta+\delta)^5}f+A^*f'+B^*\Theta=0$$

This equation can be written as

$$\Theta''-P_r f\Theta'-\left(P_r\frac{2(2m-1)}{m+1}f'-\frac{2\delta^2\lambda\beta f}{(\eta+\delta)^5}-B^*\right)\Theta=\frac{2\delta^2\lambda\beta\varepsilon}{(\eta+\delta)^5}f-A^*f' \qquad (6.23)$$

Equation (6.23) is a second order linear differential equation in setting $y(\eta)=\theta(\eta)$

which is of the form

$$P(x)y''(x)+Q(x)y'(x)+R(x)y(x)=S(x) \qquad (6.30)$$

where $P(x)=1,\ Q(x)=-P_r f,\ R(x)=-\left(P_r\frac{2(2m-1)}{m+1}f'-\frac{2\delta^2\lambda\beta f}{(\eta+\delta)^5}-B^*\right),$

$$S(x)=\frac{2\delta^2\lambda\beta\varepsilon}{(\eta+\delta)^5}f-A^*f$$

Considering $f(\eta), f'(\eta)$ and θ known, we obtain a new approximation θ_{new} for θ and this process is continue until convergence up to a small quantity ε is attained and finally we obtain θ. This process is continuing until final convergence of the solution is attained.

In order to apply to our numerical computation a proper step size $h = \Delta\eta = 0.01$ and appropriate η_∞ value as $(y \to \infty)$ must be determined. By "trial and error" we set $\eta_\infty = 8$, $\Delta\eta = 0.01$ and the tolerance between the iterations is set at $\varepsilon = 10^{-4}$ defined as $\varepsilon = \max_{i=1,N}\left(\left|\frac{f_{old}(i) - f_{new}(i)}{f_{old}(i)}\right|\right)$. Computations were also performed for $\Delta\eta = 0.001$ and no significant differences were found.

6.5 Assignment of the parameter values

The dimensionless parameters are required to allocate the values for entering into the problem in order to continue to derivation of the numerical results. For this problem, we can assume that the fluid is blood with $\rho = 1050\, kg/m^3$ and $\mu = 3.2\times10^{-3}\, kgm^{-1}s^{-1}$ (Tzirtzilakis (2008, 2015)). The electrical conductivity of blood is $\sigma = 0.8 sm^{-1}$ (Tzirtzilakis (2005)). A range is adopted for the temperature field under the influence of the applied magnetic field. The temperature of the fluid is $T_c = 41^0 c$ while the plate temperature is $T_w = 37^0 c$. For these values of temperature, the temperature number is $\varepsilon = 78.5$ and the viscous dissipation number is 6.4×10^{-14}. Generally, the specific heat under a constant pressure c_p and thermal conductivity k of any fluid are temperature dependent. However, the ratio including the above quantities expressed by the Prandtl number can be considered constant with the temperature variation. Therefore, for the temperature range consider in this problem, $c_p = 3.9\times10^3\, Jkg^{-1}k^{-1}$ and $k = 0.5\, Jm^{-1}s^{-1}k^{-1}$ and hence $P_r = 25$

As far as the parameters related with the magnetic field, in the present study we adopted the value of β to be 0 to 10, used also in the studies, Tzirtzilakis (20015), Tzirtzilakis and Kafaussian (2003). Moreover, similar range is adopted for the Magnetohydrodynamics parameter M_n which is 0 to 10

6.6 Results and Discussion

In this section, we discuss the influence of different parameters $m, \alpha, \beta, M_n, A^*, B^*$ on velocity, pressure and temperature fields. The numerical results are presented graphically in figures 6.2-6.18.

In the absence of the magnetic field i.e β=0, M_n=0 and for α=0.5 or 0.25 the numerical values for $-f''(0)$ are found to be in excellent agreement with Fang et al. (2012) and Kader and Megahed (2015) which displayed in table 6.1.

Table 6.1: Comparison of numerical values of $-f''(0)$

α	m	Present result $-f''(0)$	Fang et al. (2012)	Kader and Megahed (2015)
0.5	10	1.0602	1.0603	1.0602
	9	1.0590	1.0589	1.0589
	7	1.0557	1.0550	1.0550
	5	1.0503	1.0486	1.0486
	3	1.0397	1.0359	1.0358
	2	1.0295	1.0234	1.0235
	-0.5	1.1647	1.1667	1.1667
0.25	10	1.1432	1.1434	1.1434
	9	1.1404	1.1405	1.1405
	7	1.1327	1.1326	1.1326
	5	1.1198	1.1186	1.1186
	3	1.0933	1.0905	1.0905

For the biomagnetic flow (β=10, M_n=5), first we analyze the effects of wall thickness parameter on the fluid flow, pressure and temperature distribution. The obtained results are presented in figures 6.2, 6.3 and 6.4, respectively.

From figure 6.2 it is clear that, for the velocity power index $m = 0.1$, the velocity at any point near to the plate decreases as the wall thickness parameter α increases and the reverse is true for $m = 2$. Figure 6.3 shows that the temperature distribution is decreased with the increment of the wall thickness parameter α for $m = 0.1$, whereas, the reverse is observed for $m = 2$. Generally speaking the temperature distribution for any value of α, is greater for $m = 2$ than that observed for $m = 0.1$.

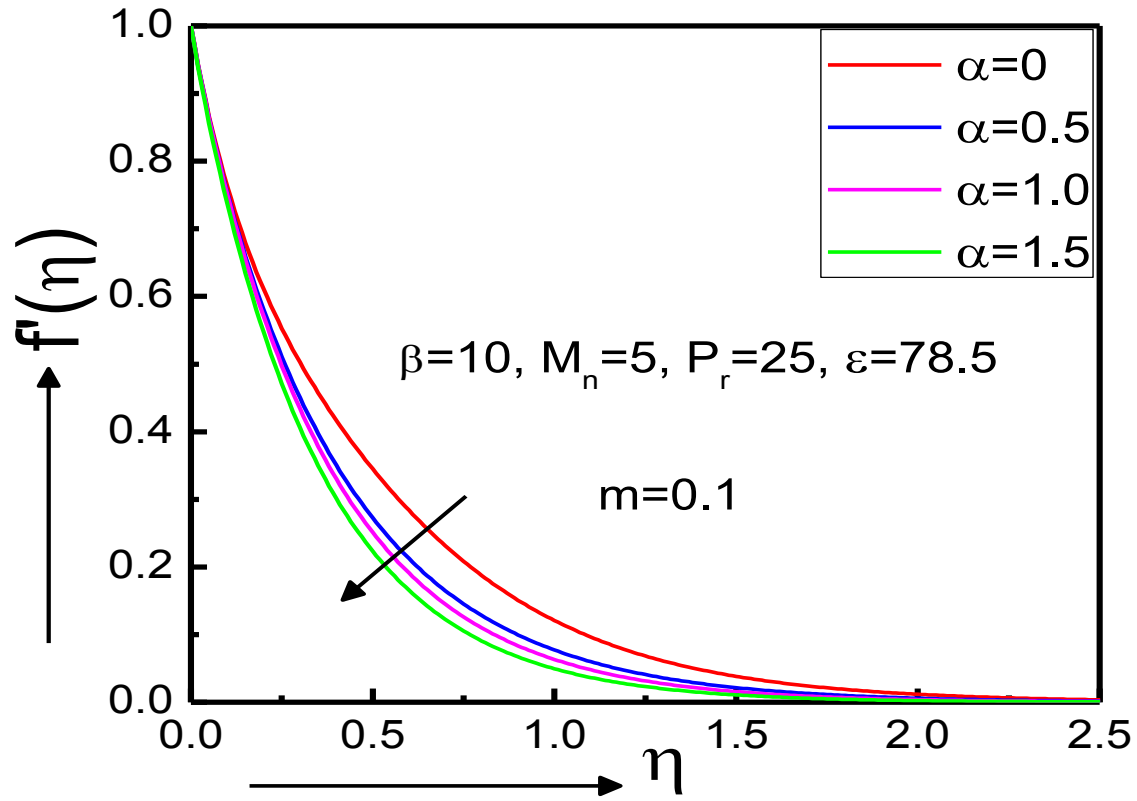

Fig 6.2(a) Velocity distribution for various values of α with $m = 0.1$

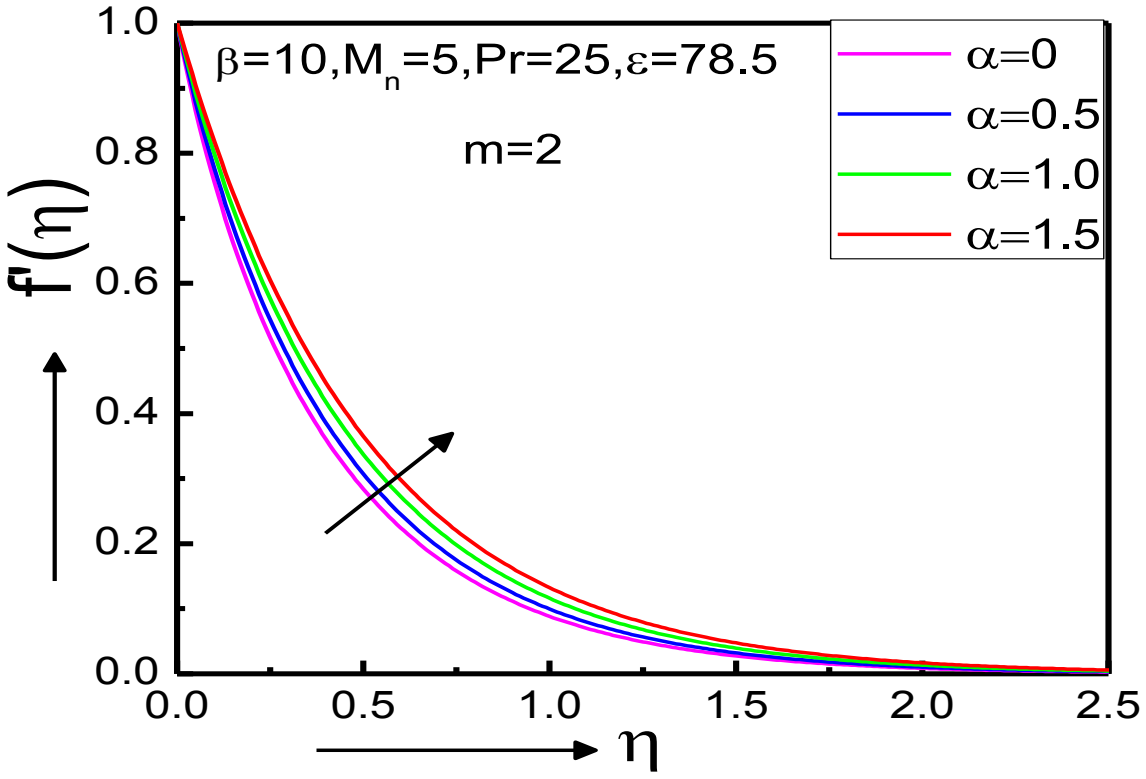

Fig 6.2(b) Velocity distribution for various values of α with $m = 2$

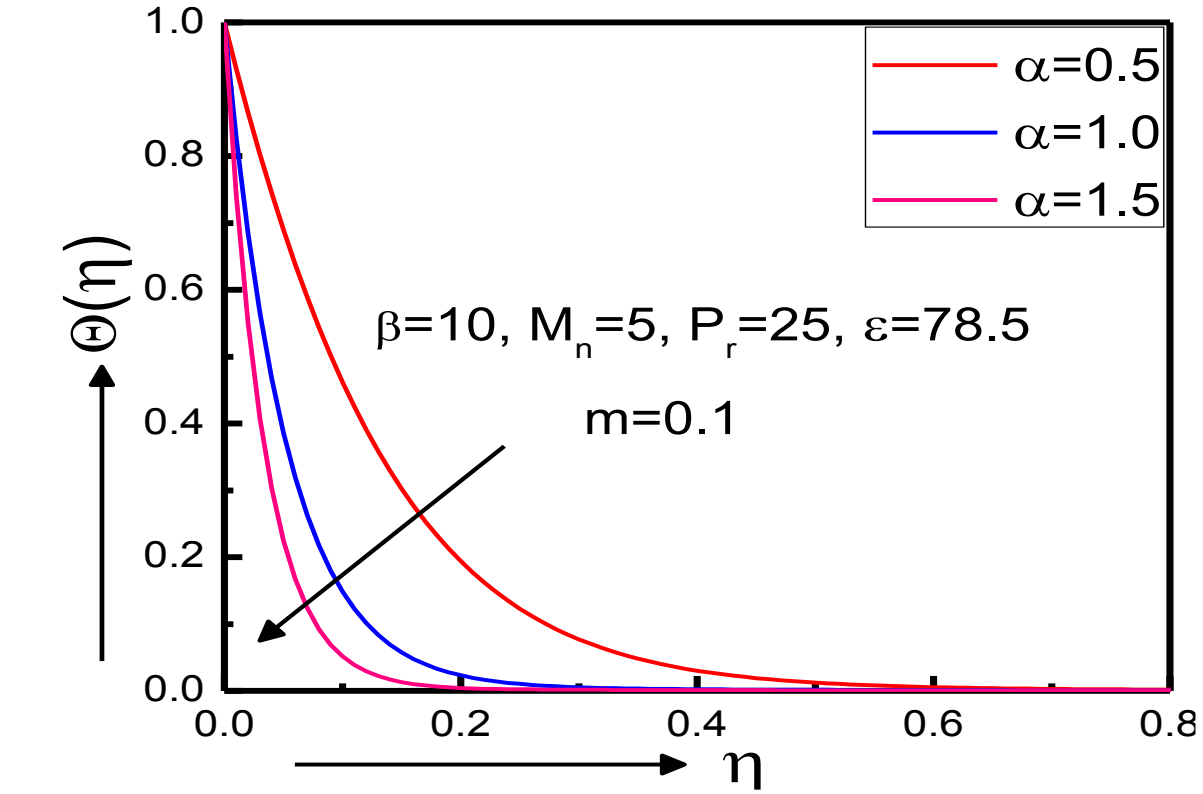

Fig 6.3(a) Temperature distribution for various values of α with $m = 0.1$

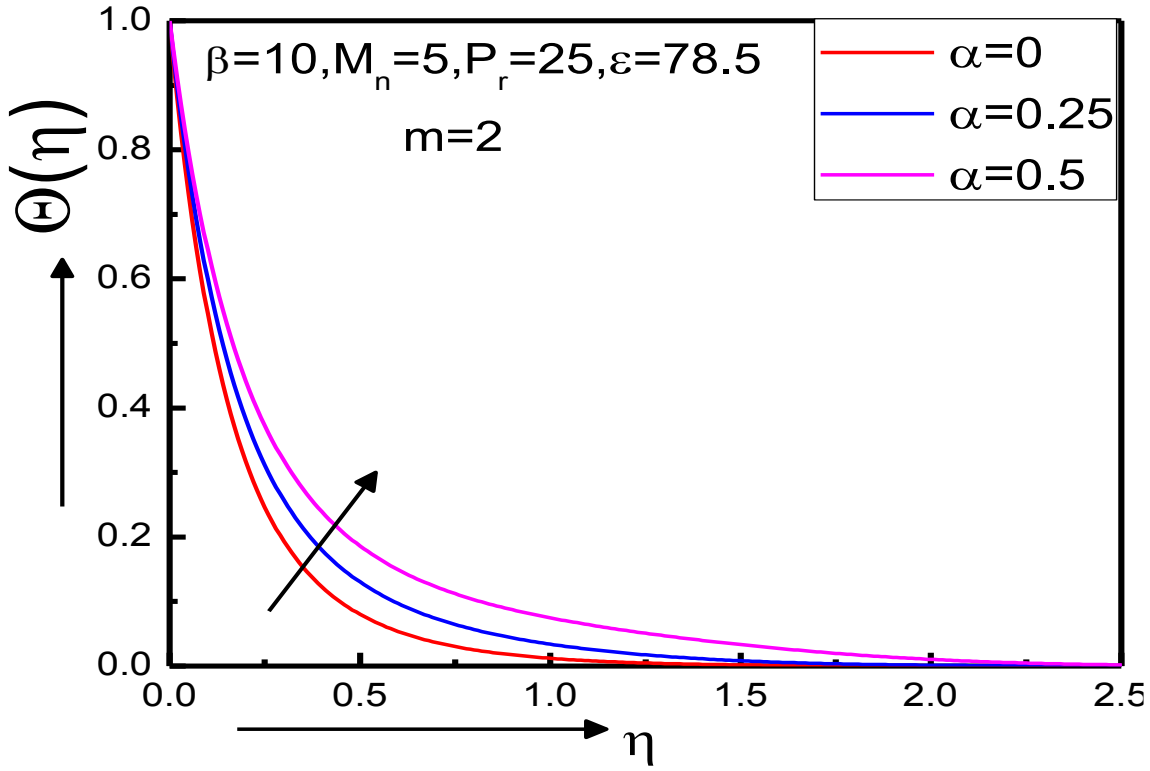

Fig 6.3(b) Temperature distribution for various values of α with $m = 2$

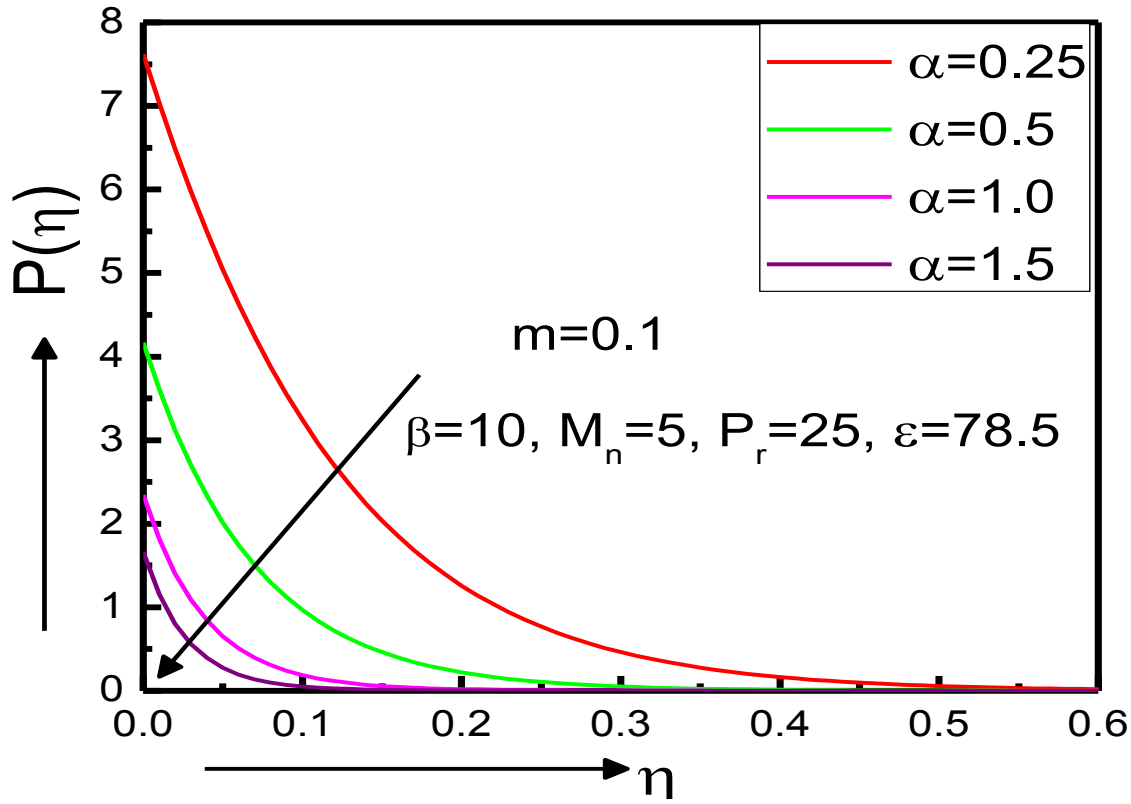

Fig 6.4(a) Variation of pressure distribution for various values of α with $m = 0.1$

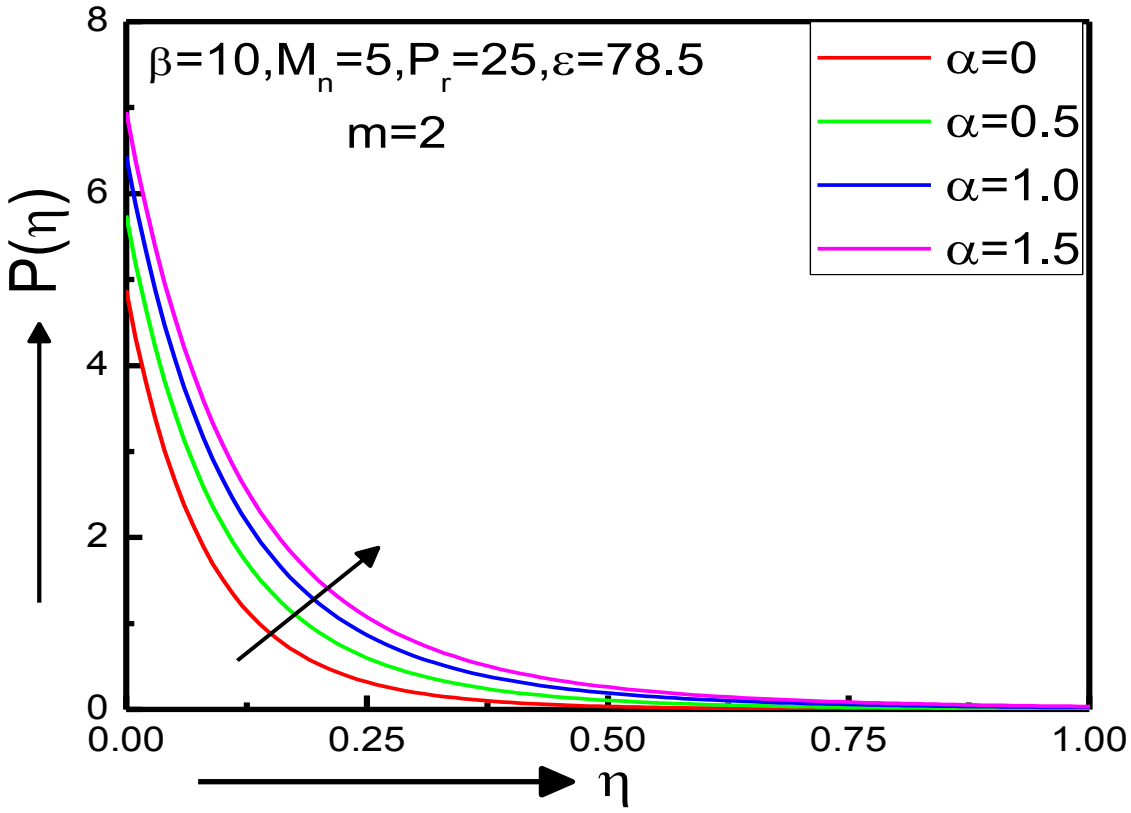

Fig 6.4(b) Variation of pressure distribution for various values of α with $m = 2$

Figure 6.4 shows the variation of the dimensionless pressure P for different values of wall thickness parameter for $m = 0.1$ and $m = 2$. It is observed that the dimensionless pressure P decreases with the increment of α for $m = 0.1$ and the reverse is true for $m = 2$ Generally speaking the values of the dimensionless pressure close to the wall are greater for $m = 2$ than those obtained for $m = 0.1$.

Figure 6.5, 6.6, 6.7 show that the effect of velocity power index m on the velocity, temperature and pressure distribution for a fixed value of α=0.5. It is observed that all the values of the aforementioned variable are increasing with the increment of m.

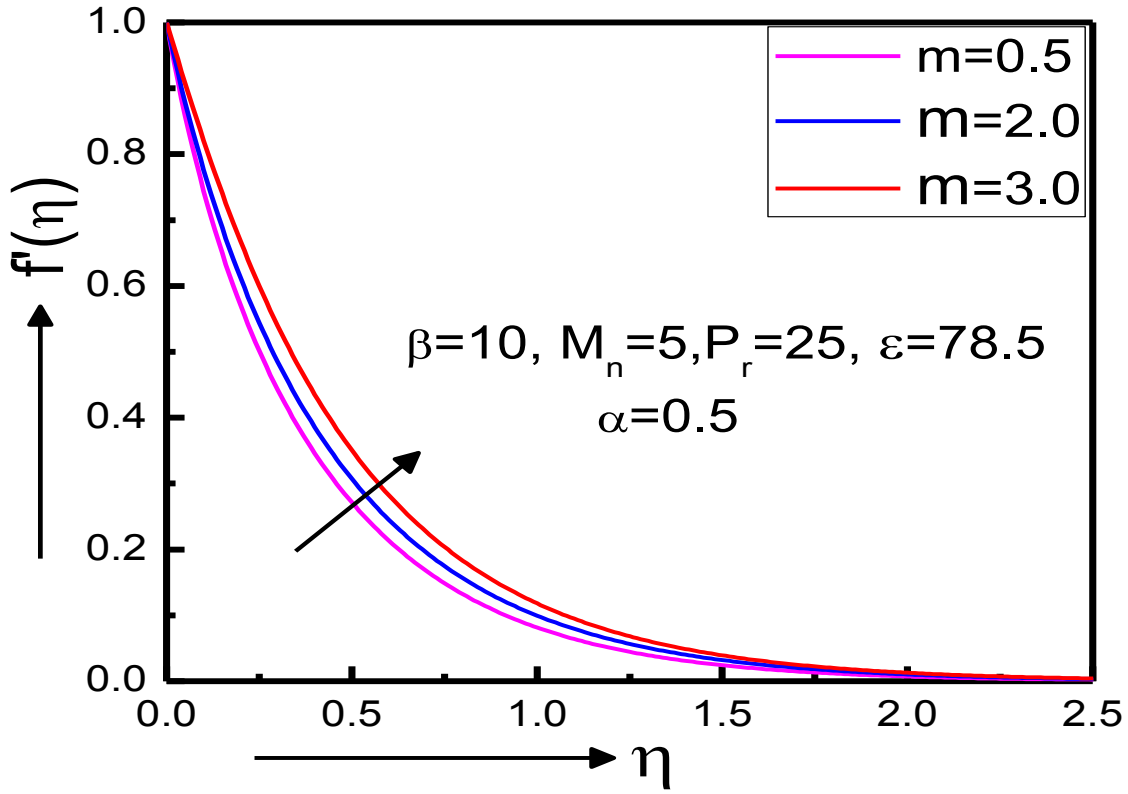

Fig 6.5 Velocity distribution for various values of m.

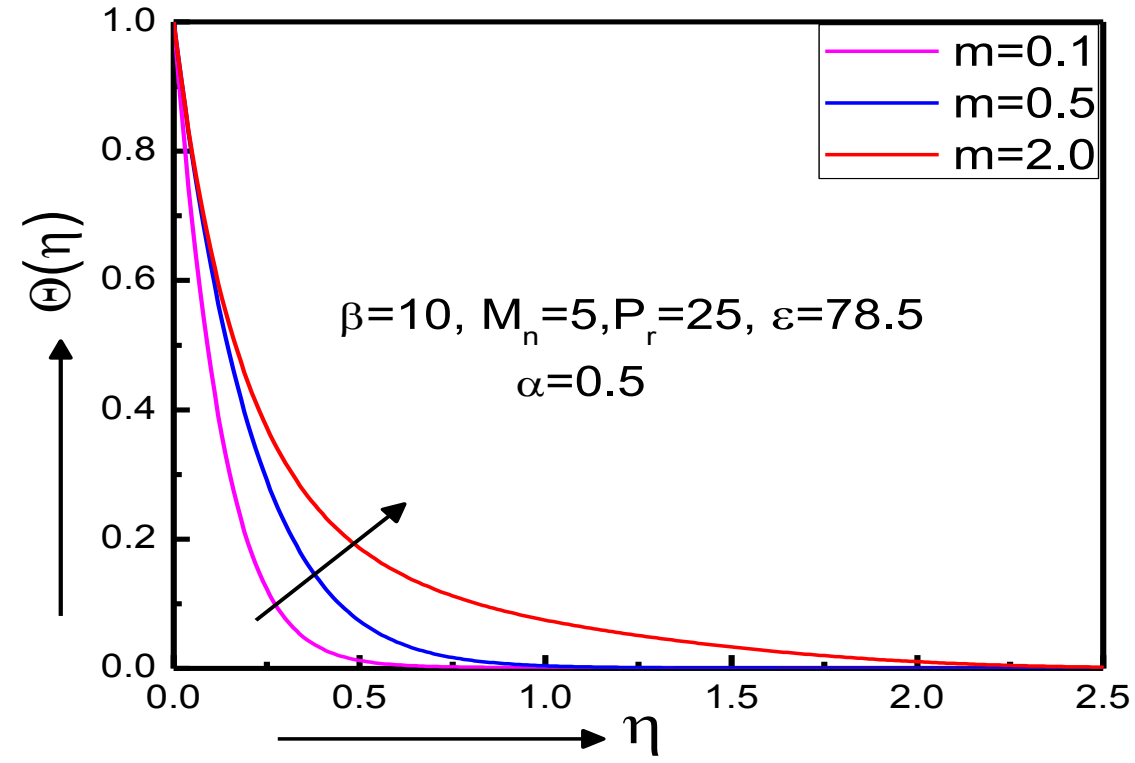

Fig 6.6 Temperature distribution for various values of m .

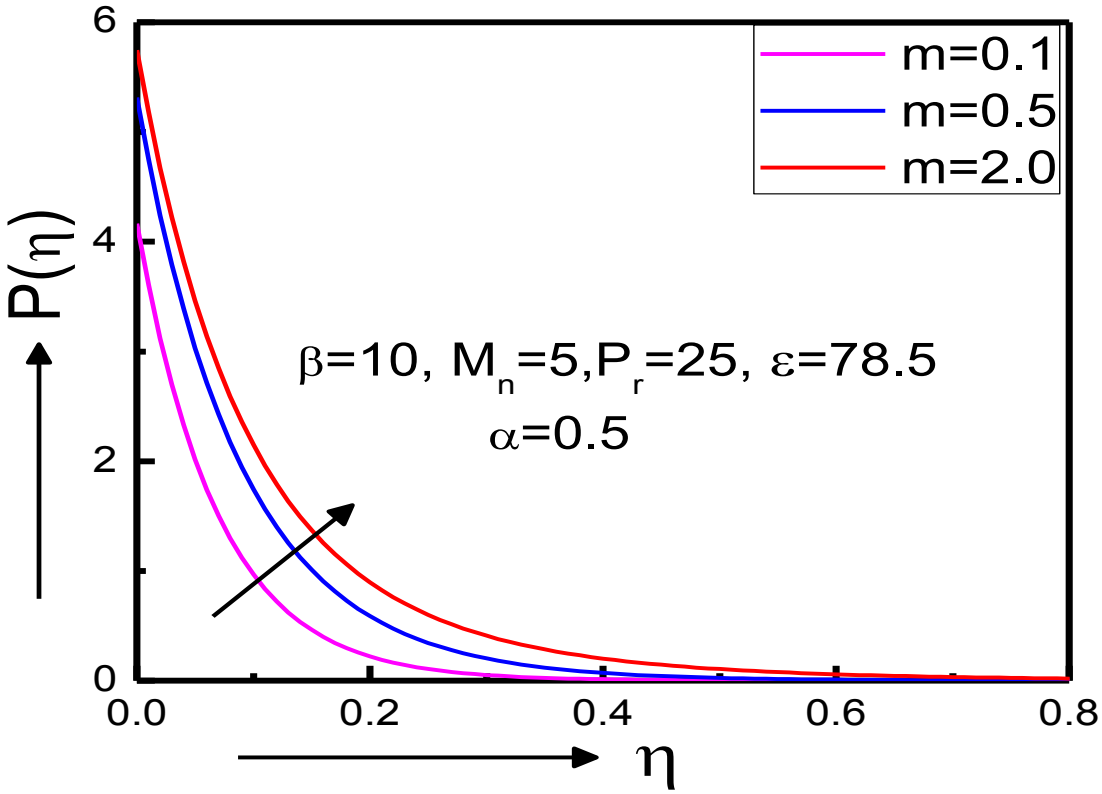

Fig 6.7 Variation of pressure distribution for different values of m.

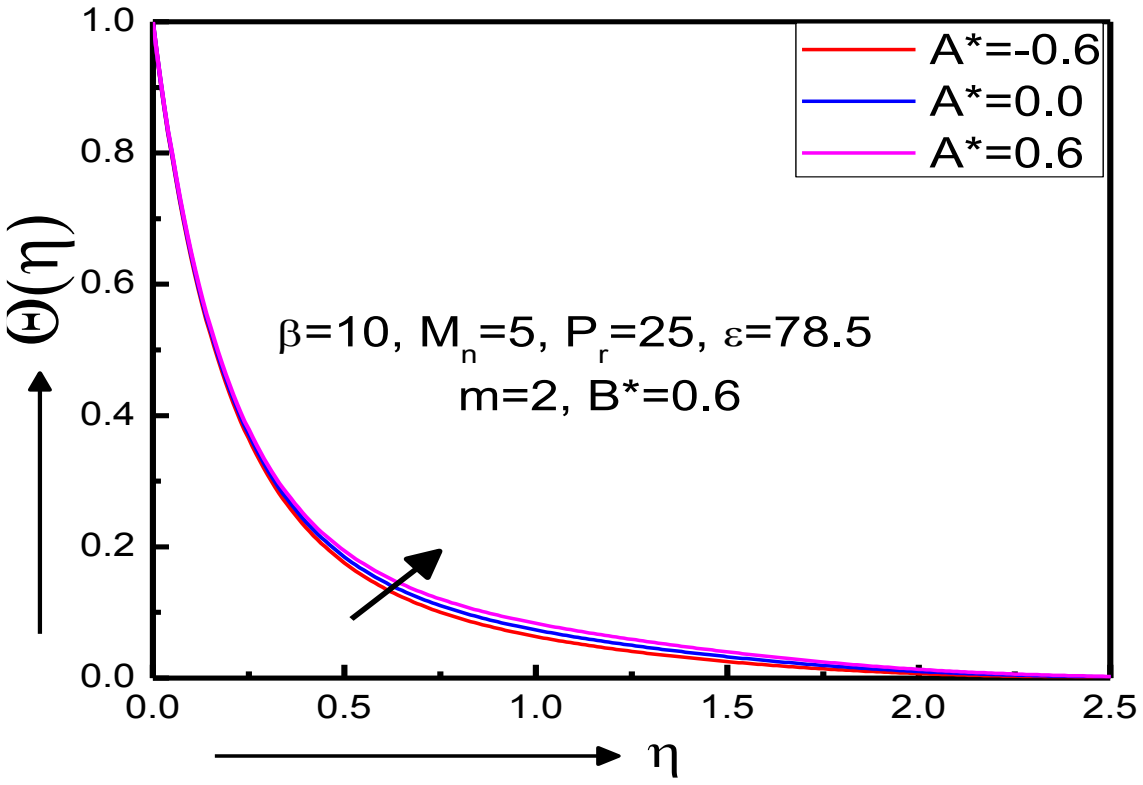

Fig 6.8 Variation of temperature distribution for different values of $A*$

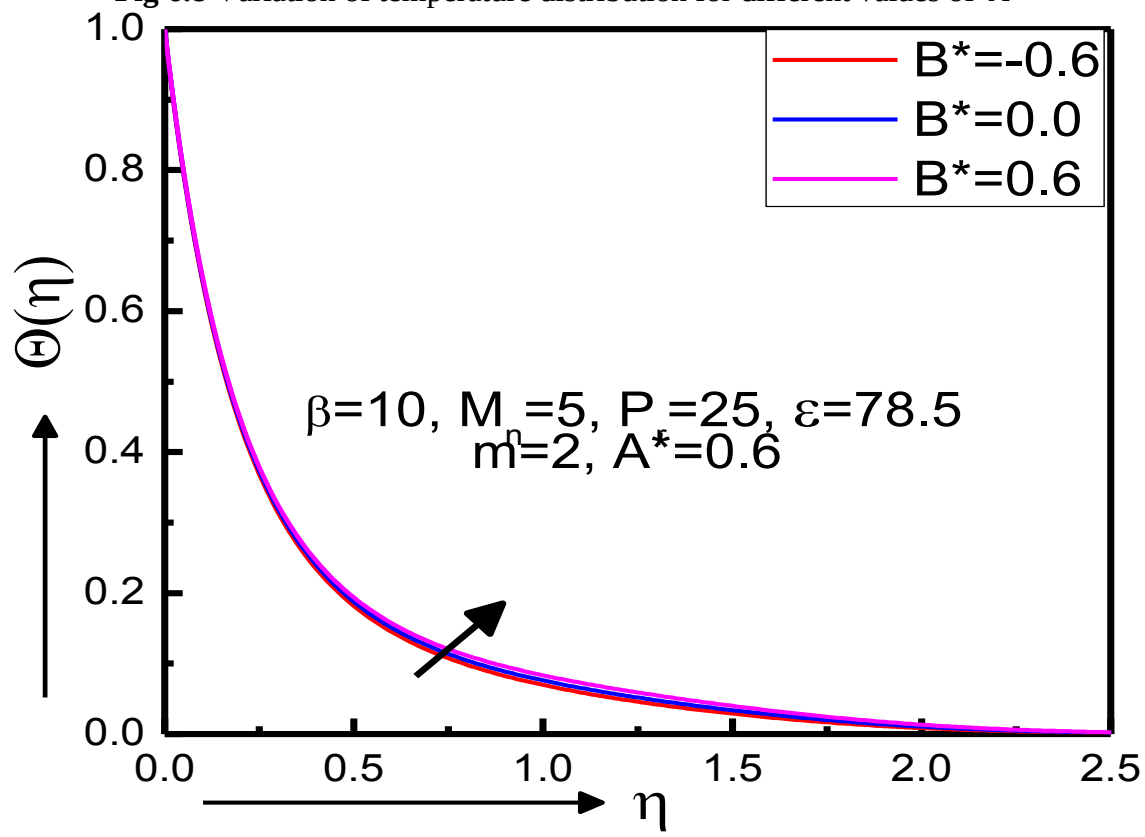

Fig. 6.9 Variation of temperature distribution for different values of B^*

Figures 6.8 and 6.9 depict the effect of space dependent heat source/sink parameter A^* and temperature dependent heat source/sink parameter B^*. It is observed that the values of the temperature distribution of the fluid are increased with the increment of A^* (heat source) for B^*=0.6 and analogous behavior is observed when $A^* = 0.6$ and B^* increases. It is concluded that the application of the magnetic field does not alter qualitatively the expected behavior of the temperature field and in the presence of heat sources or sinks is formed accordingly.

Figures 6.10, 6.11 and 6.12 depict the effect of the magnetic force applied due to the electrical conductivity of the fluid for a given polarization force $(\beta = 10)$. This is achieved by setting $\beta = 10$ and letting M_n vary from 0 to 10. It is obtained from Figure 6.10 that the dimensionless velocity $f'(\eta)$ is significantly reduced throughout the flow field as M_n is increased. On the contrary, the temperature and the pressure values throughout the flow field are increased with the increment of M_n shown in Fig. 6.11-6.12.

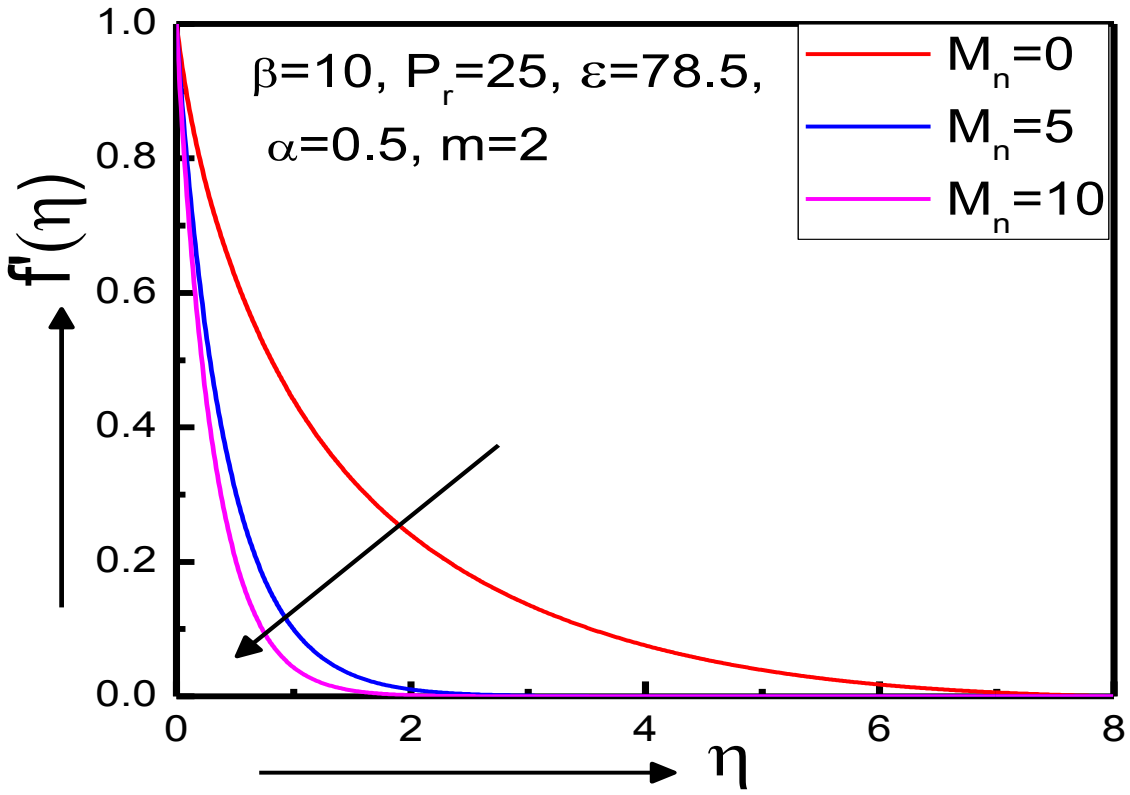

Fig. 6.10 Variation of velocity profile with different values of M_n

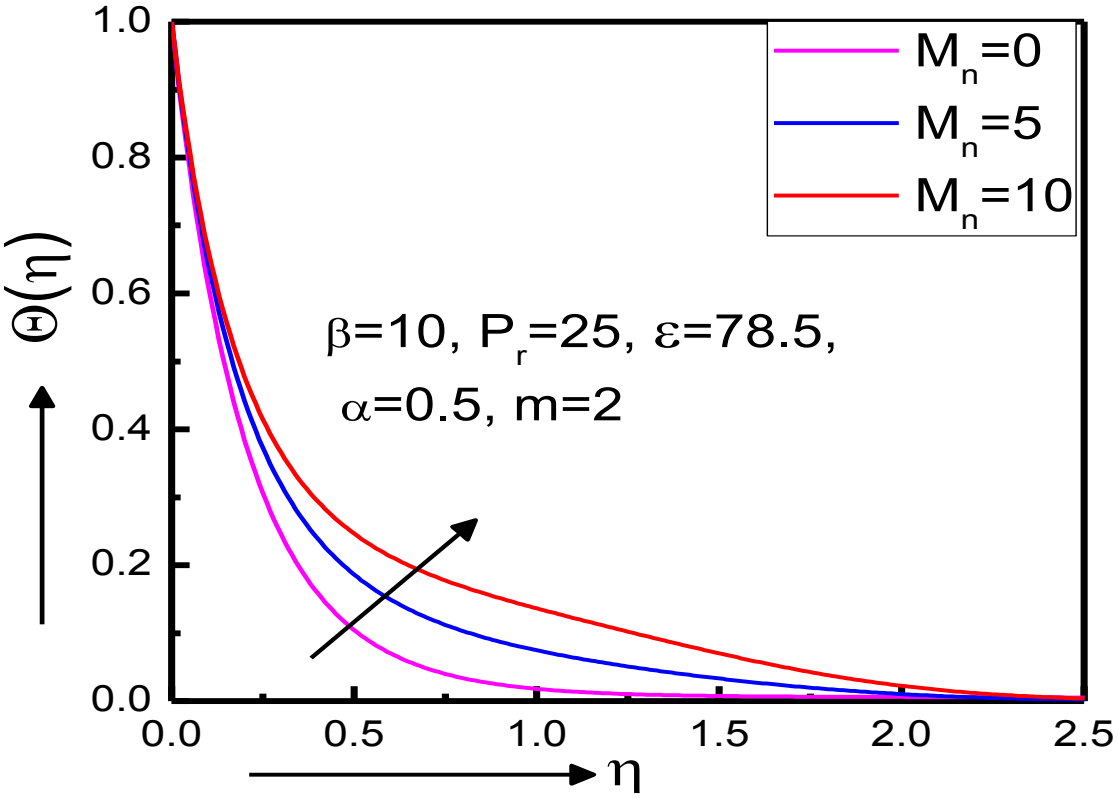

Fig. 6.11 Variation of temperature distribution profile with different values of M_n

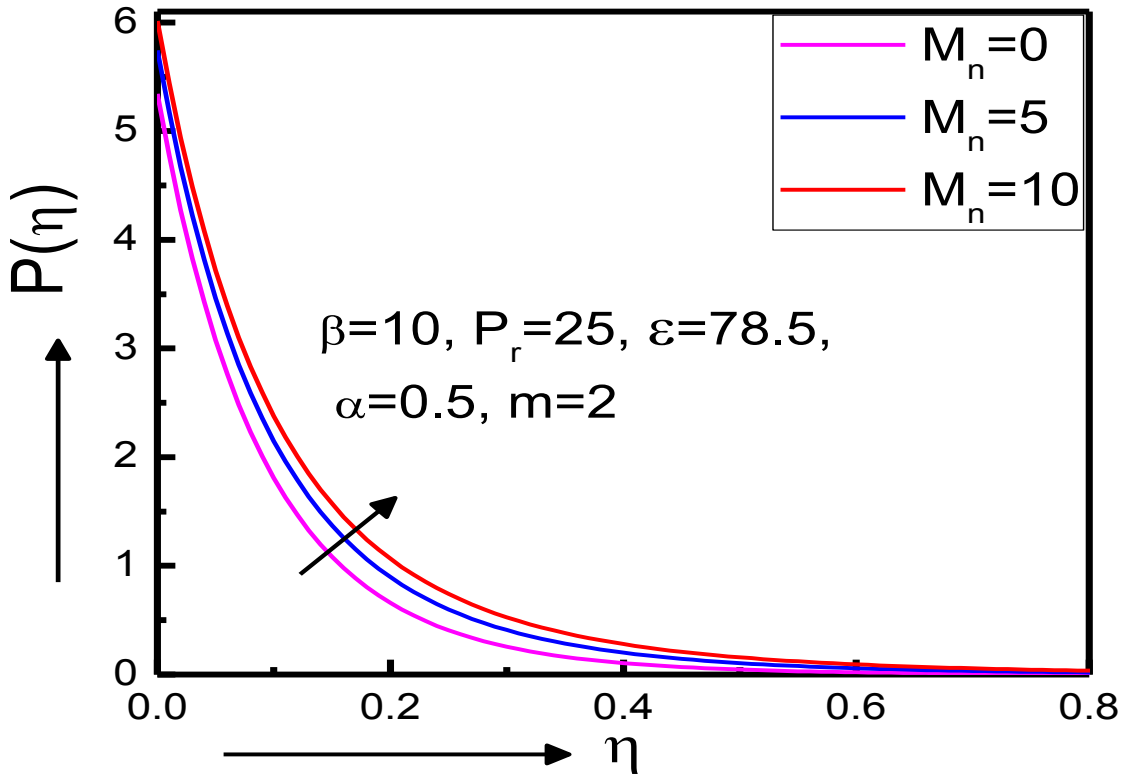

Fig. 6.12 Variation of Pressure distribution with different values of M_n

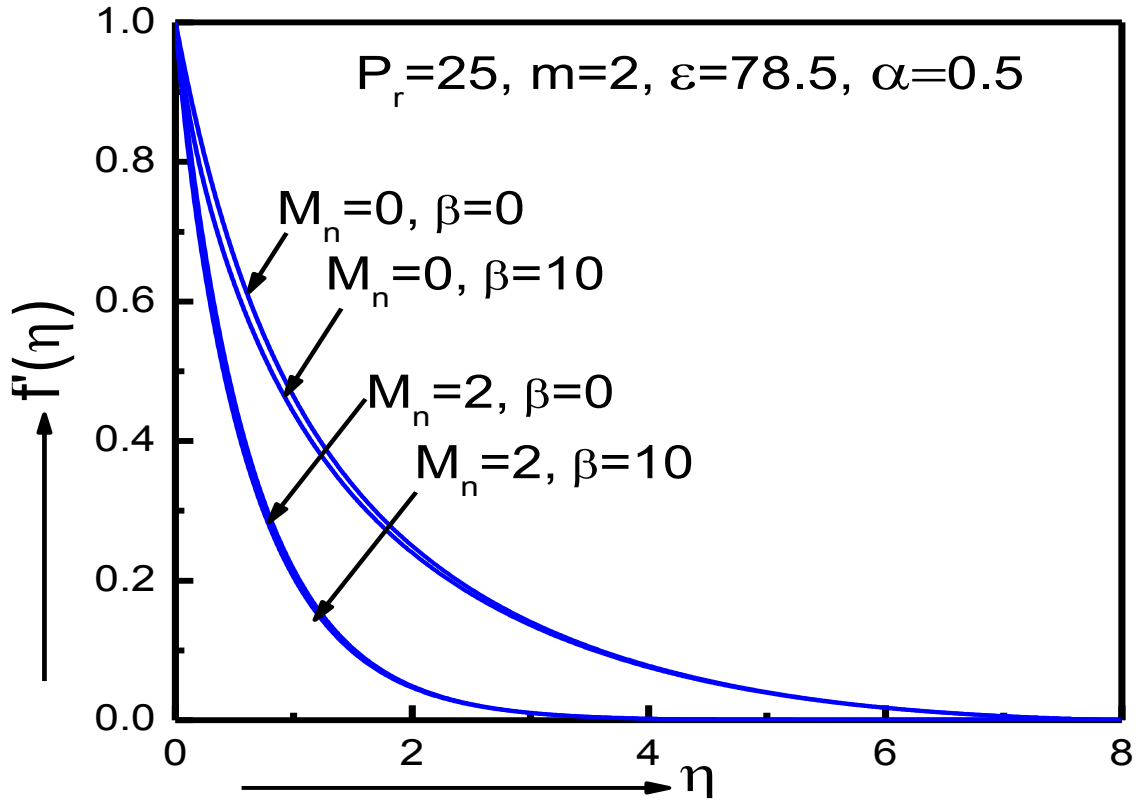

Fig 6.13 Variation of velocity profile with different values of β and M_n

Figures 6.13, 6.14 and 6.15 picture the dimensionless velocity, pressure and temperature distribution profiles, respectively. The curves are plotted for pure hydrodynamic flow $(\beta = 0,\ M_n = 0)$, pure FHD flow $(\beta \neq 0,\ M_n = 0)$, pure MHD flow $(\beta = 0,\ M_n \neq 0)$ and BFD flow $(\beta \neq 0,\ M_n \neq 0)$. It is observed that the velocity is reduced with the increment of β or M_n. It is noted that the major impact on the velocity is observed with the increment of magnetohydrodynamic parameter M_n which is also shown in fig 6.10. Generally speaking the impact of ferromagnetic interaction parameter β is negligible comparable to that caused by the increment of M_n, whereas the reverse is observed for the temperature and pressure distribution shown at figures 6.14 and 6.15. Namely, the temperature and pressure profiles are increased with the increase of magnetohydrodynamics parameter M_n and ferromagnetic interaction parameter β, but the major impact is observed with the increment of the magnetohydrodynamics parameter M_n as shown at fig. 6.11 and fig. 6.12.

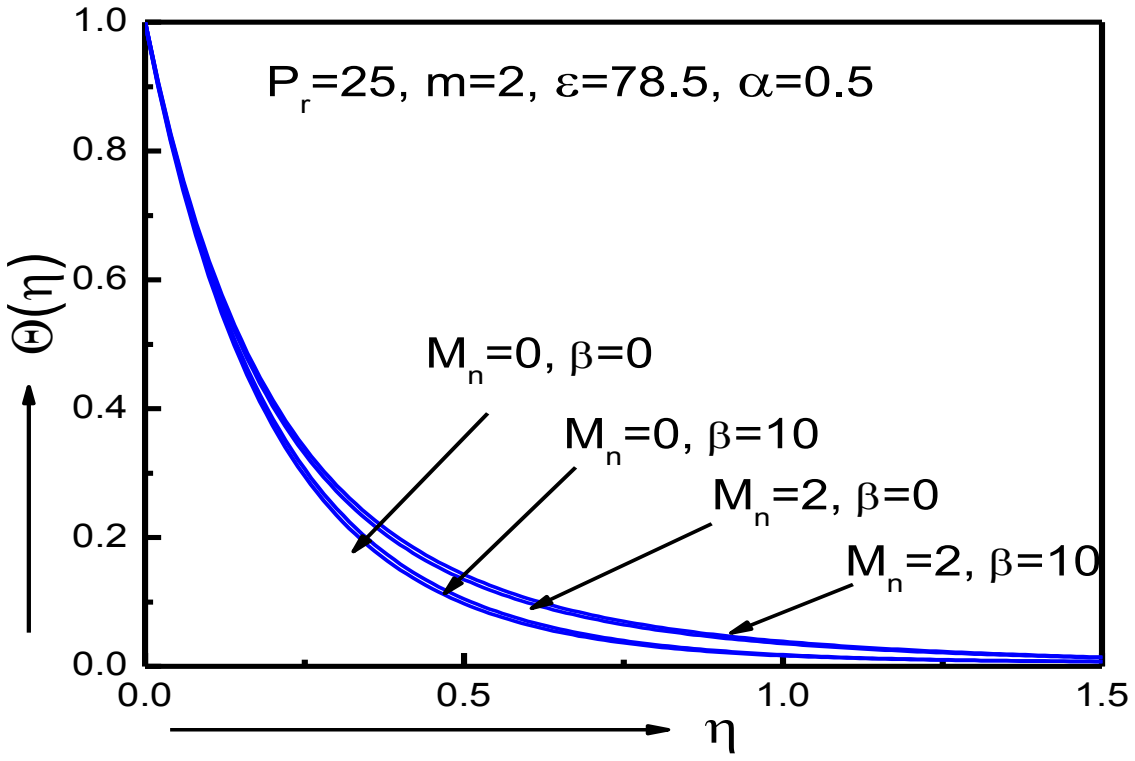

Fig. 6.14 Variation of temperature distribution with different values of β and M_n

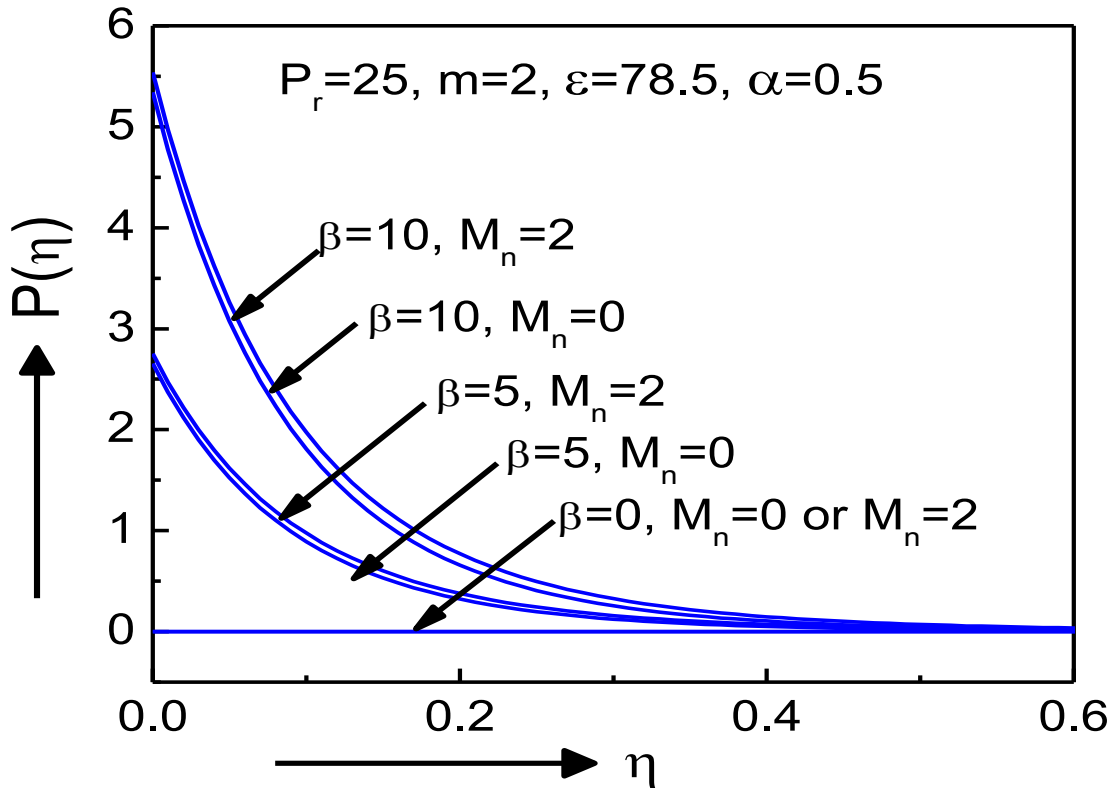

Fig. 6.15 Variation of dimensionless pressure with different values of β and M_n

The important characteristics of the present study are the local skin friction coefficient $\left(f''(0)\right)$ and local rate of heat transfer $\left(\theta*(0)\right)$ and wall pressure $P(0)$. The skin friction at the surface as shown at figure 6.16. It is found that the skin friction is increased with the increment of the ferromagnetric parameter β for specific value of M_n and its increment is linear. Furthermore, $f''(0)$ is increased, not linearly this time, with the increment of M_n for specific values of β, (see fig 6.16(b)). The variation of the dimensionless wall shear parameter $f''(0)$ with the increment of m is shown at Fig 6.16 (c) and 6.16(d). In figure 6.16(c) observed that as m increased and up to $m=7$, the wall shear parameter is increased as β increases. The opposite is happening when m exceeds the value of 7. It is worth mentioning here, that as β increases, there is a value of m for which the dimensionless wall shear parameter takes its maximum value and this is attained for $m \approx 3$. For $m=7$ the value of the wall shear parameter is not affected by the application of the magnetic field and the polarization effect.

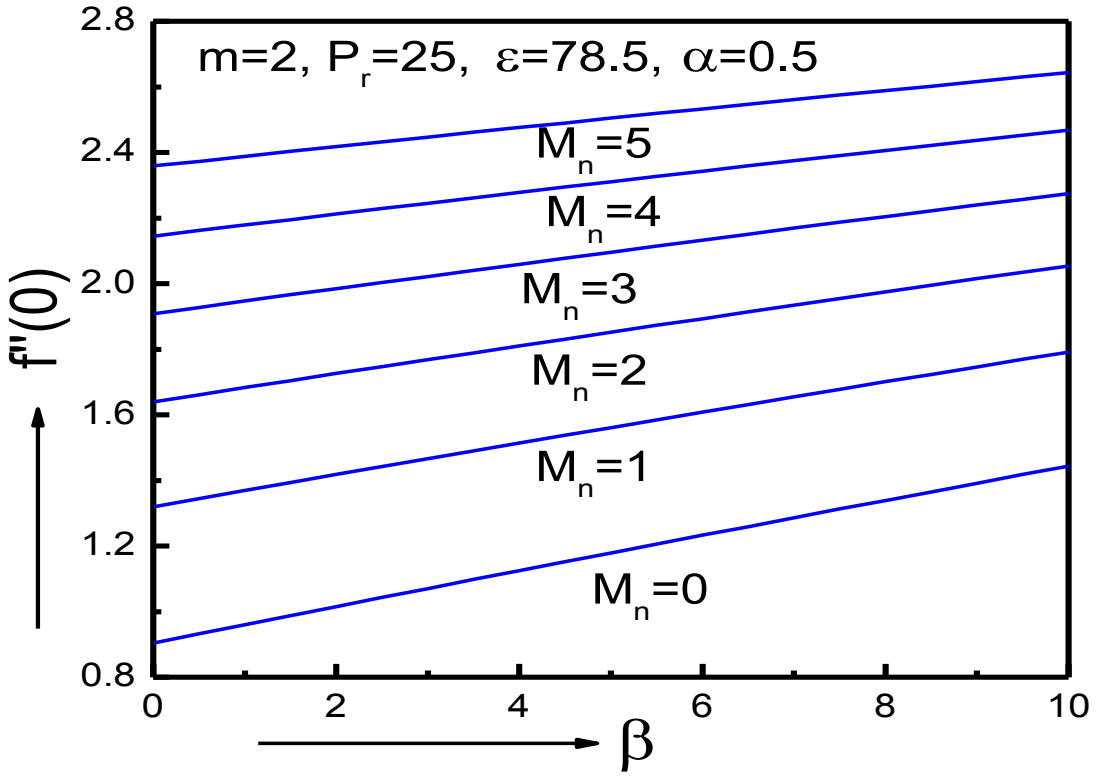

Fig. 6.16(a) Variation of the wall shear parameter with β for different values of M_n.

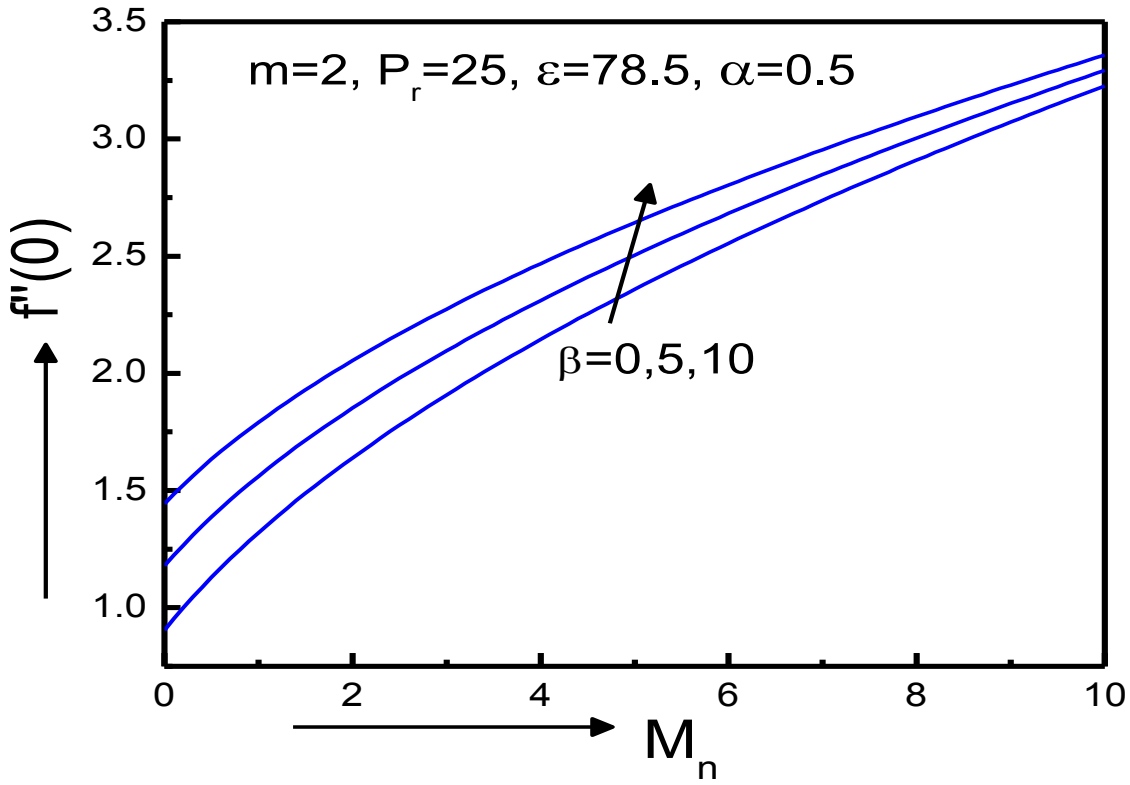

Fig. 6.16(b) Variation of the wall shear with M_n for different values of β.

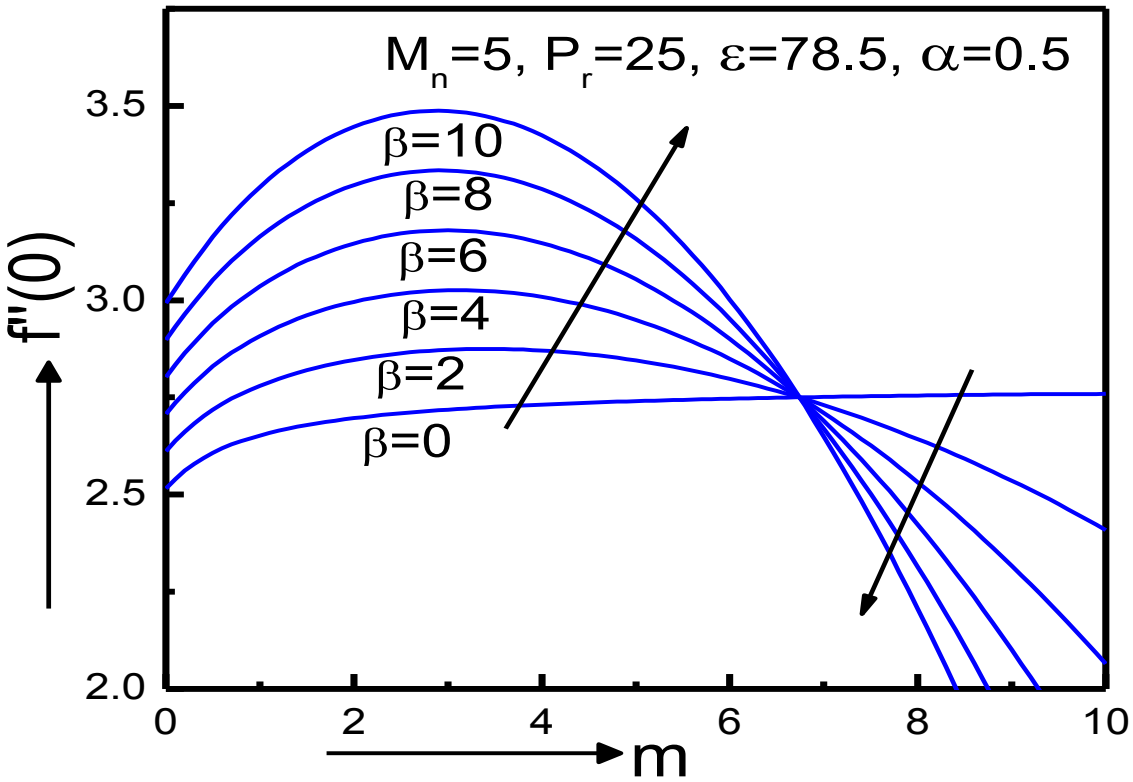

Fig. 6.16(c) Variation of the wall share parameter with m for different values of β.

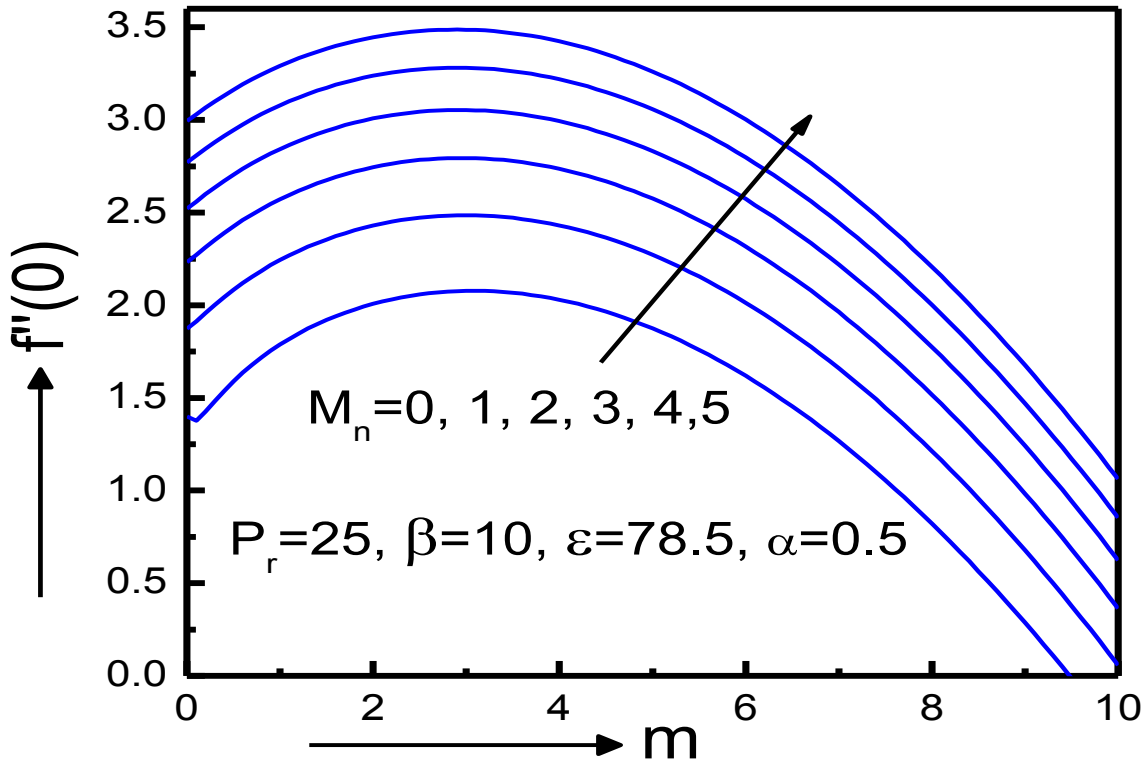

Fig. 6.16(d) Variation of the wall shear parameter with m for different values of M_n.

At figure 6.16(d) it is observed that as m is increased and up to $m \cong 3$, the wall share parameter increases as M_n increases, and the reverse is true when m exceeds the value of 3. It is mention that its increase or decrease is not linear.

The heat transfer rate at the sheet can be measured by the ratio $\Theta*(0) = \dfrac{\Theta'(0)}{\Theta'(0) \mid \beta = M_n = 0}$. The variation of the wall heat transfer parameter $\Theta^*(0)$ with β and M_n is shown at figures 6.17. For the case of the variation with β pictured at figure 6.17(a), $\Theta^*(0)$ reduces linearly. Figure 6.17(b) shows the variation of $\Theta^*(0)$ which is decreased with the increment of M_n in a non-linear way. The variation of the wall pressure $P(0)$ is displayed at figure 6.18 which shows that the wall pressure is monotonically increased with the increment of the magnetic parameter β. It is interesting to note that all over the sheet the skin friction coefficient $\left(f''(0)\right)$ and rate of heat transfer $\left(\Theta^*(0)\right)$ and wall pressure $P(0)$, all vary linearly with the ferromagnetic parameter but nonlinearly with magnetohydrodynamic and velocity power index parameter.

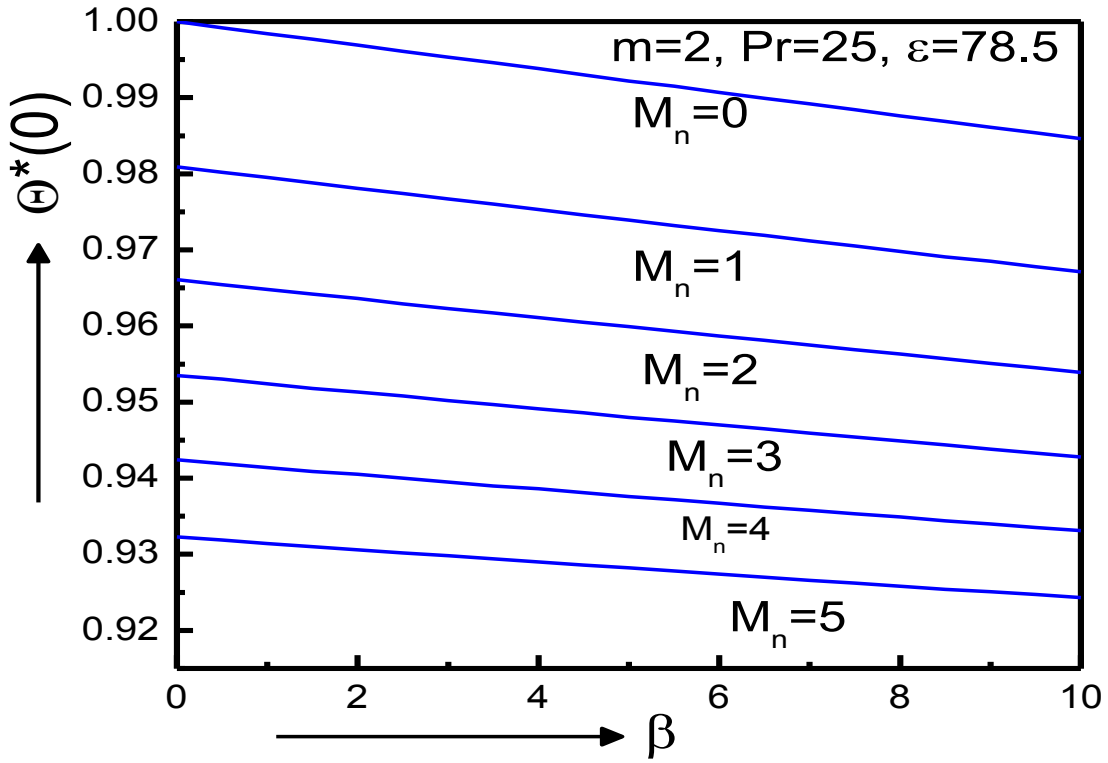

Fig. 6.17(a) Variation of the wall heat transfer parameter with β for different values of M_n.

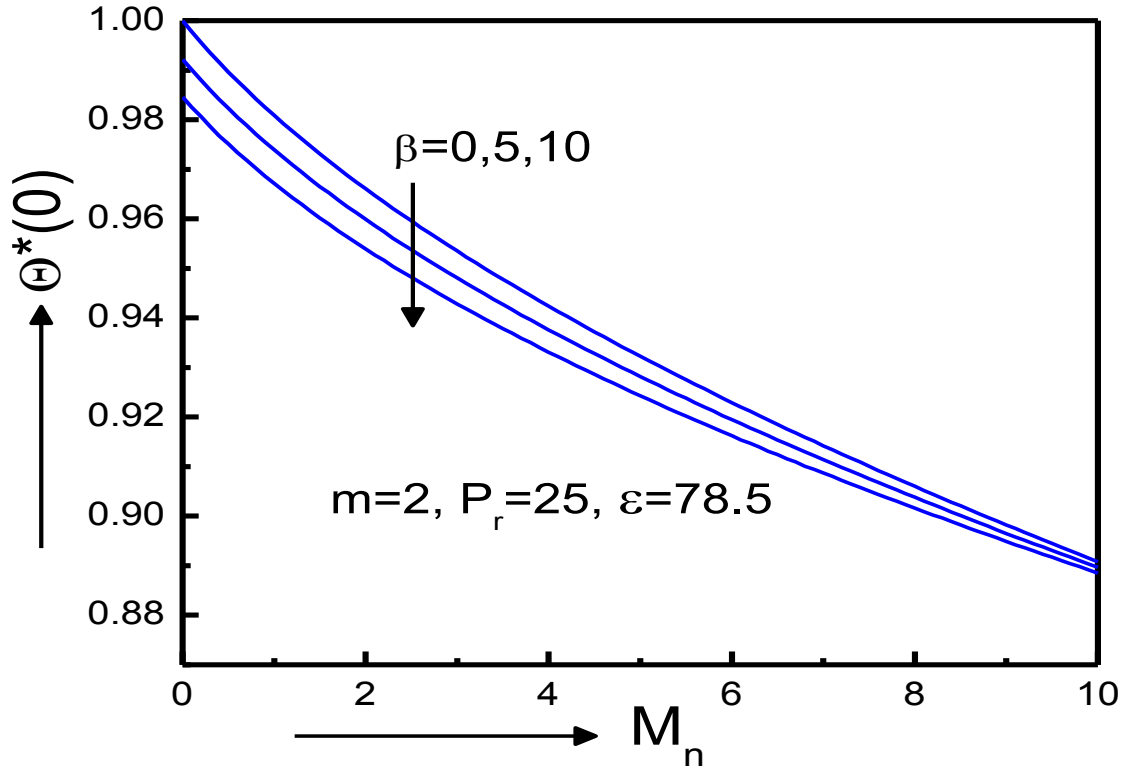

Fig 6.17(b) Variation of the wall heat transfer parameter with M_n for different values of β

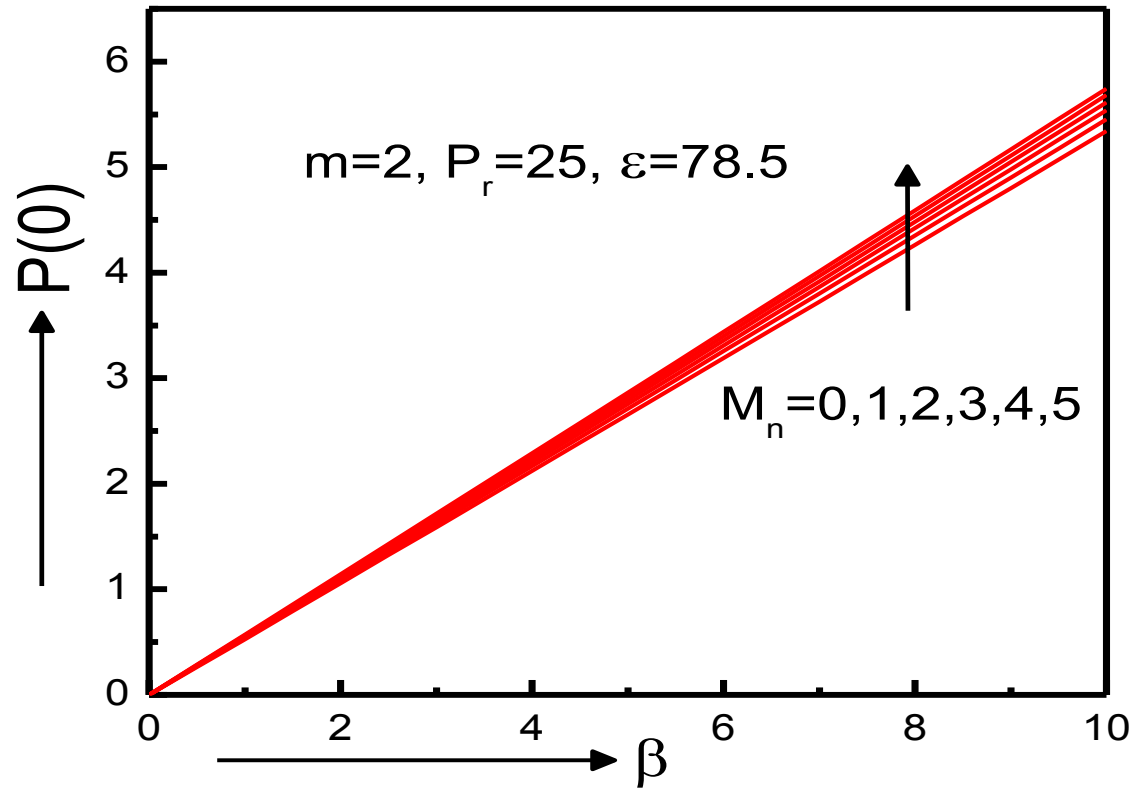

Fig 6.18 Variation of the wall pressure parameter with β for different values of M_n.

6.7 Summary of the chapter

In this study of biomagnetic fluid flow over a stretching sheet with variable thickness in the presence of applied magnetic field which is generated by a magnetic dipole. This model takes into accounts both magnetization and electrically conductivity.

The observations on the effect of various physical parameter, the velocity and temperature of fluid is increased or decreased with wall thickness parameter in depend on velocity power index. It is generally observed that the thickness of the boundary layer plays very important role in the determination of the BFD flow field.

In FHD and MHD case the velocity component decreases with both ferromagnetic interaction parameter and magnetohydrodynamics parameter, but the major impact on the fluid velocity is causes rather than the variation of the magnetohydrodynamics parameter rather than the ferrohydrodynamics one. On the contrary, pressure and temperature profiles are increased on the effect of ferromagnetic interaction parameter and magnetohydrodynamics parameter.

Another important characteristic of biofluid are wall shear parameter, wall pressure and rate of heat transfer. The wall shear parameter and wall pressure increase with the increment of the value of β, M_n. but the rate of heat transfer is decreased with the increment of β, M_n. It is noted that wall share parameter, wall pressure and rate of heat transfer are linearly increase/decrease with the value of β but nonlinearly with M_n. This information is useful for all kinds of applications that deal with blood flow in the presence of a magnetic field and also use in medical diagnosis such as for clearer imaging, MRI etc.

Chapter 7

Three dimensional Biomagnetic flow and heat transfer over a stretching surface with variable fluid properties

In this chapter, we investigate the effects of variable fluid properties on the flow and heat transfer of three dimensional biomagnetic fluid over a stretching surface in the presence of magnetic dipole. In our model, we assume that the fluid viscosity and thermal conductivity are varying with temperature and the wall temperature varies in the (x, y) plane. The model used takes into account both magnetization and electrically non-conductivity which described by the principle of FHD. The governing equations are transformed into system of ordinary differential equations by using similarity transformations and solved by using an efficient numerically technique. The influence of various parameters namely the viscosity parameter, thermal conductivity parameter, ferromagnetic interaction parameter on the velocity and temperature fields is analyzed and presented graphically. This result analysis shows that the magnetic force controls the fluid behavior and the friction coefficient. The accuracy of the numerical result is checked by comparisons with previously published work and the results are found to be in good agreement, Murtaza et al. (2018).

7.1 Introduction

Biomagnetic fluid flow has a relatively new area in fluid dynamics because there are numerous applications in bioengineering and medicine. Hyperthermia or hypothermia is one of the treatments in which body tissue is exposed to slightly higher temperatures to destroy and kill cancer cells. By the magnetic fluid application, hyperthermia can also be used for the eye injuries treatment. The magnetic devices development for cell separation, high-gradient magnetic separation, reduction of blood flow during surgeries, targeted transport of drugs using magnetic particles as drug carries, treatment of cancer tumor causing magnetic

hyperthermia and magnetic wound treatment and development of magnetic tracers are some applications.

The mathematical model for flow of BFD, has been developed first Haik et al. (1999). This model is conformed with the principles of FHD by Rosensweig (1985, 1987). According to this model, they consider that biomagnetic fluid is Newtonian, electrically non-conducting magnetic fluid formulated on the principles of ferrohydrodynamics (FHD). An extended mathematical model developed by Tzirtzilakis (2005). According to this model, the biofluid flow under the influence of an applied magnetic field is consistent with the principles of Ferrohydrodynamics (FHD) and the Magnetohydrodynamics (MHD) by Davidson (2001). Tzirtzilakis and Kafoussias (2003) analyzed the mathematical model of the flow of a heated ferrofluid over a linearly stretching sheet under the action of a magnetic field which is generated by a magnetic dipole. Tzirtzilakis and Tanoudis (2003) presented a numerical method for the study of laminar incompressible two dimensional biofluid over a stretching sheet with heat transfer. He assumed that the magnetization of the fluid varied with the magnetic field strength H and the temperature T. Further Misra and Shit (2009) investigated the Biomagnetic viscoelastic fluid flow over a stretching sheet and he indicate that the presence of an external magnetic field influences the flow of biomagnetic fluid quite appreciably.

The magnetization property M is the behaviour of a biological fluid when it is exposed to magnetic field. Anderson and Valnes (1998) used a linear and temperature dependent magnetization equation where as Tzirtzilakis and Kafoussias (2003, 2010) used a nonlinear and temperature dependent one. Haik et al. (2001) studied the viscosity of human blood in a high static magnetic field. They used the magnetization equation which is not temperature dependent.

All the above studies, they consider the uniform fluid viscosity and thermal conductivity. However, it is evident that the physical properties of fluid may change with temperature, especially the fluid viscosity and the fluid thermal conductivity. Vajravelu et al. (2013) investigated the Effects of variable fluid properties on the thin film flow of Ostwald-de Waele fluid over a stretching surface. Prasad et al. (2010) studied the effects of variable fluid properties on the hydromagnetic flow and heat transfer over a non-linearly stretching sheet. Salawu and Dada (2016) studied the radiative heat transfer of variable viscosity and thermal conductivity effects on inclined magnetic field with dissipation in a non-Darcy medium. Makinde et al. (2016) investigated the MHD variable viscosity reacting flow over a convectively heated plane in a porous medium with thermophoresis and radiative heat

transfer. All above authors assume that the fluid viscosity and thermal conductivity very as a linear function of temperature. Kafoussias et al. (2008) investigated that free-forced convective boundary-layer flow of a biomagnetic fluid under the action of a localized magnetic field. They conclude that for increasing viscosity parameter, the skin friction coefficient increases, whereas the Nusselt number decreases.

The aim of the present study is to examine the temperature dependent viscosity and thermal conductivity of biomagnetic fluid flow over a three dimensional stretching sheet with variable surface temperature. Here we conclude that the effect of variable viscosity and thermal conductivity, the flow characteristic are significantly changed compared to constant physical properties. This study will help the development of medical treatment by controlling blood velocity and blood temperature.

7.2 Mathematical Formulation

Let us consider a steady three-dimensional boundary layer flow and heat transfer of a viscous incompressible and electrically non-conducting biomagnetic fluid over a stretching surface in the presence of applied magnetic field. A magnetic dipole is placed parallel to the $x-$ axis and at a distance d below it. It is also assumed that this magnetic dipole gives rise to a magnetic field of sufficient strength to saturate the magnetic fluid so that the equilibrium magnetization is accounted. Assume that the flat surface is stretching in two lateral directions x and y with the velocities ax and by. The stretching sheet is placed in the plane $z=0$, whereas the fluid occupies the upper half plane $z \geq 0$. Here we consider the plates are kept at a constant temperature T_w, while the fluid is at temperature T_c, such that $T_w < T_c$. Let the surface be maintained at a power law temperature. The geometry and magnetic dipole of the problem is shown in Fig. 7.1.

The boundary layer equations of the fluid and energy equation in the presence of variable fluid properties can be written as

Continuity equation:

$$\frac{\partial \mathrm{u}}{\partial \mathrm{x}} + \frac{\partial \mathrm{v}}{\partial \mathrm{y}} + \frac{\partial w}{\partial \mathrm{z}} = 0 \tag{7.1}$$

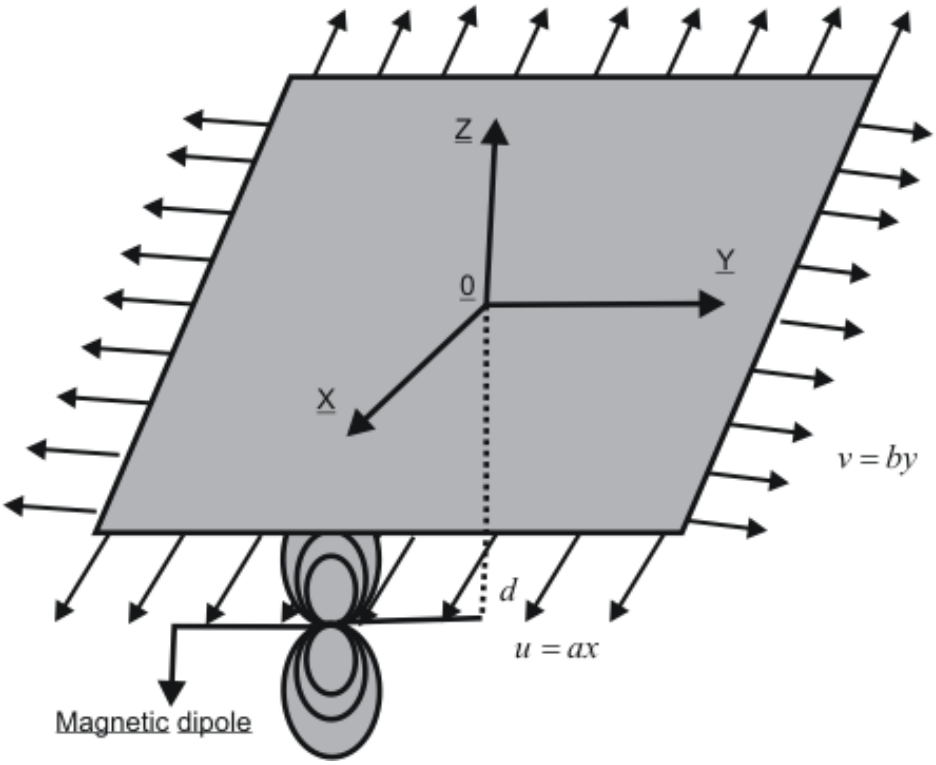

Fig. 7.1 Physical configuration and coordinate system

Momentum equation:

$$u\frac{\partial \mathrm{u}}{\partial \mathrm{x}} + w\frac{\partial \mathrm{u}}{\partial \mathrm{z}} = \frac{1}{\rho_\infty}\frac{\partial}{\partial \mathrm{z}}\left(\mu\frac{\partial u}{\partial \mathrm{z}}\right) \tag{7.2}$$

$$v\frac{\partial v}{\partial \mathrm{y}} + w\frac{\partial \mathrm{v}}{\partial \mathrm{z}} = \frac{1}{\rho_\infty}\frac{\partial}{\partial \mathrm{z}}\left(\mu\frac{\partial v}{\partial \mathrm{z}}\right) + \frac{1}{\rho_\infty}\mu_0 M\frac{\partial H}{\partial y} \tag{7.3}$$

$$w\frac{\partial \mathrm{w}}{\partial \mathrm{z}} = -\frac{1}{\rho_\infty}\frac{\partial p}{\partial \mathrm{z}} + \frac{1}{\rho_\infty}\frac{\partial}{\partial \mathrm{z}}\left(\mu\frac{\partial w}{\partial \mathrm{z}}\right) + \frac{1}{\rho_\infty}\mu_0 M\frac{\partial H}{\partial \mathrm{z}} \tag{7.4}$$

Energy equation:

$$\rho_\infty C_p\left(u\frac{\partial T}{\partial x} + v\frac{\partial T}{\partial y} + w\frac{\partial T}{\partial \mathrm{z}}\right) + \mu_0 T\frac{\partial M}{\partial T}\left(v\frac{\partial H}{\partial y} + w\frac{\partial H}{\partial \mathrm{z}}\right) = \frac{\partial}{\partial \mathrm{z}}\left(k\frac{\partial T}{\partial \mathrm{z}}\right) \tag{7.5}$$

With boundary conditions are

$$u = u_w = ax, v = v_w = by, w = 0, \qquad T = T_w = T_c + Ax^m y^n \qquad \text{at} \qquad z = 0 \tag{7.6}$$

$$u \to 0,\ v \to 0,\ T \to T_c,\ p + \frac{1}{2}\rho q^2 = p_\infty = const \quad \text{at } z \to \infty \tag{7.7}$$

Here u, v and w are the velocity components along the x, y and z axes, respectively. μ is the fluid viscosity, ρ_∞ is the fluid density far away from the sheet, μ_0 is the magnetic permeability, H is the magnetic field. The terms $\mu_0 M \frac{\partial H}{\partial y}$ and $\mu_0 M \frac{\partial H}{\partial z}$ in (7.3) and (7.4), respectively, represent the components of the magnetic force, per unit volume of the fluid, and depend on the existence of the magnetic gradient. These two terms are well known from FHD which is so-called Kelvin forces and the term $\mu_0 T \frac{\partial M}{\partial T}\left(v\frac{\partial H}{\partial y} + w\frac{\partial H}{\partial z} \right)$ of the thermal energy equation (7.5) represents the thermal power per unit volume due to magnetization that takes place as an adiabatic process. The power indices m and n indicate the variable surface temperature in the (x, y) plane.

Assumed that the viscosity and thermal conductivity of fluid is a temperature dependent and is of the form Salawu and Dada (2016)

$$\frac{1}{\mu} = \frac{1}{\mu_\infty}\left[1 + \gamma\left(T - T_\infty\right)\right] \text{ or } \frac{1}{\mu} = s\left[\left(T - T_r\right)\right] \tag{7.8}$$

Where $s = \frac{\gamma}{\mu}$ and $T_r = T_\infty - \frac{1}{\gamma}$

Here s and T_r are the constant and their values depend on the reference state and γ is a constant connected with the thermal property of the fluid. Generally for the liquids $s > 0$ and for gases $s < 0$.

On the other hand, for most liquids the thermal conductivity k is assumed to very as a linear function of temperature in the form Salawu and Dada (2016)

$$k = k_\infty\left(1 + a\theta\right), \tag{7.9}$$

where $a = \frac{k_w - k_\infty}{k_\infty}$ is the thermal conductivity parameter.

The biomagnetic fluid flow is affected by the magnetic field generated by the presence of a magnetic dipole and assumed that the magnetic dipole is located at distance d below the sheet. The magnetic dipole gives rise to a magnetic field, sufficiently strong to saturate the fluid and its scalar potential for the magnetic dipole whose components H_y, H_z of the magnetic field $H = \left(H_y, H_z\right)$, due to the electric current with the wire with intensity I, are given by Tzirtzilakis and Kafoussias (2010)

$$H(x,y,z)=\frac{I}{2\pi}\frac{1}{\sqrt{y^2+(z+d)^2}}=\frac{I}{2\pi}\left(\frac{1}{(z+d)}-\frac{1}{2}\frac{y^2}{(z+d)^3}\right)$$

A linear equation involving the magnetic intensity H and Temperature T is given by Tzirtzilakis and Kafoussias (2010)

$$M=KH(T_c-T), \tag{7.10}$$

where K is a constant

7.3 Mathematical Analysis

We are now introducing the non-dimensional coordinates as following Tzirtilakis and Kafoussias (2010).

$$\xi(x)=\sqrt{\frac{a}{\nu}}\ x\ ,\zeta(y)=\sqrt{\frac{a}{\nu}}\ y\ ,\eta(z)=\sqrt{\frac{a}{\nu}}\ z$$

the dimensionless velocity, pressure $P(\xi,\zeta,\eta)$ and temperature $\theta(\xi,\zeta,\eta)$ of the magnetic fluid are given by the following expressions:

$$u=\sqrt{a\nu}\xi f'(\eta),\ v=\sqrt{a\nu}\zeta g'(\eta),\ w=-\sqrt{a\nu}\left(f(\eta)+g(\eta)\right). \tag{7.11}$$

$$p(\xi,\zeta,\eta)=a\mu_\infty P(\eta) \tag{7.12}$$

$$\theta(\xi,\zeta,\eta)=\frac{T_c-T}{T_c-T_w}=\theta(\eta) \tag{7.13}$$

And the magnitude H of the magnetic field strength is given by the expression

$$H(\zeta,\eta)=\frac{I}{2\pi}\sqrt{\frac{a}{\nu}}\left[\frac{1}{\eta+\alpha}-\frac{1}{2}\frac{\zeta^2}{(\eta+\alpha)^3}\right] \tag{7.14}$$

Where α is the dimensionless distance of the electric wire from the $\xi-$axis $\alpha=d\sqrt{\frac{a}{\nu}}$. By substituting equation (7.10) and all the above expressions (7.11)-(7.14) into the momentum equations (7.2)-(7.4) and energy equation (7.5), and equating the coefficients of equal power of ξ,ζ we get the following system of ordinary differential equations.

$$f'''+\frac{\theta-\theta_r}{\theta_r}\left[f'^2-(f+g)f''\right]-\frac{\theta'}{\theta-\theta_r}f''=0 \tag{7.15}$$

$$g'''+\frac{\theta-\theta_r}{\theta_r}\left[g'^2-(f+g)g''\right]-\frac{\theta'}{\theta-\theta_r}g''+\frac{\theta-\theta_r}{\theta_r}\frac{B\theta}{(\eta+\alpha)^4}=0 \tag{7.16}$$

$$P'-\frac{\theta_r}{\theta-\theta_r}\left(f''+g'\right)'+\frac{\theta_r\theta'}{\left(\theta-\theta_r\right)^2}\left(f'+g'\right)+\frac{\beta\theta}{\left(\eta+\alpha\right)^3}=0 \tag{7.17}$$

$$\left(1+a\theta\right)\theta''+a\theta'^2-\Pr\left(mf'\theta+ng'\theta-\left(f+g\right)\theta'\right)-\frac{B\lambda(f+g)(\theta-\varepsilon)}{\left(\eta+\alpha\right)^3}=0 \tag{7.18}$$

The boundary conditions are

$$f'=1,\ g'=\frac{b}{a}=\delta,\ \theta=1,\quad f=g=0 \text{ at } \eta=0 \tag{7.19}$$

$$f'\to 0, g'\to 0, P\to -P_\infty, \theta\to 0 \text{ as } \eta\to\infty \tag{7.20}$$

The dimensionless parameters appearing in these equations are:

Prandtl number, $P_r=\frac{\mu_\infty c_p}{k_\infty}$, viscous dissipation parameter, $\lambda=\frac{a{\mu_\infty}^2}{\rho_\infty k_\infty(T_c-T_w)}$, dimensionless Curie temperature, $\varepsilon=\frac{T_c}{T_c-T_w}$,ferromagnetic interaction parameter, $\beta=\frac{I^2}{4\pi^2}\frac{K\mu_0(T_c-T_w)\rho_\infty}{{\mu_\infty}^2}$, dimensionless distance, $\alpha=d\sqrt{\frac{a}{\nu}}$, viscosity parameter, $\theta_r=\frac{T_r-T_\infty}{T_w-T_\infty}=-\frac{1}{\gamma\left(T_w-T_\infty\right)}$ where θ_r is negative for liquids and θ_r is positive for gases.

The local Skin friction coefficient and local Nusselt number are important physical parameters of this flow and heat transfer which is define respectively

$C_f=-\frac{\tau_w}{\frac{1}{2}\rho_\infty u_w^2}$ and $N_u=-\frac{xq_w}{k_\infty\left(T_w-T_\infty\right)}$ where $\tau_w=-\mu\left(\frac{\partial u}{\partial z}\right)_{z=0}$ and $q_w=-k\left(\frac{\partial T}{\partial z}\right)_{z=0}$

and the corresponding dimensionless quantities can be written as

$$C_{fx}=C_f(\mathrm{Re}_x)^{1/2}=-\frac{2\theta_r}{\theta_r-1}f''(0) \quad \text{and} \quad Nu_x=Nu(\mathrm{Re}_x)^{-1/2}=-\theta'(0)$$

7.4 Numerical Method

For the numerical solution of the problem under consideration we apply an approximate technique that has better stability characteristics than classical Runge-Kutta combined with a shooting method, is simple, accurate and efficient. The essential features of this technique are the following: (i) It is based on the common finite difference method with central differencing (ii) on a tridiagonal matrix manipulation and (iii) on an iterative procedure. This numerical method is described in detail in Kafoussias and Williams (1993). For reasons of completeness of this study we demonstrate the application of this methodology for the numerical solution of the system of equations (7.15), (7.16) and (7.18), subject to the boundary conditions (7.19) and (7.20).

The momentum Equation (7.15) can be written as

$$f'''+\frac{\theta-\theta_r}{\theta_r}\left[f'^2-(f+g)f''\right]-\frac{\theta'}{\theta-\theta_r}f''=0 \tag{7.21}$$

The above equations can be considered as a second order linear differential equation by setting $y(x)=f'(\eta)$ provided that P and $f(\eta)$ are considered known functions. In this case equation (7.21) can be written as

$$(f')''+\left(\frac{\theta-\theta_r}{\theta_r}(f+g)-\frac{\theta'}{\theta-\theta_r}\right)(f')'+\frac{\theta-\theta_r}{\theta_r}f'f'=0$$

which is of the form

$$P(x)y''(x)+Q(x)y'(x)+R(x)y(x)=S(x) \tag{7.22}$$

where $P(x)=1,\ Q(x)=\left(\frac{\theta-\theta_r}{\theta_r}(f+g)-\frac{\theta'}{\theta-\theta_r}\right),\ R(x)=\frac{\theta-\theta_r}{\theta_r}f',\quad S(x)=0$

In an analogous manner all equations of the system can be reduced in this form of equation (7.22) except for equation (7.17) which are already first order differential equations. Equation (7.22) can be solved by a common finite difference method, based on central differencing and tridiagonal matrix manipulation.

To start the solution procedure, we assume initial guesses (distribution curves) for $f'(\eta)$ between $\eta=0$ and $\eta=\eta_\infty(\eta\to\infty)$ which satisfy the boundary conditions (7.19) and (7.20). For this problem indicative initial guesses are

$$f(\eta)=g(\eta)=\frac{\eta}{\eta_\infty}\left(1-\frac{\eta}{\eta_\infty}\right),\ f'(\eta)=1-\frac{\eta}{\eta_\infty},\ g'(\eta)=\delta\left(1-\frac{\eta}{\eta_\infty}\right),\ \theta(\eta)=1-\frac{\eta}{\eta_\infty}.$$

The $f(\eta)$ distribution is obtained by the integration from $f'(\eta)$ curve. The next step is to consider the f, P, θ known and to determine a new estimation for $f'(\eta)$, $f'_{new}(\eta)$ by solving the non-linear equation (7.22) using the above method. The distribution is updated by the integration of new $f'(\eta)$ curve. These new profiles of $f'(\eta)$ and $f(\eta)$ are then used for new inputs and so on. In this way the momentum equation (7.21) and consequently (7.15) and (7.16) are solved iteratively until convergence up to a small quantity ε is attained.

After $f(\eta)$ is obtained the solution of the energy equation (7.18) with boundary conditions (7.19) and (7.20) is solved by using the same algorithm, but without iteration now as far as equation (7.19) is linear. Equation (7.19) is

$$(1+a\theta)\theta''+a\theta'^2-\Pr(mf'\theta+ng'\theta-(f+g)\theta')-\frac{B\lambda(f+g)(\theta-\varepsilon)}{(\eta+\alpha)^3}=0$$

This equation can be written as

$$(1+a\theta)\theta''+(a\theta'-\Pr(f+g))\theta'+\left((mf'+ng')-\frac{B\lambda(f+g)}{(\eta+\alpha)^3}\right)\theta=\frac{B\lambda(f+g)\varepsilon}{(\eta+\alpha)^3} \qquad (7.23)$$

Equation (7.23) is a second order linear differential equation in setting $y(\eta)=\theta(\eta)$

which is of the form

$$P(x)y''(x)+Q(x)y'(x)+R(x)y(x)=S(x)$$

where $P(x)=(1+a\theta),\ Q(x)=(a\theta'-\Pr(f+g)),\ R(x)=-\left((mf'+ng')-\frac{B\lambda(f+g)}{(\eta+\alpha)^3}\right),$

$$S(x)=\frac{B\lambda(f+g)\varepsilon}{(\eta+\alpha)^3}.$$

Considering $f(\eta), f'(\eta), g(\eta), g'(\eta)$ and θ known, we obtain a new approximation θ_{new} for θ and this process is continue until convergence up to a small quantity ε is attained and finally we obtain θ. This process is continuing until final convergence of the solution is attained.

In order to apply to our numerical computation a proper step size $h = \Delta\eta = 0.01$ and appropriate η_∞ value as $(y \to \infty)$ must be determined. By "trial and error" we set $\eta_\infty = 6$, $\Delta\eta = 0.01$ and the tolerance between the iterations is set at $\varepsilon = 10^{-4}$ defined as $\varepsilon = \max_{i=1,N}\left(\left|\frac{f_{old}(i) - f_{new}(i)}{f_{old}(i)}\right|\right)$. Computations were also performed for $\Delta\eta = 0.001$ and no significant differences were found.

7.4.1 Numerical validation

First we verify the accuracy of the present method, the present numerical results for $\theta'(0)$ are compared with the published results obtained by setting $\beta = 0$ *and* $f'(0) = 1,\ g'(0) = 0.5, \Pr = 1$ in boundary conditions (7.19). The comparisons are found to be in complete agreement, and thus we are confident that the present method is accurate with Liu et al. (2008).

Table 7.1 Validation of the present results by comparing with the published literature for wall heat transfer rate coefficients $\theta'(0)$ when $\Pr = 1,\ \beta = 0$ *and* $f'(0) = 1,\ g'(0) = 0.5$

stretching ratio	$m = 0, n = 0$		$m = 2, n = 0$		$m = 0, n = 2$	
	Present	Liu et al. (2008)	Present	Liu et al. (2008)	Present	Liu et al. (2008)
$\delta = 0.25$	-0.66721	-0.665933	-1.36331	-1.364890	-0.88301	-0.883125
$\delta = 0.5$	-0.73546	-0.735334	-1.39377	-1.395356	-1.10544	-1.106491
$\delta = 0.75$	-0.79599	-0.796472	-1.42341	-1.425038	-1.29056	-1.292003

7.5 Results and Discussion

The values of the governing parameters are chosen to be physically representative of the actual blood fluids. We considered by Loukopoulos and Tzirtzilakis (2004), human blood as a biomagnetic fluid. At $T_w = 37^0 C$ (human body temperature) where as the body curie temperature is $T_c = 41^0 C$, For these values of temperature, the temperature number is

$\varepsilon = 78.5$. Since the fluid is blood so we can assume $\rho = 1050\, kg/m^3$ and $\mu = 3.2\times10^{-3}\, kgm^{-1}s^{-1}$ by Tzirtzilakis (2008). Generally, the specific heat under a constant pressure c_p and thermal conductivity k of any fluid are temperature dependent. For the temperature range consider in this problem, $C_p = 14.65\, JKg^{-1}.K^{-1}$ and $k = 2.2\times10^{-3}\, Jm^{-1}s^{-1}k^{-1}$ respectively by Tzirtzilakis and Xenos (2013) and hence $P_r = 21$, Ferromagnetic interaction parameter $\beta = 0$ to 10 as in Tzirtzilakis and Kafoussias (2003). Noted that $\beta = 0$ corresponds to hydrodynamic flow. Viscous dissipation parameter $\lambda = 6.4\times10^{-14}$

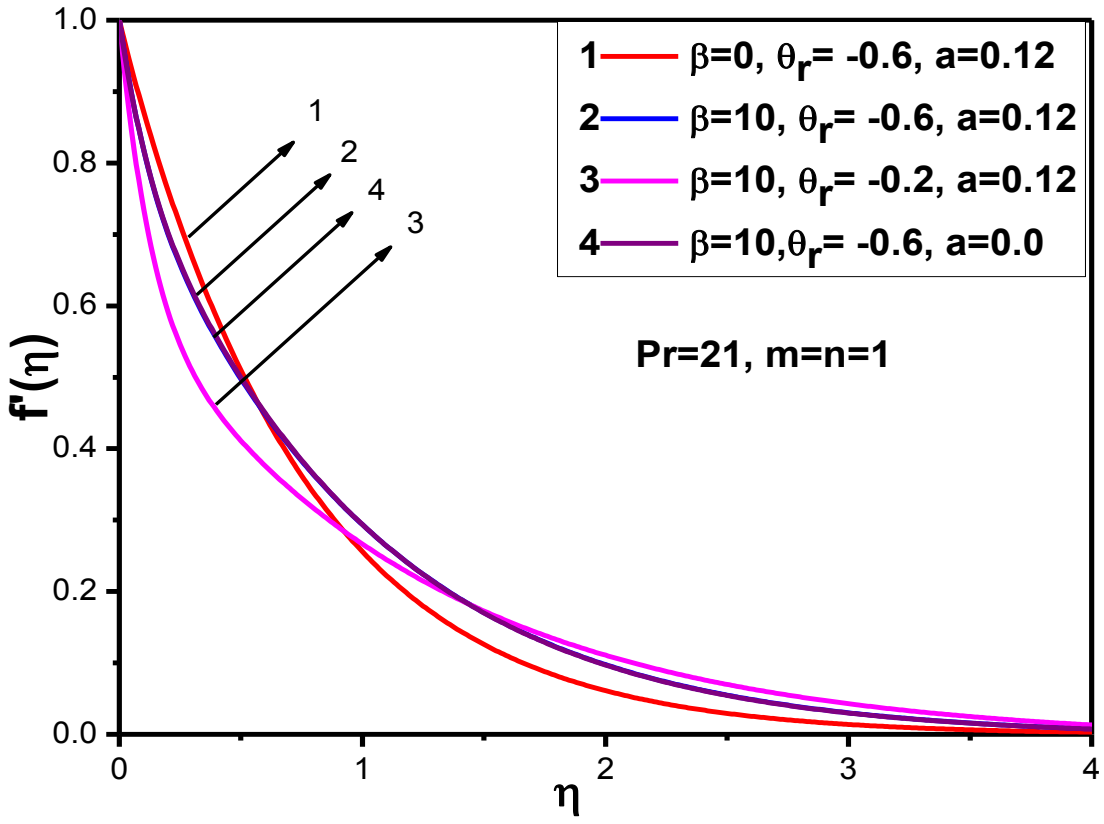

Fig. 7.2 Velocity profile for various values of β, θ_r, a

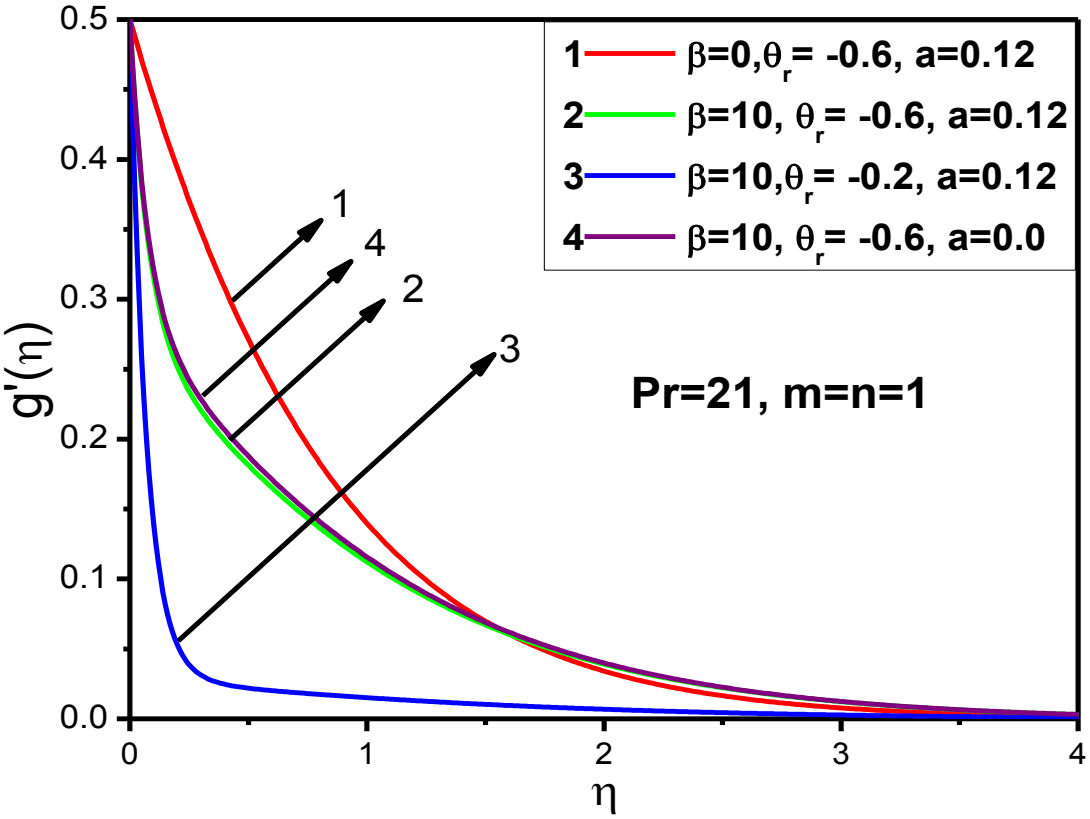

Fig. 7.3 Velocity profile for various values of β, θ_r, a

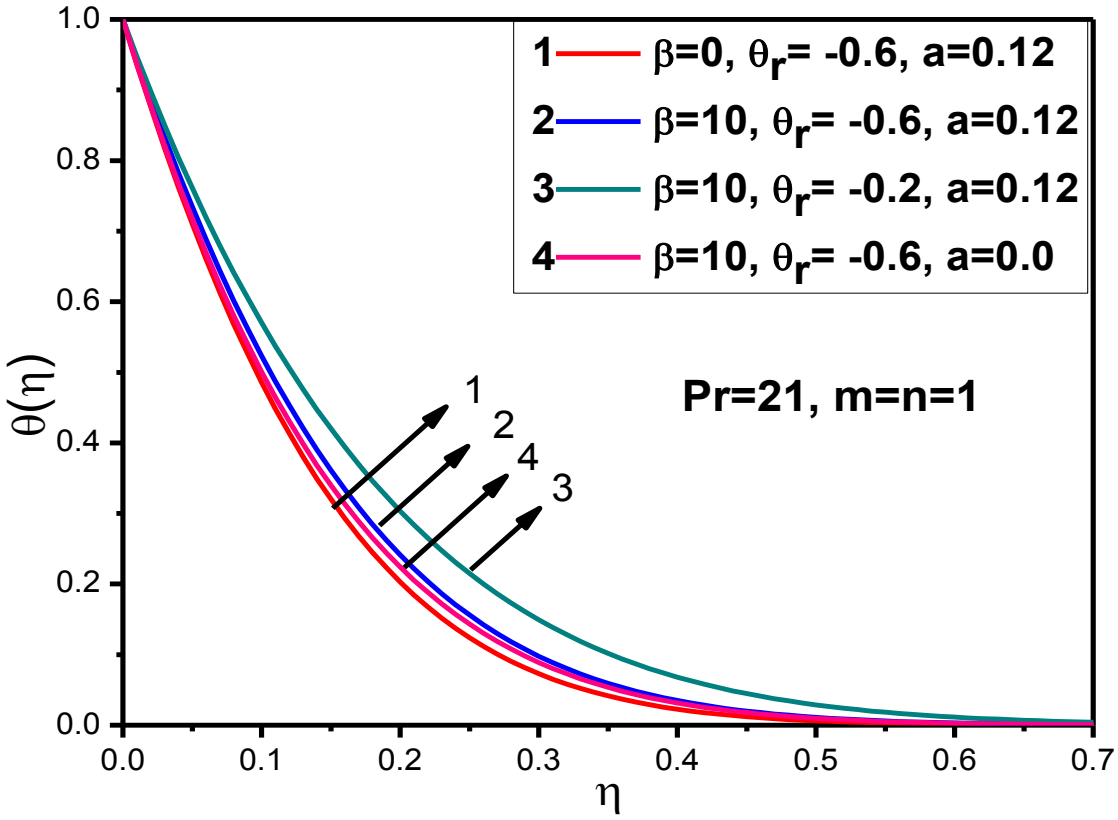

Fig. 7.4 Temperature profile for various of β, θ_r, a

Figures 7.2 to 7.4 display the influence of ferromagnetic parameter, viscosity parameter and thermal conductivity parameter on velocity and temperature distributions. It is evident from figures that an increase of the magnetic parameter results to greater the velocity profiles $f'(\eta)$ than the corresponding hydrodynamics ones. However, the opposite is true for the velocity component $g'(\eta)$ (fig 7.3). This fact is due to the influences of Kelvin forces on the flow field in the y direction.

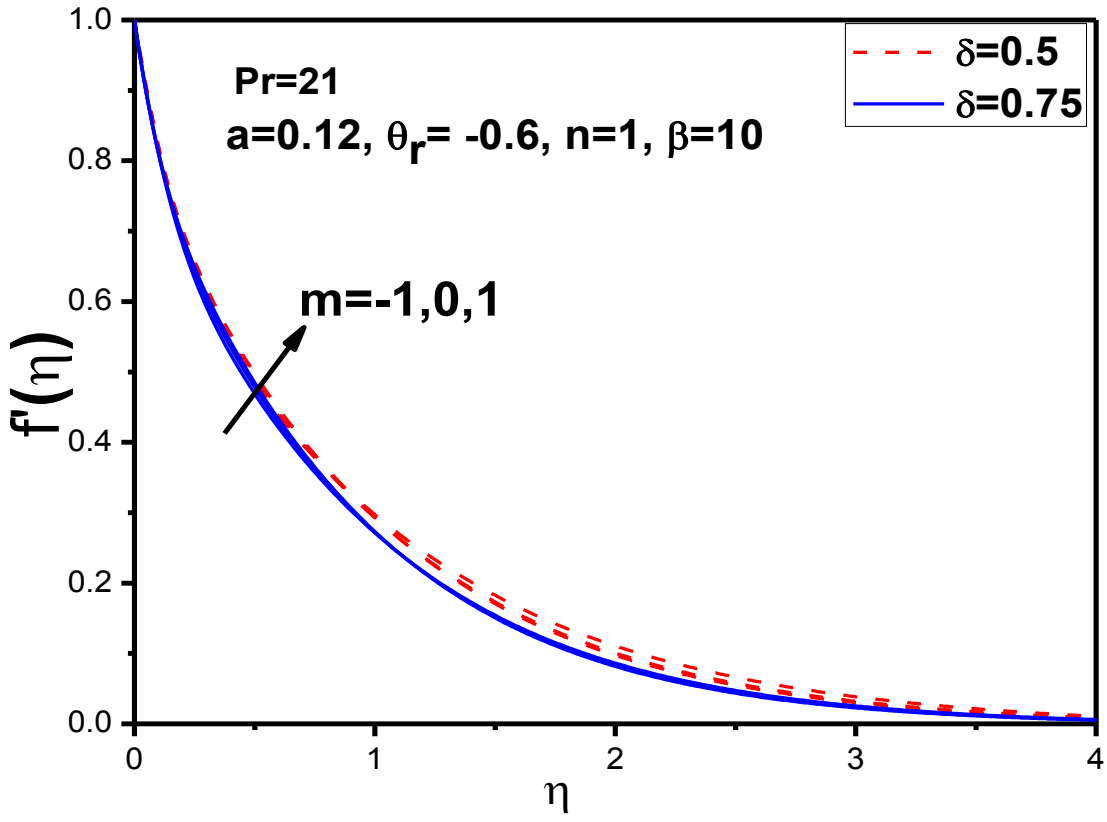

Fig. 7.5 Velocity profile $f'(\eta)$ for values various values of δ, m

From figure 7.4, it is observed that increase in magnetic field parameter increases the temperature profiles. The reason behind this is that increment of the magnetic field reduces the boundary layer thickness and enhances the thermal conductivity of the fluid. These figure also indicates that increment of the values of θ_r, results to decrement of the velocity and enhances the temperature profile. This is due to fact that increment of θ_r results to an increment in the thermal boundary layer thickness which results to decrement the velocity and increment of the temperature.

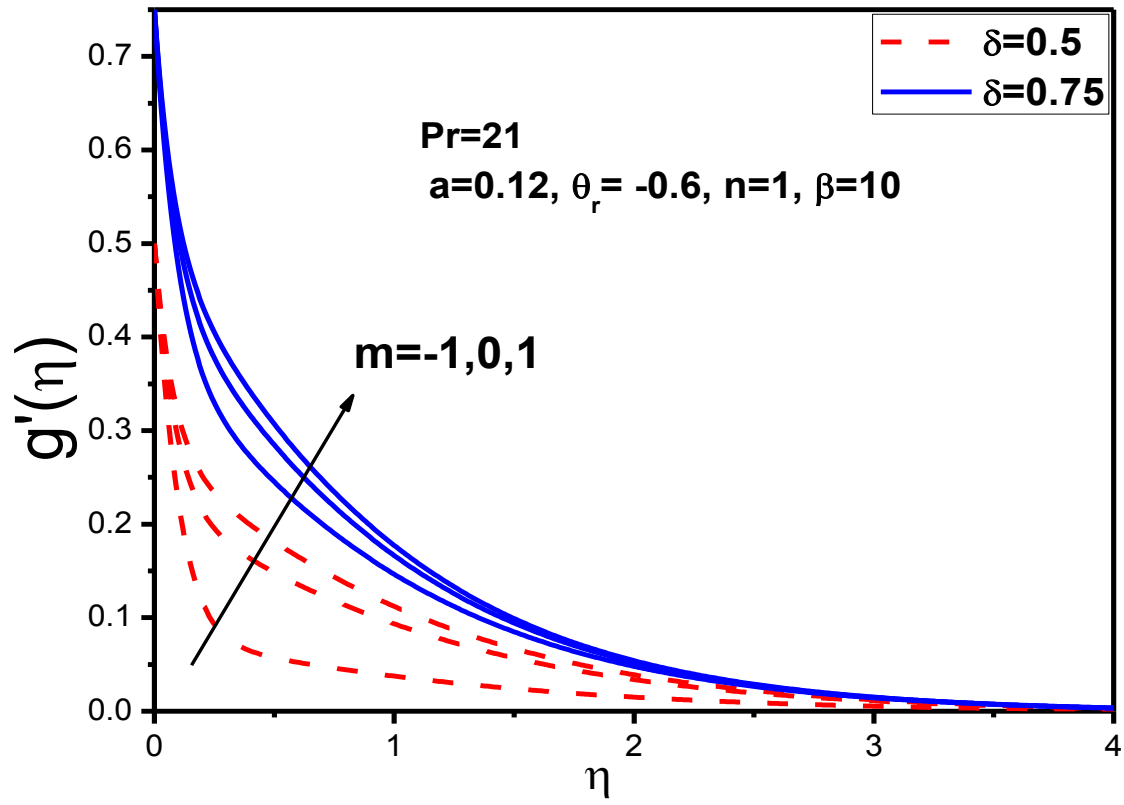

Fig. 7.6 Velocity profile $g'(\eta)$ for various values of δ, m

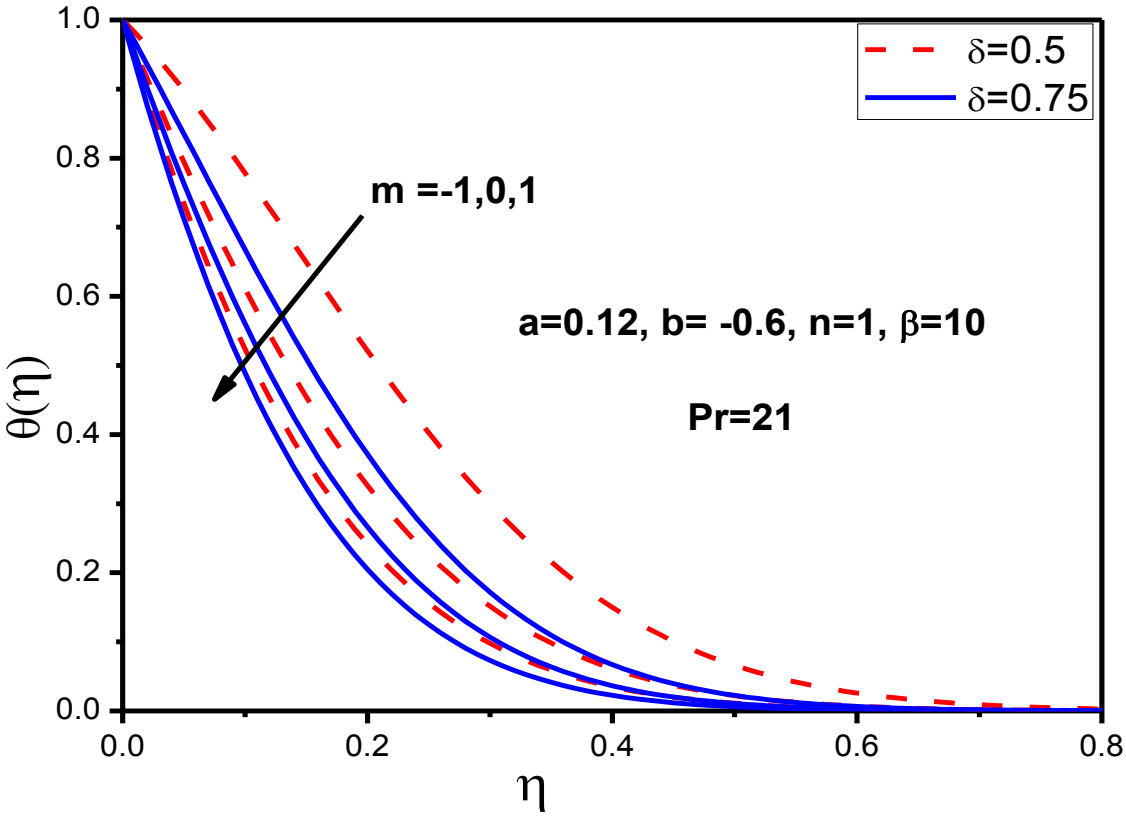

Fig. 7.7 Temperature profile for various values of δ, m

Figure 7.5 to 7.9 exhibits effect of wall temperature parameter on velocity and temperature distribution. For this figure it is observed that the variation of sheet temperature has a significantly effect on the velocity and temperature profile. From the figure we conclude that increment of the wall temperature parameter results to increment the velocity profile and the opposite behaviour occurs for the temperature profile. This is due to fact that, when $m, n > 0$ the heat flows from the stretching sheet into the fluid and when $m, n < 0$ the temperature gradient is positive and the heat flows from the fluid into the stretching sheet. When m and n are both increased, then the temperature profile is decreased whereas the velocity is increased i.e. thermal boundary layer becomes thinner and momentum boundary layer is thicker.

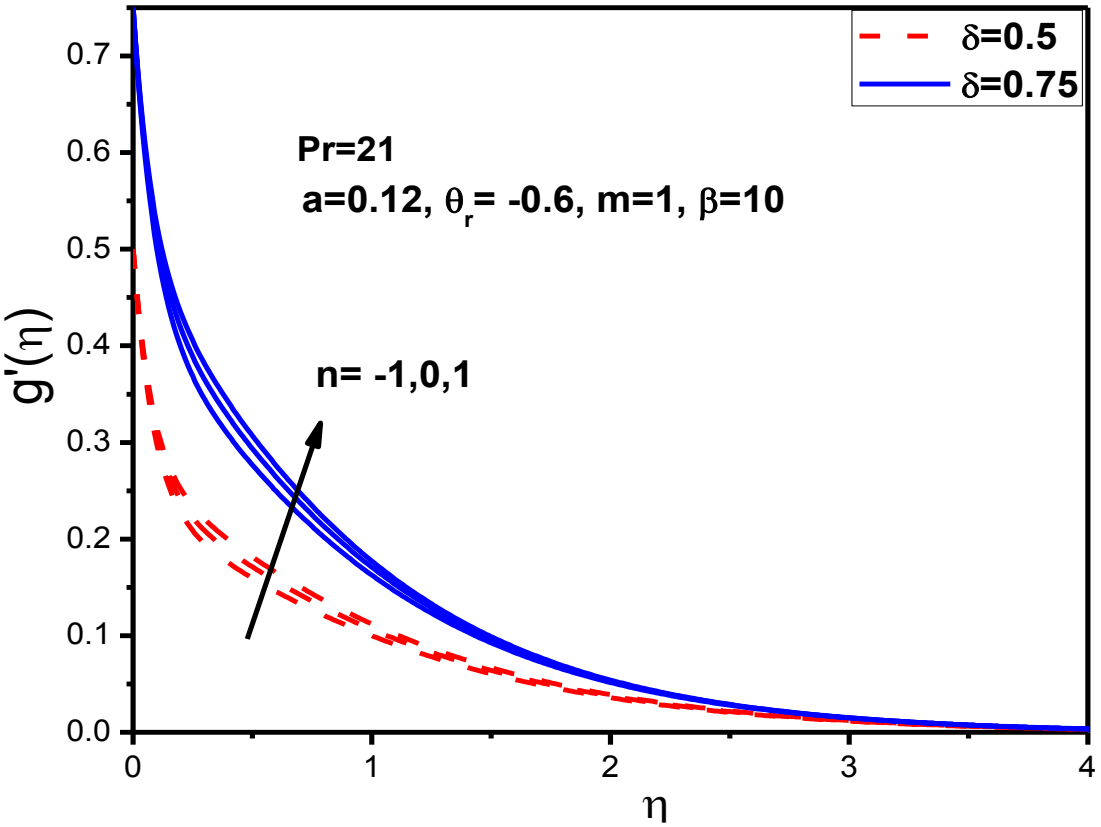

Fig. 7.8 Velocity profile for various values of δ, n

Figure 7.10 to 7.14 depicts the skin friction coefficient and rate of wall heat transfer with respect to the viscosity parameter and thermal conductivity parameter for various values of magnetic number β. It is observed from this figure that when the viscosity parameter is increase, the velocity gradient at the wall is increased and its reverse trend was found for the wall temperature gradient.

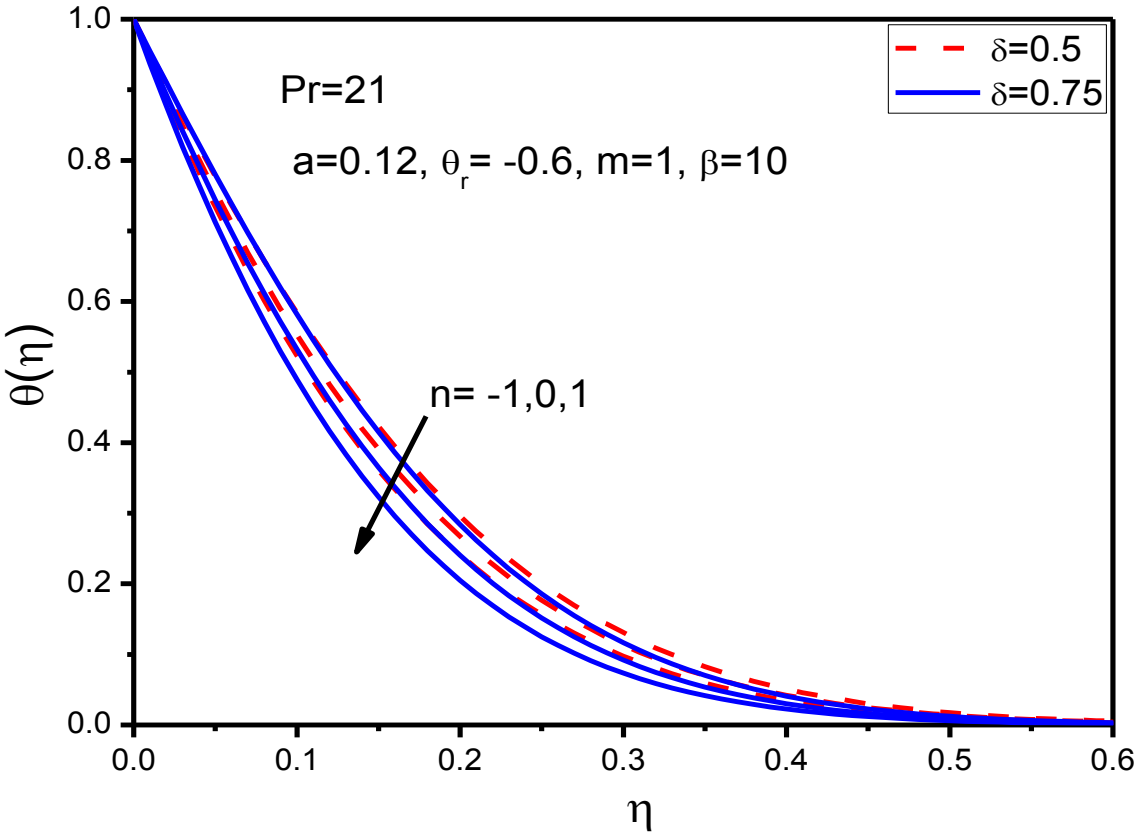

Fig. 7.9 Temperature profile for various values of δ, n

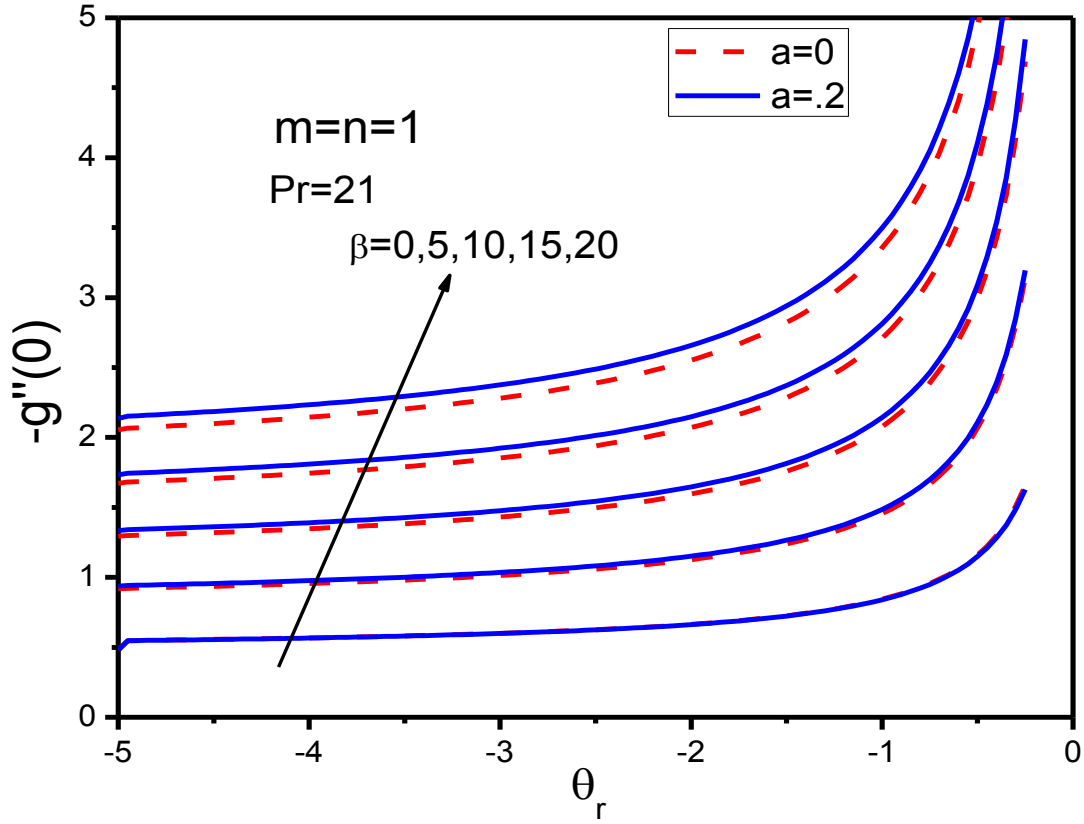

Fig. 7.10 Skin friction for various values for various of β with respect θ_r

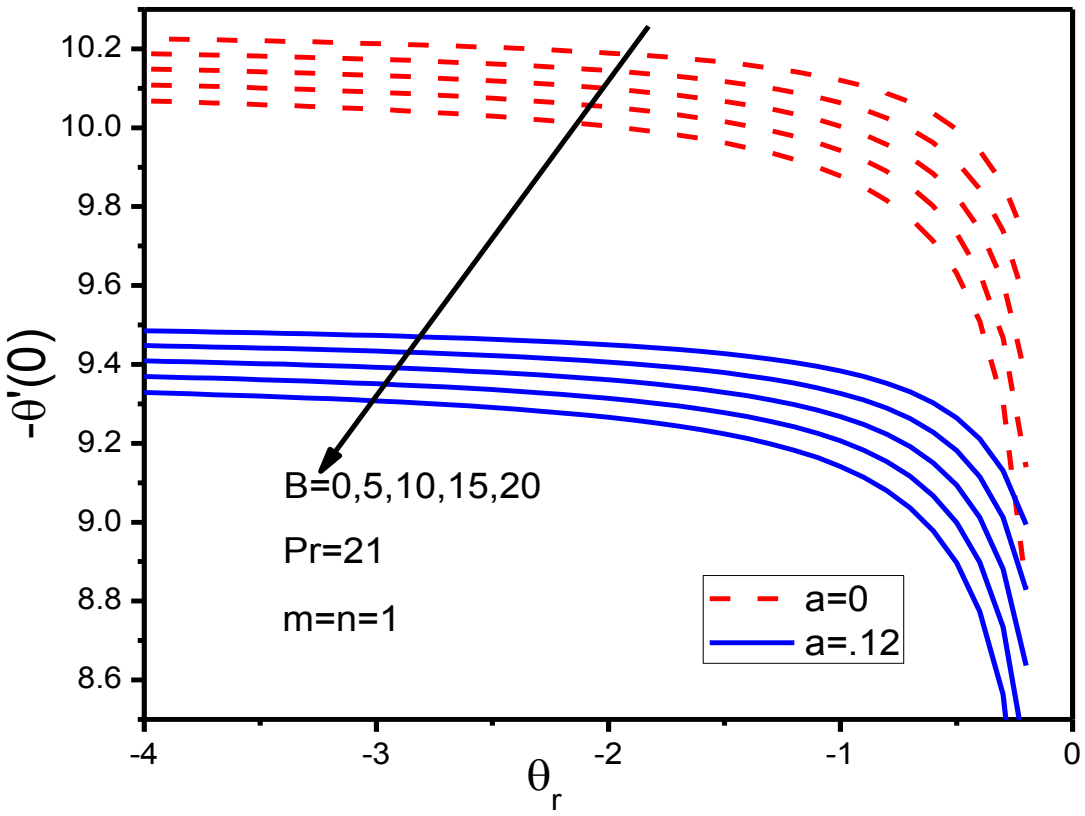

Fig. 7.11 Rate of heat transfer values of β with respect θ_r

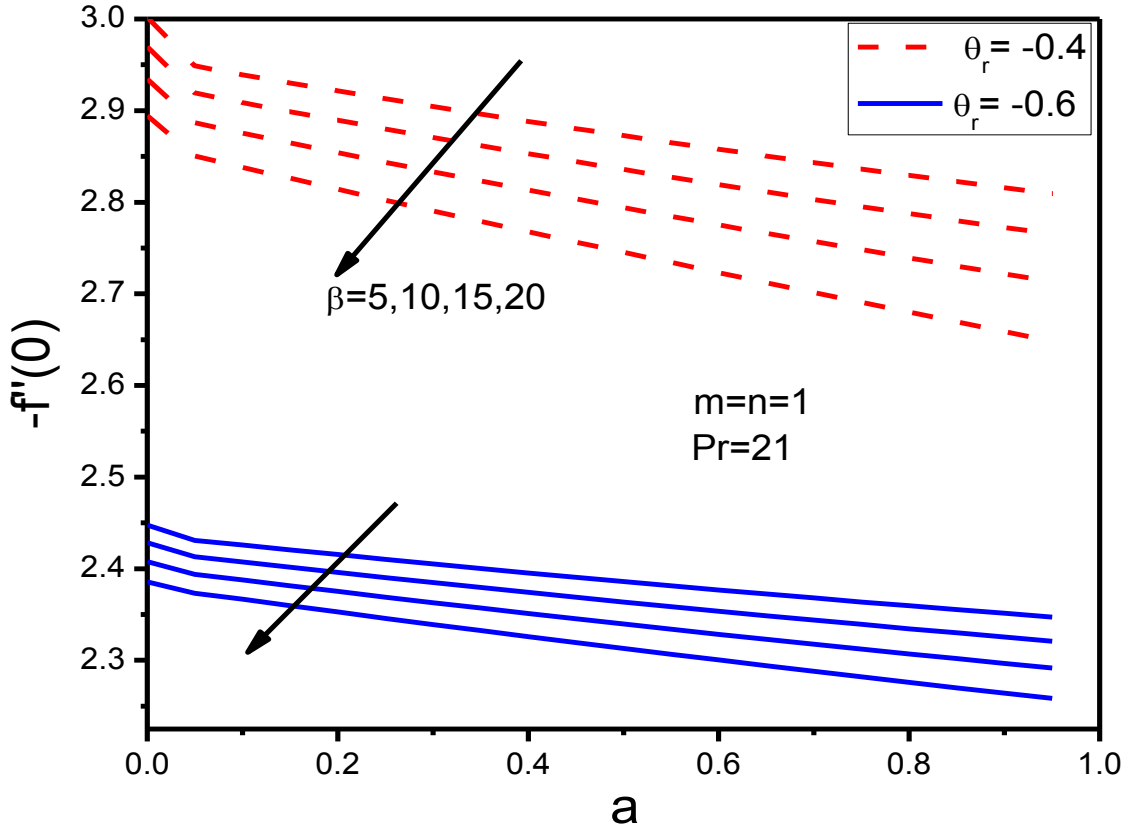

Fig. 7.12 Skin friction for various values of β and θ_r with respect a

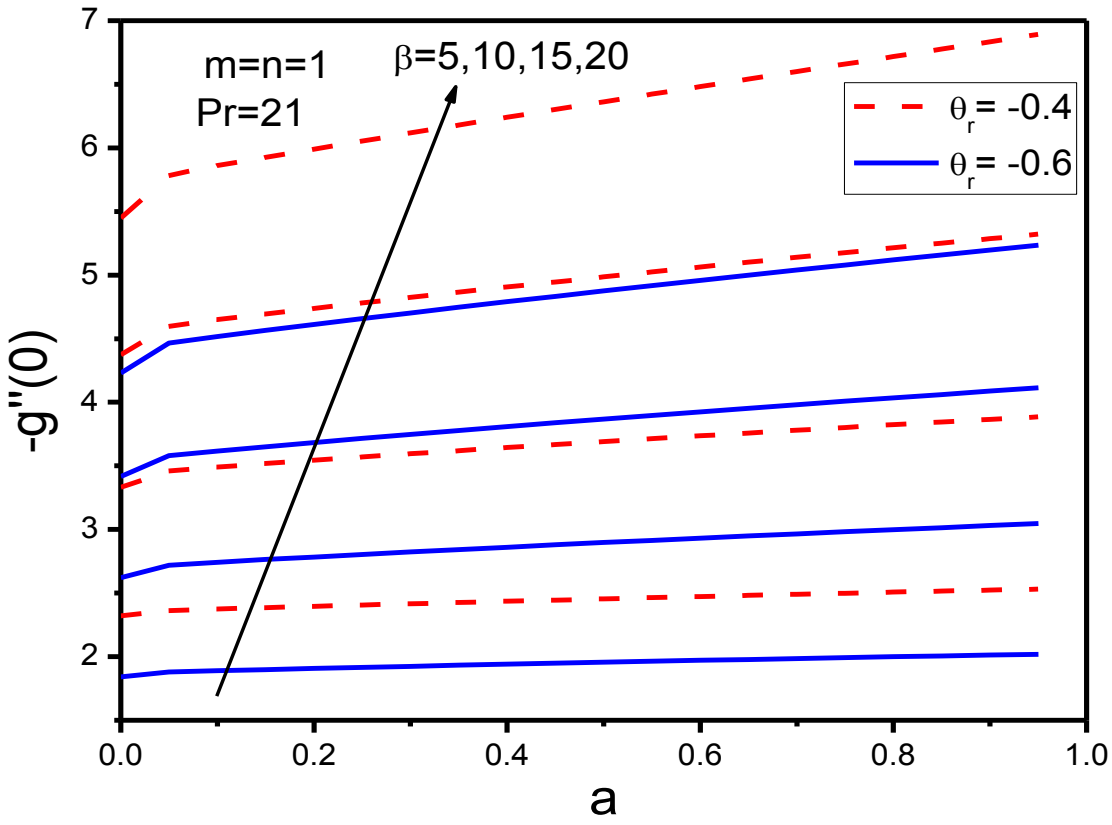

Fig. 7.13 Skin friction $g''(0)$ for various values of β and θ_r with respect a

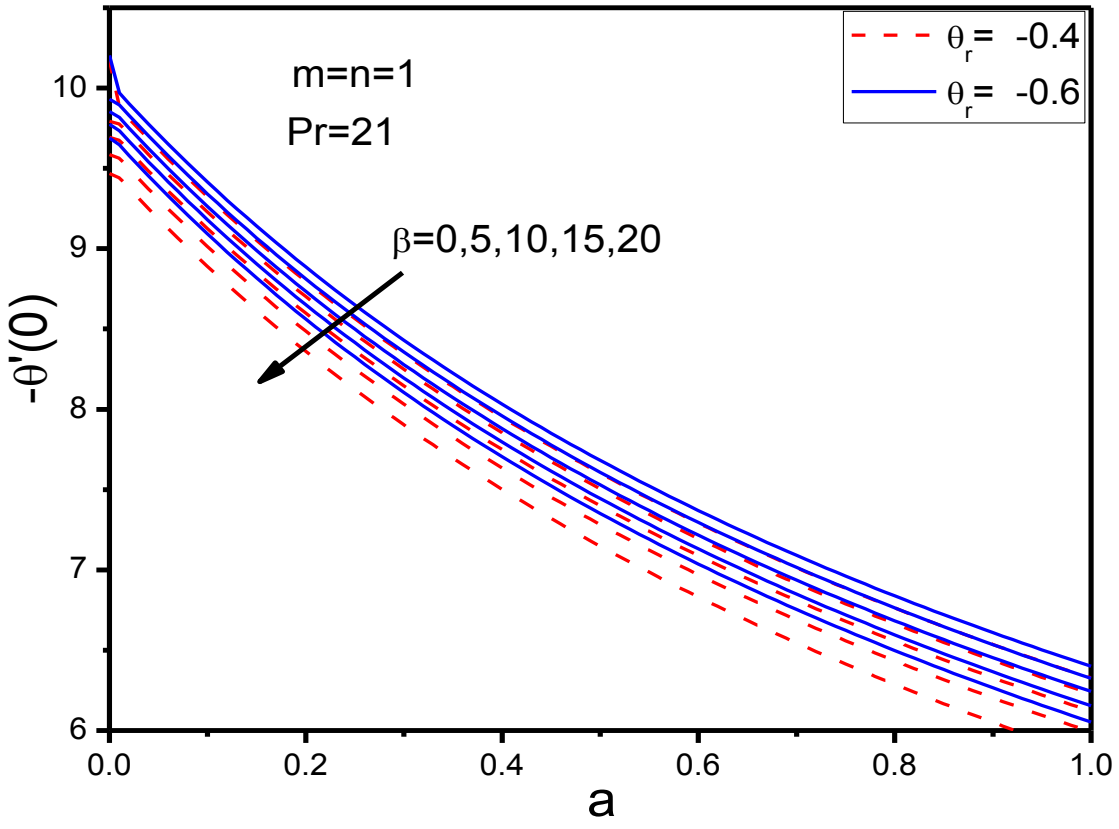

Fig. 7.14 Rate of heat transfer for various values of β and θ_r with respect a

7.6 Summery of the chapter

In this chapter, we studied the effect of variable fluid properties on BFD in the presence of applied magnetic field. The results are presented graphically to investigate influence of pertinent parameters on velocity and temperature field. Some important result are:

(i) The effect the increment of variable thermal conductivity parameter is to enhance the temperature in the flow region and the reverse is true in the case of the wall temperature parameter. This parameter effect is negligible for velocity and skin friction.

(ii) The effect of increasing value of viscosity parameter θ_r is to enhance the temperature and decrease the velocity. This parameter variation is more effective on the velocity profile and skin friction but negligible on the wall temperature gradient.

(iii) For the effect of the magnetic parameter, as the magnetic number increases, it is apparent that the velocity profile $f'(\eta)$ is increased but the velocity profile $g'(\eta)$ decreases with the increment of the magnetic field. This is happen due to the Lorentz forces.

(iv) The effect of thermal conductivity is more profound on the temperature gradient than other physical quantities. On the other hand the viscosity parameter is more affected from the skin friction than the temperature gradient variation.

Chapter 8

Dual Solutions in Biomagnetic Fluid Flow and Heat Transfer over a nonlinear stretching/shrinking sheet: Application of Lie Group Transformation Method

Of concern in this chapter is a theoretical investigation of boundary layer flow of a biomagnetic fluid and heat transfer on a stretching/shrinking sheet in the presence of a magnetic dipole. The problem has been treated mathematically by using Lie group transformation. The governing nonlinear partial differential equations are thereby reduced to a system of coupled nonlinear ordinary differential equations subject to associated boundary conditions. The resulting equations subject to boundary conditions are solved numerically by using bvp4c function available in MATLAB software. The plots for variations of velocity, temperature, skin friction and heat transfer rate have been drawn and adequate discussion has been made. The study reveals that the problem considered admits of dual solutions in particular ranges of values of the suction parameter and nonlinear stretching/shrinking parameter. A stability analysis has also been carried out and presented in the chapter. This enables one to determine which solution is stable that can be realized physically, and which is not. The results of the present study have been compared with those reported by previous investigators in order to ascertain the validity/reliability of the computational results.

8.1 Introduction

Studies on biomagnetic fluid flow and heat transfer under the influence of external magnetic fields have been receiving growing attention of researchers owing to their important applications in bioengineering and clinical sciences. Observations derived from related investigation are useful in the design and development of magnetic devices for cell separation, reduction of blood flow during surgery, targeted transport of drugs through the

use of magnetic particles as drug carriers, magnetic resonance imaging (MRI) of specific parts of the human body, electromagnetic hyperthermia in cancer treatment etc., as mentioned in earlier communications, Misra and Shit (2009a, 2009b), Misra et al. (2010).

Base on the principles of Ferrohydrodynamics (FHD), a biomagnetic fluid model was developed by Haik et al. (1996). This was further extended by Tzirtzilakis (2005) by combining the principles of Magnetohydrodynamics with those of FHD and applied his model to analyze the flow of blood under the influence of a magnetic field. Tzirtzilakis and Kafoussias (2003) studied the flow of a heated ferrofluid over a linearly stretching sheet under the action of a magnetic field generated due to the presence of a magnetic dipole. Laminar two-dimensional flow of an incompressible biofluid over a stretching sheet was studied numerically by Tzirtzilakis and Tanoudis (2003). The effect of heat transfer on the flow behaviour was also studied by these authors. Flows of biomagnetic viscoelastic fluids in different situations were investigated theoretically by Misra and Shit (2009a, 2009b). These studies reveal that the presence of external magnetic field bears the potential of influencing the flow behaviour of biomagnetic viscoelastic fluids quite appreciably.

Existence of dual solutions have been reported in various studies by different researchers. Some of them have presented stability analysis also. Mukhopadhyay (2011) while dealing with a problem of heat transfer in a moving fluid over a moving flat surface observed the existence of dual solutions. Vajravelu et al. (2017) while studying the unsteady flow and heat transfer over a shrinking sheet with consideration of thermal radiation and viscous dissipation, reported the existence of dual solutions for the flow field. Krisna et al. (2016) observed dual solutions for an unsteady problem of flow past an inclined sheet. Naganthran and Nazar (2017) found the existence of dual solutions during MHD stagnation point flow over a stretching/shrinking sheet. It was reported by Hafidzuddin et al. (2016) that dual solutions exist for boundary layer flow and heat transfer over an exponentially stretching/shrinking sheet. Ray Mahapatra et al. (2014) also discussed the existence of dual solutions for MHD stagnation point flow over a shrinking surface with partial slip. Stability analysis has presented in several studies (cf. Ghosh et al. (2016), Yasin et al. (2016), Awaludin et al. (2016) and Mishra and Singh (2014)).

Use of Lie group transformation method has been found to be very effective in finding the solutions of highly nonlinear differential equations. It helps determine the invariants and similarity solutions for partial differential equations (Pakdemirli and Yurusoy (1998), Bluman and Kumei (1991)). Several researchers (cf. Prabhu et al., (2009), Jalil et al. (2010), Reddy,

(2012), Rashidi et al. (2014), Ferdows et al. (2013)) have used Lie group analysis method for dealing with various problems of fluid flow and heat transfer.

Several problems of flow and heat transfer on sheets/channels under the action of external magnetic/electric fields that have applications to physiological fluid dynamics have been treated mathematically, among others are those of Misra and Sinha (2013), Sinha and Misra (2014), Misra and Chandra (2013), Misra and Adhikary (2016, 2017), Misra et al. (2013, 2015, 2017, 2018). However, in none of these studies, stability analysis/existence of multiple solutions has been considered. More particularly, to the best of our knowledge, there has not been any attempt to explore the existence of multiple solutions or to discuss the stability for any theoretical analysis for the flows of biomagnetic fluids. Considering this an attempt has been made, in this chapter to explore the stability and existence of dual solutions in the context of flow and heat transfer of biomagnetic fluids on stretching/shrinking sheets. The governing equations are highly nonlinear so we have made use of the Lie group transformation method. Finally, the computational results have been obtained with the help of bvp4c function available in Matlab software. Detailed discussion has been made for variations of biomagnetic fluid velocity, temperature, skin friction and heat transfer rate. The study reveals that there exist dual solutions in specific ranges of the vital parameters involved and that one of the two solutions is stable and physically realistic. The validity of the numerical results presented has also been established.

8.2 Mathematical Formulation

Let us consider the two-dimensional incompressible boundary layer flow and heat transfer of a biomagnetic fluid over a stretching/shrinking sheet (Fig. 8.1), where x-axis is taken along the sheet and y-axis along the normal direction. We assume that stretching/shrinking has a velocity $u = ax^n$, where $a(>0)$ is a constant that signifies the stretching situation. When $a < 0,$ we have the case of a shrinking sheet. It is assumed that the free stream velocity is $U_\infty(x) = bx^n$, where b is a positive constant. A magnetic dipole is supposed to be located below the sheet at a distance d which generates a magnetic field of constant strength. Also, we denote the temperature of the sheet by $T_w(x)$ and the ambient temperature by $T_c(x)$.

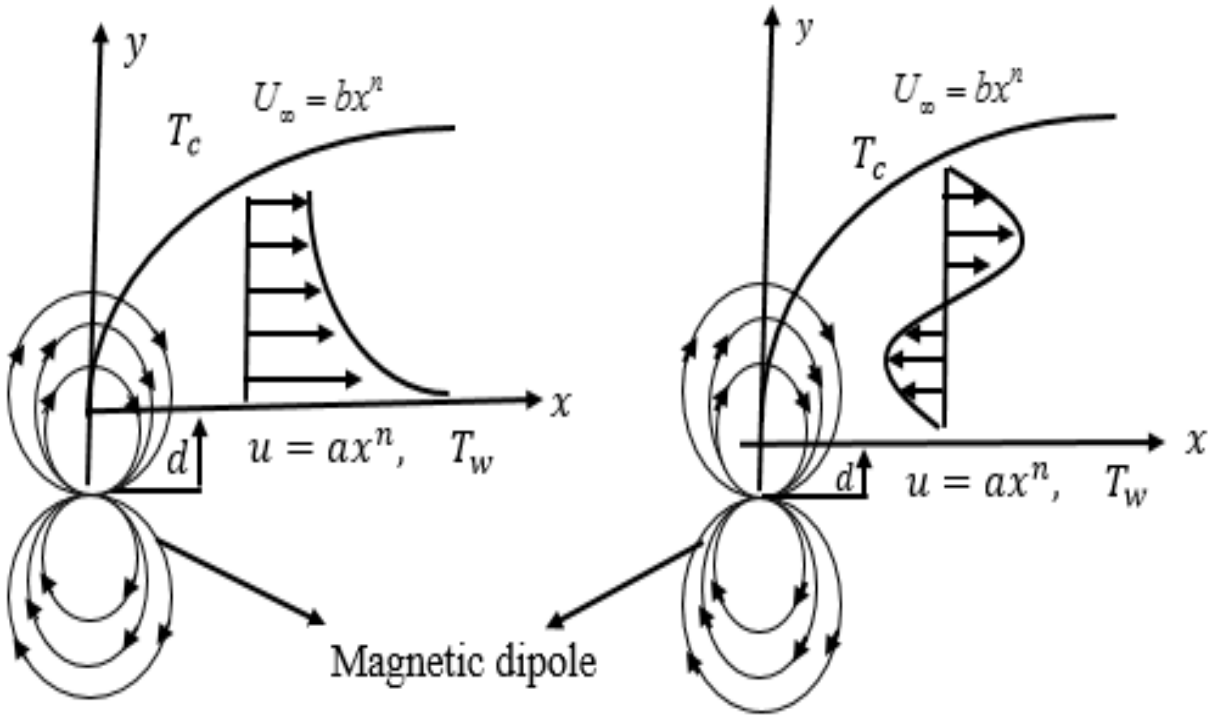

Stretching sheet Shrinking sheet

Fig. 8.1. The geometry of the problem.

Under the assumptions of boundary layer approximation, the governing equations for the problem can be written as

$$\frac{\partial \bar{u}}{\partial \bar{x}} + \frac{\partial \bar{v}}{\partial \bar{y}} = 0 \tag{8.1}$$

$$\bar{u}\frac{\partial \bar{u}}{\partial \bar{x}} + \bar{v}\frac{\partial \bar{u}}{\partial \bar{y}} = \bar{U}_\infty \frac{\partial \bar{U}_\infty}{\partial \bar{x}} + \bar{\nu}\frac{\partial^2 \bar{u}}{\partial \bar{y}^2} + \frac{\mu_0}{\rho} M \frac{\partial \bar{H}}{\partial \bar{x}} + \frac{\sigma B^2(\bar{x})}{\rho}\left(\bar{U}_\infty - \bar{u}\right) \tag{8.2}$$

$$\rho c_p \left(\bar{u}\frac{\partial T}{\partial \bar{x}} + \bar{v}\frac{\partial T}{\partial \bar{y}}\right) + \mu_0 T \frac{\partial M}{\partial T}\left(\bar{u}\frac{\partial H}{\partial \bar{x}} + \bar{v}\frac{\partial H}{\partial \bar{y}}\right) = k\frac{\partial^2 T}{\partial \bar{y}^2} \tag{8.3}$$

and the boundary conditions as

$$\bar{u} = u_w(x) = ax^n,\ v(x) = v_w(x),\ T = T_w = \left(T_\infty - Dx^m\right) \ \ at\ y = 0$$

$$\bar{u} = U_\infty(x) = bx^n,\ T \to T_c \ \ as\ y \to \infty. \tag{8.4}$$

u and *v* being the velocity components along the *x*- and *y*-axes, respectively. Other parameters ρ and k represent respectively the fluid density and the thermal conductivity, c_p is the specific heat at constant pressure, μ the fluid viscosity and μ_0 the magnetic permeability.

We consider that the magnetic field strength varies linearly with temperature T, M as a linear function of temperature T, given by $M = K(T_c - T)$, K being a constant.

The horizontal and vertical components of the magnetic field generated by a magnetic dipole located at a distance d below the sheet are given by Tzirtzilakis and Tanoudis, (2003).

$$H_x(x,y) = -\frac{\gamma}{2\pi}\frac{y+d}{x^2+(y+d)^2} \quad \text{and} \quad H_y(x,y) = \frac{\gamma}{2\pi}\frac{x}{x^2+(y+d)^2}$$

Then, the magnitude $\|H\| = H$ of the magnetic field is given by

$$H(x,y) = \left[H_x^2 + H_y^2\right]^{1/2} = \frac{\gamma}{2\pi}\frac{1}{\sqrt{x^2+(y+d)^2}} \approx \frac{\gamma}{2\pi}\left[\frac{1}{(y+d)^2} - \frac{1}{2}\frac{x^2}{(y+d)^4}\right] \tag{8.5}$$

8.3 Mathematical Analysis

We now introduce the following dimensionless quantities:

$$x = \frac{b}{c}\bar{x},\ y = \sqrt{\frac{(n+1)b}{2\nu}}\bar{y},\ u = \frac{\bar{u}}{c},\ v = \sqrt{\frac{(n+1)b}{2\nu b}}\bar{v},\ U_\infty = \frac{\bar{U}_\infty}{c},\ \theta(\eta) = \frac{T_c - T}{T_c - T_w} \tag{8.6}$$

Substituting (8.6) into Equation (8.2), one obtains the non-dimensional equations:

$$cu.c.\frac{b}{c}\frac{\partial u}{\partial x} + \sqrt{\frac{(n+1)b}{2\nu}}.cu.\sqrt{\frac{2\nu b}{(n+1)}}\frac{\partial u}{\partial y} = cU_\infty.c.\frac{b}{c}.\frac{\partial U_\infty}{\partial x} + \nu.c.\frac{(n+1)b}{2\nu}\frac{\partial^2 u}{\partial y^2} +$$

$$\frac{\sigma}{\rho}B_0^2\left(\frac{c}{b}\right)^{n-1}(cU_\infty - cu)x^{n-1} + \frac{\mu_0}{\rho}k(T_c - T).\left(-\frac{\gamma}{2\pi}\right)\frac{2.\frac{c}{b}.x}{(y+d)^4\left\{\frac{2\nu}{(n+1)b}\right\}^2}$$

$$\Rightarrow bc.u\frac{\partial u}{\partial x} + bc.v\frac{\partial u}{\partial y} = bcU_\infty\frac{\partial U_\infty}{\partial x} + bc.\frac{(n+1)}{2}\frac{\partial^2 u}{\partial y^2} + c\frac{\sigma B_0^2}{\rho}\left(\frac{c}{b}\right)^{n-1}(U_\infty - u)x^{n-1}$$

$$-\frac{\gamma}{2\pi}\frac{\mu_0}{\rho}k(T_c - T_w).\theta\frac{2.\frac{c}{b}.x}{(y+d)^4}\left\{\frac{(n+1)b}{2\nu}\right\}^2$$

$$\Rightarrow u\frac{\partial u}{\partial x} + v\frac{\partial u}{\partial y} = U_\infty\frac{\partial U_\infty}{\partial x} + \frac{n+1}{2}\frac{\partial^2 u}{\partial y^2} - \frac{(n+1)^2}{4}\frac{2\beta\theta x}{(y+d)^4} + M_n.x^{n-1}(U_\infty - u) \tag{8.7}$$

Again, substituting (8.6) into Equation (8.3), one obtains the non-dimensional equations:

$$-cu\frac{\partial\theta}{\partial x}\frac{b}{c}(T_c-T_w)-\sqrt{\frac{2\nu b}{n+1}}\nu\frac{\partial\theta}{\partial y}\sqrt{\frac{(n+1)b}{2\nu}}(T_c-T_w)+$$

$$\frac{\mu_0}{\rho c_p}[T_c-(T_c-T_w)\theta](-k)\left(cu\frac{\partial H}{\partial x}\frac{b}{c}+\sqrt{\frac{2\nu b}{n+1}}\nu\frac{\partial H}{\partial y}\sqrt{\frac{(n+1)b}{2\nu}}\right)=\alpha\frac{\partial^2\theta}{\partial y^2}\frac{(n+1)b}{2\nu}(T_c-T_w)$$

Divided by $b(T_c-T_w)$, we obtain

$$u\frac{\partial\theta}{\partial x}+\nu\frac{\partial\theta}{\partial y}+\frac{k\mu_0}{\rho c_p}[\varepsilon-\theta]\left(u\frac{\partial H}{\partial x}+\nu\frac{\partial H}{\partial y}\right)=\frac{\alpha}{\nu}\frac{\partial^2\theta}{\partial y^2}\frac{(n+1)}{2}$$

$$\Rightarrow\left(u\frac{\partial\theta}{\partial x}+\nu\frac{\partial\theta}{\partial y}\right)+\frac{k\mu_0}{\rho c_p}(\varepsilon-\theta)\left(u\frac{\partial H}{\partial x}+\nu\frac{\partial H}{\partial y}\right)=\frac{1}{\Pr}\frac{n+1}{2}\frac{\partial^2\theta}{\partial y^2} \tag{8.8}$$

in which $\beta=\frac{\gamma}{2\pi}\frac{\mu_0 k(T_c-T_w)\rho}{\mu^2}$ and $\Pr=\frac{\mu c_p}{k}$

Further, by introducing a stream function ψ, where $u=\frac{\partial\psi}{\partial y},v=-\frac{\partial\psi}{\partial x}$, the equations (8.7) and (8.8) take the form

$$\frac{\partial\psi}{\partial y}\frac{\partial^2\psi}{\partial x\partial y}-\frac{\partial\psi}{\partial x}\frac{\partial^2\psi}{\partial^2 y}=U_\infty\frac{\partial U_\infty}{\partial x}+\frac{n+1}{2}\frac{\partial^3\psi}{\partial y^3}+M_n x^{n-1}\left(U_\infty-\frac{\partial\psi}{\partial y}\right)-\frac{(n+1)^2}{4}\frac{2\beta\theta x}{(y+d)^4} \tag{8.9}$$

$$\frac{\partial\psi}{\partial y}\frac{\partial\theta}{\partial x}-\frac{\partial\psi}{\partial x}\frac{\partial\theta}{\partial x}+\frac{k\mu_0}{\rho c_p}(\varepsilon-\theta)\left(\frac{\partial\psi}{\partial y}\frac{\partial H}{\partial x}-\frac{\partial\psi}{\partial x}\frac{\partial H}{\partial y}\right)=\frac{1}{\Pr}\frac{n+1}{2}\frac{\partial^2\theta}{\partial y^2} \tag{8.10}$$

where the dimensionless form of the boundary conditions, expressed in terms of ψ, is obtained as

$$\frac{\partial\psi}{\partial y}=ax^n,\ \frac{\partial\psi}{\partial x}=x^{\frac{n-1}{2}},\ \theta=1\quad at\ \ y=0$$

and $\frac{\partial\psi}{\partial y}=U_\infty=bx^n,\ \ \theta=0\quad as\ \ y\to\infty$. (8.11)

8.4 Lie Group Transformation

Since it is extremely difficult to solve the coupled nonlinear equations (8.9) and (8.10) subject to the boundary conditions (8.11) even numerically, we resort to the application of a novel type of similarity transformation, called the Lie group transformation (alternatively called the scaling group transformation) (cf. Ferdows et al. (2013)) given by

$$\Gamma: x^*=xe^{\varepsilon\alpha_1},\ y^*=ye^{\varepsilon\alpha_2},\ \psi^*=\psi e^{\varepsilon\alpha_3},\ u^*=ue^{\varepsilon\alpha_4},\ v^*=ve^{\varepsilon\alpha_5},\ U_\infty{}^*=U_\infty e^{\varepsilon\alpha_6},$$
$$\theta^*=\theta e^{\varepsilon\alpha_7},\ H^*=He^{\varepsilon\alpha_8} \tag{8.12}$$

Here ε is the group scaling parameter and α_i $(i = 1,2,...,8)$ are arbitrary real numbers. Now we find out the values of α_i such that the form of (8.9)-(8.11) is invariant under the scaling group transformation (8.12). This transformation can be treated as point transformation, which transforms the coordinates $(x, y, \psi, u, v, U_\infty, \theta, H)$ to $(x^*, y^*, \psi^*, u^*, v^*, U_\infty^*, \theta^*, H^*)$

Substituting (8.12) into (8.9) and (8.10), we get

$$e^{\varepsilon(\alpha_1+2\alpha_2-2\alpha_3)}\left(\frac{\partial\psi^*}{\partial y^*}\frac{\partial^2\psi^*}{\partial x^*\partial y^*}-\frac{\partial\psi^*}{\partial x^*}\frac{\partial^2\psi^*}{\partial y^{*2}}\right)=e^{\varepsilon(\alpha_1-2\alpha_6)}U_\infty^*\frac{\partial U_\infty^*}{\partial x^*}+\frac{n+1}{2}e^{\varepsilon(3\alpha_2-\alpha_3)}\frac{\partial^3\psi^*}{\partial y^{*3}}$$

$$+M_n x^{*n-1}e^{\varepsilon(\alpha_1-n\alpha_1-\alpha_6)}U_\infty^*+M_n x^{*n-1}e^{\varepsilon(\alpha_1-n\alpha_1+\alpha_2-\alpha_3)}\frac{\partial\psi^*}{\partial y^*}-\frac{(n+1)^2}{4}\frac{2\beta\theta^* x^*}{\left(y^*+d\right)^4}e^{\varepsilon(4\alpha_2-\alpha_1-\alpha_7)} \quad (8.13)$$

and $e^{\varepsilon(\alpha_1+\alpha_2-\alpha_3-\alpha_7)}\left(\frac{\partial\psi^*}{\partial y^*}\frac{\partial\theta^*}{\partial x^*}-\frac{\partial\psi^*}{\partial x^*}\frac{\partial\theta^*}{\partial y^*}\right)+\frac{k\mu_0}{\rho c_p}e^{\varepsilon(\alpha_1+\alpha_2-\alpha_3-\alpha_8)}\left(\frac{\partial\psi^*}{\partial y^*}\frac{\partial H^*}{\partial x^*}-\frac{\partial\psi^*}{\partial x^*}\frac{\partial H^*}{\partial y^*}\right)$

$$-\frac{k\mu_0}{\rho c_p}\theta^* e^{\varepsilon(\alpha_1+\alpha_2-\alpha_3-\alpha_7-\alpha_8)}\left(\frac{\partial\psi^*}{\partial y^*}\frac{\partial H^*}{\partial x^*}-\frac{\partial\psi^*}{\partial x^*}\frac{\partial H^*}{\partial y^*}\right)=\frac{1}{\Pr}\frac{n+1}{2}\frac{\partial^2\theta^*}{\partial y^{*2}}e^{\varepsilon(2\alpha_2-\alpha_7)} \quad (8.14)$$

The transformed equations (8.13) and (8.14) are invariant under the Lie group of transformation, if the following relations among the transform parameters are satisfied.

$$\alpha_1+2\alpha_2-2\alpha_3=\alpha_1-2\alpha_6=3\alpha_2-\alpha_3=\alpha_1-n\alpha_1-\alpha_6=\alpha_1-n\alpha_1+\alpha_2-\alpha_3=4\alpha_2-\alpha_1-\alpha_7$$

$$\alpha_1+\alpha_2-\alpha_3-\alpha_7=\alpha_1+\alpha_2-\alpha_3-\alpha_8=\alpha_1+\alpha_2-\alpha_3-\alpha_7-\alpha_8=2\alpha_2-\alpha_7 \quad (8.15)$$

By using the equations (8.15) and the boundary conditions we obtain

$$3\alpha_2-\alpha_3=\alpha_1-n\alpha_1+\alpha_2-\alpha_3$$

$$\Rightarrow 2\alpha_2=-(n-1)\alpha_1$$

$$\Rightarrow \alpha_2=-\frac{(n-1)}{2}\alpha_1$$

Again $\alpha_1+2\alpha_2-2\alpha_3=3\alpha_2-\alpha_3$

$$\Rightarrow \alpha_1-\alpha_2=\alpha_3$$

$$\Rightarrow \alpha_3=\alpha_1+\frac{n-1}{2}\alpha_1=\frac{n+1}{2}\alpha_1$$

also from equation (8.15) we have

$$3\alpha_2-\alpha_3=4\alpha_2-\alpha_1-\alpha_7$$

$$\Rightarrow \alpha_7=\alpha_2-\alpha_1+\alpha_3$$

$$\Rightarrow \alpha_7 = \left(-\frac{n-1}{2} - 1 + \frac{n+1}{2}\right)\alpha_1$$

$$\Rightarrow \alpha_7 = \left(\frac{-n+1-2+n+1}{2}\right)\alpha_1 = 0$$

and $\alpha_1 - 2\alpha_6 = \alpha_1 - n\alpha_1 - \alpha_6$

$\Rightarrow \alpha_6 = -n\alpha_1$

from equation (8.15) we have

$\alpha_1 + \alpha_2 - \alpha_3 - \alpha_7 = \alpha_1 + \alpha_2 - \alpha_3 - \alpha_8$

$\Rightarrow -\alpha_3 - \alpha_7 = \alpha_8$

$\Rightarrow -\alpha_3 = \alpha_8$, since $\alpha_7 = 0$.

Finally, using the equations (8.15) and the boundary conditions we obtain

$$\alpha_2 = -\frac{n+1}{2}\alpha_1, \alpha_3 = \frac{n+1}{2}\alpha_1, \alpha_6 = n\alpha_1, \alpha_7 = 0, \alpha_8 = 0, \alpha_4 = n\alpha_1, \alpha_5 = \frac{n-1}{2}\alpha_1 \tag{8.16}$$

If we insert (8.16) into the scaling (8.12), the set of transformations reduces to a one parameter group of transformations given by

$\Gamma: x^* = xe^{\varepsilon\alpha_1}, y^* = ye^{\varepsilon\frac{n-1}{2}\alpha_1}, \psi^* = \psi e^{\varepsilon\frac{n+1}{2}\alpha_1}, u^* = ue^{\varepsilon n\alpha_1}, v^* = ve^{\varepsilon\frac{n-1}{2}\alpha_1}, U_\infty^* = U_\infty e^{\varepsilon n\alpha_1}, \theta^* = \theta$ and

$H^* = H.$ (8.17)

Expanding by Tailor's method and remaining terms up to $O(\varepsilon^2)$ of the one parameter group, we further get

$$x^* - x = x\varepsilon\alpha_1 + o(\varepsilon^2),\ y^* - y = -y\varepsilon\frac{n-1}{2}\alpha_1 + o(\varepsilon^2),\ \psi^* - \psi = \psi\varepsilon\frac{n+1}{2}\alpha_1 + o(\varepsilon^2),$$

$$u^* - u = u\varepsilon n\alpha_1 + o(\varepsilon^2),\ v^* - v = v\varepsilon\frac{n-1}{2}\alpha_1 + o(\varepsilon^2),\ U_\infty^* - U_\infty = U_\infty\varepsilon n\alpha_1,\ \theta^* - \theta = 0$$

and $H^* - H = 0.$ (8.18)

From Eq. (8.18), one can easily deduce the set of transformation in the form of the following characteristic equations:

$$\frac{dx}{x\alpha_1} = \frac{dy}{-\frac{n-1}{2}y\alpha_1} = \frac{d\psi}{\frac{n+1}{2}\psi\alpha_1} = \frac{du}{un\alpha_1} = \frac{dv}{\frac{n-1}{2}v\alpha_1} = \frac{dU_\infty}{nU_\infty\alpha_1} = \frac{d\theta}{0} = \frac{dH}{0} \tag{8.19}$$

Integrating the subsidiary equations

$$\frac{dx}{x\alpha_1} = \frac{dy}{-\frac{n-1}{2}y\alpha_1},$$

we get $yx^{\frac{n-1}{2}} = \text{constant} = \eta$ (say)

From the subsidiary equations

$$\frac{dx}{x\alpha_1} = \frac{d\theta}{0},$$

we get $d\theta = 0$, that is $\theta(\eta) = \text{constant} = \theta$ (say).

Also by integrating the equation $\frac{dx}{x\alpha_1} = \frac{d\psi}{\frac{n+1}{2}\psi\alpha_1}$,

we get $\frac{\psi}{x^{\frac{n+1}{2}}} = \text{constant} = f(\eta)$ (say)

i.e. $\psi = x^{\frac{n+1}{2}} f(\eta)$

Thus the new similarity transformations are obtained as follows:

$$\eta(x,y) = yx^{\frac{n-1}{2}},\ \psi(x,y) = x^{\frac{n+1}{2}} f(\eta),\ \theta = \theta(\eta) \tag{8.20}$$

where ψ is the stream function and η is the dimensionless similarity variable, f is the dimensionless stream function and θ is the dimensionless temperature function. For the velocity field we define the dimensionless stream function $\psi(x,y)$ as

$$u = \frac{\partial\psi}{\partial y},\ v = -\frac{\partial\psi}{\partial x}$$

Now,

$$u = \frac{\partial\psi}{\partial y} = x^{\frac{n+1}{2}} f' x^{\frac{n-1}{2}} = x^n f'$$

$$v = -\frac{\partial\psi}{\partial x} = -\left[\frac{1}{2}x^{\frac{n-1}{2}}\left((n+1)f(\eta) + (n-1)\eta f'(\eta)\right)\right]$$

$$\frac{\partial u}{\partial y} = x^n f'' x^{\frac{n-1}{2}}$$

$$\frac{\partial u}{\partial x} = nx^{n-1} f' + \frac{n-1}{2}\eta f'' x^{n-1}$$

$$\frac{\partial^2 u}{\partial y^2} = x^{2n-1} f'''$$

$$\frac{\partial\theta}{\partial x} = \frac{n-1}{2}\frac{\eta}{x}\theta'$$

$$\frac{\partial \theta}{\partial y} = x^{\frac{n-1}{2}}\theta'$$

$$\frac{\partial^2 \theta}{\partial y^2} = x^{n-1}\theta''$$

Now from the above transformation, equation (8.7) becomes

$$x^n f'\left[nx^{n-1}f' + \frac{n-1}{2}\eta f'' x^{n-1}\right] - \left[\frac{1}{2}x^{\frac{n-1}{2}}\left((n+1)f + (n-1)\eta f'\right)\right]x^n f'' x^{\frac{n-1}{2}} = x^n n x^{n-1}$$
$$+ \frac{n+1}{2}x^{2n-1}f''' + M_n x^{n-1}\left[x^n - x^n f'\right] - \frac{(n+1)^2}{4}\frac{2\beta\theta x}{(\eta+\alpha)^4}x^{2n-2}$$

$$\Rightarrow\ nx^{2n-1}f'^2 + \frac{n-1}{2}\eta x^{2n-1}f'f'' - \frac{(n+1)}{2}x^{2n-1}ff'' - \frac{(n-1)}{2}x^{2n-1}\eta f'f'' = nx^{2n-1}$$
$$+ \frac{n+1}{2}x^{2n-1}f''' + M_n x^{2n-1}\left[1 - f'\right] - \frac{(n+1)^2}{4}\frac{2\beta\theta}{(\eta+\alpha)^4}x^{2n-1}$$

By equating the coefficient of x^{2n-1}, we get

$$f''' + ff'' - \frac{2n}{n+1}(f'^2 - 1) + \frac{2M_n}{n+1}(1 - f') - \frac{n+1}{2}\frac{2\beta\theta}{(\eta+\alpha)^4} = 0 \qquad (8.\ 21)$$

and equation (8.8) becomes,

$$x^n f'\left(\frac{n-1}{2}\frac{\eta}{x}\theta'\right) - \left[\frac{1}{2}x^{\frac{n-1}{2}}\left[\left((n+1)f + (n-1)\eta f'\right)\right]\right]x^{\frac{n-1}{2}}\theta' + \frac{k\mu_0}{\rho c_p}(\varepsilon - \theta)\left[x^n f'.\left(-\frac{\gamma}{2\pi}\right)\frac{2x}{(y+d)^4}\right.$$
$$\left. - \frac{1}{2}x^{\frac{n-1}{2}}\left[\left((n+1)f + (n-1)\eta f'\right)\right]\left(\frac{\gamma}{2\pi}\right)\left(-\frac{1}{(y+d)^3} + \frac{4x^2}{(y+d)^5}\right)\right] = \frac{1}{\mathrm{Pr}}\frac{n+1}{2}x^{2n-1}\theta''$$

By equating the coefficient of x^{n-1}, we get

$$\theta'' - \mathrm{Pr}\left(\frac{2m}{n+1}f'\theta - f\theta'\right) + \frac{2\lambda_a\beta(\varepsilon-\theta)f}{(\eta+\alpha)^3} = 0 \qquad (8.22)$$

The associated boundary conditions are:

$$\begin{aligned} &f = s,\ f' = \lambda,\ \theta = 1 \quad at \quad \eta = 0 \\ &f' \to 1,\ \theta \to 0 \qquad as \quad \eta \to \infty \end{aligned} \qquad (8.23)$$

in which $\beta = \frac{\gamma}{2\pi}\frac{\mu_0 k(T_c - T_w)\rho}{\mu^2}$, $\lambda_a = \frac{\mu^2}{\rho k(T_c - T_w)}$ and $\mathrm{Pr} = \frac{\mu c_p}{k}$

The important physical characteristics skin friction coefficient C_{fx} and the local Nusselt number Nu_x are described as $C_{fx} = \frac{\tau_w}{\frac{1}{2}\rho u_w^2}$ and $Nu_x = \frac{xq_w}{k(T_c - T_w)}$ (8.24)

In Eqn. (8.24), τ_w is the shear stress at wall, while q_w represents the wall heat flux, defined by

$$\tau_w = \mu\left(\frac{\partial u}{\partial y}\right)_{y=0} \text{ and } q_w = -k\left(\frac{\partial T}{\partial y}\right)_{y=0} \tag{8.25}$$

Introducing (8.25) into Eqn. (8.24), the skin friction coefficient and local Nusselt number can be written in dimensionless form as

$$\frac{1}{2}C_{fx}\sqrt{\mathrm{Re}_x} = f''(0) \quad \text{and} \quad Nu_x / \sqrt{\mathrm{Re}_x} = -\theta'(0) \tag{8.26}$$

where $\mathrm{Re}_x = \dfrac{u_w(x)x}{\nu}$ is the local Reynolds number based on the stretching velocity $u_w(x)$.

8.5 Stability Analysis

In this section, we present a stability analysis for the unsteady flow of the biomagnetic fluid, by considering the momentum equation in the form

$$\frac{\partial u}{\partial t} + u\frac{\partial u}{\partial x} + v\frac{\partial u}{\partial y} = U_\infty \frac{\partial U_\infty}{\partial x} + \frac{n+1}{2}\frac{\partial^2 u}{\partial y^2} - \frac{(n+1)^2}{4}\frac{2\beta\theta x}{(y+d)^4} + M_n.x^{n-1}(U_\infty - u) \tag{8.27}$$

where t denotes the time. Here we define another set of dimensionless variables (in tune with equation (8.20)) as

$$\psi = x^{\frac{n+1}{2}} f(\eta,\tau),\ \eta = yx^{\frac{n-1}{2}},\ \tau = tx^{n-1},\ \theta = \theta(\eta,\tau)$$

In terms of these variables, the expression for the axial and transverse velocities read

$$u = x^n \frac{\partial f}{\partial \eta}(\eta,\tau) \text{ and } v = -x^{\frac{n-1}{2}}\frac{n+1}{2}\left[f(\eta,\tau) + \frac{n-1}{n+1}\eta\frac{\partial f}{\partial \eta}(\eta,\tau) - 2\frac{n-1}{n+1}\tau\frac{\partial f}{\partial \eta}(\eta,\tau)\right] \tag{8.28}$$

Substituting the above expression in equation (8.27), we have

$$x^{2n-1}\frac{\partial^2 f}{\partial\eta\partial\tau} + nx^{2n-1}\left(\frac{\partial f}{\partial\eta}\right)^2 + x^{2n-1}\frac{n-1}{2}\eta\frac{\partial f}{\partial\eta}\frac{\partial^2 f}{\partial\eta^2} - x^{2n-1}\left[\frac{n+1}{2}f\frac{\partial^2 f}{\partial\eta^2} + \frac{n+1}{2}\eta\frac{\partial f}{\partial\eta}\frac{\partial^2 f}{\partial\eta^2}\right.$$
$$\left. - (n-1)\tau\frac{\partial f}{\partial\tau}\frac{\partial^2 f}{\partial\eta^2}\right] = nx^{2n-1} + \frac{n+1}{2}x^{2n-1}\frac{\partial^3 f}{\partial\eta^3} + M_n x^{2n-1}\left(1 - \frac{\partial f}{\partial\eta}\right) - \frac{(n+1)^2}{4}\frac{2\beta\theta}{(\eta+\alpha)^4}x^{2n-1}$$

By equating the coefficient of x^{2n-1}, we get

$$\frac{\partial^3 f}{\partial \eta^3} + f\frac{\partial^2 f}{\partial \eta^2} - \frac{2n}{n+1}\left(\frac{\partial f}{\partial \eta}\right)^2 + \frac{2n}{n+1} + \frac{2M_n}{n+1}\left(1 - \frac{\partial f}{\partial \eta}\right) - \frac{n+1}{2}\frac{2\beta\theta}{(\eta+\alpha)^4} - \frac{2}{n+1}\frac{\partial^2 f}{\partial \eta \partial \tau}$$

$$-\frac{2(n-1)}{n+1}\tau\frac{\partial f}{\partial \tau}\frac{\partial^2 f}{\partial \eta^2} = 0, \tag{8.29}$$

The associated boundary conditions are:

$$f(0,\tau) = S,\ \frac{\partial f}{\partial \eta}(0,\tau) = \lambda$$

and $\frac{\partial f}{\partial \eta}(\eta,\tau) \to 0 \quad as \eta \to \infty.$ (8.30)

To test the stability of the steady flow solution $f(\eta) = F(\eta)$ that satisfy the boundary value problem (8.2), we write

$$f(\eta,\tau) = F(\eta) + e^{-\gamma\tau} g(\eta,\tau), \tag{8.31}$$

where γ is an unknown eigenvalue parameter and $g(\eta,\tau)$ is small as compared to $F(\eta)$.

Now we have

$$\frac{\partial f}{\partial \eta} = \frac{\partial F}{\partial \eta} + e^{-\gamma\tau}\frac{\partial g}{\partial \eta}$$

$$\frac{\partial^2 f}{\partial \eta^2} = \frac{\partial^2 F}{\partial \eta^2} + e^{-\gamma\tau}\frac{\partial^2 g}{\partial \eta^2}$$

$$\frac{\partial^3 f}{\partial \eta^3} = \frac{\partial^3 F}{\partial \eta^3} + e^{-\gamma\tau}\frac{\partial^3 g}{\partial \eta^3}$$

$$\frac{\partial^2 f}{\partial \eta \partial \tau} = -\gamma e^{-\gamma\tau}\frac{\partial g}{\partial \eta} + e^{-\gamma\tau}\frac{\partial^2 g}{\partial \eta \partial \tau}$$

$$\frac{\partial f}{\partial \tau} = -\gamma e^{-\gamma\tau} g + e^{-\gamma\tau}\frac{\partial g}{\partial \eta}$$

By substituting the above expression into equation (8.29), we get

$$\left(\frac{\partial^3 F}{\partial \eta^3}+e^{-\gamma\tau}\frac{\partial^3 g}{\partial \eta^3}\right)+\left(F(\eta)+e^{-\gamma\tau}g(\eta,\tau)\right)\left(\frac{\partial^2 F}{\partial \eta^2}+e^{-\gamma\tau}\frac{\partial^2 g}{\partial \eta^2}\right)-\frac{2n}{n+1}\left[\frac{\partial F}{\partial \eta}+e^{-\gamma\tau}\frac{\partial g}{\partial \eta}\right]^2$$
$$+\frac{2n}{n+1}+\frac{2M_n}{n+1}\left(1-\frac{\partial F}{\partial \eta}-e^{-\gamma\tau}\frac{\partial g}{\partial \eta}\right)-\frac{n+1}{2}\frac{2\beta\theta}{(\eta+\alpha)^4}-\frac{2}{n+1}\left(-\gamma e^{-\gamma\tau}\frac{\partial g}{\partial \eta}+e^{-\gamma\tau}\frac{\partial^2 g}{\partial \eta\partial\tau}\right)-$$
$$\frac{2(n-1)}{(n+1)}\tau\left(-\gamma e^{-\gamma\tau}g+e^{-\gamma\tau}\frac{\partial g}{\partial \eta}\right)\left(\frac{\partial^2 F}{\partial \eta^2}+e^{-\gamma\tau}\frac{\partial^2 g}{\partial \eta^2}\right)$$

The linearized problem of the above expression as follow:

$$\frac{\partial^3 g}{\partial \eta^3}+F\frac{\partial^2 g}{\partial \eta^2}+g\frac{\partial^2 F}{\partial \eta^2}-\frac{2n}{n+1}2\frac{\partial g}{\partial \eta}\frac{\partial F}{\partial \eta}-\frac{2M_n}{n+1}\frac{\partial g}{\partial \eta}+\frac{2}{n+1}\gamma\frac{\partial g}{\partial \eta}-\frac{2}{n+1}\frac{\partial^2 g}{\partial \eta\partial\tau}-$$
$$\frac{2(n-1)}{n+1}\tau\left(\frac{\partial^2 g}{\partial \eta\partial\tau}-\gamma g\right)\frac{\partial^2 F}{\partial \eta^2}=0 \qquad (8.32)$$

subject to the boundary conditions:

$$g(0,\tau)=0,\frac{\partial g}{\partial \eta}(0,\tau)=0$$

and $\frac{\partial g}{\partial \eta}(\eta,\tau)\to 0\ as\ \eta\to\infty$ (8.33)

For $\tau=0,$ we have $f(\eta)=F(\eta),$ we have the case of steady flow of the fluid characterized by equation (8.21), while $g(\eta)=g_0(\eta)$ in (8.32) characterizes the initial growth or decay of the solution (8.31). To test our numerical procedure, the following linear eigenvalue problem corresponding to the steady state problem:

$$g_0'''+Fg_0''+g_0F''-\frac{4n}{n+1}F'g_0'-\frac{2M_n}{n+1}g_0'+\frac{2}{n+1}\gamma g_0'=0 \qquad (8.34)$$

along with the conditions:

$$g_0(0)=0,\ g_0'(0)=0$$

and $g_0'(\eta)\to 0 \quad as \quad \eta\to\infty.$ (8.35)

The smallest eigenvalue γ will determine the stability of the corresponding steady flow solution $F(\eta)$ for all the parameters involved.

8.6 Numerical Method

Now we solve the set of nonlinear ordinary differential equations (8.21) and (8.22) with boundary conditions (8.23) numerically by using bvp4c function technique in MATLAB package. We consider $f = y_1, f' = y_2, f'' = y_3, \theta = y_4, \theta' = y_5$. Then the equations (8.7) and (8.8) are transformed into a system of first order ordinary differential equations as given below.

$$\left.\begin{aligned} f' &= y_2 \\ f'' &= y_2' = y_3 \\ f''' = y_3' &= -y_1 y_3 + \frac{2n}{n+1}(y_2^2 - 1) - \frac{2M_n}{n+1}(1 - y_2) + \frac{n+1}{2}\frac{2\beta y_4}{(\eta+\alpha)^4} \\ \theta' &= y_5 \\ \theta'' = y_5' &= -\Pr y_1 y_5 + \frac{2m}{n+1}\Pr y_2 y_4 - \frac{2\lambda_a \beta(\varepsilon - y_4) y_1}{(\eta+\alpha)^3} \end{aligned}\right\} \tag{8.36}$$

along with the initial boundary conditions:

$$y_1(0) = S,\ y_2(0) = \lambda,\ y_4(0) = 1,\ y_2(\infty) = 1,\ y_4(\infty) = 0. \tag{8.37}$$

Equations (8.36) and (8.37) are integrated numerically as an initial value problem to a given terminal point. All these simplifications are made by using bvp4c function available in MATLAB software.

8.7 Results and Discussion

The nonlinear ordinary differential equations (8.21) and (8.22) with boundary conditions (8.23), can be solved numerically using the bvp4c programme in MATLAB software. To have an insight of the flow physics, we have carried out numerical computation of various physical quantities, such as velocity, temperature, skin friction etc. Variations of the physical quantities with change in different parameters have been presented graphically/in tabular form. In order to establish the validity and accuracy of the method, we have computed the

skin friction coefficient for steady flow with $\beta = 0,\ S = 0, M_n = 0,\ n = 1$ and compared with those reported by Naganthran et al. (2016) in table 8.1. This table shows very clearly that our results are in good agreement with those of Naganthran et al. (2016). This observation serves as a confirmation of the accuracy of the results that are reported in this communication.

Table 8.1: Comparison of skin friction coefficient for different values of λ

λ	Present		Naganthran et al. (2016)	
	First solution	Second solution	First solution	Second solution
-0.25	1.40224		1.402240	
-0.5	1.49567		1.495669	
-0.75	1.48929		1.489298	
-1.0	1.32882	0.00126	1.328816	0
-1.15	1.08225	0.11576	1.082231	0.116702
-1.2	0.93253	0.23286	0.932473	0.233649

While carrying out numerical computations, we observe that dual solutions exist for a certain range of stretching/shrinking of the sheet and suction parameter. Since the dual solutions exist, we need to ascertain which solution is physically meaningful. With this end in view, we have performed stability analysis. For the sake of brevity, the details of the stability analysis are not being presented here. However, on the basis of the stability test, we find that one set of solutions is stable and physically realizable, while the other solution set is not so.

Figs. 8.2-8.7 depict the existence of dual solutions for skin friction $f''(0)$ and wall heat transfer gradient $\theta'(0)$ for different values of the stretching/shrinking parameter and the suction parameter, when the value of ferromagnetic parameter and nonlinear stretching parameter changes.

The graphs presented in Figs. 8.2 and 8.3 have been plotted by considering different values of the ferromagnetic parameter and so they clearly depict the ferromagnetic effect of the fluid. It is interesting to note that there exist two solution branches. The first branch

represents the stable solution, while the second branch denotes the unstable solution for each value of λ corresponding to a given value of β.

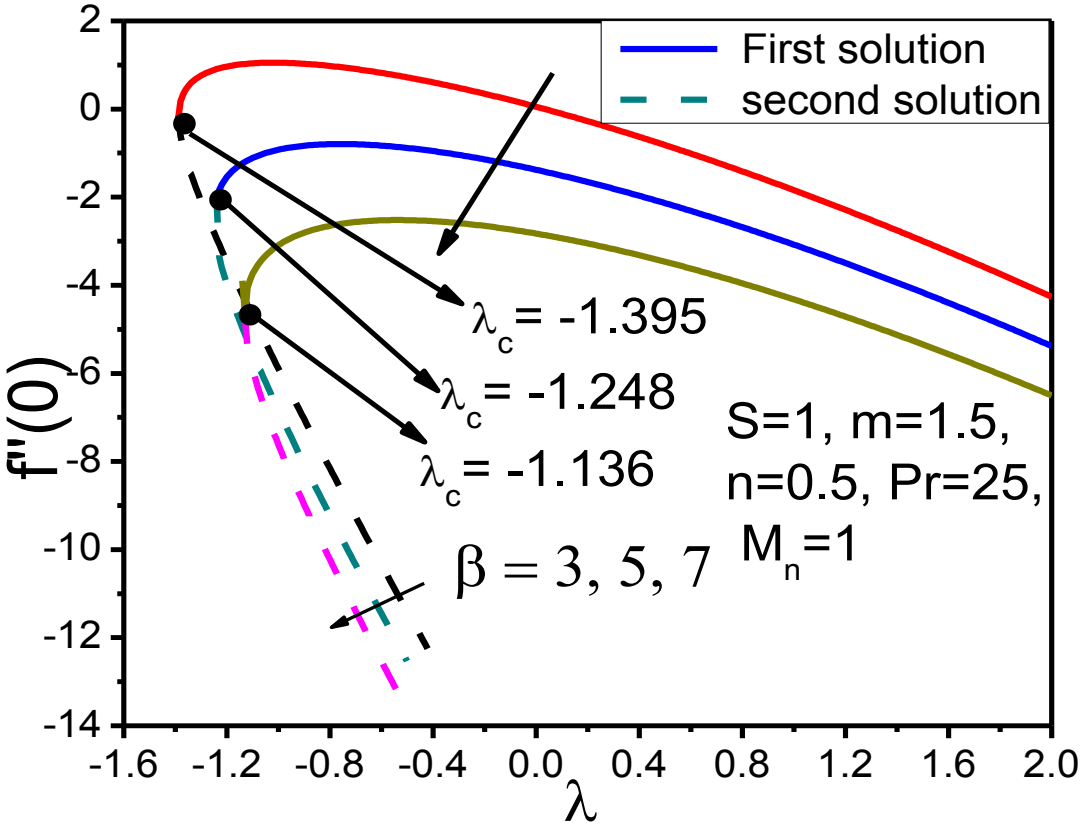

Fig. 8.2. Variation of skin friction coefficient with λ for various values of β

From Fig. 8.2, we observe that unique solution exists for $\lambda > -0.2$ or $\lambda > -0.3$ or $\lambda > -0.4$ when $\beta = 3,5,7$ respectively, while dual solutions exist when $-1.395 < \lambda < -0.4$ for $\beta = 7$, when $-1.248 < \lambda < -0.3$ for $\beta = 5$ and when $-1.136 < \lambda < -0.2$ for $\beta = 3$. Also no solution exists when $\lambda < \lambda_c$, where $\lambda_c = -1.136, -1.248, -1.395$ for $\beta = 3,5,7$. respectively, λ_c being the critical value of λ, at which the two solution branches meet each other and thus a unique solution is obtained.

Variation of wall heat transfer rate $\theta'(0)$ with stretching parameter for various values of the ferromagnetic parameter are shown in Fig. 8.3. From this figure, it can be seen that the solution is unique when $\lambda = \lambda_c$, while dual solutions exist when $\lambda_c < \lambda < 0.5$ and no solutions exist, when $\lambda < \lambda_c$, where λ_c is the critical value of λ and the value of $\lambda_c = -1.392, -1.235, -1.144$ with specific values of $\beta = 3,5,7$.

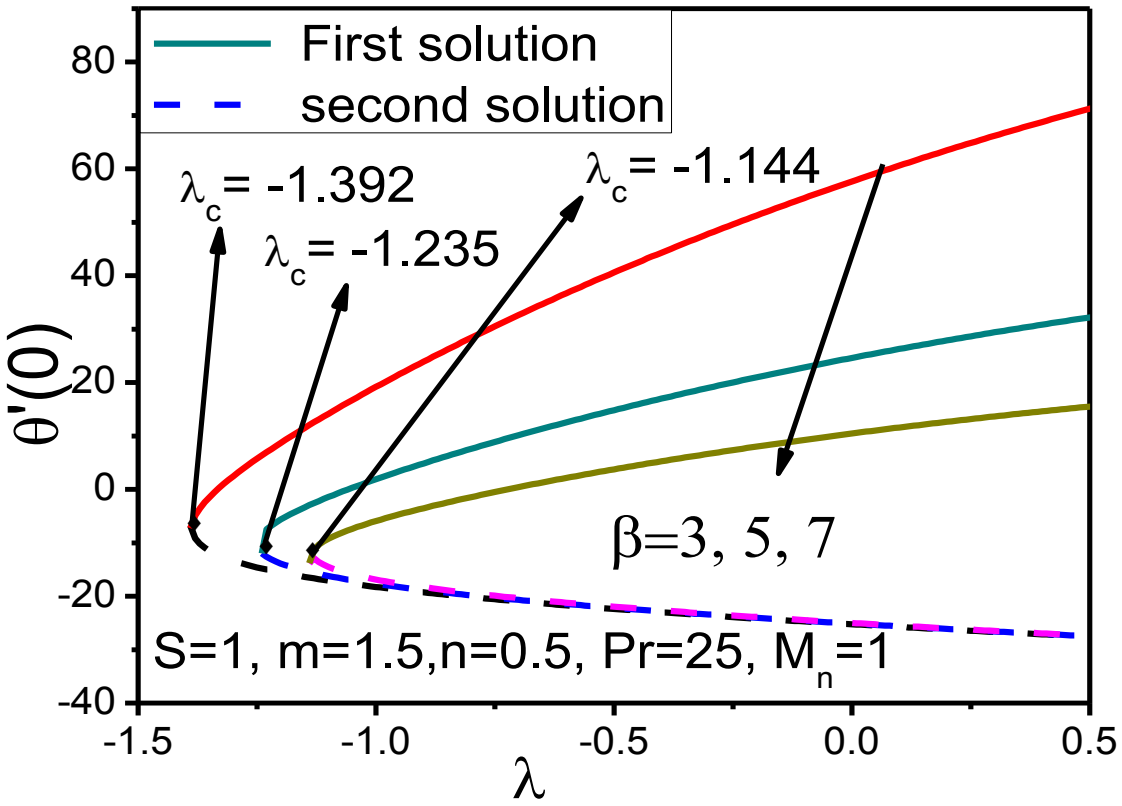

Fig. 8.3. Variation of heat transfer rate with λ for different values of β

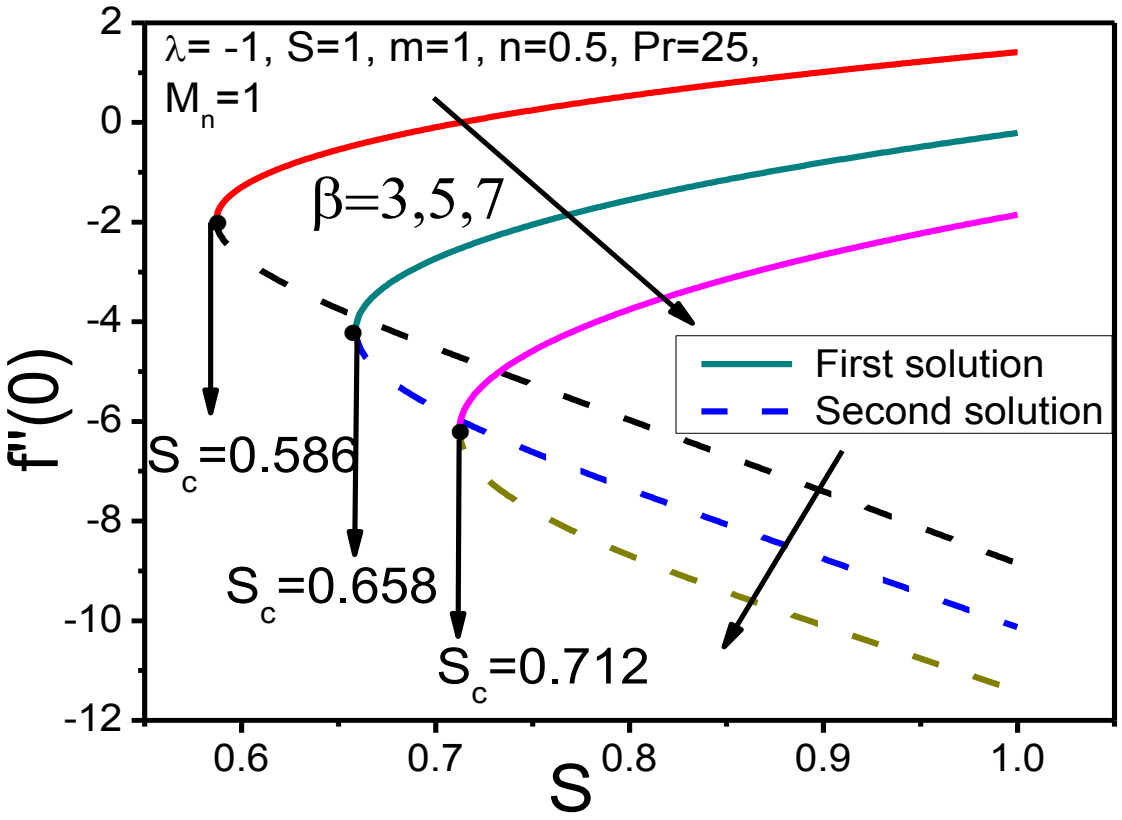

Fig. 8.4. Variation of skin friction coefficient with S for various values of β

From this figure we also observe that the critical value λ_c decreases, as the value of the ferromagnetic parameter increases and that of the skin friction coefficient decreases. One way further observe that the effect of the ferromagnetic parameter diminishes in the range of λ for which the solution exists.

The variations of the skin friction coefficient $f''(0)$ and the local Nusselt number $\theta'(0)$ with suction parameter for different values of the ferromagnetic parameter are shown in Figs. 8.4 and 8.5 respectively. From these figures, it reveals that the solution is unique when $S = S_c$, while dual solution exists up to $S_c < S < 1$ and no solutions for $S < S_c$. One way further note that as the ferromagnetic parameter increases, both the skin friction coefficient and the heat transfer rate at the wall surface decrease.

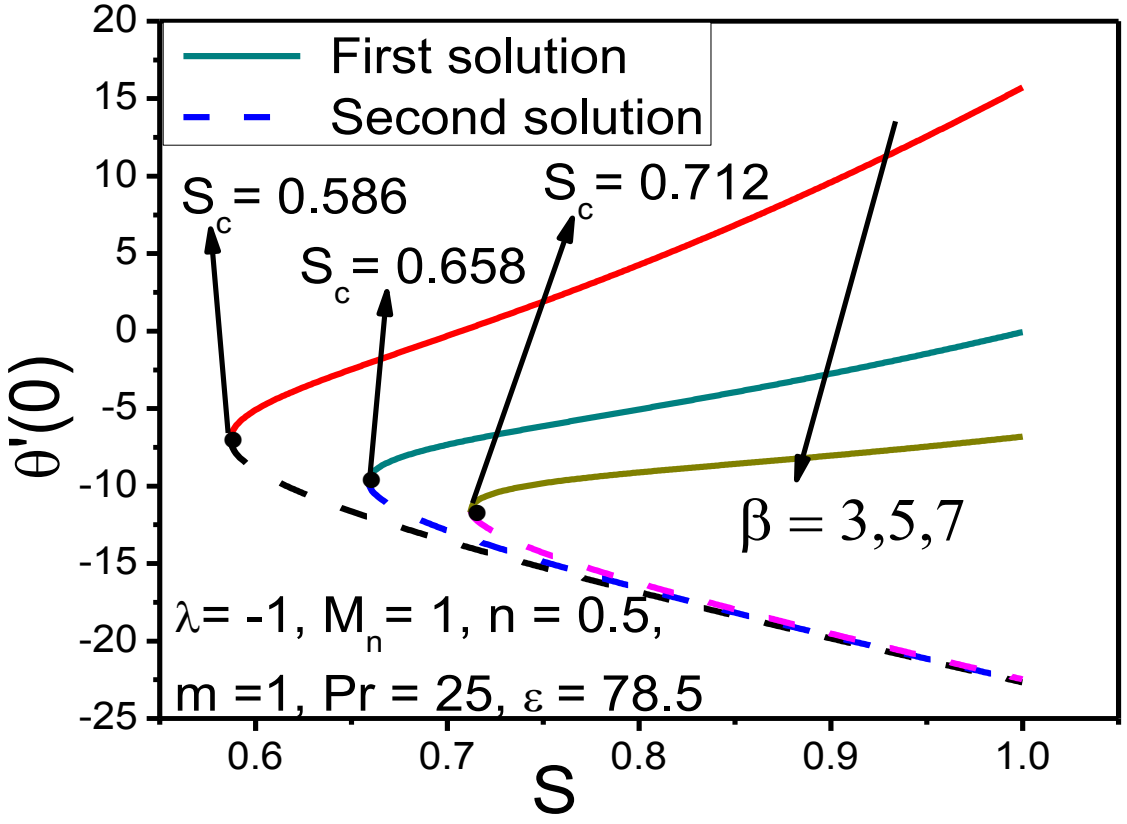

Fig. 8.5. Variation of heat transfer rate with S for various values of β

Figs. 8.6 and 8.7 depict the variation of the skin friction coefficient $f''(0)$ and heat transfer rate $\theta'(0)$ with the stretching/shrinking parameter λ, for different values of nonlinear stretching parameter n. We also note that dual solution exists for a specific range of values of

the nonlinear stretching parameter. The aforesaid observations may be summarized as follows:

(i) For $\lambda_c < \lambda < 0$, dual solutions exist.

(ii) When $\lambda = \lambda_c$, the solution exists and is unique.

(iii) For $\lambda < \lambda_c$, no solution exists.

(iv) With an increase in n, there is a reduction in the skin friction coefficient and the heat transfer rate.

(v) As the nonlinear stretching parameter n increases, the range of similarity solution and that of the existence of dual solutions are both enlarged.

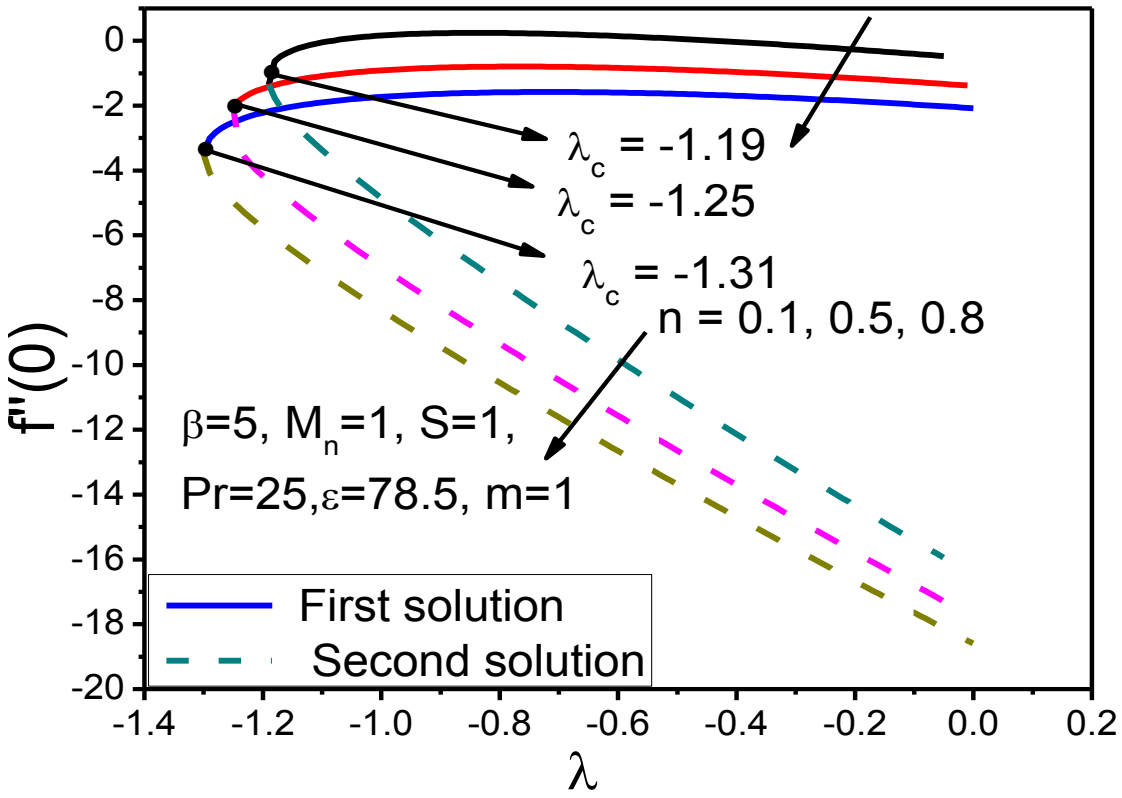

Fig. 8.6 Change in skin friction coefficient for different values of n and λ_c

The effects of ferromagnetic parameter β on velocity and temperature distribution are shown in Figs. 8.8 and 8.9. These figures reveal that although the biomagnetic fluid velocity is enhanced as the ferromagnetic parameter increases for both cases (first and second solution), the fluid temperature is diminished, as the value of β rises. This reduction in fluid temperature may be attributed to be due to the influence of the external magnetic field.

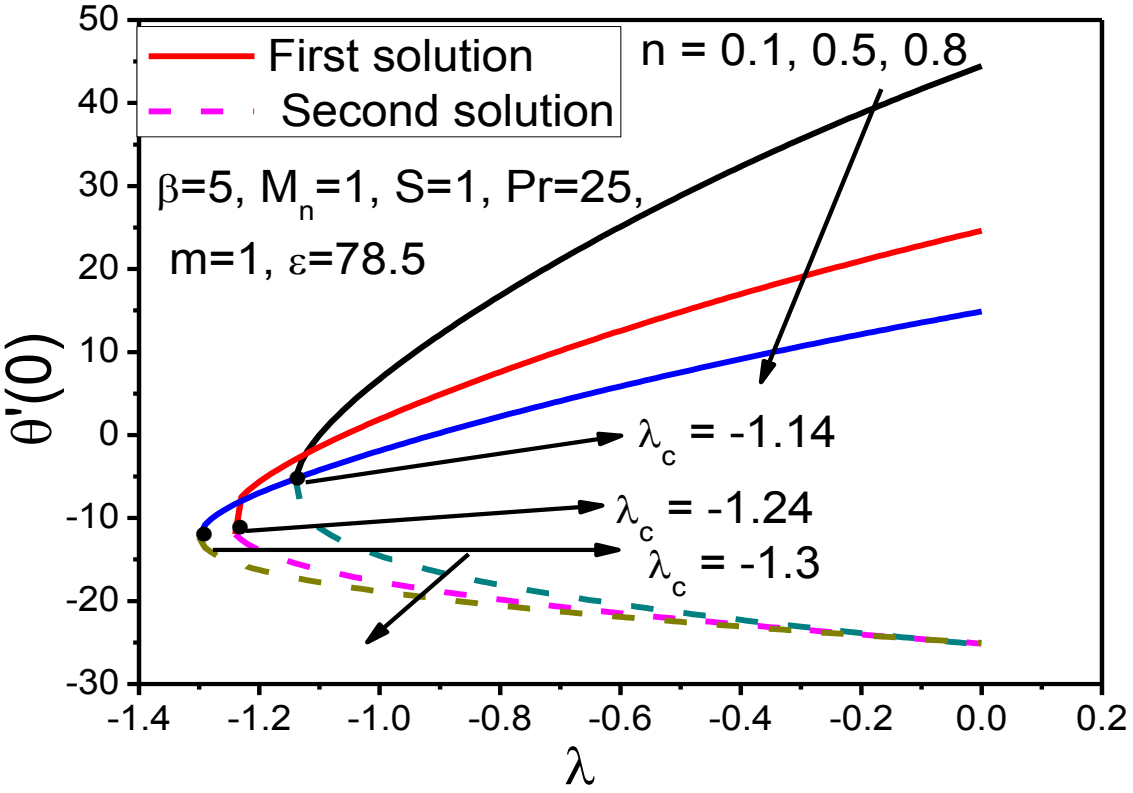

Fig. 8.7 Change in heat transfer rate for different values of n and λ_c

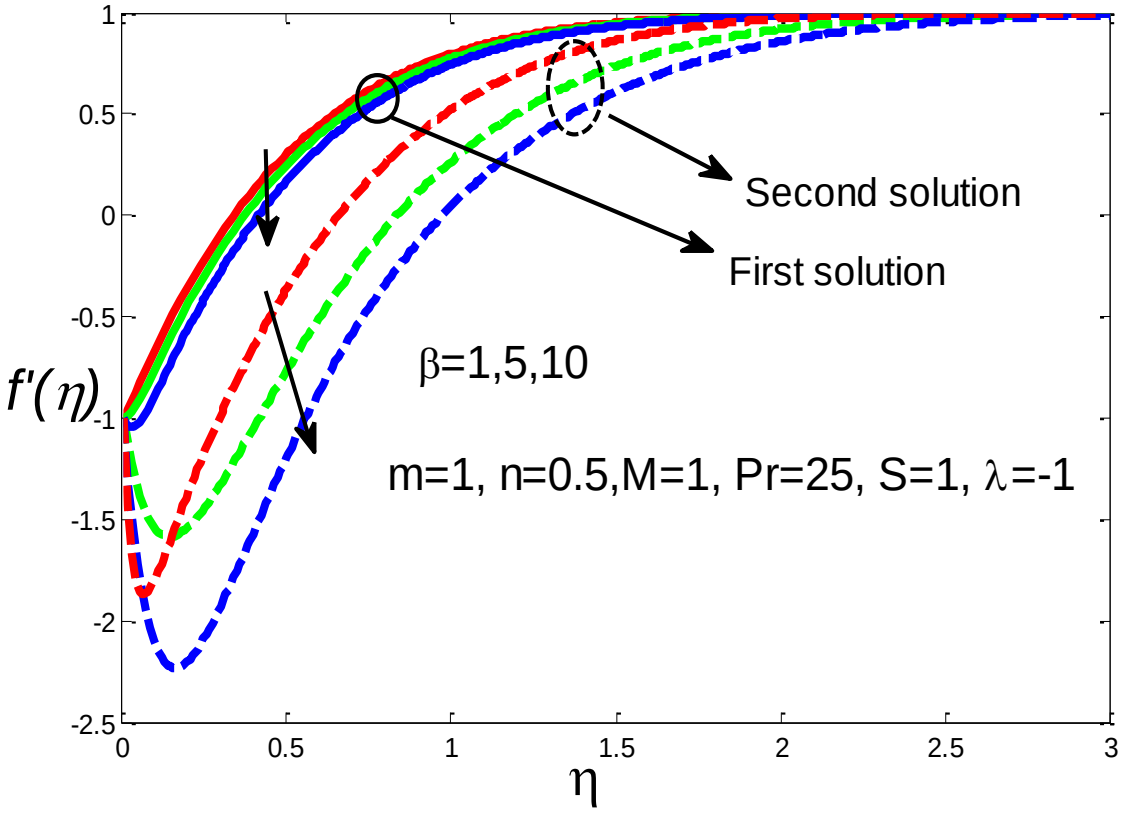

Fig. 8.8 Velocity profiles, $f'(\eta)$ for different values of β

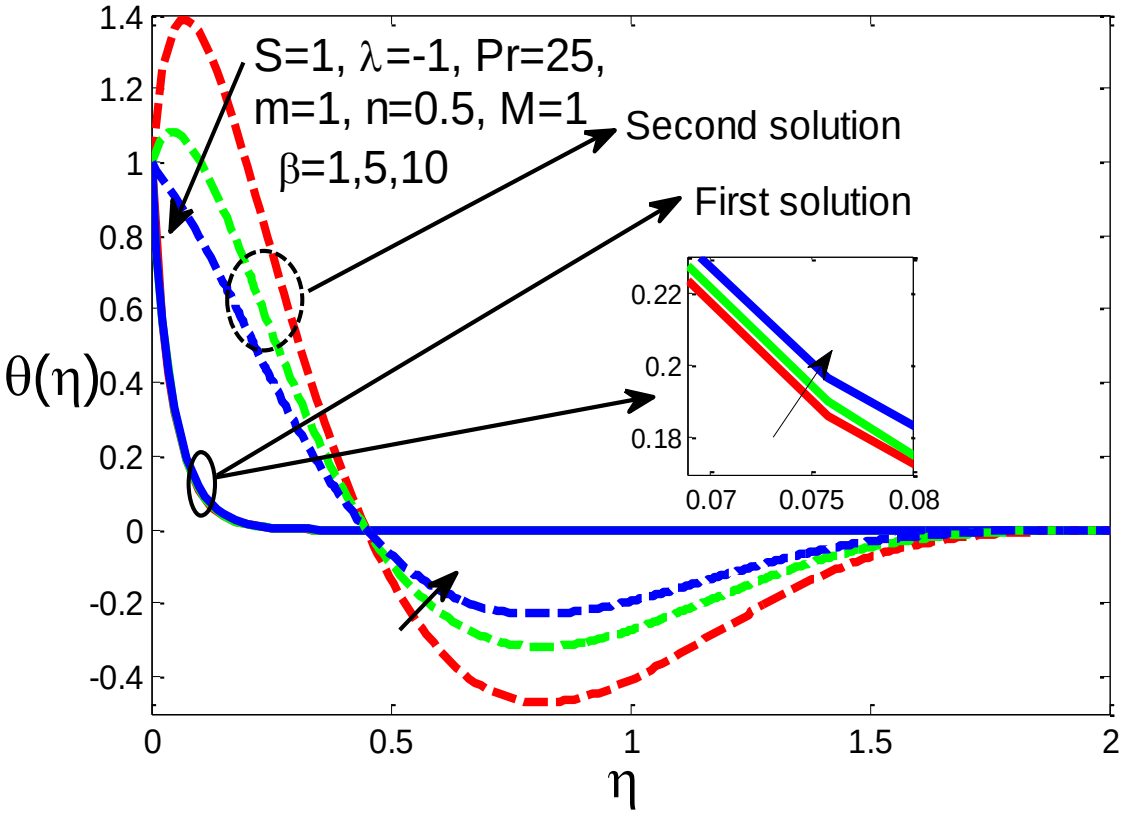

Fig. 8.9 Temperature profiles, $\theta(\eta)$ for different values of β

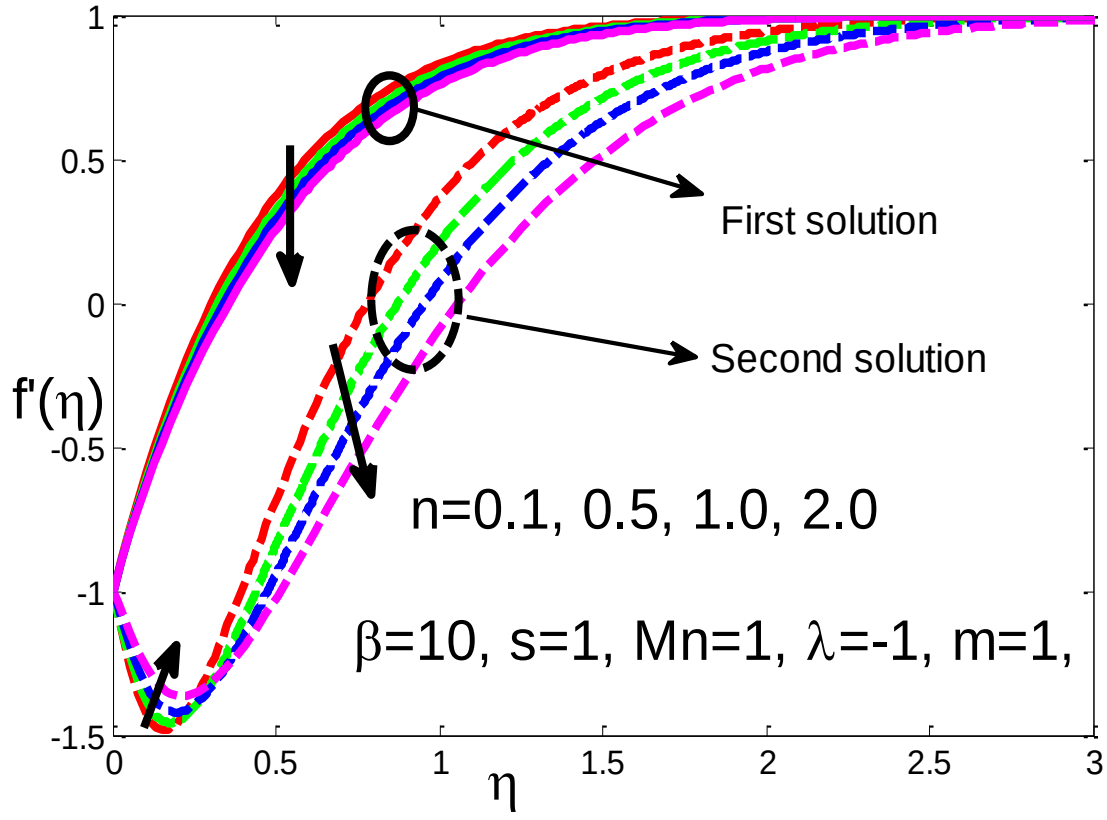

Fig. 8.10. Velocity profiles, $f'(\eta)$ for different values of n

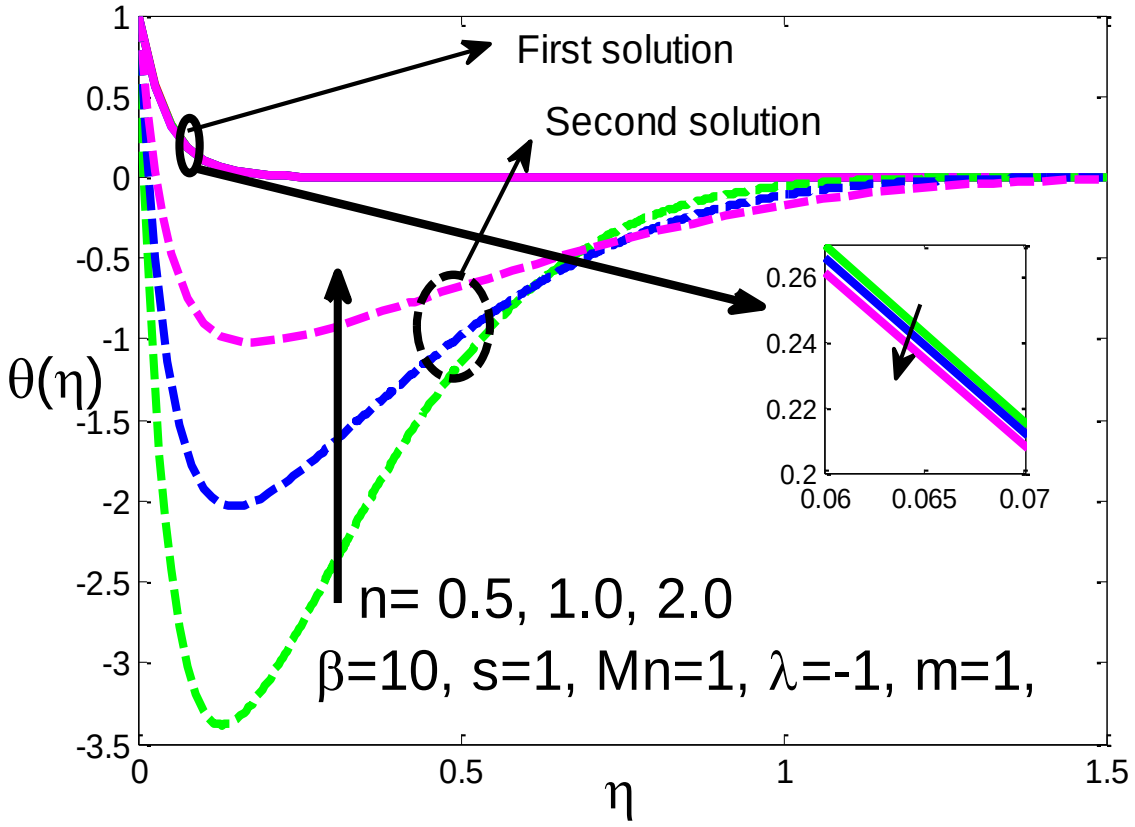

Fig. 8.11. Temperature profiles, $\theta(\eta)$ for different values of n

Figs. 8.10 and 8.11 show that the effect of nonlinear stretching parameter (n) on the velocity and temperature distributions for a particular situation, when $\beta = 10,\ S = 1,\ M_n = 1,\ \lambda = 1,\ m = 1$. Figure 8.10 indicates that the velocity of the biomagnetic fluid is significantly reduced throughout the flow field as n is increased, in the case of the first solution. This signifies that the momentum boundary layer thickness becomes thinner with a rise in the value of the parameter n. But the result is to the contrary in the case of the second solution, except at points very close to the sheet. Fig. 8.11 shows that temperature reduces with increase in n, in the case of the first solution, while for the second solution, a reverse trend is observed.

The effect of suction parameter S on velocity and temperature distributions can be found from Figs. 8.12 and 8.13. According to the first solution (cf. Fig. 8.12), the fluid velocity increases, as the suction velocity enhances, while a reverse trend is observed in the case of the second solution. This can be interpreted physically by saying that since during suction, the fluid in the vicinity of the wall is sucked away, the boundary layer thickness is reduced due to suction and thereby the fluid velocity is enhanced. Fig. 8.13 demonstrates that the fluid temperature is reduced as the quantum of suction increases. This implies that the

thermal boundary layer thickness decreases with as suction proceeds. This causes an increase in the rate of heat transfer. However, this is the observation from the first solution. A reverse trend is found to occur, if we consider the second solution. This observation implies that as the fluid is brought closer to the surface, the thermal boundary layer thickness diminishes.

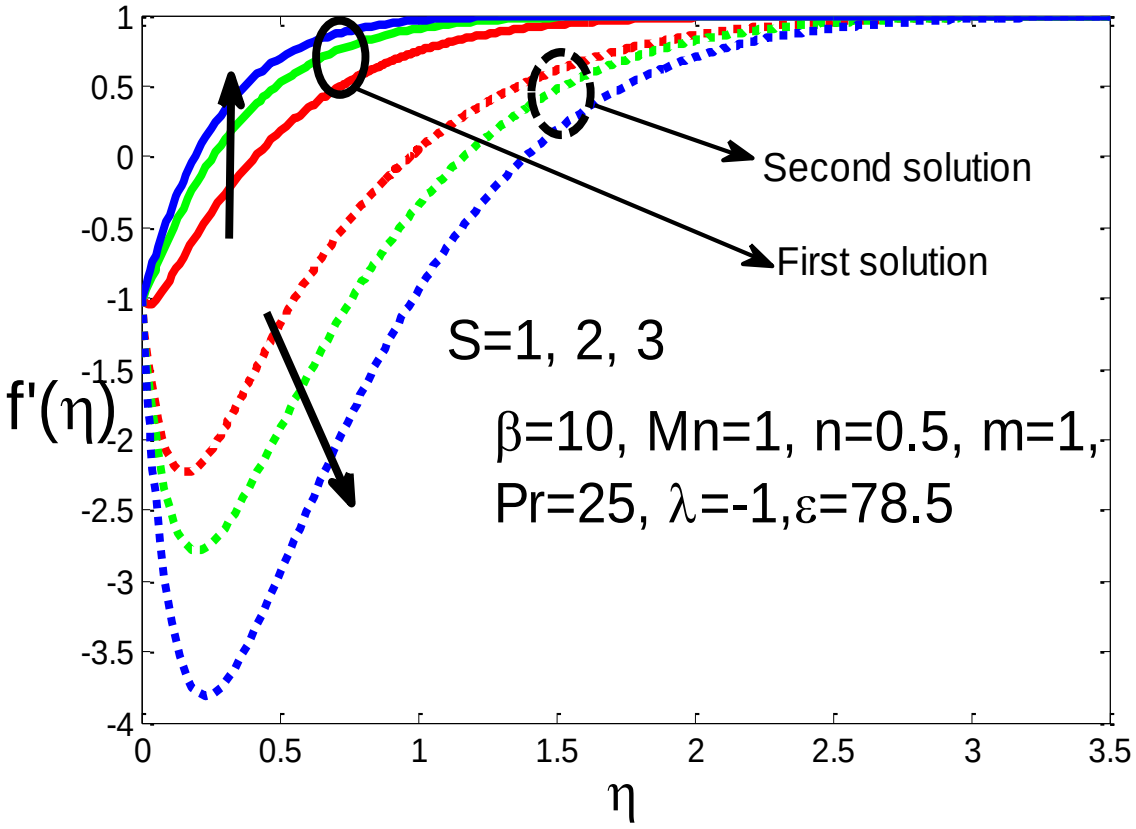

Fig. 8.12. Velocity distribution for different values of S

The impact of temperature exponent (m) on velocity and temperature distributions are displayed in Figs. 8.14 and 8.15, respectively. The dual velocity and temperature distributions are also presented in the same figures, alongside the first solutions. It may be noted that in the case of the first solution, as m increases the velocity decreases. But a reverse trend is observed in the case of the second solution. The results imply that increase in the fluid index is accompanied by a reduction in temperature boundary layer thickness also. These are the observations, when we consider the first solution. But for the second solution, the observations are a bit different. Also, the temperature exponent (m) parameter enhances the thermal overshoot near the sheet for the second solution.

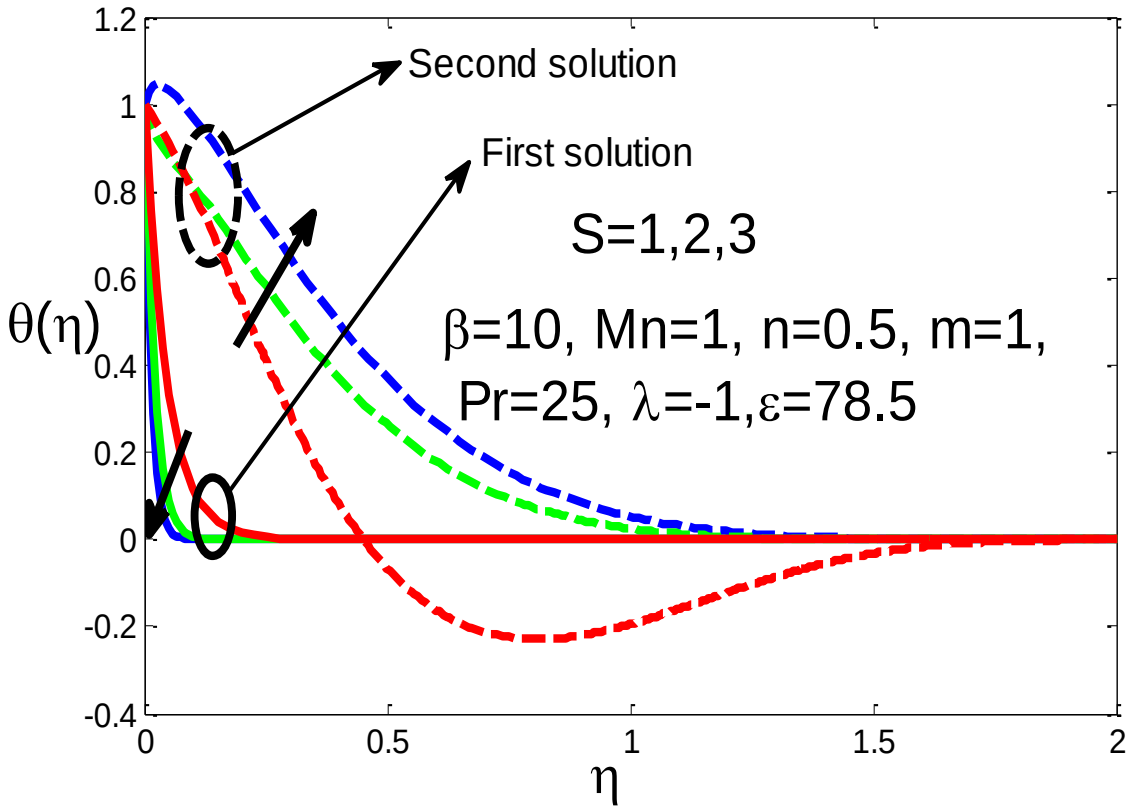

Fig. 8.13. Temperature distributions for different values of S

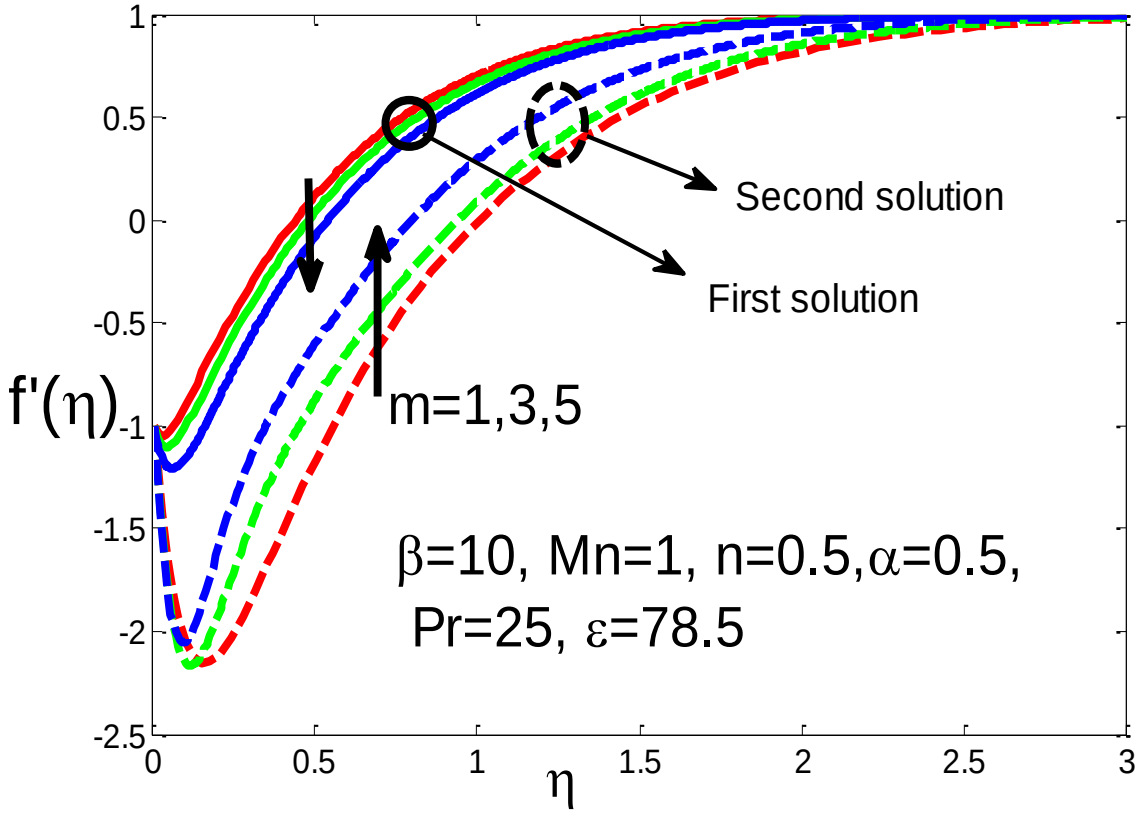

Fig. 8.14 Velocity profiles, $f'(\eta)$ for different values of m

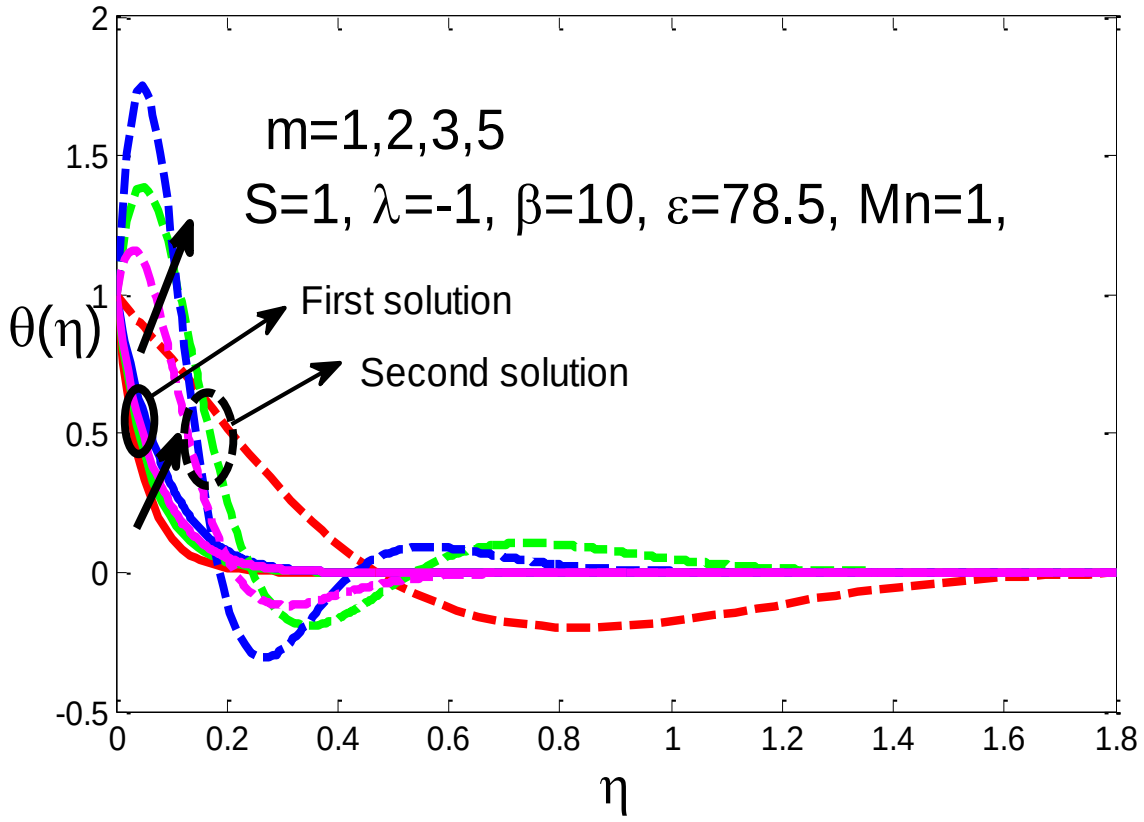

Fig. 8.15 Temperature profiles, $\theta(\eta)$ for different values of m

8.8 Summary of the chapter

This chapter is devoted to a theoretical study on the flow of a biomagnetic fluid, by using Lie group transformation method. The flow is considered to take place over a stretching/shrinking sheet, under the influence of a magnetic field generated owing to the presence of a magnetic dipole. The study has been conducted under the purview of Biomagnetic Fluid Dynamics (BFD). Similarity solutions have been obtained for BFD boundary layer equations. The invariants and symmetries of equations were obtained for the determination of the similarity variables. This process could bring about a reduction in the number of independent variables. Stability analysis has been duly carried out. The resulting differential equation was then solved subject to appropriate boundary conditions by using bvp4c function available in the Matlab software. Adequate discussion has been made in respect of the dual solutions. The associated heat transfer has also been studied. On the basis of the computational results, we can draw the following conclusions:

(i) Dual solutions exist for some specific range of values of the suction parameter and stretching/shrinking parameters.

(ii) The stability analysis emphasizes the existence of dual solutions, one of them being

stable and can be realized physically. But the second solution is not so.

(iii) The ferromagnetic parameter has a dominating control over the flow of the biomagnetic fluid and heat transfer.

(iv) As the ferromagnetic effect increases, the velocity, temperature and thermal boundary layer thickness are reduced.

(v) The skin friction coefficient fluid temperature increase as suction rate increases.

(vi) With an increase in nonlinear stretching, the heat transfer rate and skin friction are both diminished.

(vii) The range of similarity solution and that for the existence of dual solutions are enlarged, as the (nonlinear) stretching increases.

Chapter 9

Dual solutions in boundary layer flow and heat transfer of biomagnetic fluid over a stretching/shrinking sheet in the presence of a magnetic dipole and prescribed heat flux

This chapter analyzes the steady boundary layer flow and heat transfer of biomagnetic fluid over a stretching/shrinking sheet with prescribed surface heat flux under the influence of a magnetic dipole. The governing equations are transformed into a set of ordinary differential equations (ODEs) by using similarity transformations. Numerical results are obtained using the boundary value problem solver bvp4c of MATLAB. The effect of various physical parameters on the velocity and temperature profiles as well as skin friction coefficient are discussed. Dual solutions exist for certain values of stretching/shrinking sheet and suction parameters. Stability analysis is performed to determine which solution is stable and physically valid. Results from the stability analysis depict that the first solution (upper branch) is stable and physically realizable, while the second solution (lower branch) is unstable, Murtaza et al. (2018).

9.1 Introduction

Biomagnetic fluid dynamics (BFD) is a relatively new research area in fluid mechanics which is the study of the interaction of biological/physiological fluids in the presence of magnetic field. The investigation of biomagnetic fluid has been increasing due to its numerous potential applications in bioengineering and medical sciences. Among them are magnetic devices development for cell separation, high-gradient magnetic separation, reducing bleeding during surgeries, targeted transport of drugs using magnetic particles as drug carries, Magnetic Resonance imaging for imaging technique of a specific part of a body using strong magnetic fields and treatment of cancer tumor causing magnetic hyperthermia

by Haik et al. (1999), Ruesetski and Ruuge (1993), Lauva and Plavins (1993), Pulfer and Gallo (2000).

Biomagnetic fluid dynamics model which is conformed to the principles of FHD has been developed first by Haik et al. (1996). Recently, an extended biofluid dynamics (BFD) mathematical model, which includes the initial BFD model of Haik et al. (1996) was developed by Tzirtzilakis (2005). According to this model, the biofluid flow under the influence of an applied magnetic field is consistent with the principles of Ferrohydrodynamics (FHD) and the Magnetohydrodynamics (MHD). Tzirtzilakis and Kafoussias (2003) analyzed the mathematical model of the flow of a heated ferrofluid over a linearly stretching sheet under the action of a magnetic field which is generated by a magnetic dipole. Tzirtzilakis and Tanoudis (2003) presented a numerical method for the study of laminar incompressible two dimensional biofluid over a stretching sheet with heat transfer. Further Misra and Shit (2009) investigated the flow of a biomagnetic viscoelastic fluids in different situations and they indicated that the presence of an external magnetic field influences the flow of biomagnetic fluid quite appreciably. The problem of biomagnetic fluid flow under the influence of a spatially varying magnetic field was studied also by Nor Amirah Idris et al. (2014).

Recently, Murtaza et al. (2017) investigated the combined effect of electrical conductivity and magnetization on biomagnetic fluid over a stretching sheet. Reddy et al. (2018) analyzed the magnetohydrodynamic flow of blood in a permeable inclined stretching surface in the presence of an external magnetic field with heat and mass transfer. Siddiqa et al. (2018) investigated the effect of thermal radiation and magnetic field on the two dimensional biomagnetic fluid. This study is conducted to determine the behavior of blood flow and heat transfer in the presence of magnetic field combined with thermal radiation effects. Sushma et al. (2018) studied the slip flow effect of MHD blood flow in the presence of heat source/sink and chemical reaction and reported that the blood velocity near the wall is decreased as the slip parameter is increased.

Most of the researchers reported the existence of the dual solutions of their study. Some of them have also presented stability analysis. Stability analysis is performed to determine which solution is stable and physically realistic and which is not. Mukhopadhyay (2011) analyzed prescribed surface temperature and reported the dual solutions exist. Naganthran et al. (2016) studied the flow and heat transfer of a third grade fluid and proved the presence of dual solutions for the flow field. Krishna et al. (2016) reported the dual solutions existence for the unsteady flow with inclined stretching sheet. Naganthran and Nazar (2017) studied the

MHD Stagnation-point Flow and Heat Transfer over a Stretching/Shrinking Sheet and found dual solutions existence. Hafidzuddin et al. (2016) reported the dual solutions existence for the boundary layer flow and heat transfer with slip velocity over an exponentially stretching/shrinking sheet. It is worth mentioning that the stable and unstable solution (dual solutions) and stability analysis are also found in the papers of Ghosh et al. (2016), Yasin et al. (2016), Awaludin (2016), Mishra and Singh (2014) and Bhattacharyya (2011).

The study of MHD flow over a stretching sheet still constitutes a topic of current ongoing research. The two-dimensional MHD flow of a viscous nanofluid over a nonlinear stretching surface with the slip effects of the velocity, the temperature and the concentration was studied by Hayat et al. (2015). Das et al. (2015) studied the unsteady MHD flow of nanofluids over an accelerating, convectively heated stretching sheet, in the presence of a transverse magnetic field with heat source/sink. The MHD stretching sheet flow was also investigated in three-dimensions considering velocity and thermal slip boundary conditions by Hayet et al. (2015) or in two dimensions considering the effects of the induced magnetic field by Ali et al. (2011).

The aim of the present study is to investigate the effects of the magnetic parameter and suction parameter on the flow and heat transfer of the biomagnetic fluid over a stretching/shrinking sheet with prescribe heat flux. The computational results have been obtained using the built-in bvp4c function in MATLAB. The study reveals that there exist dual solutions for some specific values of suction parameter, stretching parameter and ferromagnetic parameter. Stability analysis has also been carried out that determine which solution is stable and physically realistic. The validity of the numerical results presented, has also been established.

9.2 Mathematical Formulation

Consider the two-dimensional incompressible boundary layer flow and heat transfer of a biomagnetic fluid over a stretching/shrinking sheet as illustrated in Fig. 9.1, where x *and* y are Cartesian coordinates measured along the sheet and normal to it. It is assumed that the free stream velocity is $U_\infty(x) = bx$ and the sheet is stretched or shrunk with the velocity $U_w(x) = ax,$ where $a > 0$ implies the stretching situation and $a < 0$ indicates the shrinking condition and b as a positive constant. A magnetic dipole is located below the sheet, at a distance d, i.e. at the point $(0, d), d < 0,$ giving rise to a magnetic field of magnetic field

strength intensity H. Moreover, we assumed that temperature of the sheet is $T_w(x)$ while the temperature of the ambient far from the surface of the sheet is $T_c(x)$ where $T_c(x) > T_w(x)$.

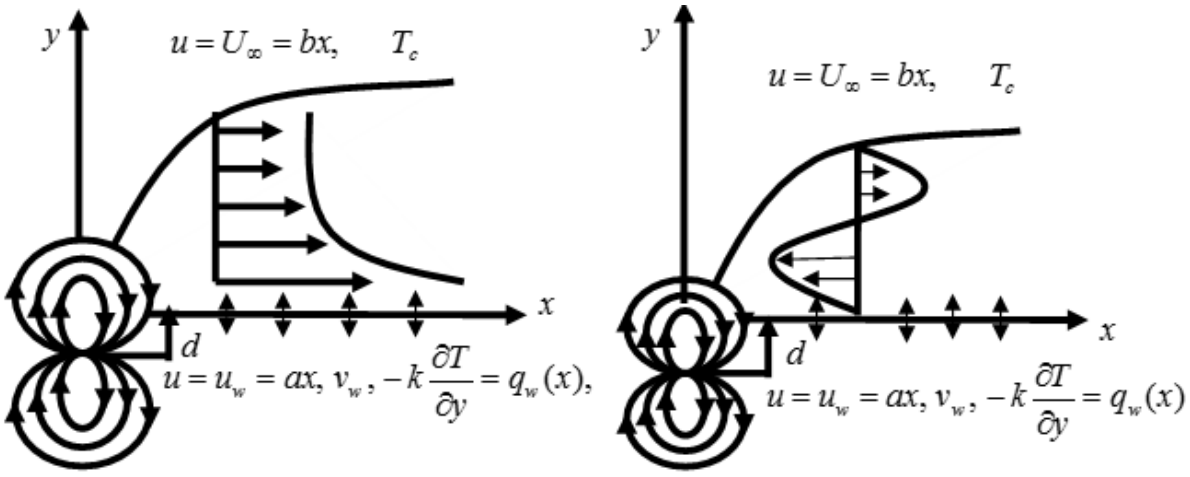

Stretching sheet Shrinking sheet

Fig 9.1. The geometry of the problem.

Under the boundary layer approximation the governing equation for the problem can be written as indicated in the studies of Tzirtzilakis and Kafoussias (2003), Murtaza et al.(2017), Naganthran et al. (2016) and Majeed et al. (2016),

$$\frac{\partial u}{\partial x} + \frac{\partial v}{\partial y} = 0 \tag{9.1}$$

$$u\frac{\partial u}{\partial x} + v\frac{\partial u}{\partial y} = U_\infty \frac{\partial U_\infty}{\partial x} + \nu\frac{\partial^2 u}{\partial y^2} + \frac{\mu_0}{\rho} M \frac{\partial H}{\partial x} \tag{9.2}$$

$$\rho C_p\left(u\frac{\partial T}{\partial x} + v\frac{\partial T}{\partial y}\right) + \mu_0 T\frac{\partial M}{\partial T}\left(u\frac{\partial H}{\partial x} + v\frac{\partial H}{\partial y}\right) = k\frac{\partial^2 T}{\partial y^2} \tag{9.3}$$

subject to the boundary conditions, Majeed et al. (2016)

$$u = U_w(x) = ax,\ v_w(x) = v_w, -k\frac{\partial T}{\partial y} = q_w(x) = T_c - Dx \quad at\ y = 0$$

$$u = U_\infty(x) = bx, T \to T_c \quad as\ y \to \infty. \tag{9.4}$$

where u and v are the velocity components along the x- and y-axes, respectively, ρ is the fluid density, k is the thermal conductivity, c_p is the specific heat at constant pressure, μ is

the fluid viscosity, μ_0 is the magnetic permeability. We considered the variation of magnetization M as a linear function of temperature T, that is $M = K(T_c - T)$.

The magnetic dipole lies on the y-axis and a distance d below the x-axis which gives rise to a magnetic field, sufficiently strong to saturate the biofluid and H_x, H_y are the component of the magnetic field $\overrightarrow{H} = (H_x, H_y)$

$$H_x(x,y) = -\frac{\gamma}{2\pi}\frac{x^2 - (y+d)^2}{\left[x^2 + (y+d)^2\right]^2} \text{ and } H_y(x,y) = \frac{\gamma}{2\pi}\frac{2x(y+d)}{\left[x^2 + (y+d)^2\right]^2}$$

Therefore, the magnitude $\|H\| = H$ of the magnetic field is given by

$$H(x,y) = \left[H_x^2 + H_y^2\right]^{1/2} \approx \frac{\gamma}{2\pi}\left[\frac{1}{(y+d)^2} - \frac{1}{2}\frac{x^2}{(y+d)^4}\right] \tag{9.5}$$

The mathematical analysis of the problem is simplified by introducing the following dimensionless coordinates, Murtaza et al. (2017), Majeed et al. (2016),

$$\xi(x) = \sqrt{\frac{b}{\nu}}x,\ \eta = \sqrt{\frac{b}{\nu}}y,\ \psi = \left(\frac{\nu}{\rho}\right)\xi f(\eta),\ \theta(\eta) = \frac{T_c - T}{T_c - T_w} \tag{9.6}$$

where $T_c - T_w = \frac{Dx}{k}\sqrt{\frac{\nu}{b}}$ and we assumed that temperature of the sheet is $T_w(x)$ while the temperature of the ambient far from the surface of the sheet is $T_c(x)$. This implies that the magnetization, $M = K(T_c - T)$, far from the surface becomes zero and the magnetic field no longer affects the flow field.

Finally, ψ is the stream function defined by $u = \frac{\partial \psi}{\partial y} and v = -\frac{\partial \psi}{\partial x}$ which identically satisfy equation (9.1).

By substituting (9.6) and (9.5) into equations (9.2) and (9.3), we obtain:

$$f''' + ff'' - f'^2 + 1 - \frac{2\beta\theta}{(\eta+\alpha)^4} = 0 \tag{9.7}$$

$$\theta''+\Pr f\theta'-\frac{2\lambda_a\beta(\theta-\varepsilon)}{(\eta+\alpha)^3}f=0 \tag{9.8}$$

The corresponding transformed boundary conditions are

$$f'(0)=\lambda,\ f(0)=S,\ \theta'(0)=-1$$

$$f'(\infty)\to 1,\ \theta(\infty)\to 0 \tag{9.9}$$

The dimensionless parameters appearing in the above governing equations are the Prandtl number $P_r=\frac{\mu C_p}{k}$, the ferromagnetic parameter $\beta=\frac{\gamma}{2\pi}\frac{\mu_0 k(T_c-T_w)\rho}{\mu^2}$, the viscous dissipation parameter $\lambda_a=\frac{c\mu^2}{\rho k(T_c-T_w)}$, the dimensionless temperature parameter $\varepsilon=\frac{T_c}{(T_c-T_w)}$ and the dimensionless distance $\alpha=\sqrt{\frac{c\rho}{\mu}}$. Also $\lambda=\frac{b}{a}$ is the stretching/shrinking parameter, where $\lambda>0$ indicates the stretching sheet, $\lambda<0$ represents the shrinking sheet and S is the suction/injection parameter where suction defined by $S>0$ and $S<0$ refers to injection.

9.3. Stability Analysis

In order to carry out a stability analysis, we consider the unsteady case for (9.1)-(9.3). The continuity equation (9.1) holds while equations (9.2) and (9.3) can be written as

$$\frac{\partial u}{\partial t}+u\frac{\partial u}{\partial x}+v\frac{\partial u}{\partial y}=U_\infty\frac{\partial U_\infty}{\partial x}+\nu\frac{\partial^2 u}{\partial y^2}+\frac{\mu_0}{\rho}M\frac{\partial H}{\partial x} \tag{9.10}$$

$$\frac{\partial T}{\partial t}+\left(u\frac{\partial T}{\partial x}+v\frac{\partial T}{\partial y}\right)+\frac{\mu_0}{\rho C_p}T\frac{\partial M}{\partial T}\left(u\frac{\partial H}{\partial x}+v\frac{\partial H}{\partial y}\right)=\frac{k}{\rho C_p}\frac{\partial^2 T}{\partial y^2} \tag{9.11}$$

where *t* denotes the time. Based on the variables (9.6), we introduce the following new dimensionless variables:

$$u=bx\frac{\partial f}{\partial\eta}(\eta,\tau),\ v=-\sqrt{b\nu}\,f(\eta,\tau),$$

$$\eta = \sqrt{\frac{b}{\nu}} y,\ \tau = bt,\ \theta(\eta,\tau) = \frac{k(T-T_c)}{Dx}\sqrt{\frac{b}{\nu}} \tag{9.12}$$

Then equations (9.10) and (9.11) can be written as

$$\frac{\partial^3 f}{\partial \eta^3} + f\frac{\partial^2 f}{\partial \eta^2} - \left(\frac{\partial f}{\partial \eta}\right)^2 + 1 - \frac{\partial^2 f}{\partial \eta \partial \tau} - \frac{2\beta\theta}{(\eta+\alpha)^4} = 0 \tag{9.13}$$

$$\frac{\partial^2 \theta}{\partial \eta^2} + \Pr\left(f\frac{\partial \theta}{\partial \eta} - \frac{\partial \theta}{\partial \tau}\right) - \frac{2\lambda_a \beta(\varepsilon-\theta) f}{(\eta+\alpha)^3} = 0 \tag{9.14}$$

and are subject to the boundary conditions

$$f(0,\tau) = S, \frac{\partial f}{\partial \eta}(0,\tau) = \lambda, \frac{\partial \theta}{\partial \eta}(0,\tau) = -1$$

$$\frac{\partial f}{\partial \eta}(\eta,\tau) \to 0, \theta(\eta,\tau) \to 0\ as \eta \to \infty \tag{9.15}$$

To test the stability of the steady flow solution we consider $f(\eta) = f_0(\eta), \theta(\eta) = \theta_0(\eta)$ that satisfy the boundary value problem (9.1)-(9.3), we write

$$f(\eta,\tau) = f_0(\eta) + e^{-\gamma\tau} F(\eta,\tau)$$

$$\theta(\eta,\tau) = \theta_0(\eta) + e^{-\gamma\tau} G(\eta,\tau) \tag{9.16}$$

where γ is an unknown eigenvalue parameter, and $F(\eta,\tau)$ and $G(\eta,\tau)$ are small as compared to $f_0(\eta)$ and $\theta_0(\eta)$. By substituting (9.16) into equations (9.13) and (9.14), we get the following linearized governing equations

$$\frac{\partial^3 F}{\partial \eta^3} + f_0\frac{\partial^2 F}{\partial \eta^2} + f_0'' F - 2f_0'\frac{\partial F}{\partial \eta} - \frac{\partial^2 F}{\partial \eta \partial \tau} + \gamma\frac{\partial F}{\partial \eta} - \frac{2\beta G_0}{(\eta+\alpha)^4} = 0 \tag{9.17}$$

$$\frac{\partial^3 G}{\partial \eta^3} + \Pr\left(f_0\frac{\partial G}{\partial \eta} + \gamma G + \theta_0' F\right) - \frac{2\beta\lambda_a \varepsilon F}{(\eta+\alpha)^3} + \frac{2\beta\lambda_a (f_0 G + \theta_0 F)}{(\eta+\alpha)^3} = 0 \tag{9.18}$$

subject to the boundary conditions

$$F_0(0,\tau)=0,\frac{\partial F}{\partial \eta}(0,\tau)=0,G(0,\tau)=0$$
$$\frac{\partial F}{\partial \eta}(\eta,\tau)\to 0,G(\eta,\tau)\to 0 \;\; as \;\; \eta\to\infty \tag{9.19}$$

Consider $\tau=0$, then the solution of the steady state equations (9.7) and (9.8) is $f(\eta)=f_0(\eta)$ and $\theta(\eta)=\theta_0(\eta)$. Hence, $F(\eta)=F_0(\eta)$ and $G(\eta)=G_0(\eta)$ in (17) and (18) identify initial growth or decay of the solution (9.16). To test our numerical procedure, the following linear eigenvalue problems will be solved:

$$F_0''' + f_0F_0'' + f_0''F_0 - 2f_0'F_0' + \gamma F' - \frac{2\beta G_0}{(\eta+\alpha)^4}=0 \tag{9.20}$$

$$G_0'' + \Pr\left(f_0G_0' + \gamma G_0 + F_0\theta_0'\right) - \frac{2\beta\lambda\varepsilon F_0}{(\eta+\alpha)^3} + \frac{2\beta\lambda\left(f_0G_0+\theta_0F_0\right)}{(\eta+\alpha)^3}=0 \tag{9.21}$$

along with the new boundary conditions:

$$F_0(0)=0,\; F_0'(0)=0, G_0(0)=0$$

$$F_0'(\eta)\to 0,\;\; G_0(\eta)\to 0 \;\; as \;\eta\to\infty \tag{9.22}$$

The smallest eigenvalue γ will determine the stability of the corresponding steady flow solution $f_0(\eta)$ and $\theta_0(\eta)$ for all parameters involved.

Harris et al. (2009) suggests relaxing a boundary condition on $F_0(\eta)$ or $G_0(\eta)$ to better find the range of possible eigenvalues. Hence, for the present problem, we relax the condition that $F_0'(\eta)\to 0$ *as* $\eta\to\infty$ and for a fixed value of γ we solve the system (9.20-9.21) along with the new boundary condition $F_0''(0)=1$.

9.4 Numerical Method

The system of nonlinear ordinary differential equations (ODEs) (9.7) and (9.8) subject to boundary conditions (9.9) have been solved numerically by using the boundary value problem solver, bvp4c function technique in MATLAB. To obtain the solution we need three necessary conditions: (i) first order ODEs which are to be solved (ii) their associated boundary conditions and (iii) initial guesses for these functions.

Since our transformed governing equations are of third order we reduce them to a system of first order differential equations. New variables are now defined by the equations $f = y_1, f' = y_2, f'' = y_3, \theta = y_4, \theta' = y_5$. Thus, the two coupled higher order differential equations and the corresponding boundary conditions, can be transformed to five equivalent first ODEs subject to corresponding boundary conditions. The system of first order ODEs is:

$$\left.\begin{aligned} f' &= y_2 \\ y_2' &= y_3 \\ y_3' &= -y_1 y_3 + y_2^2 - 1 + \frac{2\beta y_4}{(\eta+\alpha)^4} \\ \theta' &= y_5 \\ y_5' &= -\Pr y_1 y_5 - \frac{2\lambda_a \beta(\varepsilon - y_4) y_1}{(\eta+\alpha)^3} \end{aligned}\right\} \tag{9.23}$$

subject to the initial boundary conditions:

$$y_1(0) = S, y_2(0) = \lambda, y_5(0) = -1,\ y_2(\infty) = 0, y_4(\infty) = 0 \tag{9.24}$$

Eq. (9.24), and Eq. (9.23) is then integrated numerically as an initial valued problem to a given terminal point. All these simplifications are done for using the MATLAB package. This programme is performed with the step size of $\eta = 0.01$ and then solved for the interval of $0 \le \eta \le \eta_\infty$ where by trial and error we set $\eta_\infty = 3$.

9.5 Results and Discussion

In order to continue to the derivation of the numerical results it is necessary to allocate values to the dimensionless parameters. For this problem, we can assume that the fluid is blood with $\rho = 1050\, kg/m^3$ and $\mu = 3.2 \times 10^{-3}\, kgm^{-1}s^{-1}$, Murtaza et al. (2017). The

electrical conductivity of blood is $\sigma = 0.8 sm^{-1}$, Tzirtzilakis (2005), and the temperature of the fluid is $T_c = 41^0 c$ whereas the plate temperature is $T_w = 37^0 c$. As it is known, for temperatures above 41°C, blood cell irreversible structural damages occur and this is the reason why someone's life is in danger if he/she is exposed to such high fever. This biological limit of 41°C is by definition the Curie temperature, T_c, of blood since the definition of T_c in general Ferrohydrodynamics is the temperature, beyond of which, we no longer have the magnetization effect on the fluid $(M = 0)$, Tzirtzilakis (2005). For the above values of temperature, the temperature number is $\varepsilon = 78.5$ and the viscous dissipation number is 6.4×10^{-14}, Murtaza et al. (2017). Generally, the specific heat under a constant pressure c_p and thermal conductivity k of any fluid are temperature dependent. However, the ratio including the above quantities expressed by the Prandtl number can be considered constant with the temperature variation. Therefore, for the temperature range consider in this problem, $c_p = 3.9 \times 10^3 \, Jkg^{-1}k^{-1}$ and $k = 0.5 \, Jm^{-1}s^{-1}k^{-1}$ and hence $P_r = 25$, Murtaza et al. (2017).

As far as the parameters related with the magnetic field, in the present study we adopted the values of β to be from 0 to 10, used also in the study of Tzirtzilakis and Kaffoussias (2003). We note here that for a specific fluid, where k, ρ, μ are considered constants and at constant temperatures T_c and T_w in the flow field, increasing β means increment the magnetic field strength of the magnetic dipole, whereas, $\beta = 0$ corresponds to the pure hydrodynamic flow. For the validation of the numerical method, the numerical results for the skin friction coefficient (for some limitation case) are compared with those of Naganthran et al.(2016) The obtained results for variable stretching parameter are presented in Table 9.1 and found to be in good agreement with those derived by Naganthran et al. (2016).

The effects of various physical parameters on the velocity and the temperature profiles are discussed through graphs Fig. 9.2 to Fig. 9.11. We also observe that dual solutions exist by setting different initial guesses of missing slope where all profiles satisfy the far field boundary conditions (9.9) asymptotically.

Table 9.1: Comparison of skin friction coefficient for $\beta = 0, S = 0, \Pr = 0.72$

λ	Present		Naganthran et al. (2016)	
	First solution	Second solution	First solution	Second solution
-0.25	1.40224		1.402240	
-0.5	1.49567		1.495669	
-0.75	1.48929		1.489298	
-1.0	1.32882	0.00126	1.328816	0
-1.15	1.08225	0.11576	1.082231	0.116702
-1.2	0.93253	0.23286	0.932473	0.233649

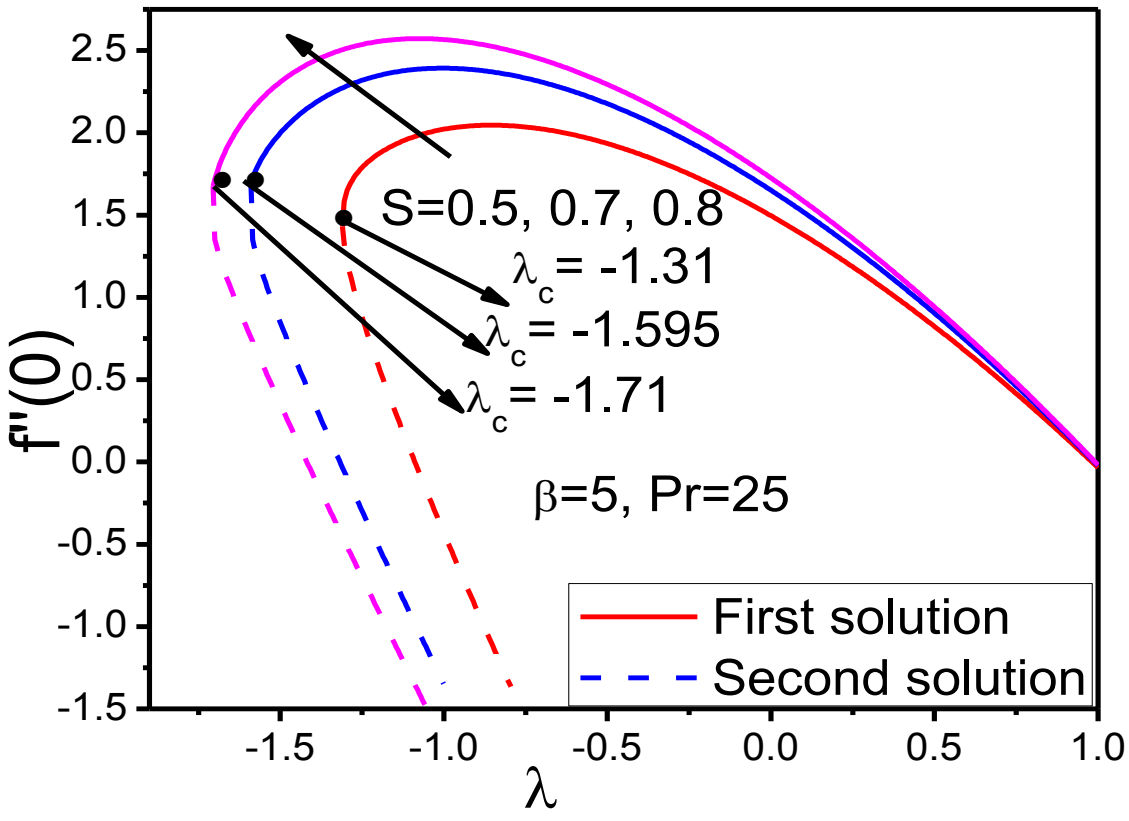

Fig. 9.2 Skin friction coefficient with λ for various value of S

Fig. 9.2 illustrates the variation of skin friction coefficient $f''(0)$ with the stretching/shrinking parameter for different values of suction parameter. It is interesting to note that there exist two solutions branches. The first branch represents the stable solution, while the second branch denotes the unstable solution commencing for a critical value of λ, λ_c which corresponds to a given value of S. From Fig 9.2, we observe that the unique solution exists for $\lambda > -0.75$ when $S = 0.5$, $\lambda > -0.9$ when $S = 0.7$ and $\lambda > -1.1$ when $S = 0.8$, while dual solutions exist for $-1.31 < \lambda < -0.75$ when $S = 0.5$, $-1.595 < \lambda < -0.9$ when $S = 0.7$ and $-1.71 < \lambda < -1.1$ when $S = 0.8$, and no solution exists when $\lambda < \lambda_c$ where $\lambda_c = -1.31, -1.595, -1.71$ *for* $S = 0.5, 0.7, 0.8$, respectively, where λ_c is the critical value of λ at which the two solution branches meet with each other thus a unique solution is obtained.

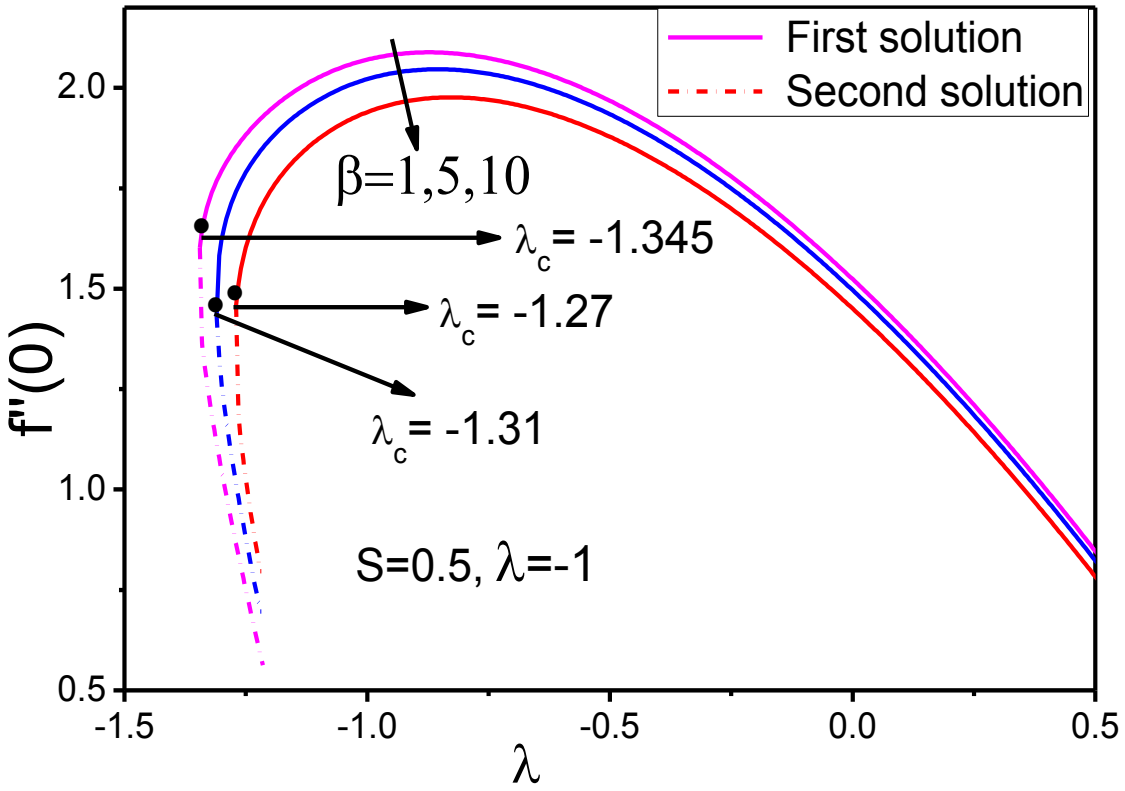

Fig. 9.3 Skin friction coefficient with λ for various values of β

The variation of the skin friction coefficient with stretching/shrinking parameter for different values of ferromagnetic number is displayed at Fig 9.3. In this figure, we observe that the solution is unique when $\lambda > -1.21$, multiple (dual) solutions exist up to

$\lambda_c < \lambda < -1.21$ and no solutions exists when $\lambda < \lambda_c$ where λ_c is critical value of λ and the value of $\lambda_c = -1.27, -1.31, -1.345$ for $\beta = 1, 5, 10$.

We also observe that the magnitude of the critical value λ_c are stated in Figs 9.2 and 9.3, which show that increasing the suction parameter results to increment of the range of λ for which the similarity solution exists. The skin friction coefficient at the surface increases as the suction parameter increases.

Further, we observe that the range of λ for which the similarity solution exists is increased, as the ferromagnetic parameter β increases. The skin friction coefficient at the surface decreases as the ferromagnetic parameter increases. Conclusively, the effect of the increment of the suction parameter, is the enlargement of the range of λ for which unique solution exists. On the other hand, the increment of the ferromagnetic parameter results to reduced range of λ for which the unique solution exists.

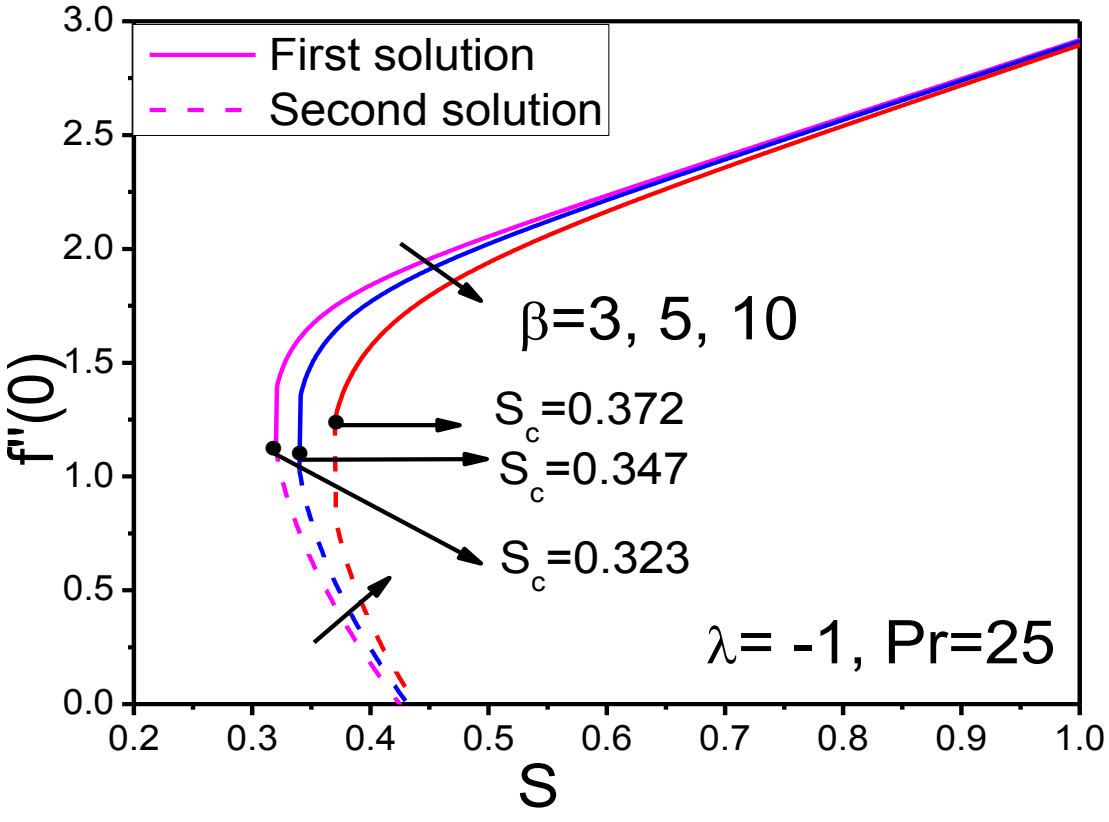

Fig. 9.4: Skin friction coefficient with S for various values of β

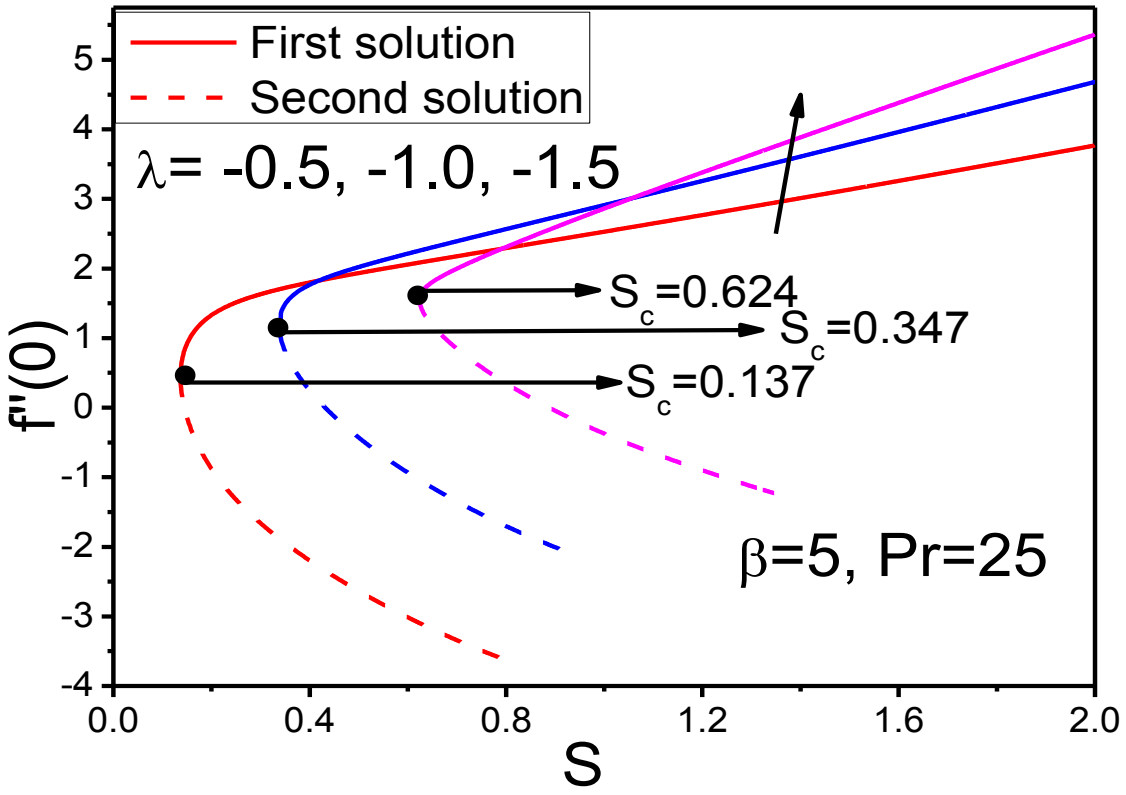

Fig. 9.5: Skin friction coefficient with S for various values of λ.

Figs. 9.4 and 9.5 show the variation of skin friction coefficient $f''(0)$ with suction parameter S for different values of stretching parameter and ferromagnetic number. It is observed that, dual solutions exist for some specific values of the suction parameter with different values of ferromagnetic parameter and stretching parameter. Numerically it is seen that for $\beta = 3$, the unique solution exists for $S > 0.42$, dual solutions exist for $0.323 < S < 0.42$ and no solutions for $S < 0.323$. Again for $\beta = 5$, the solution is unique for $S > 0.43$, dual solutions for $0.347 < S < 0.43$ and no solution for $S < 0.347$. Also, for $\beta = 10$, the solution is unique for $S > 0.44$, dual solutions for $0.372 < S < 0.44$ and no solutions for $S < 0.372$. From fig. 9.4, it is seen that the critical values of $S_c = 0.137, 0.347, 0.624$ for $\lambda = -0.5, -1.0, -1.5$, respectively. We also observe that for $\beta = 5, \lambda = -1.0$, the solution is unique for $S > 1$, no solution for $S < 0.347$ and multiple solutions is found for $0.347 < S < 1$.

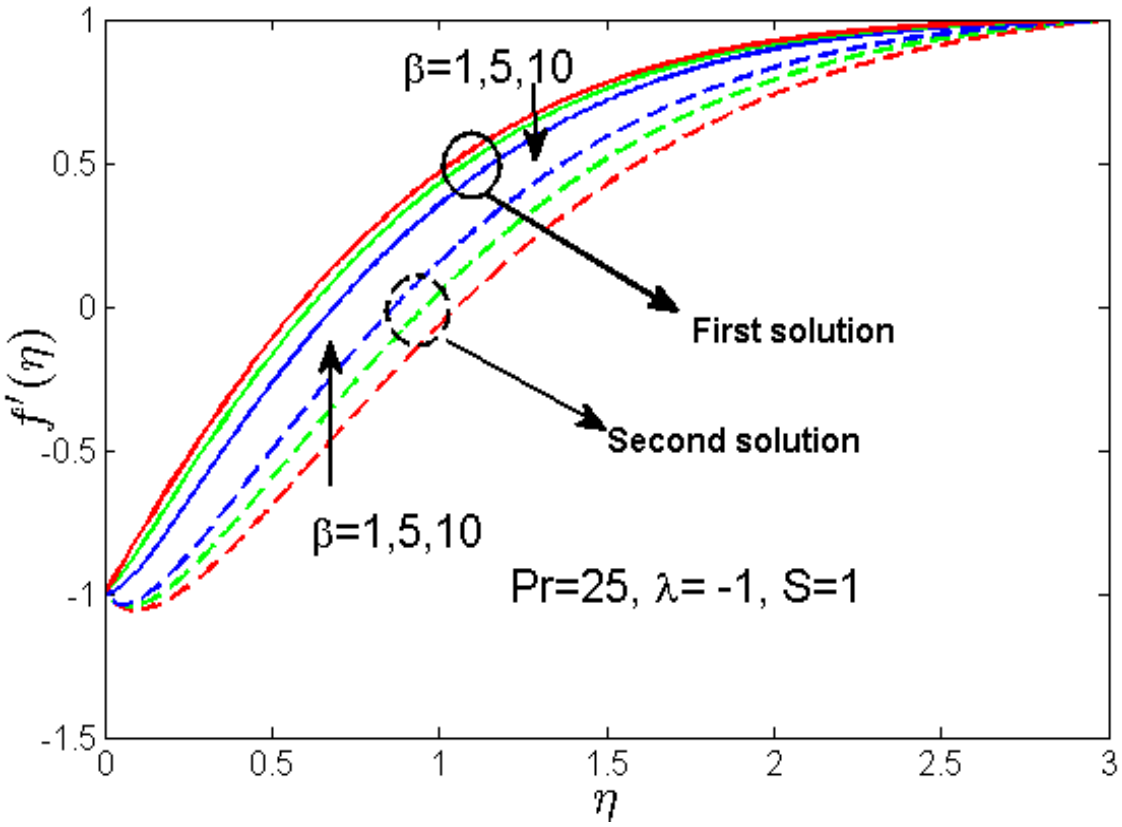

Fig. 9.6 Velocity profile $f'(\eta)$ for different values of β

Clearly, the increment of the ferromagnetic parameter β results in the increment of the range of the values of the suction parameter for which the unique solution exists. Moreover, the skin friction coefficient at the surface decreases as the ferromagnetic parameter increases. On the other hand, the range of the suction parameter S for which unique solution exists, is increased with the increment of the stretching parameter. Finally, the skin friction coefficient at the surface increases as the stretching parameter increases.

Figs. 9.6-9.11 depict the velocity and temperature profiles for different values of β, S, λ. Figure 9.6 indicates that the velocity of the biomagnetic fluid is significantly reduced throughout the flow field as the ferromagnetic parameter increases, in the case of the first solution. This signifies that the momentum boundary layer thickness becomes thinner with a rise in the value of the parameter β. But the result is to the contrary in the case of the second solution. The observation that the increment of the ferromagnetic parameter β results in the reduction of the velocity in the boundary layer is consistent with previous studies by Tzirtzilakis and Kafoussias (2003), Tzirtzilakis and Taoudis (2003), Murtaza et al. (2017). It is apparent that the magnetic field retards the flow and this resistance leads to the increment of the temperature inside the boundary layer as well as Tzirtzilakis and Kafoussias (2003),

Tzirtzilakis and Taoudis (2003), Murtaza et al. (2017). This is observed for the temperature profile of the first solution and opposite effects are observed for the second solution with the increment of the ferromagnetic parameter (See fig 9.7). From Fig. 9.7 it is also observed that thermal boundary layer increases for the first solution and decreases for the second solution with the increment of the ferromagnetic parameter.

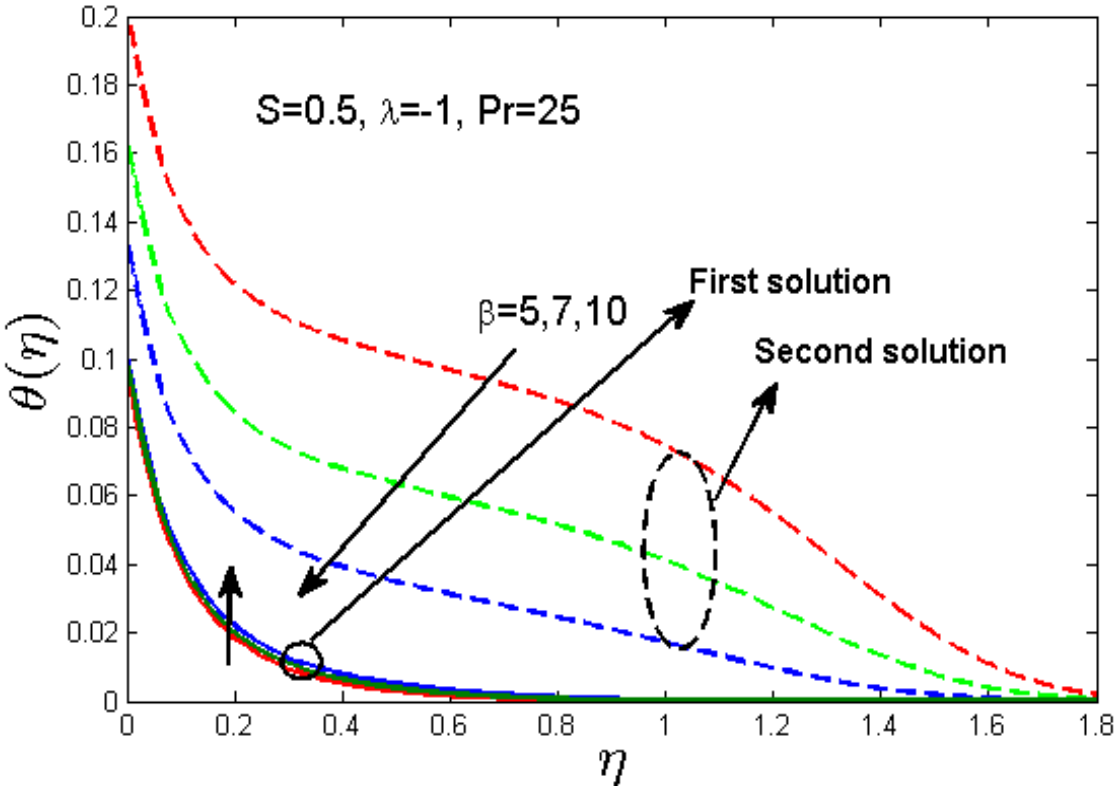

Fig. 9.7 Temperature profile $\theta(\eta)$ for different values of β

Figs. 9.8 and 9.9 display the velocity and temperature profiles for different values of the suction parameter. According to the first solution (cf. Fig. 9.8), the fluid velocity increases, as the suction velocity enhances, while a reverse trend is observed in the case of the second solution. This can be interpreted physically by saying that since during suction, the fluid in the vicinity of the wall is sucked away, the boundary layer thickness is reduced due to suction and thereby the fluid velocity is enhanced. Fig. 9.9 demonstrates that the fluid temperature is reduced as the quantum of suction increases. This implies that the thermal boundary layer thickness decreases as suction proceeds. This causes an increase in the rate of heat transfer. However, this is the observation from the first solution. A reverse trend is found to occur, if we consider the second solution. This observation implies that as the fluid is brought closer to the surface, the thermal boundary layer thickness diminishes.

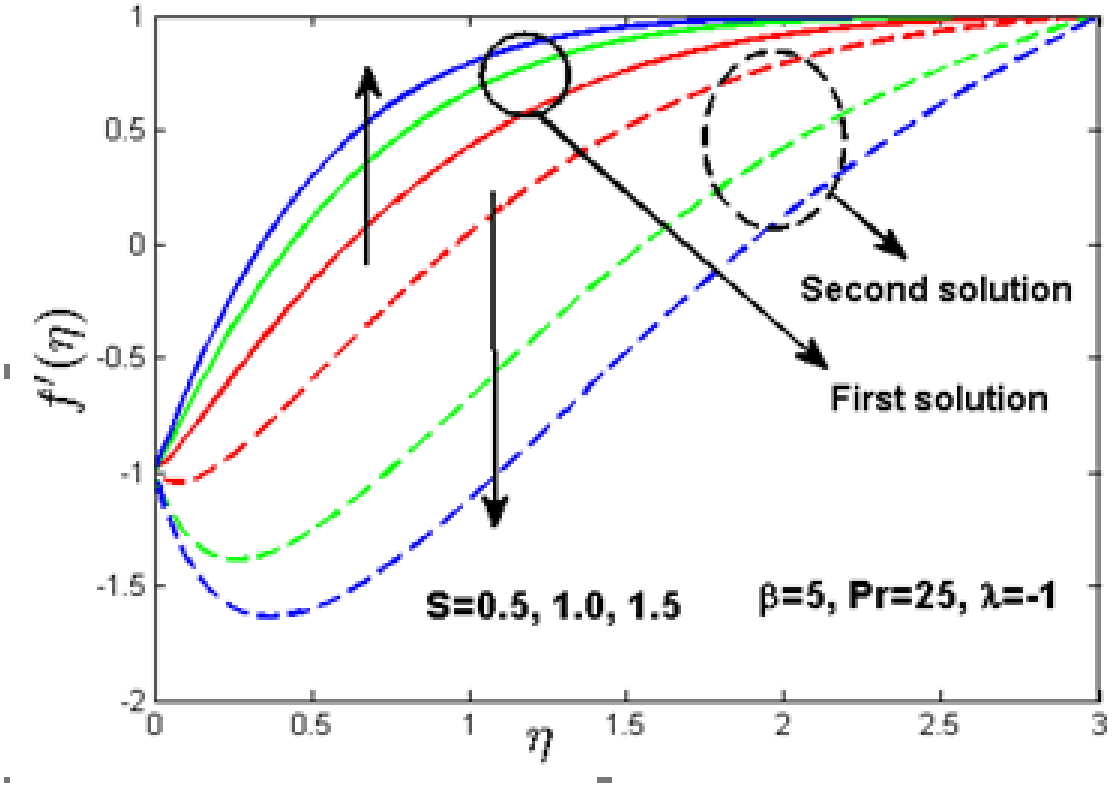

Fig. 9.8 Velocity profile $f'(\eta)$ for different values of S

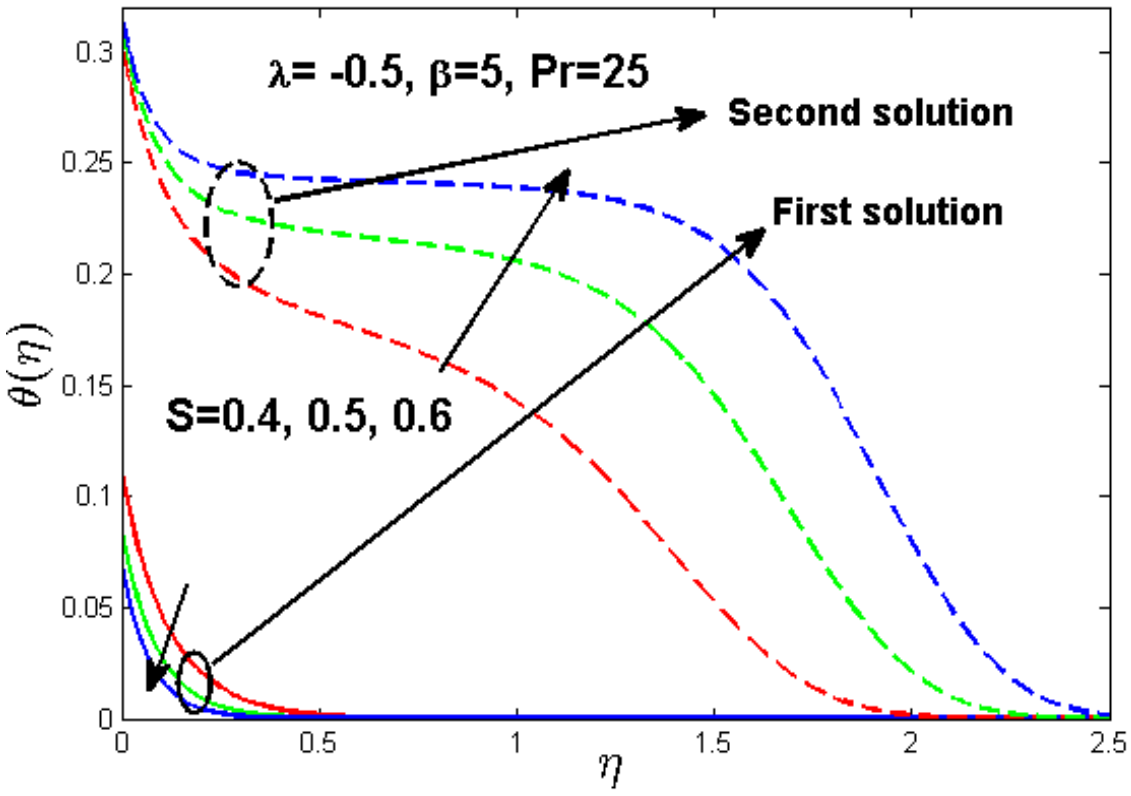

Fig. 9.9 Temperature profile $\theta(\eta)$ for different values of S

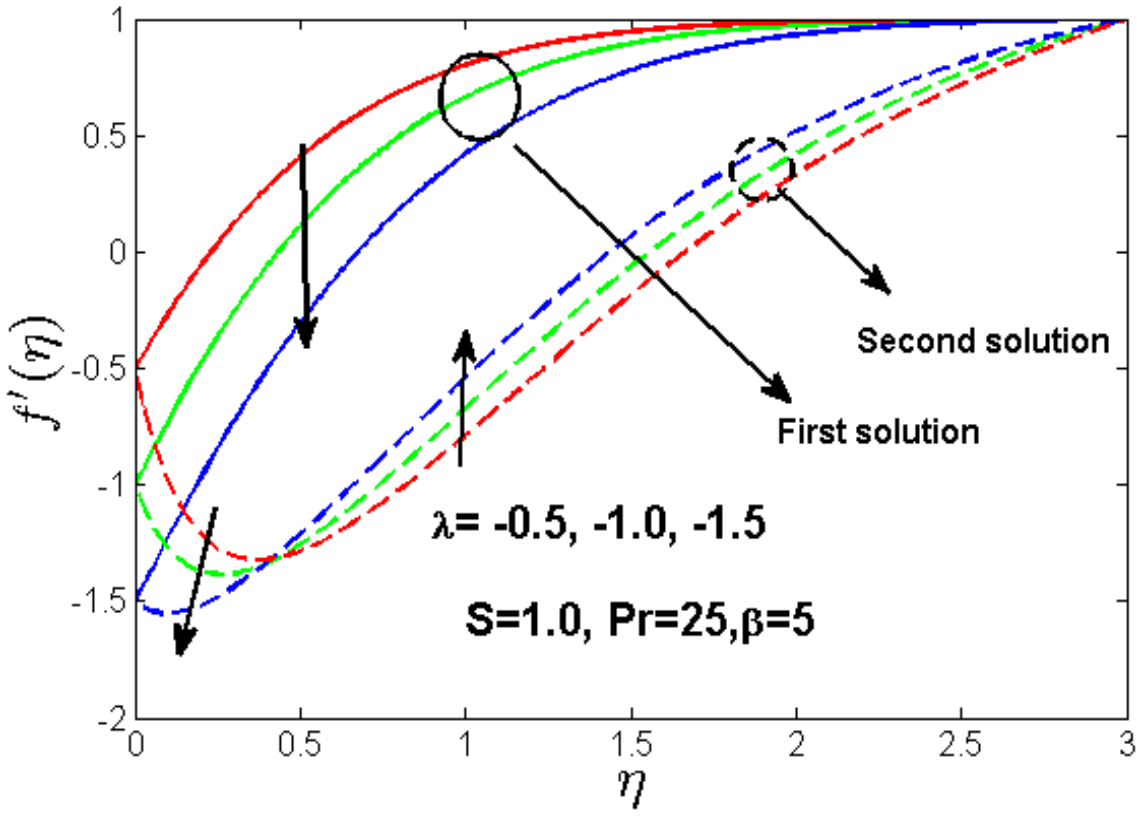

Fig. 9.10 Velocity profile $f'(\eta)$ for different values of λ

Fig. 9.10 depicts the velocity profiles for different values of shrinking parameter $\lambda(<0)$. From this figure, we can notice that when the shrinking parameter increases then it is strongly beneficial in decelerating the fluid flow. This is caused due to the opposite directions of shrinking and free stream velocities.

Fig. 9.11 illustrates the effect of shrinking parameter $\lambda(<0)$ on the temperature profiles. In this case the thermal boundary layer increases as shrinking parameter increases for the first solution and completely opposite behaviour is observed for the second solution. From Figs. 9.6 to 9.11, it can be seen that the boundary layer thickness for the second solution is always larger than the first solution.

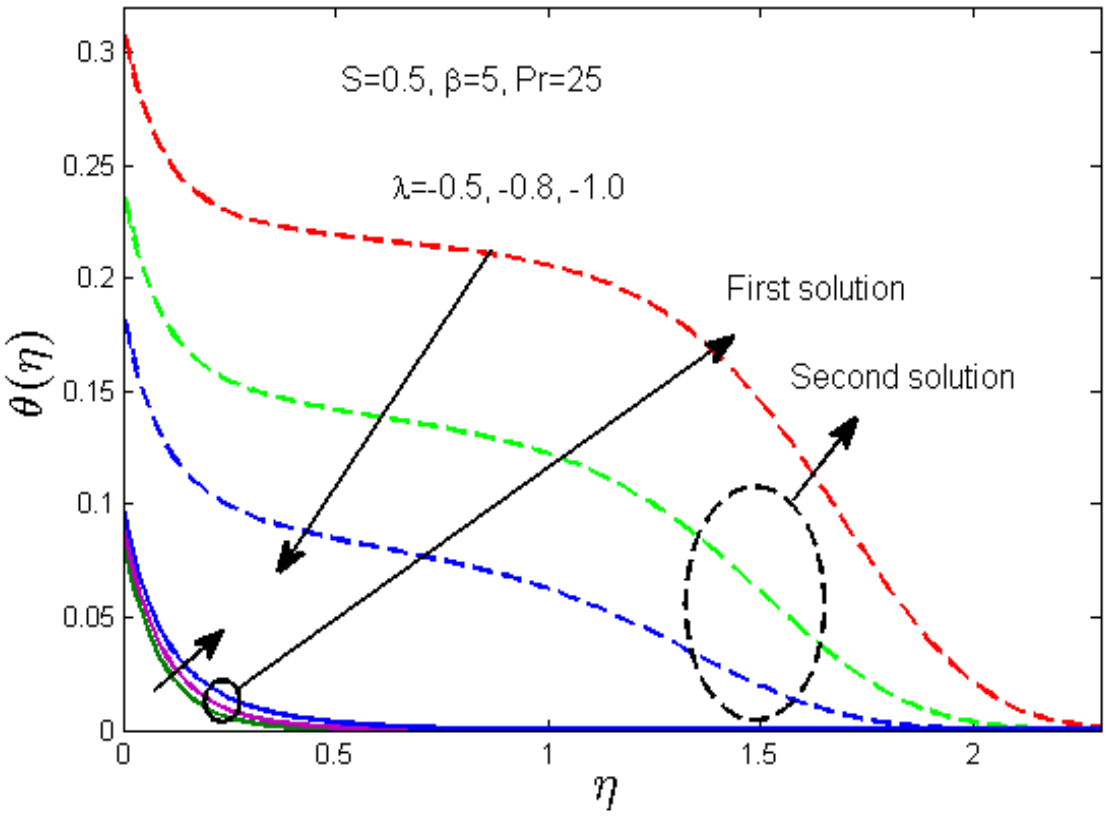

Fig. 9.11 Temperature profile $\theta(\eta)$ for different values of λ

9.6 Summary of the chapter

This chapter considered the stability analysis of dual solutions of flow and heat transfer of biomagnetic fluid with prescribed heat flux over a stretching/shrinking sheet. Numerical solutions were obtained using bvp4c function in MATLAB. Dual solutions can be obtained for a certain range of stretching/shrinking parameter and suction parameter. The stability analysis was performed and showed that the first solution was stable and physically reliable while second solution was unstable. From this study, we concluded that the skin friction coefficient increases with suction parameter and stretching parameter but decreases with the increment of the ferromagnetic parameter. Moreover, the boundary layer thickness of the velocity as well as temperature in the second solution is always larger than that observed for the first solution.

Chapter 10

Conclusion and future scope

In this thesis, we have analyzed the biomagnetic fluid flow over a different type of stretched sheet/surface. The flow is considered for steady/unsteady and linear/nonlinear under the influence of a magnetic field. Basic principles of magnetohydrodynamics (MHD) and ferro-hydrodynamics (FHD) have been employed in this thesis. The governing PDEs are transformed into a system of couple non-linear ODEs subject to appropriate boundary conditions by using similarity transformations. Similarity solutions have been obtained for BFD boundary layer equations. The resulting differential equation subject to appropriate boundary conditions was solved by using efficient numerical technique based on (i) the common finite difference method with central differencing (ii) on a tridiagonal matrix manipulation and (iii) on an iterative procedure in FORTRAN programming with the help of CodeBlocks software and BVP4C function available in the MATLAB software.

This thesis has started with introductory chapter in which a brief discussion of biomagnetic fluid namely, blood and its properties, applications of biofluid, aims, objectives and important of this study. Then, we investigate the Biomagnetic Fluid Flow (BFD) (blood) over a stretching/shrinking sheet in the presence of magnetic field. After that, the biomagnetic fluid flow and heat transfer in three-dimensional unsteady stretching/shrinking sheet in the presence of ferromagnetic interaction parameter has also been investigated. Then, we investigate the time-dependent two-dimensional biomagnetic fluid flow (BFD) over a stretching sheet under the action of strong magnetic field. A study of BFD flow and heat transfer over a non-linearly stretching sheet with variable thickness has been carried out has also been investigated. Later on, we have analyzed the temperature dependent viscosity and thermal diffusivity on BFD boundary layer flow and heat transfer over a stretching sheet. Finally, we have analyzed the dual solutions in biomagnetic fluid flow and heat transfer over a nonlinear stretching/shrinking sheet in the presence of a magnetic dipole with/without prescribed heat flux using Lie group transformation. Effects of various parameters, such as, magnetohydrodynamic parameter, ferromagnetohydrodynamic parameter, viscosity parameter, stretching parameter, wall thickness parameter, velocity index parameter and

internal heat generation parameter on velocity, pressure and temperature distributions, as well as on skin friction, relative wall pressure and heat transfer rate have been investigated numerically.

Based on the present thesis, the following conclusions can be drawn.

1) The magnetic parameter has a dominating control over the flow of the biomagnetic fluid and heat transfer.
2) In FHD and MHD case the velocity component decreases with both ferromagnetic interaction parameter and magnetohydrodynamics parameter increases, but the major impact on the fluid velocity is magnetohydrodynamics parameter than ferrohydrodynamics.
3) The pressure and temperature profiles are increased on the effect of ferromagnetic interaction parameter and magnetohydrodynamics parameter.
4) The temperature of the fluid increases with the increment of the MHD or FHD parameter. The greater increment found for BFD flows.
5) For the effect of magnetic parameter, the velocity profile $f'(\eta)$ is increased with the increment of the magnetic number in stretching sheet but this observation is reversed for the shrinking sheet. On the other hand the velocity profiles $g'(\eta)$ and $-(f(\eta)+g(\eta))$ are decreased with the increment of the magnetic number in both stretching and shrinking sheet.
6) The thermal boundary layer thickness is increased in both stretching and shrinking sheet with the increment of the unsteady parameter and magnetic number. Note that the profile is higher in shrinking sheet than that of the stretching one.
7) The effect of variable thermal conductivity parameter is to enhance the temperature in the flow region and this effect reversed in the case of the wall temperature parameter. This parameter effect is negligible for velocity and skin friction.
8) The effect of increasing value of viscosity parameter θ_r is to enhance the temperature but decreases the velocity. This parameter are more affected on velocity profile and skin friction but negligible on wall temperature gradient.
9) The effect of thermal conductivity is more affect in temperature gradient than other physical significance. On the other hand viscosity parameter is more affected in skin friction than temperature gradient.

10) The skin friction coefficient is increased with the increment of FHD and MHD parameters. Also the rate of heat transfer at the wall and the relative pressure are reduced with FHD and MHD parameter.
11) Dual solutions exist for some specific range of values of the suction parameter and stretching/shrinking parameters.
12) The stability analysis emphasizes the existence of dual solutions, one of them being stable and can be realized physically. But the second solution is not so.
13) The range of similarity solution and that for the existence of dual solutions are enlarged, as the (nonlinear) stretching increases.
14) Skin friction coefficient is decreased/increased with the increment of the unsteady parameter for the shrinking/stretching sheet, respectively. Also skin friction is increased with the increment of the ferromagnetic number β in both sheets.
15) Wall temperature gradient is increased/decreased with the increase of the unsteady parameter for the shrinking/stretching sheet, respectively.
16) The skin friction coefficient fluid temperature increase as suction rate increases.
17) With an increase in nonlinear stretching, the heat transfer rate and skin friction are both diminished.

This study will extended with three dimensional blood flows pattern through channel flow in horizontal cylinder, cylindrical geometry with significant narrowing (mimicking stenosis) and cylindrical geometry with significant swelling (mimicking aneurysm) allowing magnetisation and Lorentz forces. In addition, symmetry and three dimensional cylindrical system of blood flows through an artery will also be investigated which is more realistic mathematical models to interpret and enhance the understanding of blood flow characteristics under stenosis and aneurysmal conditions through mathematical behaviour that determine the effect of mass and flow transport phenomena associated with disease on geometries stated. The establishment of new numerical techniques finite volume method (FVM), finite element method (FEM), COMSOL Multiphysics will be used as the way for the solution of more difficult bio-fluid and mathematical problems.

References

Abbasbandy, S., & Roohani Ghehsareh, H. (2013). Solutions for MHD viscous flow due to a shrinking sheet by Hankel-Pade method. *International Journal of Numerical Methods for Heat & Fluid Flow, 23*(2), 388-400.

Abel, M. S., Siddheshwar, P. G., & Nandeppanavar, M. M. (2007). Heat transfer in a viscoelastic boundary layer flow over a stretching sheet with viscous dissipation and non-uniform heat source. *International journal of heat and mass transfer, 50,* 960-966.

Abel, M. S., & Mahesha, N. (2008). Heat transfer in MHD viscoelastic fluid flow over a stretching sheet with variable thermal conductivity, non-uniform heat source and radiation. *Applied mathematical modelling, 32*, 1965-1983.

Alfred Walz. (1969). *Boundary layers of flow and temperature.* the University of Michigan: M.I.T. Press.

Alfven, H. (1942). On the existence of electromagnetic Hydromagnetic waves. *Arkiv F. Mat. Astro. O. Fysik. Bd, 2*, 295.

Ali, F. M., Nazar, R., Arifin, N. M., & Pop, I. (2011). MHD boundary layer flow and heat transfer over a stretching sheet with induced magnetic field. *Heat and mass transfer, 47*, 155- 162.

Ali, F. M., Nazar, R., Arifin, N. M., & Pop, I. (2011). MHD stagnation-point flow and heat transfer towards stretching sheet with induced magnetic field. *Applied Mathematics and Mechanics (Engl. Ed.), 32*(4), 409–418.

Ali, M., Ahmad, M., & Hussain, S. (2015). Analytical Solution of Unsteady MHD Blood Flow and Heat Transfer through Parallel Plates when Lower Plate Stretches Exponentially. *J. Appl. Environ. Biol. Sci., 5*, 1-8.

Alimohamadi, H., & Sadeghy, K. (2015). On the use of magnetic fields for controlling the temperature of hot spots on porous plaques in stenosis arteries. *Nihon Reoroji Gakkaishi, 45*(5), 135–144.

Anderson, H. I. (1992). MDH flow of a viscoelastic fluid past a stretching surface. *Acta Mechanica, 95*, 227-230.

Anderson, H. I. (1995). An exact solution of the Navier–Stokes equations for magnetohydrodynamics flow. *Acta Mech, 113*, 241–244.

Andersson, H. I. (2002). Slip flow past a stretching surface. *Acta Mech, 158*, 121-125.

Andersson, H. I., & Valnes, O. A. (1998). Flow of a heated ferrofluid over a stretching sheet in the presence of a magnetic dipole. *Acta Mech, 128*(1), 39–47.

Andersson, S., Larsson, K., Larsson, M., & Jacob, M. (1999). *Biomathematics: Mathematics of Biostructure and Biodynamics* (1st ed.). Elsevier Science.

Andra, W., & Nowak, H. (1998). *Magnetism and Medicine.* Berlin: Willy VCH.

Awaludin, I. S., Weidman, P. D., & Ishak, A. (2016). Stability analysis of stagnation-point flow over a stretching/shrinking sheet. *AIP Advances, 6*, 0453081-7.

Aziz, A., Uddin, M. J., Hamad, M. A., & Ismail, A. I. (2012). MHD flow over an inclined radiating plate with the temperature-dependent thermal conductivity, variable reactive index, and heat generation. *Heat Transfer—Asian Research, 41*(3), 241-259.

Bachok, N., Ishak , A., & Pop, I. (2012). Unsteady boundary layer flow and heat transfer of a nanofluid over a permeable stretching/shrinking sheet. *Int. J. of heat and mass transfer, 55*, 2102-2109.

Bachok, N., Ishak, A., & Pop, I. (2010). Unsteady three-dimensional boundary layer flow due to a permeable shrinking sheet. *Applied Mathematics and Mechanics, 31*, 1421-1428.

Baillie, C. T., Winslet , M. C., & Bradley, N. J. (1995). Tumour vasculature—a potential therapeutic target. *British Journal of Cancer, 72*(2), 257-267.

Balivada, S., Rachakatla, R. S., & Wang, H. (2010). A/C magnetic hyperthermia of melanoma mediated by iron(0)/iron oxide core/shell magnetic nanoparticles: a mouse study. *BMC Cancer, 10*(1), 119.

Bashtovoy, V. G., Berkovsky, B. M., & A.N. (1988). *Vislovich, Introduction to Thermomechanics of magnetic fluids.* Berlin: Hemisphere, spinger-verlag.

Berkovsky, B. M., & Bashtovoy, V. G. (1996). *Magnetic Fluids and Applications Handbook.* Begell House Inc.

Berkovsky, B. M., Medvedev, V. F., & Krakov, M. S. (1993). *Magnetic Fluids-Engineering Aplications.* Oxford, U.K: Oxford University Press.

Bhattacharyya, K. (2011). Dual Solutions in Unsteady Stagnation-Point Flow over a Shrinking Sheet. *Chin Phys.Lett, 28*(8), 084702.

Bluman, G. W., & Kumei, S. (1991). *Symmetries and differential equations, Applied mathematical sciences.* New York: Springer-Verlag.

Blums, E., Cebers , A., & Maiorov, M. (1997). *Magnetic Fluids.* New York: Walter de Gruyter, Berlin.

Callahan, G. D., & Marner, W. J. (1976). Transient free convection with mass transfer on an isothermal vertical flat plate. *International Journal of Heat and Mass Transfer, 19*, 165-174.

Cambel, A. B. (1963). *Plasma Physics and Magneto-fluid mechanics.* New York: McGraw-Hill.

Carnahan, B., Luther, H. A., & Wilkes, J. O. (1969). *Applied numerical methods.* New York: John Wiley and sons.

Caro, C. G., & Colin, G. (1978). *The Mechancs of the circullation.* New York: Oxford University Press.

Chen, H. I. (1985). Analysis of an intensive magnetic field on blood flow: part 2. *J Bioelectr, 4*, 55–61.

Chien, S., King, R. G., Skalak, R., Usami, S., & Copley, A. L. (1975). Viscoelastic properties of human blood and red cell suspensions. *Biorheology, 12*(6), 341-346.

Cramer, K., & Pai, S. (1973). *Magnetofluid Dynamics for Engineers and Applied Physicists.* New York: McGraw Hill.

Crane, L. J. (1970). Flow past a stretching plate. *J. Appl. Math. Phys. (ZAMP), 21*, 645–647.

Dailey, J. P., Phillips, I. P., Li, C., & Riffle, J. S. (1999). Synthesis of silicone magnetic fluid for use in eye surgery. *J. Magn. Magn. Mater., 194*, 140-148.

Dandapat, B. S., Santra, B., & Singh, S. K. (2010). Thin film flow over a non-linear stretching sheet in presence of uniform transverse magnetic field. *Z. Angew. Math. Phys, 61*, 685–695.

Das, K., & Saha, G. C. (2009). Arterial MHD Pulsatile Flow of Blood under Periodic Body Acceleration. *Bulletin of Society of Mathematicians Banja Luka, 16*, 21-42.

Das, S., Chakraborty, S., Jana, R. N., & Makinde, O. D. (2015). Entropy analysis of unsteady magneto-nanofluid flow past accelerating stretching sheet with convective boundary condition. *Appl. Math. Mech. (Engl. Ed.), 36*(12), 1593–1610.

Davidson, P. (2001). *An Introduction to Magnetohydrodynamics.* United Kingdom: Cambridge University Press.

Devi, S. A., & Thiyagarajan, M. (2006). Steady nonlinear hydromagnetic flow and heat transfer over a stretching surface of variable temperature. *Heat Mass Transfer, 42*, 671–677.

Dulal, C. S., & Ananda, B. (2010). Pulsatile Motion of Blood through an Axi - Symmetric Artery in Presence of Magnetic Field. *Journal of Science and Technology of Assam University, 5*(2), 12-20.

Eldesoky, I. M. (2012). Mathematical Analysis of Unsteady MHD Blood Flow through Parallel Plate Channel with Heat Source. *World Journal of Mechanics, 2*, 131-137.

El-Mistikawy, M. A. (2016). MHD flow due to a linearly stretching sheet with induced magnetic field. *Acta Mechanica, 227*(10), 3049-3053.

Evans , H. L. (1968). *Laminar boundary layer theory.* United States: Addison-Wesley Publishing Company.

Fan, H. Y. (1987). *Elements of Solid State Physics.* Wiley-Interscience.

Fang, T. G., Zhang, J., & Yao, S. S. (2009). Viscous flow over an unsteady shrinking sheet with mass transfer. *Chinese Physics Letter, 26*, 014703.

Fang, T., Zhang, J., & Zhong, Y. (2012). Boundary layer flow over a stretching sheet with variable thickness. *Applied Mathematics and computation, 228*, 7241-7252.

Farady, M. (1832). Experimental researches in electricity-second series (Bakerian lecture). *Phil. Trans. Roy. Soc*, 175.

Fenton, B. M., Paoni, S. F., Lee, J., Koch, C. J., & Lord, E. M. (1999). Quantification of tumour vasculature and hypoxia by immunohistochemical staining and HbO2 saturation measurements. *British Journal of Cancer, 79*(3-4), 464-471.

Ferdows, M., Md. Jashim Uddin , & Afify, A. A. (2013). Scaling group transformation for MHD boundary layer free convective heat and mass transfer flow past a convectively heated nonlinear radiating stretching sheet. *International Journal of Heat and Mass Transfer, 56*, 181-187.

Fiorentini, G., & Szasz, S. (2006). Hyperthermia today: Electric energy, a new opportunity in cancer treatment. *Journal of Cancer Research and Therapeutics, 21*, 41-46.

Frewer, R. A. (1974). The electrical conductivity of flowing blood. *Biomed Eng.*, 552–554.

Ghosh, S., Mukhopadhyay, S., & Vajravelu , K. (2016). Dual solutions of slip flow past a nonlinearly shrinking permeable sheet. *Alexandria Engineering Journal, 55*, 1835-1840.

Goodwin, S., Peterson, C., Hoh, C., & Bittner, C. (1999). Targeting and retention of magnetic targeted carriers (MTCs) enhancing intra-arterial chemotherapy. *J.Magn. Magn. Mater., 194*, 132-139.

Goyal, M. R. (2013). *Biofluid dynamics of Human body system.* Apple Academic Press.

Griffiths, D. (1999). *Introduction to Electrodynamics.* Prentice Hall.

Hafizuddin, E. H., Nazar, R., Arifin, N. M., & Pop, I. (2016). Boundary layer flow and heat transfer over s permeable exponentially stretching/shrinking sheet with generalized slip velocity. *Journal of applied fluid mechanics, 9*, 2025-2036.

Hafizuddin, H. M., Nazar, H., Arifin, N. M., & Pop, I. (2014). Three-Dimensional Viscous Flow over an Unsteady Permeable Stretching/Shrinking Sheet. *Proceedings of the 3rd International Conference on Mathematical Sciences. 1602*, p. 422. AIP Conf. Proc.

Haik, Y., Pai, V., & Chen, C. J. (1999). *Biomagnetic fluid dynamics, in fluid dynamics at interfaces, edited by W. Shyy and R. Narayanan.* Cambridge: Cambridge University Press.

Haik, Y., Pai, V., & Chen, C. J. (1999). Development of magnetic device for cell separation. *Journal of magnetism and Magnetic Materials, 194*(1), 254–261.

Haik, Y., Pai, V., & Chen, C. J. (2001). Apparent viscosity of human blood in a high static magnetic field. *J. Magn. Magn. Mater, 225*, 180.

Haik, Y., Chen, J. C., & Pai, V. M. (1996). Development of biomagnetic fluid dynamics. *In: Proceedings of the IX International Symposium on Transport Properties in Thermal Fluid Engineering.* Singapore.

Harald, I., & Hans, L. (2009). *Solid-State Physics: An Introduction to Principles of Materials Science (4th ed.).* Berlin: Springer.

Harris, S. D., Ingham, D. B., & Pop, I. (2009). Mixed convection boundary-layer flow near the stagnation point on a vertical surface in a porous medium: Brinkman model with slip. *Trans. Porous Media, 77*, 267-285.

Hathaway, D. B. (1979). Use of ferrofluid in moving-coil loudspeakers. *dB-Sound Engg. Mag., 13*, 42-44.

Hayat, T., Imtiaz, M., & Alsaedi, A. (2015). Partial slip effects in flow over nonlinear stretching surface. *Applied Mathematics and Mechanics (Engl. Ed.), 36*(11), 1513–1526.

Hayat, T., Shafiq, A., Alsaedi, A., & Shahzad, S. A. (2016). Unsteady MHD flow over exponentially stretching sheet with slip conditions. *Applied Mathematics and Mechanics (Engl. Ed.), 37*(2), 193–208.

He, Y., Shirazaki, M., Liu, H., Himeno, R., & Sun, Z. (2006). A numerical coupling model to analyze the blood flow, temperature, and oxygen transport in human breast tumor under laser irradiation. *Computers in Biology and Medicine, 36*(12), 1336-1350.

Higashi, T., Yamagishi, A., Atakeuchi, T., Kawaguch, N., Sagawa, S., Onishi, S., Kawaguch, N. (1993). Orientation of rythrocytes in a strong static magnetic field. *Journal of Blood, 88*, 1328.

Hollingworth , W., Todd, C. J., Bell, M. I., Arafat , Q., Girlin, S., Karia, K. R., & Dixon, A. K. (2000). The diagnostic and therapeutic impact of MRI: an observational multi-centre study. *Clinical Radiology, 55*(11), 825-31.

Ishak, A., Jafar, K., Nazar, R., & Pop, I. (2009). MHD stagnation point flow towards a stretching sheet. *Physica A, 388*, 3377-3383.

Ishak, A., Nazar, R., & Pop, I. (2006). Mixed convection boundary layers in the stagnation point flow towards a stretching vertical sheet. *Meccanica, 441*, 509-518.

Ishak, A., Bachok, N., Nazar, R., & Pop, I. (2010). MHD mixed convection flow near the stagnation point on a vertical permeable surface. *Physica A, 389*, 40-46.

Ishak, A., Nazar, R., & Pop, I. (2007). Boundary layer flow over a continuously moving thin needle in a parallel free stream. *Chinese Physics Letters., 24*(10), 2895–2897.

Jackson, J. (1998). *Classical Electrodynamics: 3rd Edition.* Wiley.

Jalil, M., Asghar, S., & Mushtaq, M. (2010). Lie group analysis of mixed convection flow with mass transfer over a stretching surface with suction or injection. *Math. Probl. Eng., 2010*, 1-14.

Jat, R. N., & Chaudhary, S. (2010). Radiation effects on the MHD flow near the stagnation point of a stretching sheet. *Z. Angew. Math. Phys, 61*, 1151–1154.

Jullien, A., & Guinier, R. (1989). *The Solid State from Superconductors to Superalloys.* U.K: Oxford Univ. Press.

Kafoussias, N. G., & Williams, E. W. (1993). An improved approximation technique to obtain umerical solution of a class of two-point boundary value similarity problems in fluid mechanics. *Int. J. Numer. Methods Fluids, 17*(2), 145–162.

Kafoussias, N. G., Tzirtzilakis, E. E., & Raptis, A. (2008). Free-force convective boundary layer flow of a biomagnetic fluid under the action of localized magnetic field. *Canadian J. of Physics, 86*, 447-457.

Khader, M. M., & Megahed, A. M. (2015). Approximate solutions for the flow and heat transfer due to a stretching sheet embedded in a porous medium with variable thickness, variable thermal conductivity and thermal radiation using Laguerre collocation method. *Application and applied mathematics, 10*(2), 817-834.

Kim, D. K., Voit, W., Zapka, W., Bjelke, B., & Muhammed, M. (2001). Biomedical application of ferrofluids containing magnetite nanoparticles. *J. Magn. Magn. Mater., 225*, 256-261.

Kleinstreuer, C. (2006). *Biofluid dynamics: Principles and selected applications.* CRC press.

Kluwick, A. (2014). *Recent advances in boundary layer theory.* Springer verlag Wien GmbH.

Kobu, Y. (1999). Effects of infrared radiation on intraosseous blood flow and oxygen tension in rat tibia. *Kobe J Med Sci, 45*, 27–39.

Kolka, A. G., Hendriksea, J., Zwanenburga, J. M., Visser, F., & Peter, R. L. (2013). Clinical applications of 7 T MRI in the brain. *European Journal of Radiology, 82,* 708-718.

Krishna, P. M., Sandeep, N., Reddy, R., & Sugunam, V. (2016). Dual solutions for unsteady flow of Powell-Eyring fluid past an inclined stretching sheet. *Journal of Naval Architecture and Marine Engineering, 13,* 89-99.

Lauva, M., & Plavins, J. (1993). Study of Colloidal Magnetite Binding Erythrocytes: Prospects for Cell Separation. *Journal of Magnetism and Magnetic Materials, 122,* 349–353.

Lee, L. L. (1967). Boundary layer over a thin needle. *Physics of Fluid, 10,* 822-828.

Liu, I. C., & Andersson, H. I. (2008). Heat transfer over a biodirectional stretching sheet with variable thermal conditions. *International journal of heat and mass transfer, 51,* 4018-4024.

Liu, J., Flores, G. A., & Sheng, R. (2001). In-vitro investigation of blood embolization in cancer treatment using magnetorhelogical fluids. *J. Magn.Magn.mater, 225,* 209.

Loukopoulos, V. C., & Tzirtzilakis, E. E. (2004). Biomagnetic channel flow in spatially varying magnetic field. *International journal of engineering science, 42,* 571-590.

Majeed, A., Zeeshan, A., & Ellahi, R. (2016). Unsteady Ferromagnetic Liquid Flow and Heat Transfer Analysis over a Stretching Sheet with the Effect of Dipole and Prescribed Heat Flux. *Journal of Molecular Liquids, 223,* 528-533.

Makinde, O. D., Khan, W. A., & Culham, J. R. (2016). MHD variable viscosity reacting flow over a convectively heated plate in a porous medium with thermophoresis and radiative heat transfer. *International Journal of Heat and Mass Transfer, 93,* 595-604.

Maruno, S., Yubakami, K., & Soga, S. (1983). Plain paper recording process using magnetic fluids. *J. Magn. Magn. Mater., 39,* 187-189.

Matsuki, H., Yamasawa, K., & Murakami, K. (1977). Experimental considerations on a new automatic cooling device using temperature sensitive magnetic fluid. *IEEE Trans. Magn, 13*(5), 1143–1145.

Mishra, U., & Singh, G. (2014). Dual solutions of mixed convection flow with momentum and thermal slip flow over a permeable shrinking cylinder. *Computers & Fluids, 93,* 107-115.

Misra, J. C. (2006). *Biomathematics modeling and simulation.* Singapore: World Scientific.

Misra, J. C., Sinha, A., & Mallick , B. (2017). Stagnation point flow and heat transfer on a thin porous sheet: Applications to flow dynamics of the circulatory system. *Physica A: Statistical Mechanics and its Applications, 470*, 330-334.

Misra, J. C., & Adhikary, S. D. (2016). MHD oscillatory channel flow, heat and mass transfer of a physiological fluid in presence of chemical reaction. *Alex. Engng. Journal, 55*, 287-297.

Misra, J. C., & Adhikary, S. D. (2017). Flow of a Bingham fluid in a porous bed under the action of a magnetic field: Application to magneto-hemorheology. *Engineering Science and Technology, an Inter. Journal, 20*, 973-981.

Misra, J. C., & Chandra, S. (2013). Electroosmotically actuated oscillatory flow of a physiological fluid on a porous micro-channel subjected to an AC electric field having dissimilar frequencies. *Cent. Euro. J. Phys., 12*, 274-285.

Misra, J. C., & Shit, G. C. (2007). Effect of magnetic field on blood flow through an artery: A numerical model. *J. Computational Technologies, 12*, 3-16.

Misra, J. C., & Shit, G. C. (2009). Biomagnetic viscoelastic fluid flow over a stretching sheet. *Appl. Math. Comput, 210*(2), 350–361.

Misra, J. C., & Shit, G. C. (2009). Flow of a biomagnetic viscoelastic fluid in a channel with stretching walls. *Journal of Applied Mechanics, Trans. ASME, 76*, 06106: 1-9.

Misra, J. C., & Sinha, A. (2013). Effect of thermal radiation on MHD flow of blood and heat transfer in a permeable capillary in stretching motion. *Heat Mass Transfer, 49*, 617–628.

Misra, J. C., Chandra, S., & Herwig, H. (2015). Flow of a micro polar fluid in a micro-channel under the action of an alternating electric field: Estimates of flow in bio-fluidic devices. *Journal of Hydrodynamics, 27*, 350-358.

Misra, J. C., Chandra, S., Shit, G. C., & Kundu, P. K. (2013). Thermodynamic and magnetohydrodynamic analysis of blood flow, considering rotation of micro-particles of blood. *J. Mechs. Med. Biol., 13*, 135003-1-13.

Misra, J. C., Mallick, B., Sinha, A., & Roy Chowdhury, A. (2018). Impact of Cattaneo-Christov heat flux on electroosmotic transport of third-order fluids in a magnetic environment. *The Euro. Phys. Journal Plus, 133*, 195.

Misra, J. C., Pal, B., & Gupta, A. S. (1998). Hydromagnetic flow of a second grade fluid in a channel: some applications to physiological system. *Math. Models Methods Appl. Sci., 8*, 1323-1342.

Misra, J. C., Shit, G. C., & Rath, H. J. (2008). Flow and heat transfer of a MHD viscoelastic fluid in a channel with stretching walls: some applications to haemodynamics. *Comput. Fluids, 37*(1), 1-11.

Misra, J. C., Shit, G. C., Chandra, S., & Kundu, P. K. (2011). Hydromagnetic flow and heat transfer of a second grade viscoelastic fluid in a channel with oscillatory stretching walls: application to the dynamics of blood flow. *J. Engn. Maths, 59*, 91-100.

Misra, J. C., Sinha, A., & Shit, G. C. (2010). Flow of a biomagnetic viscoelastic fluid: application to estimate of blood flow in arteries during electromagnetic hyperthermia, a therapeutic procedure for cancer treatment. *Appl. Math. Mech. Engl. Ed, 31*(11), 1405-1420.

Misra, J. C., Sinha, A., & Shit, G. C. (2011). A numerical model for the magnetohydrodynamic flow of blood in a porous channel. *J. Mechs. Med. Biol., 11*, 547-562.

Mitchell, A. R., & Griffiths, D. F. (1980). *The finite difference method in partial differential equations.* New York: Wiley.

Mukhopadhyay, S. (2011). Heat transfer in a moving fluid over a moving non-isothermal flat surface. *Chin Phys.Lett., 28*, 124706.

Murray, J. D. (1993). *Mathematical Biology.* New York: Springer-Verlag.

Murtaza, M. G., Tzirtzilakis, E. E., & Ferdows, M. (2018). Numerical solution of three dimensional unsteady biomagnetic flow and heat transfer through stretching/shrinking sheet using temperature dependent magnetization. *Archives of mechanics, 70*(2), 161-185.

Murtaza, M. G., Tzirtzilakis, E. E., & Ferdows, M. (2017). Effect of electrical conductivity and magnetization on the biomagnetic fluid flow over a stretching sheet. *Z. Angew. Math. Phys., 68*, 93.

Murtaza, M. G., Tzirtzilakis, E. E., & Ferdows, M. (2018). Dual solutions in boundary layer flow and heat transfer of biomagnetic fluid over a stretching/shrinking sheet in the presence of a magnetic dipole and prescribed heat flux. *Zeitschrift f¨ur Angewandte Mathematik und Physik (ZAMP), Accepted.*

Murtaza, M. G., Tzirtzilakis, E. E., & Ferdows, M. (2018). Three dimensional Biomagnetic flow and heat transfer over a stretching surface with variable fluid properties. *Advance in mechanics and mathematics, 41, 403-414.*

Naganthran, K., & Nazar, R. (2017). Dual Solutions of MHD Stagnation-point Flow and Heat Transfer past a Stretching/Shrinking Sheet in a Porous Medium. *4th International Conference on Mathematical Science AIP Conf, 1830*, 020038-1-020038-8.

Nagranthran, K., Nazar, R., & Pop, I. (2016). Unsteady stagnation point flow and heat transfer of a special third grade fluid past a permeable stretching/shrinking sheet. *Scientific Report, 6*, 24632.

Naramgari, S., & Sulochana, C. (2016). MHD flow over a permeable stretching/shrinking sheet of a nonofluid with suction/injection. *Alexandria Enginnering journal, 55*, 819-827.

Nik Long, N. M., Suali, M., Ishak, A., Bachok,, N., & Arifin, N. M. (2011). Unsteady stagnation point flow and heat transfer over a stretching/shrinking sheet. *Journal of applied sciences, 11*, 3520-3524.

Nishimoto, C., Ishiura , Y., Kuniasu, K., & Koga, T. (2006). Effects of ultrasonic radiation on cutaneous blood flow in the paw of decerebrated rats. *Kawasaki J. Med Welfare, 12*, 13-18.

Nor Amirah Idris, Norsarahaida, A., & Hamisan, R. (2014). Effect of gravitational acceleration on unsteady biomagnetic fluid flow. *Applied and computational mathematics, 3*(6), 285-294.

Nursalasawati, R., Hong, A. K., Kasiman, E. H., Yassin, Y. M., & Amin, N. (2012). Numerical computation of a two dimensional biomagnetic channel flow. *International Journal of Modern Physics: Conference Series, 9*, 178-192.

Odenbach, S. (2002). *Magnetoviscous Effects in Ferrofluids.* Berlin, Heidelberg.: Springer-Verlag.

Oka, S., & Murata, T. (1970). A theoretical study of the flow of blood in a capillary with permeable wall. *Jpn J Appl Phys*, 9:345–352.

Oleinik, O. A., & Samokhin, V. N. (1999). *Mathematical model in boundary layer theory.* New York: Chapman and Hall/CRC.

Olver, P. J. (1986). *Application of Lie group to differential equations.* New York: Springer.

Olver, P. J. (1993). *Applications of Lie Groups to Differential Equations, vol. 107 of raduate Texts in Mathematics, 2nd edition.* New York, USA: Springer.

Ovsiannikov, L. V. (1982). *Group Analysis of Differential Equations.* New York, USA.: Academic Press.

Pakdemirli, M., & Yurusoy, M. (1998). Similarity transformations for partial differential equations. *Soc Ind Appl Math., 40*, 96–101.

Papisov , M. I., Bogdannov , A., Schaffer, B., Nossiff, N., Shen, T., Weissleder, R., & Brady, T. J. (1993). Colloidal magnetic resonance contrast agents: effect of particle surface on biodistribution. *J. Magn. Magn. Mater, 122*(1-3), 383-386.

Pavlov, K. B. (1974). Magnetohydrodynamic flow of an incompressible viscous fluid caused by deformation of a plane surface. *Magnitnaya Gidrodinamika, 10*(4), 146- 148.

Plavins, J., & Lauva, M. (1993). Study of colloidal magnetic binding erythrocytes: Prospects for cell separation. *J. Magn. Magn. Mater., 122*, 349.

Pop, I., Ishak, A., & Aman, F. (2011). Radiation effects on the MHD flow near the stagnation point of a stretching sheet: revisited. *Z. Angew. Math. Phys., 62*, 953-956.

Pop, I., Natalia , C., Rosca , A., & Rosca, V. (2016). Additional results for the problem of MHD boundary-layer flow past a stretching/shrinking surface. *International Journal of Numerical Methods for Heat & Fluid Flow, 26*(7), 2283-2294.

Pop, I., & Na , T. Y. (1998). A note on MHD flow over a stretching permeable surface. *Mech Res Comm, 25*, 263–269.

Prabhu, K. S., Kandasamy, R., & Saravanan, R. (2009). Lie group analysis for the effect of viscosity and thermophoresis particle deposition on free convective heat and mass transfer in the presence of suction/injection. *Theoretical and Applied Mechanics, 36*, 275-298.

Prakash, J., & Makinde, O. D. (2011). Radiative heat transfer to blood flow through a stenotic artery in the presence of magnetic field. *Lat. Am. appl. res., 41*(3).

Prandtl, L. (1904). Uber Fliissigkeitsbewegung bei schr kleiner Reibung. *Procedding 3rd international math conference.* Heidelberg.

Prandtl, L. (1935). *The mechanics of viscous fluid, in Aerodynamic Theory, edited by W. F. Durand, Vol:III.* Berlin: Springer-Verlag.

Prasad, K. V., Vajravelu, K., & Datti, P. S. (2010). The effects of variable fluid properties on the hydromagnetic flow and heat transfer over a non-linearly stretching sheet. *International Journal of Thermal Sciences, 49*, 603-610.

Prasad, K. V., Vajravelu, K., Vaidya, & Hanumesh . (2016). MHD casson nanofluid flow and heat transfer at a stretching sheet with variable thickness. *Journal of Nanofluids, 5*, 1-13.

Pulfer, J. M., & Gallo, J. K. (2000). Targeting Tumors Using Magnetic Drug Delivery, Biomedical Chemistry: Applying Chemical Principles to the Understanding and Treatment of Disease. *John Wiley & Sons, Inc.*, 211-225.

Raj, K., & Moskowitz, R. (1990). Commercial applications of ferrofluids. *J. Magn. Magn. Mater., 85*, 233-245.

Raju, C. S., Sandeep, N., Babu, M. J., & Sugunamma, V. (2016). Dual solution for three dimensional MHD flow of a nanofluid over a nonlinearly permeable stretching sheet. *Alexandria engineering journal, 55*, 151-162.

Ramamurthy, G., & Shanker, B. (1994). Magnetohydrodynamic Effects on Blood Flow through Porous Channel. *Medical and Biological Engineering and Computing, 32*(6), 655-659.

Rashidi, M. M., Momoniat, E., Ferdows, M., & Basiriparsa, A. (2014). Lie group solution for free convective flow of a nanofluid past a chemically reacting horizontal plate in a porous media. *Math. Probl. Eng., 2014*, 1-21.

Ray Mahapatra, T., Nandy, S. K., & Pop, I. (2014). Dual solutions in magnetohydrodynamics stagnation point flow and heat transfer over a shrinking surface with partial slip. *Journal of heat transfer, ASME, 136*, 104501: 1-6.

Reddy, M. G. (2012). Lie group analysis of heat and mass transfer effects on steady MHD free convection dissipative fluid flow past an inclined porous surface with heat generation. *Theoretical and Applied Mechanics, 39,* 233-254.

Robert, L. A. (1968). *Principles of Solid State Physics.* Cambridge, United States: Academic Press.

Rosca, A. V., Rosca, N. C., & Pop, I. (2016). Numerical simulation of the stagnation point flow past a permeable stretching/shrinking sheet with convective boundary condition and heat generation. *International Journal of Numerical Methods for Heat and Fluid flow, 26*(1), 348-364.

Rosensweig, R. E. (1985). *Ferrohydrodynamics.* Cambridge university press.

Rosensweig, R. E. (1987). Magnetic fluids. *Annual Review of Fluid Mechanics, 19,* 437-461.

Ruban, A. I. (2017). *Fluid Dynamics: Part 3 Boundary Layers.* Oxford: Oxford university press.

Rusetski, A. N., & Ruuge, E. K. (1999). Magnetic Fluids as Drug Carriers: Targeted Transport of Drugs by a Magnetic Field. *Journal of Magnetism and Magnetic Materials, 122*, 335-339.

Safari, J., & Zarnegar, Z. (2014). Advanced drug delivery systems: Nanotechnology of health design A review. *Journal of Saudi Chemical Society, 18*, 85-99.

Salawu, S. O., & Dada, M. S. (2016). The radiative heat transfer of variable viscosity and thermal conductivity effects on inclined magnetic field with dissipation in a non-Darcy medium. *Journal of Nigerian Mathematical Society, 35*, 93-106.

Sassaki, M., Ehara, S., Nakasato, T., Tamakawa, Y., Kuboya, Y., Miyoshi, S., & Sato, T. (1990). MR of the shoulder with a 0.2-T permanent-magnet unit. *American Journal of Roentgenology, 154*(4), 777-8.

Schlichting, H. (1960). *Boundary layer theory* (six ed.). New York: McGraw-Hill Inc.

Schlichting, H., & Gersten, K. (2017). *Boundary layer theory.* Heidelberg: Springer-Verlag Berlin.

Schneck, D. J. (2013). *Biofluid Mechanics.* Springer.

Shampine, L. F., Reichelt, M. W., & Kierzenka, J. (2000). *Solving boundary value problem for ordinary differential equation in MATLAB with bvp4c.* U. K: Cambridge University Press.

Siddiqa, S., Naqvi, S. B., Naheed, S. E., & Awal, M. A. (2018). Thermal radiation therapy of biomagnetic fluid flow in the presence of localized magnetic field. *International Journal of Thermal Sciences, 132,* 457–465.

Singh, J., & Rathee, R. (2010). Analytical Solution of Two -Dimensional Model of Blood Flow with Variable Viscosity through an Indented Artery Due to LDL Effect in the Presence of Magnetic Field. *International Journal of Physical Sciences, 5*(12), 1857-1868.

Sinha, A., & Misra, J. C. (2012). Numerical study of flow and heat transfer during oscillatory blood flow in diseased arteries in presence of magnetic fields. *Appl. Maths. Mechs., 33,* 649-662.

Sinha, A., & Misra, J. C. (2014). Effect of induced magnetic field on magnetohydrodynamic stagnation point flow and heat transfer on a stretching sheet. *Journal of heat transfer, ASME, 136,* 112701:1-11.

Sobey, I. J. (2000). *Interactive boundary layer theory.* New York: Oxford university press.

Speziale, P., Visai, L., Rindi, S., Pietrocola, G., Provenza , G., & Provenzano , M. (2008). Prevention and Treatment of Staphylococcus Biofilms. *Current Medicinal Chemistry, 15,* 3185-3195.

Strikwerda, J. C. (1989). *Finite difference schemes and partial differential equation.* New York: Springer.

Surma , D., Takhar, H. S., & Nath, G. (1986). Unsteady, three-dimensional, boundary-layer flow due to a stretching surface. *Int. J. Heat Mass Transfer, 29,* 1996-1999.

Sushma, S., Nancy Samuel, & Neeraja, G. (2018). Slip Flow Effects on Unsteady MHD Blood Flow in a Permeable Vessel in the Presence of Heat Source/Sink and Chemical Reaction. *Global Journal of Pure and Applied Mathematics, 14*(8), 1083-1099.

Tani, I. (1977). History of boundary layer theory. *Ann. Rev. Fluid Mech., 9,* 87-111.

Thumma, T., Beg, O. A., & Kadir, A. (2017). Numerical study of heat source/sink effects on dissipative magnetic nanofluid flow from a non-linear inclined stretching/ shrinking sheet. *Journal of Molecular Liquids, 232*, 159-173.

Tollmien, W. (1931). Handbuch der Experimentalal physic. *Leipzig, Bd., 4*(1), 669-703.

Tzirtzilakis, E. E. (2005). A mathematical model for blood flow in magnetic field. *Phys. Fluids, 17*(7), 077103.

Tzirtzilakis, E. E. (2008). A simple numerical methodology for BFD problems using stream function vorticity formulation. *Commun numer methods Eng, 24*, 683-700.

Tzirtzilakis, E. E. (2008). Biomagnetic fluid flow in a channel with stenosis. *Physica D–Nonlinear Phenomena, 237*, 66-81.

Tzirtzilakis, E. E. (2015). Biomagnetic fluid flow in an aneurysm using ferrohydrodynamics principles. *Phys. Fluids, 27*(6), 061902.

Tzirtzilakis, E. E., Xenos, M., Loukopolos, V. C., & Kafoussias, N. G. (2006). Turbulent biomagnetic fluid flow in a rectangular channel under the action of localized magnetic field. *International journal of engineering science, 44*(18-19), 1205-12.

Tzirtzilakis, E. E., & Kafoussias, N. G. (2003). Biomagnetic fluid flow over a stretching sheet with nonlinear temperature dependent magnetization. *Z. Angew. Math. Phys. (ZAMP), 54*(4), 551–565.

Tzirtzilakis, E. E., & Kafoussias, N. G. (2010). Three dimensional magnetic fluid boundary layer flow over a linearly stretching sheet. *Journal of heat transfer, 132*, 011702-1-8.

Tzirtzilakis, E. E., & Tanoudis, G. B. (2003). Numerical study of biomagnetic fluid flow over a stretching sheet with heat transfer. *International Journal of Numerical Methods for Heat & Fluid Flow, 13*(7), 830-848.

Tzirtzilakis, E. E., & Xenos, M. A. (2013). Biomagnetic fluid flow in a driven cavity. *Meccanica, 48*(1), 187-200.

Vajravelu , K., Sarojamma, G., Sreelakshmi, K., & Kalyani, C. H. (2017). Dual solutions of an unsteady flow, heat and mass transfer of an electrically conducting fluid over a shrinking sheet in the presence of radiation and viscous dissipation. *International Journal of Mechanical Sciences, 130*, 119-132.

Vajravelu, K., Prasad, K. V., & Raju, B. T. (2013). Effects of variable fluid properties on the thin film flow of Ostwald-de Waele fluid over a stretching surface. *Journal of Hydrodynamics Series B, 25*, 10-19.

Varcaccio, G., Carriero, C., & Loizzo, M. R. (1995). Analgesic properties of electromagnetic field therapy in patients with chronic pelvic pain. *Clin Exp Obstet Gynecol, 22*, 350-354.

Voltairas, P. A., Fotiadis, D. I., & Michalis, L. K. (2002). Hydrodynamics of magnetic drug targeting. *Journal of biomechanics, 35*, 813-821.

Wilson, D. H. (1974). Comparison of short wave diathermy and pulsed electromagnetic energy in treatment of soft tissue injuries. *Physiotherapy, 60*, 309-310.

Yanase, M., Shinkai, M., Honda, H., Wakabayashi, T., Yoshida, J., & Kobayashi, T. (1998). Intracellular Hyperthermia for Cancer Using Magnetite Cationic Liposomes: An in vivo Study. *Jpn. J. Cancer Res., 89*, 463–470.

Yasin, M. H., Ishak , A., & Pop, I. (2016). MHD heat and mass transfer flow over a permeable stretching/shrinking sheet with radiation effect. *Journal of Magnetism and Magnetic Materials, 407*, 235-240.

Yasmeen, T., Hayet, T., Khan, M. I., Imtiaz, M., & Alsaedi, A. (2016). Ferrofluid flow by a stretched surface in the presence of magnetic dipole and homogeneous-heterogeneous reactions. *Journal of Molecular liquids, 223*, 1000-1005.

Young, A. D. (1989). *Boundary layer*. Washington, DC: American Institute of Aeronautics and Astronautics.

Zeeshan, A., Majeed, A., & Ellahi, R. (2016). Effect of magnetic dipole on viscous ferro-fluid past a stretching surface with thermal radiation. *J. Mol. Liq., 215*, 549-554.